COMPARATIVE ANALYSIS OF CORROSION INHIBITION EFFECTS OF ESTERS OF CASTOR SEED AND RUBBER SEED OILS IN FLOW PIPES

BY:

OFFURUM, JULIUS CHIGOZIE B.ENG, M.ENG

(20124471448)

A THESIS SUBMITTED TO POSTGRADUATE SCHOOL

FEDERAL UNIVERSITY OF TECHNOLOGY, OWERRI

IN PARTIAL FULFILMENT OF THE REQUIREMENTS

FOR THE AWARD OF A DEGREE OF

DOCTOR OF PHILOSOPHY (PhD)

IN CHEMICAL ENGINEERING

FEBRUARY, 2021

CERTIFICATION

This is to certify that this work "Comparative Analysis of Corrosion Inhibition Effects of Esters of Castor Seed and Rubber Seed Oils in Flow Pipe" was carried out by I, **Offurum, Julius C.** ***(20124471448)*** in partial fulfillment for the award of the Degree of Doctor of Philosophy (PhD) in Chemical Engineering, in the Department Chemical Engineering of the Federal University of Technology, Owerri, Imo State.

---------- DATE 3/5/2021

ENGR PROF. M.S. NWAKAUDU
(Supervisor)

---------- DATE 19/05/2021

PROF. O.C. NDUKWE
(Co-Supervisor)

---------- DATE 3/05/2021

ENGR DR C.I.O. KAMALU
(Co-Supervisor)

---------- DATE 04/05/2021

ENGR PROF. C.N. ANYAKWO
(Co-Supervisor)

---------- DATE 19/05/2021

ENGR DR I.S. IKE
(Head of Department)

---------- DATE 19/05/2021

ENGR PROF. J.C. EZEH
(Dean, School of Engineering and Eng. Tech.)

---------- DATE ----------

PROF. C.C. EZE
(Dean, Postgraduate School)

---------- DATE 4/5/2021

ENGR PROF. O.D. ONUKWULI
(External Examiner)

DEDITCATION

This research work is, specially, dedicated to my children- **Miss Sylvia Eberechi and Master Anthony Odinakachi Offurum**, whose arrival to the family has continuously been an added companionship.

ACKNOWLEDGMENTS

I am mostly grateful to God Almighty for the life, strength and wisdom He has granted me out of His unfading love and mercy. I wish to acknowledge the good works of my Supervisors- Engr Prof. M.S. Nwakaudu, Prof. O.C. Ndukwe, Engr Dr C.I.O. Kamalu and Engr Prof. C.N. Anyakwo, whose combined efforts have furnished this work properly. I, also, commend the efforts of my Head of department- Engr Dr I.S. Ike for his efforts in giving the administrative backups. I wish to appreciate the former head of Chemical Engineering Department, Engr Dr O.E. Onyelucheya, who has regularly made very useful inputs to give this work an enviable academic touch. I am, also, grateful to all staff of Chemical Engineering Department, especially the lecturers that taught me during the course work activities. I wish to appreciate the efforts of the dean of School of Engineering and Engineering Technology- Prof. J.C. Ezeh and the dean of Postgraduate School- Prof. C.C. Eze for their good works in their respected offices. I appreciate the great assistance offered to me by Prof. E.E. Oguzie and Dr M.A. Chidiebere who supervised the electrochemical part of the study.

I commend, in a special way, the relentless support of my dear wife – Mrs. Sussan .O. Offurum, who has continuously stood by me at the nick of time, and has selflessly made

valuable commitments throughout the period of this work; I owe her an unquantifiable reward. I wish to acknowledge the efforts of my lovely parents- Ezinna Boniface Offurum and Nneoma Bernadette Nwulu for their unflinching love, care and supports in all spheres of my life. I would continue to be grateful to my teaming siblings and their respective families, especially the Rev. Fr Sam C. Offurum, whose financial, moral and material supports have been sources of encouragement to me all the time.

I wish to acknowledge the efforts of my friends and colleagues – Engr Dr Chukwu Monday Morgan, Engr Chika Onu and Engr Okere Princewill, whose team spirit of work and diverse attributes have continued to carry us along the positive track. I wish to acknowledge the management of the Imo State Polytechnic, Umuagwo-Ohaji, for believing so much in my ability, engaging me meaningfully and securing TETFUND sponsorship for me during the programme. This page cannot be considered complete without acknowledgement of my students, of the Department of Chemical Engineering- Imo State Polytechnic, Umuagwo-Ohaji, whose continuous academic problems have challenged me to useful actions; these, of course, improved this work greatly; notably among them are Martin Onyinyechi, Eunan Chiemiziem and Comfort Chidinma. I would not fail to acknowledge the management of the New Concept

Laboratory, Obinze-Owerri for demonstration of expertise during the laboratory experiments I conducted with them. My gratitude goes, also, to Mr Paul .C. Oduocha of the PAULO'S Computer Services, who typed the manuscript of this work and has diligently given it a proven quality of professionalism. It is my pleasure, also, to commend the authors of the materials I referenced in the course of this research work.

Finally, I am very grateful to everyone, who in one way or the other, has contributed to the realization of this work but could not have his/her name included in this little space; I solemnly pray that God Almighty would bless and favour you in all your endeavors both now and always, Amen!

TABLE OF CONTENT

LIST OF TABLES

Table Number Title

Page

LIST OF FIGURES

Figure Number Title

Page

ABSTRACT

Research work on "Comparative analysis of corrosion inhibition effects of ester of castor seed oil (ECSO) and Ester of Rubber Seed Oil (ERSO) in mildsteel flow pipes" was carried out. The oil samples were extracted using solvent-extraction techniques (n-hexane for castor seed oil and petroleum ether for rubber seed oil). The castor and rubber seeds were ground, and respectively soaked in the n-hexane and petroleum ether before subsequent subjection to soxhlet extraction, to obtain purer oils. The oils were esterified to obtain ECSO and ERSO. Phytochemical analysis of the esterified oils was conducted to reveal the presence of alkaloid, flavonoid, tannins, cardiac glycocide, phenol, phytate, saponin and oxalate that are responsible for protection of the mild steel specimen. The mild steel samples were immersed in a flowing sulphuric acid solution held at various temperatures and pressures. Potentiodynamic polarization was used to determine the influence of the inhibitors on corrosion potential. Scanning electron microscopy provided surface-distorted information about the interaction between the acid medium/inhibitors and the mild steel, while Fourier transform infrared spectroscopy revealed the functional groups present in the inhibitors. The phytochemical evaluation results obtained showed that ECSO has alkaloid value of 2.2%, flavonoid (1.2%), tannic acid (8.6%), cardiac glycocide (7.0%), phenol (0.912mg/100g), Phytate (11.3%), Saponin (1.4%) and Oxalate (12937.5mg/100g), while those of ERSO have values of 2.1%, 43.5%, 12.0%, 28.0%, 1.605mg/100g, 10.8%, 11%, 59062.5mg/100g respectively. Inhibition efficiencies of ERSO-treated dynamic runs at 10g/*l*, 15g/*l*, 20g/*l* concentrations and at all treatment temperatures were higher than those of ECSO; maximum inhibition efficiencies for ERSO and ECSO applications were respectively 64.4% and 34.4% at 50% stroke, 20g/*l* dosage and 40^{o}C. Furthermore, increase in treatment temperatures and pressures drastically lowered the

inhibition efficiency; the results obtained fit the Langmuir model for both inhibitors, with $\mathbf{R^2}$ values tending towards unity. Inhibition efficiencies of ERSO-reacted static runs, obtained from potentiodynamic polarization measurements were also higher than those of ECSO, peaking at 81.70% whereas that of ECSO peaked at 75.40%, both for 20g/l treatments at ambient temperature. Scanning electron microscope, SEM pictures of the mildsteel immersed in ECSO and ERSO showed the existence of absorbate species, while Fourier transform infrared spectroscopy, FTIR spectra revealed that there were shifts due to O-H/N-H and C=O stretching frequencies from 3386cm^{-1} to 3209cm^{-1} and from 1743cm^{-1} to 1203cm^{-1} respectively. The inhibitor samples were able to inhibit mildsteel corrosion substantively, but ERSO gave better corrosion inhibition effects than ECSO.

Keywords: Castor Seed Oil, Rubber Seed Oil, Corrosion Inhibition, Mildsteel Pipe.

CHAPTER ONE

INTRODUCTION

1.1 Background Information

Corrosion inhibition is a process of adding an inhibitive substance (inhibitor) to an environment in a given concentration, in order to reduce the corrosion rate of a metal exposed to that environment (Hubert *et al*, 2002). In other words, a corrosion inhibitor is a chemical compound that, when added to a liquid or gas, decreases the corrosion rate of the material (typically a metal or an alloy). The effectiveness of a corrosion inhibitor depends largely on fluid composition, quantity of water, and flow regime. A common mechanism for inhibiting corrosion involves formation of a coating, often a passivation layer, which prevents access of the corrosive substance to the metal. Permanent treatments (such as chrome plating) are not usually considered inhibition process; instead corrosion inhibitors are seen as additives to the fluids that surround the metal or related object (Finsgarand and Milosev, 2010). Corrosion inhibitors are common in industry, and also found in over-the-counter products, typically in spray form, in combination with a lubricant and sometimes penetrating oils. Corrosion inhibition usually results from one or more of three general mechanisms. Firstly, the inhibitor molecule is adsorbed on the metal surface by the process of chemisorption, forming a thin protective film either by itself or in conjunction with metallic ions. Then, the inhibitor causes the metal to form its own protective film of metal oxides, thereby increasing its resistance. And finally, the inhibitor reacts with a potentially corrosive substance in the water.

Several things are considered when choosing the corrosion inhibitor for effective application/performance. Some of these include materials to be protected, method of application (such as dip, spray, brush, and so on), type of protection required (in process, storage or shipping), type and thickness of coating residue desired, storage, packaging and/or shipping conditions (temperature, humidity seasonal conditions), interaction with subsequent processes (if not removed), environmental, health and safety requirements, as well as type of product (such as oil/solvent or water-based). Electrochemical methods are routinely used for the evaluation of corrosion inhibitor efficiency. The advantages of electrochemical methods are their short measurement time and mechanistic information, which help in the design of corrosion protection strategies, as well as the design of new inhibitors ((Hubert *et al*, 2002; Amadi, 2006; Kelly *et al*, 2013).

1.2 Problem Statement

In our oil industries today, corrosion inhibition ranks high in issues of concern. It only takes one leak, due to corrosion, to render a length of pipeline inoperative. Occasionally, poor or no corrosion inhibition could lead to a whole plant being shut down. In the deep, hot oil and gas wells, equipment is often subjected to aggressive corrosive conditions. High temperatures and pressures combine with constituents (such as hydrogen sulphide, chloride and salts) to form an environment in which many low alloy and stainless steels perform unsatisfactorily.

In the petroleum industry, metallic failures are seen mostly in transmission networks of pipelines. In spite of much protection undertaken on the pipelines, they are still usually damaged by corrosion. As soon as the pipes are put into service, their integrity is compromised, and since corrosion is a natural

phenomenon, coupled with the fact that compatibility in engineering systems seems hard to predict, attack on the pipelines becomes obvious at its given time and rate. The local communities are now apprehensive of their environments more than ever before, and hence, their stringent demands to make almost any kind of spillage in the environment unacceptable.

The present study is therefore, motivated by the need to establish the potentials of esters of castor and rubber seed oils as corrosion inhibitors in flow pipes.

1.3 Objectives of the Study

The main objective of this research work is the comparative analysis of corrosion inhibition effects of esters of castor seed oil (ECSO) and rubber seed oil (ERSO) in flow pipes. The specific objectives include the following:

(a) Extraction and characterization of the castor seed oil (CSO) and rubber seed oil (RSO).

(b) Esterification of the oil extracts and characterization of the esters.

(c) To determine the physical, chemical and phytochemical properties of the ECSO and ERSO.

(d) Development of a flow system for the corrosion inhibition experiments.

(e) Assessment of corrosion inhibition ability of ECSO and ERSO using gravimetric method.

(f) Electrochemical study of the process.

(g) Use of scanning electron microscopy to show the effect of the acid medium and the inhibitors on the mildsteel, and Fourier transform infrared spectroscopy to identify the functional groups present in the inhibitors.

(g) Thermodynamics and isotherm studies of the process.

1.4 Justification for the Study

The dangers associated with corrosion hazards are better conceived than witnessed. These range from material thickness reduction, infliction of injuries on humans (resulting from structural failure), fluid contamination in pipes/vessels, indiscriminate deterioration of materials (leading to leakages), loss of surface properties of materials and value reduction of goods, to heavier effects, such as mechanical damage of valves/pumps and pipe blockage by solid corrosion products. The results of all these will constitute an added complexity and expensiveness of the equipment, which need to be designed to withstand the contending corrosion effects, and/or allow corroded components to be conveniently replaced. A study of this kind, therefore, becomes important in order to create room for an affordable, reliable and effective alternative of nipping corrosion and its associates to the bud. As much as the present study could offer the needed guidance on handling corrosion issues to firms that use corrodible materials (especially the oil and gas sector), it could also be a formidable benchmark to researchers whose intentions border on corrosion studies and applications.

1.5 Scope of the Study

The present study is limitated to the extraction of oil from castor and rubber seeds, characterization of the oil extracts (to obtain the inherent features) and analysis of phytochemical parameters. The study will also cover the development of the flow system unit for the study, as well as examination of the corrosion inhibition effect of the study samples on mildsteel using gravimetric and electrochemicals methods. Thermodynamic and adsorption isotherm studies will also be conducted.

CHAPTER TWO

LITERATURE REVIEW

2.1 Overview of Corrosion

Corrosion of metals or alloys occurs due to chemical or electrochemical reactions with their environment, which often results in drastic deterioration in the properties of the metals or materials comprising them thereof. Corrosion takes place on a metal (steel) surface, due to the development of anodic and cathodic areas (through oxidation and reduction reactions), forming oxides of metal alloy. This is contained in the report of Eddy *et al* (2010), as well as in Ha-Won and Vehu (2007), where it was reviewed that there are several corrosion-causing agents (corrodents) such as soot, sand, gravels, sulphate salts, chlorides, ions, temperature, and salinity, pH, dissolved gases, humidity, bacteria, stones and mechanical stresses.

Also, several protection methods could be employed to check the menace of corrosion; such methods include application of alloys, composites, inhibitors, cathodic and anodic protections, protective linings and coatings, as reviewed by Bierwagen (2011), Ghali *et al* (2011), Oluwadare *et al* (2009) and Asuquo *et al* (2012b). Notwithstanding these remedial approaches, corrosion has become a gigantic problem today for almost every nation of the world. The colossal detrimental impact of corrosion on the economy of a country can be manifested in very huge amount of money expendable annually to combat or control it. Asuquo *et al* (2012b) reported that corrosion inhibitors contain homologous series that form protective coatings on the metals. The report also identifies the iodine value of an inhibitor as an important factor in measuring the degree of unsaturation in the substance, and this measurement determines

the stability of the inhibitor oil to oxidation, which allows the overall unsaturation of the fat/oil to be determined qualitatively.

In the past two decades, research and development efforts in the field have undergone vast changes globally, because of the everyday growing consumer expectations of good quality and performance. The predictions, regulations and innovations that govern corrosion inhibition have posed constant threats and challenges for anti-corrosion industries, forcing them to change their gears world-wide. The corrosion chemists, researchers and engineers (in the industries and academics) are actively engaged to explore and formulate new strategies to meet the mandatory limits of performance, cost and legislations.

Consequently, environmental-friendly technologies (Water-borne, powder, high-solid, hyper-branched and radiation-curable) have evolved, with special emphasis on the excessive utilization of naturally available renewable resources thriving on the acres of our agricultural lands (Derksen *et al*, 1996; Gandini and Belgacem, 2002). These resources, as reviewed, may be formulated as corrosion resistant alloys, corrosion resistant composites, corrosion resistant pigments, corrosion resistant coatings, paints and corrosion inhibitors.

Metzger (2001), Weiss (2012) and Ahmed (2007) reported that renewable resources provide cheaper and abundant biological feedstocks with numerous advantages, such as cost effectiveness, low toxicity, inherent biodegradability and environmental friendliness. This yields versatile materials through chemical transformations, with plethora of applications, particularly in corrosion resistance against various corrodents as illustrated in figure 2.1.

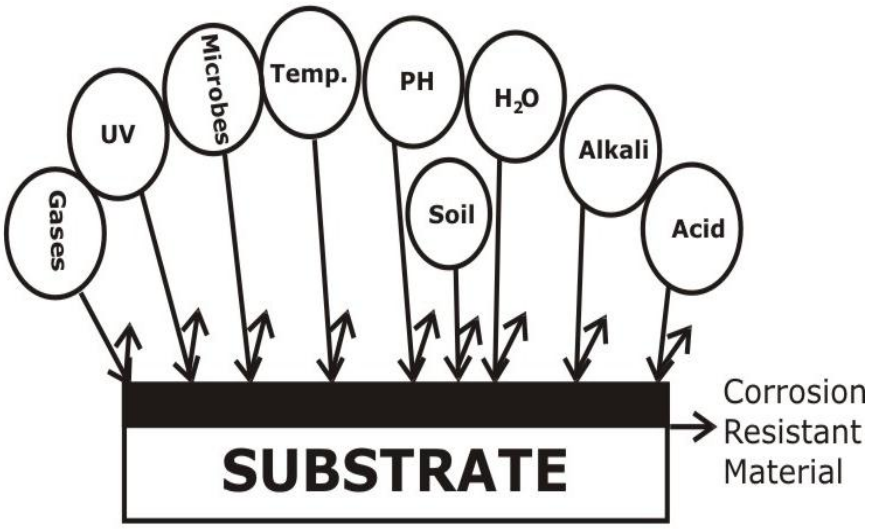

Figure 2.1: Renewable resources-based materials, providing corrosion resistance against various corrodents

The Nigerian crude oil contains, amongst other materials, some cycloparaffinic carboxylic acids. These acids have a general name known as "nepthenic acids" (with a general formula – $R([CH_2]_n$ COOH); ***R*** is a cycle nucleus, composed of one or more rings, predominantly C_5, and sometimes, C_6. In deep, hot oil and gas wells, the process equipment are often subjected to aggressive corrosion conditions. High temperatures and pressures combine with constituents such as hydrogen sulphide, chlorine and salts to form an environment in which many low alloyed and stainless steels do not perform very efficiently. Since most corrosion processes occur in an acqueous environment, complete immersion of the metal in water, or exposure to rain and moist atmosphere, or immersion in damp earth leads to corrosion of the metals in these solutions (acqueous) due to their thermodynamic instability, as compared to their compounds.

This is apparent from the fact that with the exception of the noble metals (gold, silver, copper and platinum), others are normally found in nature in the combined state as minerals, that is oxides, carbonates, silicates or sulphides of

the metals. One of the most common techniques of corrosion evaluation is the weight loss technique, and it is obviously not suited for highly localized attack (such as pitting corrosion), or corrosion dynamics (as seen in flow pipes). However, for most engineering applications, the rate of penetration or change in thickness of a structure is usually considered as the most direct and practicable measure of corrosion rate. Even when weight losses are recorded (as always the case), they are often recalculated to thickness losses using suitable corrosion factors (as could be seen in corrosion kinetics).

2.2 Sources of Green Corrosion Inhibitors

Corrosion, generally, occurs when mild steel comes in contact with oxygen and water. Witte *et* al (2006) reported that the presence of anodic and cathodic sites on steel surface and their reaction with water and oxygen transforms the metal (iron) atom to ions; through a series of chemical reactions, hydrated ferric oxide forms rust (of iron). Another anaerobic corrosion (microbiological corrosion) may occur if conditions favour the growth and multiplication of microbes.

The preliminary steps to reduce, combat or completely eradicate corrosion require the elimination or suppression of such chemical reactions by the use of corrosion inhibitors, pigments, cathodic protection, coatings and so on, providing barrier properties, adhesion between substrate and coating, as well as corrosion reducing activity and overall active anti-corrosion effect. The effectiveness of coatings as potential anti-corrosion agents depends upon their type, the type of substrate, corrodents to which these are exposed and other factors, as reviewed by Witte *et al* (2006). But for efficient service, coatings

should bear very good adhesion to the substrate, resulting in low permeability (to both oxygen and water), as well as good *wet* adhesion.

In this regard, the renewable resources or natural biopolymers (such as lignin, starch, cellulose, cashewnut shell liquid, sucrose, caffeic acid, lactic acid, tannic acid, furan, proteins, glycerol and vegetable oils) contain carboxyls, double bonds, esters, ethers and other functional groups, which impart good adhesion and corrosion resistance performance to the substrate. Also, the performance can be further improved by chemical transformations, use of modifiers (inorganic reinforcements, nanomaterials and other methods. Some of the natural (renewable) biopolymers that could be utilized in corrosion resistance are enumerated below.

2.2.1 Cellulose

Cellulose is one of the largest biopolymer obtained by photosynthesis; this was reported by Grassino *et al* (1999). According to the report, it is a crystalline polysaccharide that is mainly obtained from wood pulp and other plants; it can also be extracted from algae and bacteria for industrial purposes. Its structural formula is shown in Fig.2.2.

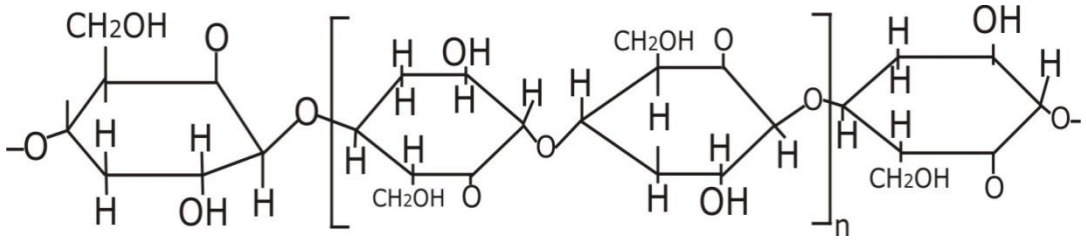

Figure 2.2: Structure of cellulose

In desirable quantities, cellulose may be used as a modifier, rendering toughness in fragile coatings. The primary hydroxyl groups present in the

chain may further facilitate adhesion to the substrate. Hydrophoebically modified hydroxyethl cellulose, used in coatings and paints, has been reported by Krone (1993) to have provided good gloss, leveling and sagging resistance. Also, Liu *et al* (2011) reported that films obtained from regenerated cellulose (from cotton linter) through coating of castor oil polyurethane/benzyl konjac glucomannan semi-interpenetrating polymer networks were observed to be water-resistant and biodegradable.

In various reports (Tarvainena *et al*, 2003; Tamborim *et al*, 2011), ethyl cellulose-based aqueous dispersions and solvent based films were plasticized with *n*-alkenyl succinic anhydrides to overcome the brittleness of cellulose films. From the reports, the films obtained showed excellent mechanical properties, low permeability and good flexibility.

Amoxicillin doped cellulose acetate films showed good corrosion inhibition on *AA2024-T3* substrate, while films doped with 2000ppm of the drug showed good anti-corrosion bahaviour, as observed by elechemical impedance spectroscopy (EIS) results. In contrast to the documentation of Liu *et al* (2011) that prepared cellulose acetate-free films with diethyl phythalate/triethyl citrate as plasticizer, Liu and Williams (2007) indicated a decrease of the electrochemical activity in the doped cellulose acetate films, relative to their undoped counterparts. The later (despite retaining higher content of plasticizer due to suppressed evaporation) provided increased mechanical strength and decreased water vapour permeability of the films. The report further indicated that triethyl acetate films showed increased elongation, decreased tensile strength and elastic modulus, relative to diethyl phythalate films.

2.2.2 Lignin

Lignin is also a very common organic polymer. About 50 million tons of lignin is produced worldwide annually as residue in paper production processes. According to Xu (2012), it consists of methoxylated phenyl propane structures. The biosynthesis of complex structure of lignin is thought to involve the polymerization of three primary monomers/ monolignols (*P*-coumaryl, coniferyl and sinapyl alcohols), which are linked together by different ether and carbon-carbon bonds, forming a 3-dimensional network. The monolignols are present in the form of *p*-hydroxylphenol, guaiacyl and syringyl residues in lignin structure. Lignin is non-toxic, inexpensive and abundantly available; this is contained in the report of Sena- Martins *et al* (2008). Also, Park *et al* (2008) reported that lignin is hydrophoebic, smaller in size and forms stables mixtures. It is used commonly in dispersants for crop protection products, dyes, and for the production of low molecular weight chemicals (like dimethyl sulphide). In various documentations (Stewart, 2008; Park *et al*, 2008; Mulder *et al*, 2011), it was reviewed that lignin could serve as filler in inks, for wood composites, chelating agents, for treating porous materials, as well as in coatings and paintings.

However, the inherent components of lignin (such as hydroxyl, carboxyl, benzyl alcohol, methoxyl, aldehidic and phenolic functional groups) form its fundamentals in corrosion resistance actions. Altwaiq *et al* (2011) observed that lignin, adsorbed on metal surface, is capable of forming a barrier between the metal and corrodents. Extracted alkali lignin, as investigated by Alwaiq *et al* (2011), has shown corrosion inhibition behaviour in the corrosion of different alloys immersed in HCl solutions. This was done by weight loss analysis, surface analysis on the corroded metals (by scanning electron

microscope, SEM) and microbeam X-ray fluorescence (N-XRF). Also, lignin doped conductive polymers (polyanilline) are used in corrosion protection. Sulphonated kraft lignin conductive polymers are more dispersible in water. Electrochemical analysis by Xu (2002) revealed that ligno-PANI (polyaniline) is an effective corrosion inhibitor. A very low loading (1-2%) of the inhibitor brings much reduction (10-20 fold) in corrosion.

Corrosion behaviour of lignosulphonate doped PANI coatings on mild steel in neutral saline conditions (salt spray/immersion) was investigated by Sakhir *et al* (2011) using electron immersion spectrophotometer, potentiodynamic measurements, as well as visual observations, and it was discovered that the coatings with highest PANI performed well both in the salt spray and immersion tests. Fig.2.3 shows the structure of lignin.

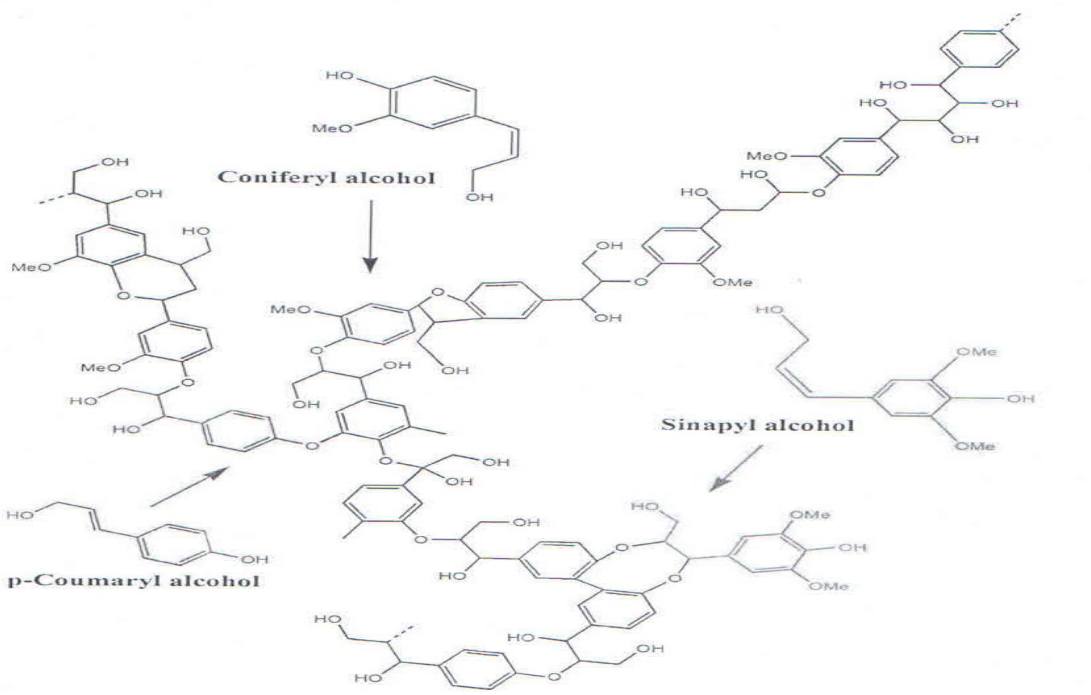

Figure 2.3: Structure of lignin

2.2.3 Tannic acid

Tannic acid (TA) is a commercial form of tannin. It is a polymer of gallic acid molecules and glucose. The pure form of TA is a light, yellowish, amorphous powder. It is contained in roots, husks, galls and leaves of plants. It is also found in bark of trees (oak, walnut, pine, mahogany), in tea, nettle wood, berries and horse chestnut. TA has astringent, antibacterial, antiviral and antienzymatic properties. It is used in tanning of leather, staining wood, as a mordant for cellulose fibres, dyeing cloth, disinfectant cleaners, in pharmaceutical industries, food additives, metal corrosion resistance (as rust convertor), slime treatment of petroleum drilling, paper, ink production and oil industry. TA can be structurally presented as shown in Fig 2.4.

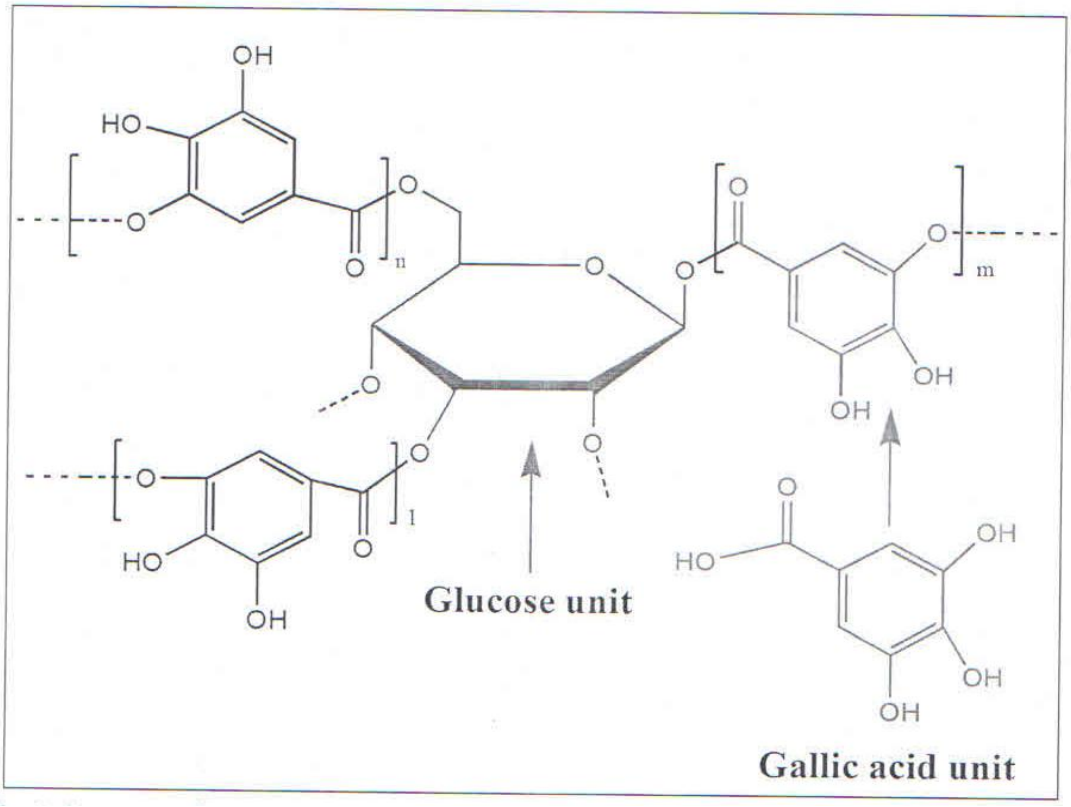

Figure 2.4: Structure of tannic acid

In corrosion resistance, tannic acid has been extensively utilized in anticorrosion methods as investigated via infrared, Mossbauer, Raman spectroscopies, electron immersion spectrophotometer and potentiodynamic measurement in different reviews by varying scholars (Morcillo *et al* 1992; Nasrazadani; 1997; Jaen *et al*, 2011; Al- Mayouf, 1999; Ocampo *et al*, 2004; Galvan Jr *et al*, 2012; Chen *et al*, 2008). The works showed that TA could be used as a conversion coating to prevent corrosion of iron, zinc, copper and their alloys. The (ortho) hydroxyls react with metals, forming metaltanic acid complexes, which protect metal from rusting.

Chen *et al* (2009) reported that TA-based conversion coating can be formed on *AZ91D* magnesium alloy. The study, further, revealed that the formation of organic chromium-free conversion coating on *AZ91D* magnesium alloy from solution containing TA and ammonium metavanadate. The potentiodynamic (PD) measurements revealed that the said coating showed more positive potential and obvious lower corrosion current density relative to traditional chromate conversion coating; salt spray tests also showed an improved anticorrosion behavior of the former.

In another report (Singh and Yadav, 2008), mildly rusted steel surface were pretreated with TA based rust converters, followed by application of a zinc-reach coating. The rust converters reacted with iron and rust, to form a sparingly soluble iron tannate film on the metal surface. This renders low pH adjacent to the corroding interface, by the diffusion of the unreacted acidic constituents of the rust converter in alkaline concrete solution. The low pH facilitated the formation of passive hydrozincite layer within 50hours of exposure to chloride-contaminated concrete pore solution, relative to 150hour for normal zinc coating (without rust converter). The mechanism of film

formation was investigated via electron immersion spectrophotometer (EIS), potential-time studies, raman spectroscopy (RS), scanning electron microscope (SEM), energy dispersive x-ray analysis (EDXA) and x-ray diffraction studies (XRD).

The report further reviewed that methocrylic derivatives of TA (M-digallic acid), toluylene 2,4- diisocyanate (TDI) and 2-hydroxyethyl methacrylate (HEMA) formed UV curable urethane coatings (in molar ratio of 1:3:3). The formation, as documented by Grassino *et al* (1999), occurred by the coupling reaction between TA and TDI, followed by HEMA addition.

2.2.4 Chitosan

Chitin and Chitosan (CHTO) are polysaccharide, and are most often, used interchangeably. They are chemically similar to cellulose, differing only by the presence or absence of nitrogen. Chitosan is a deacetylated chitin (with degree of the deacetylation as 50%), and is obtained from the outer shell of crustaceans (crabs, lobsters, krills and shrimps). Chitosan, primarily, consists of β-linked 2-amino-2-deoxy-β-D-glucopyranose units. CHTO shows biocompatibility, low toxicity, biodegrability, osteoconductivity and antimicrobial properties as could be observed in Figs. 2.5 and 2.6.

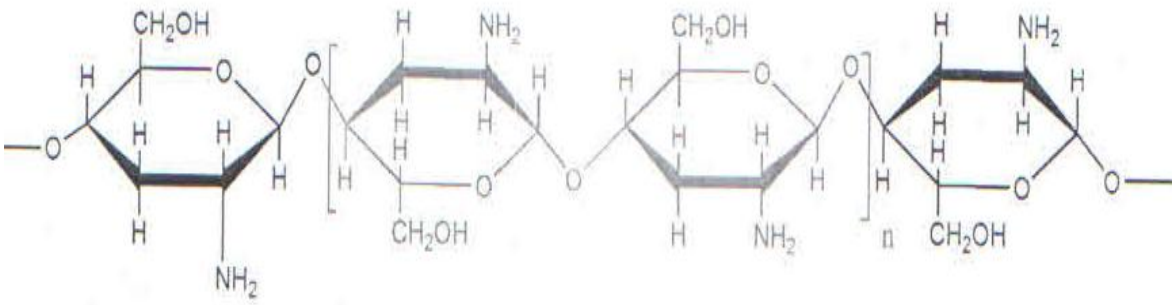

Figure 2.5: Structure of chitosan

According to reports by different scholars (Rinaudo, 2006; Bautista-Banos *et al*, 2006; Lundvall *et al*, 2007), CHTO is a cationic polyelectrolyte, and it forms complexes with metal ions and can gel with polyanions. It contains reactive hydroxyl and amine groups that undergo chemical transformations, producing chemical derivatives with plethora of applications. It is used in cosmetics, as preservative, antioxidant, antimicrobial agent and as coating in foods, fabrics, drugs, artificial organs and fungicides, as metal adsorbents for the removal of metals (such as mercury, copper, chromium, silver, iron and cadmium) from wastewater.

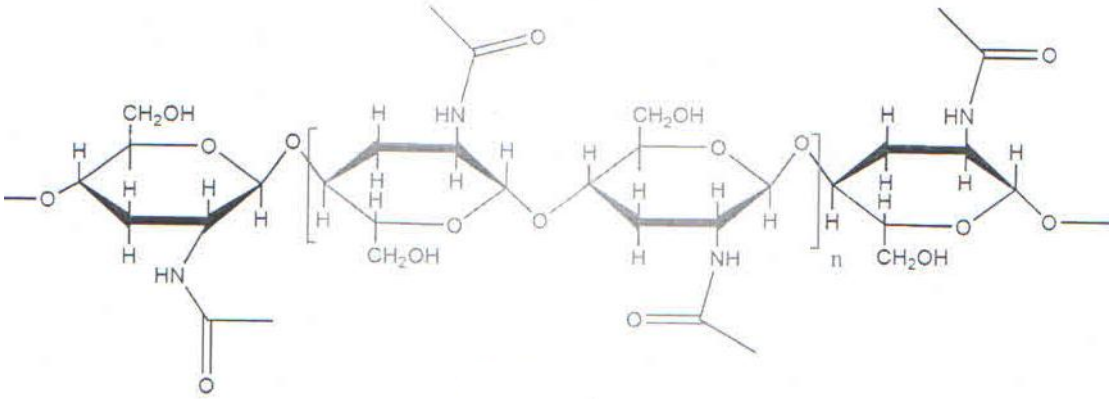

Figure 2.6: Structure of chitin

Considering its corrosion resistance ability, chitosan dissolves in acqueous solution to form tough and flexible films, and is utilized as anti-corrosion

material; this is contained in the report of Lundvall *et al* (2007). However, CHTO was found to absorb moisture from atmosphere, which penetrates the film easily and deteriorates its performance. As a remedial approach to employ the inhibitor as an environmentally green water-based coating system for aluminum substrates, Sugama and Millia-Jemenez (1999) modified CHTO with polyacid electrolyte, polyitaconic acid (PI), containing two negatively charged carboxylic acid groups. In the study, however, increased grafts and crosslinks formed coatings that were less susceptible to moisture and prevented the penetration of corrosive electrolyte species, providing good corrosion protection to the substrate. CHTO was found to be an ideal composition for efficient corrosion protection (at CHTO-PI ratio of 4:1). The study also modified CHTO with corn-starch derived dextrin, and applied it on aluminum (*Al-6063*). Also, Sugama and Duvall (1996) observed that CHTO-dextrin ratio of 7:3 provided low moisture resistance, and could withstand salt spray test up to 720hours. In this case, CHTO shows high hydrophilicity and poor adhesive strength with *Al-2024 T3* alloy.

Various studies (Kumar and Buhheit, 2006; Fekry and Mohamed, 2010; Cheng *et al*, 2007) have reviewed that the derivatives of CHTO (such as acetylthiourea CHTO and carboxymethyl CHTO) are used as efficient corrosion inhibitors through assessments by PD measurements, EIS, SEM, weight loss measurements, conductometric titrations and other related studies. Also, Eram *et al* (2011) documented that hydroxyapatite – CHTO composite coatings on *AZ31* Mg alloy by aerosol deposition produces well adherent corrosion resistant biocompatible coatings.

2.2.5 Starch

As a carbohydrate consisting of a number of glucose units joined together by glycosidic bonds, starch is a low cost, renewable and biodegradable natural polymer. It consists of two types of molecules - amylose (linear) and amylopectin (branched) as indicated in fig. 2.7.

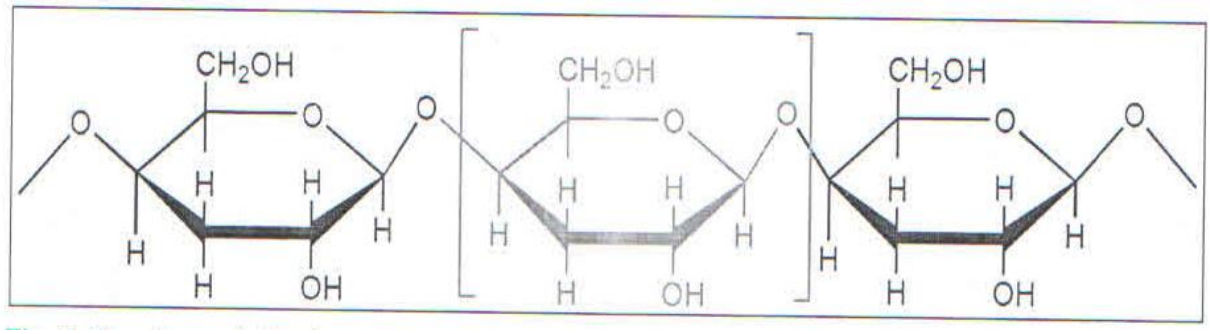

Figure 2.7: Structure of Starch

Starch is the energy store of plants. According to Sugama and DuVall (1996), commercially refined starchy foods include corn-starch, tapioca, wheat and potato starch. Industrial applications are seen in pharmaceuticals, paper-making, textile and in food preparations. Considering its role in corrosion resistance, the report reviewed that starch is widely utilized as a natural corrosion inhibitor; when used at low pH, starch shows low water solubility and poor stability. Thus, for improved performance, certain physical and chemical modifications become necessary. These involve the reactions of their hydroxyl groups with functional groups of the synthetic polymers such as carboxylic acids, anhydrides, epoxides, urethanes, oxazolines and others. Another alternative method is via free-radical ring-opening polymerization occurring between their glucose rings and vinyl monomers.

Sugama and DuVall (1999) demonstrated the preparation of poly-organosiloxane grafted starch coatings for the protection of aluminum from corrosion. The protocol involved the modification of potato starch (PS) with N-[3-(triethoxysilyl) propyl]-4, 5-dihydromidazole, TSPI. The constant threat with the use of PS was active bacterial and fungal growth, which caused the diminution of its corrosion resistance behaviour. TSPI protects the bacterial and fungal growth on PS solution. According to the report, this could be analyzed using SEM technique. The grafting of organosiloxane occurs by the opening of glycosidic rings. The coating properties are investigated by EIS and salt spray tests. PS/TSPI derived coatings display good protection on aluminum against corrosion. In another report, Sugama (1997) attempted to investigate the effects of cerium (IV) ammonium nitrate modified PS as primer coatings for aluminum substrates.

Also Bello *et al* (2010) used modified cassava starch as corrosion inhibitor of carbon steel in an alkaline solution of sodium chloride in contact with air at 25^{o}C; one was cassava starch, modified through gelatinization and activation (GAS) and the other was carboxymethylated starch (CMS) with different degrees of substitution (DS). These were characterized by NMR spectroscopy; estimation of DS was also performed, which was about 0.13$\pm$ 0.03 *($CMS_{0.13}$)* and 0.24$\pm$ 0.04 *($CMS_{0.24}$)*. Electrostatic potential mapping of the repetitive unit of GAS and CMS was based on the model proposed by Politzer and Sjoberg in Bello *et al* (2010). According to the report, corrosion studies were performed by EIS, coupled with a rotating disk electrode with a fixed rotation speed of 1000rpm. The polarization resistance values followed the order: $CMS_{0.13} < CMS_{0.24} <$ GAS. The studies confirmed that starch acts as corrosion inhibitor of carbon steel; the extent of protection against corrosion depended

on the amount and type of active groups present, that is carboxylate (-COO-) and alkoxy (-CO-) groups for CMS, and alkoxy (-CO-) groups or GAS and also on DS.

Rosliza and Nik (2010) studied the corrosion inhibition conferred by tapioca starch (TS) to AA6061 alloy in seawater. During the study, it was found that the weight loss of AAA6061 alloy specimen in the seawater diminished with increasing TS concentration as a result of corrosion deposits. PD results revealed that as the concentration of TS increased, corrosion potential (E_{corr}) values shift to more positive value, corrosion current density (i_{corr}) reduced remarkably, the numerical values of both anodic and cathodic Tafel slopes decreased, polarization resistance (R_P) value of AA6061 alloy increased (that is the higher the R_P value, the lower the corrosion rate), and double layer capacitance value (C_{dl}) decreased. The indication is that anodic and cathodic processes are suppressed by TS that acts as corrosion inhibitor, preferably reacting with Al^{3+} to form a precipitate of salt or complex on the surface of the aluminum substrate. The study maintained that inhibition efficiency (%) values obtained from all measurements viz: gravimetric, PD, linear polarization resistance (LPR) and EIS were in close agreement with other.

Inhibition Efficiency of TS increased with the corrosion inhibitor concentrations (ranging from 200 to 100 ppm). The protection conferred by TS is attributed to the adsorption on the AA6061 alloy surface through all the functional groups present in starch. This is linear amylose constituted by glucose monomer units joined to one another (head-to-tail), forming alpha-1,4 linkage and highly branched amylopeptin with an alpha-1,6 linkage every 24-30 glucose monomer units).

2.2.6 Plant Extracts

Plants, naturally, synthesize chemical compounds in defence against fungi, insects and herbivorous mammals. This is contained in varying reports of Pagella *et al* (2002) and Tangestaniana *et al* (2001). The reports reviewed that some of these phytochemical compounds (such as alkaloids, terpenoids, flavonoids, polyphenols and glycosides) prove beneficial to humans in unique manner for the treatment of several diseases. Extracts from parts of plants (such as roots, stems and leaves) also contain such extraordinary phytochemicials that are used as pesticides, antimicrobials, drugs and herbal medicines.

Plant extracts are extensively used as corrosion inhibitors. An interesting review in this context was compiled by Raja and Sethuraman (2008), who stated that plant extracts contain a variety of organic compounds such as alkaloids, flavonoids, tannins, cellulose and polycyclic compounds. These compounds with hetero-atoms (N, O, S and P) coordinate with (corroding) metal atoms or ions, consequently, forms a protective layer on the metal surface that prevents corrosion. These serve as cheaper, readily available, renewable and environmentally benign alternatives to the costly and hazardous corrosion inhibitors (such as chromates). Plant extracts serve as anti-corrosion agents to various metals such as mild steel, copper, zinc, tin, nickel, aluminum and its alloys. Theses extracts, as documented by various researchers (Zucchi and Omar, 2008; Ostovaria *et al*, 2009; Satapathy *et al*, 2009) include: Swertia angustifolia, Accacia conicianna, Embilica officianilis, Terminalia chebula, Terminalia belivia, Sapindus trifolianus, Pongamia glabra, Eucalyptus leaves, Annona squamosa, Eugenia, Jambolans, Azadirachta indica, Accacia arabica, Vernonia amydalina, Carica papaya,

Rosmarinus officinalis, Hisbiscus subdariffa, Opuntia extracta, Mentha pulegium, Occium viridis, Datura metel, Recinus communis, Chelidonium majus, Papaia, Poinciana pulcherrima, Cassica occidentalis, Datura stramonium seeds, Calotropis procera-B, Azydracta indica, Justicia gendarussa, Artemisia pallens, Auforpio turkiale sap, Black pepper extract, Henna extract.

2.2.7 Vegetable oils

Vegetable oils (simply referred to as VO) are triglycerides of fatty acids, as indicated in Fig. 2.8. They find versatile applications as biofuels, lubricants, adhesive, antimicrobial agents, coatings and paints. The extensive utilization of *VO* in several diverse fields is manifested in their rich double bonds, active methylenes and other features.

Vasconeza *et al* (2009) reported that the functional groups on *VO* backbone may undergo a host of chemical transformations, yielding green polymer derivatives (such as alkyds, epoxies, polyurethanes, polyesters, polyesteramides, polyetheramides and other related/similar compounds), with versatile applications. In terms of corrosion resistance, vegetable oil is among the largest, well-established, non-polluting, non-toxic and biodegradable substances used in coatings and paints since primeval times, particularly in corrosion inhibition. Depending on their iodine value, vegetable oils are classified as non-drying, semi-drying and drying, as indicated by their drying index. Usually, drying vegetable oils are used in coatings and paints; they are film formers, and they have the tendency to form films over the substrate on self-drying basis (that is without the use of any drier).

In drying vegetable oils, drying occurs as a natural phenomenon through auto-oxidation, initiating from the active methylene groups on *VO* backbone; this is contained in the report of Dahamani *et al* (2010). According to the report, the presence of hydroxyls, esters, oxiranes, amides, carbonyl, acrylics, carboxyls and urethanes impacts good adhesion to the substrate due to good elestatic interactions with the metal substrate.

However, since the films are not tough enough to meet the desirable performance characteristics, vegetable oils are chemically transformed into several derivatives as polyesters, alkyds, polyesteramides, polyetheramides, and polyurethans, as indicated in Fig. 2.8. This is basically done in order to meet the stringent environmental conditions. They have, however, been further modified through chemical pathways (including acrylation, vinylation, metallation and so on), for improvement of the drying ability, gloss, scratch hardness, impact resistance, flexibility and corrosion resistance of coatings produced thereof.

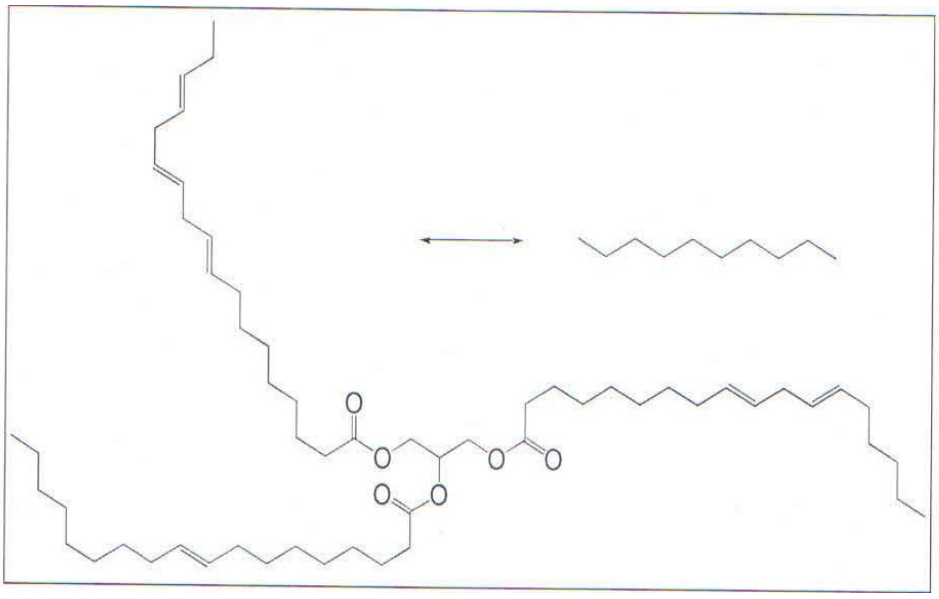

Figure 2.8 Chemical Structure of Vegetable Oil

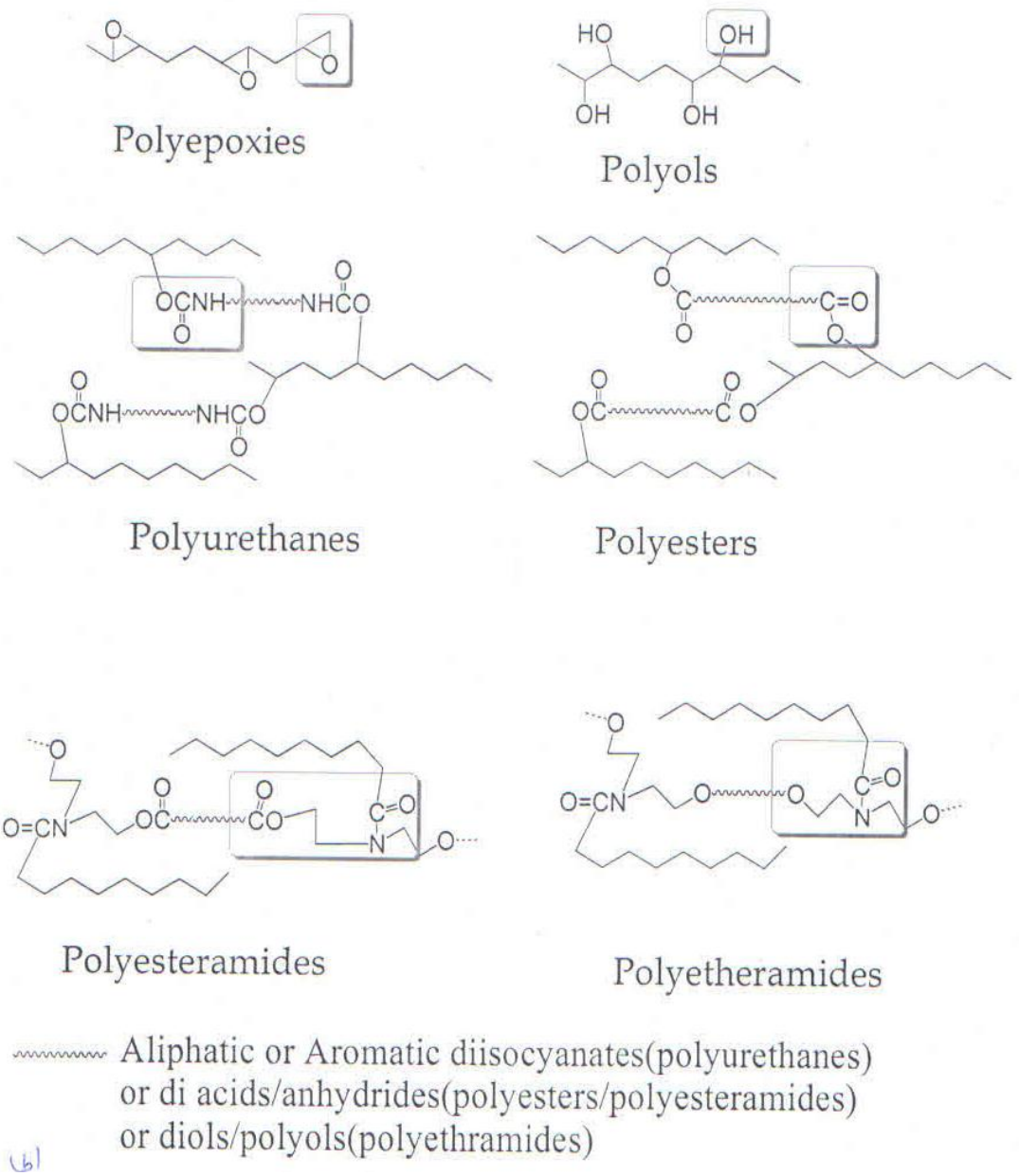

Figure 2.9 VO Derivatives used in corrosion inhibition

Today, the advancements in knowledge, rise of several innovative technologies, human awareness and concerns related to energy consumption and environmental contamination have brought about manifold changes in the world of vegetable oil based coatings and paints. These include VO based low/no solvent coatings, high solid coatings, hyper-branched coatings, WB-coatings, UV-curable, organic-inorganic hybrids and nano-composite

coatings. Aigbodion *et al* (2001, 2003 and 2010) prepared WB-coatings from rubber seed oil, in which *WB*-polyurethanes with dimer fatty acids showed excellent water hydrolytic resistance. Also, Aigbodion and Pillai (2000), Liu *et al* (2011) and Chen *et al* (2011) reviewed that commercially procured acrylate soyabean oil, modified with acrylated sucrose (ACSU) and hyper-branched acrylates (HYAC), was formulated into UV-curable coatings. The addition of ACSU and HYAC improved the adhesion and toughness of coatings respectively. ACSU acted as reactive flexibilizers in coating formulations. ACSU (in an optimum concentration) modified coatings showed good stability in water after immersion for seven days, except for slight haziness in smaller portion of the films.

In another vein, Alam *et al* (2009) reviewed that soy alkyd/PANI conducting coatings showed good scratch hardness (SH), impact resistance (IRt), flexibility (FL) and conductivity due to good adhesion between PANI and metal substrate. While the virgin soy alkyd coating succumbed to corrosion resistance tests in different corrosive media after 2 hours, relatively, soy alkyd/PANI showed higher performance as monitored for a period of 960 hours. Results of the work showed that corrosion rate decreased with increased concentration of PANI, being minimum for the highest PANI loading in alkyd. Minimum corrosion rate of 35 x 10^{-2} *mpy* in 5% HCl, 32 x 10^{-2} mpy in 5% NaOH and 30 x 10^{-2} mpy in 3.5% NaCl were observed for 2.5% - soy alkyd/PANI.

Also, it has been reported metals containing VO coatings have shown anti-microbial behaviour due to the presence of metal either being embedded or incorporated into the matrix. This is contained in the works of Konwar *et al* (2010), which further stated that metal/VO corrosion resistant materials

interact with the microbes by adhering to their surface; the long hydrophobic *VO* chains engulf the microbes, completely cutting off their nutrients, making the cell weak and finally dead. Also, *Mesuea ferra L.* seed oil polyester/clay silver nano-composite coatings have shown antimicrobial behaviour against *Escherichia coli* and *Pseudomonas aeruginosa*.

Again, Zafar *et al* (2006 and 2007) have reported antimicrobial activity of zinc containing linseed polyester-amide coatings. More recently, Sharmin *et al* (2012) investigated the coating properties of copper oxide containing poly (ester urethane) metallohybrids from linseed oil. Castor polyurethane organo-clay composite coatings prepared by Heidarani *et al* (2010) showed good corrosion resistance properties. At 3wt% loading of clay, good corrosion resistance properties could be achieved as determined by PP and EIS. At higher clay loading (>3wt %), the coating material became viscous and the adhesion of the coatings to the substrate deteriorated.

The composites prepared through ultrasonicaton technique did not show any phase separation contrary to their counterparts via mechanical agitation. Zafar *et al* (2011) reported the microwave assisted preparation and characterization of castor oil based zinc containing metallopolyurethane amide coating material. Metallopolyurethane-amide, containing 5% metal showed the best performance (compared with those of lower metal percentages). The coatings showed good SH (3.5kg), IRt (150lb/inch), FL (1/8 in) and gloss (tested by standard methods and techniques). Ahmad *et al* (2012) reported the preparation and corrosion resistance performance of linseed oil based polyurethanefattyamide/tetraoxyorthosilane (TEOS-20, 25, 30 *phr*) based organic-inorganic PULFAS prepared at ambient temperature. *PD* measurements were conducted in HCl (3.5%), NaOH (3.5%), NaCl (5%) and

tap water (Cl^- ion-63mg/l; conductivity-0.953mS/A). Asuquo *et al* (2012a) reported that the lauric and saponification values of vegetable oils play great roll in their industrial applications. According to the report, the lower the saponification value of an oil sample, the lower its lauric acid content. In the determination of rubber seed oil characteristics, Asuquo (2012a) and Asuquo *et al* (2010) observed that the rubber seed is woody (herbaceous) in nature, and as such possess low triglyceride properties.

Salt spray test of PULFAS coatings was carried out in 3.5% NaCl solution; while hybrid coatings could withstand the test for 240hours, the coatings of virgin polyurethaneamide showed loss in weight and gloss after this time period. Arajuo *et al* (2010) investigated the influence of the type of vegetable oil on the barrier properties of alkyd paints, pigmented with zinc phosphate. In the study, they selected linseed and soybean oils as modifiers of alkyd paints. However, the research works on the use of vegetable oils in corrosion resistance are enormous, and numerous innovations in the field have occurred in recent years, and more innovations are still in view.

2.2.8 Biofilms

A biofilm consists of a highly organized bacterial community, with cells entrapped in an extracellular polymer matrix. Various reports (Zuo, 2007; O'Toole *et al*, 2000; Videla and Characklis, 1992) have reviewed that bacteria in biofilms show higher resistance to antibiotics, increased production of exopolysaccharide, morphological changes in cells, different responses to environmental stimuli and distinct gene expression profile. Figure 2.10 is a typical representation of corrosion resistance by biofilm.

However, biofilm formation on metal surfaces may either enhance or hamper corrosion process. Videla and Herrera (2005) and Lopes *et al* (2006) reviewed that the bacterial colonies on metal substrates form anodic (area below thicker colonies, due to more respiration activity and lower energy concentration) and cathodic (areas below thinner colonies, due to less respiration activities and higher oxygen concentration) areas, resulting in the corrosion of metal surface. Often, the corrosion products themselves form a passive layer that may impede corrosion. The overall process (corrosion and/or anti-corrosion) depends upon the type of metal and activity of microbes. Some bacteria may become protective or corrosive, depending upon the pH of the medium.

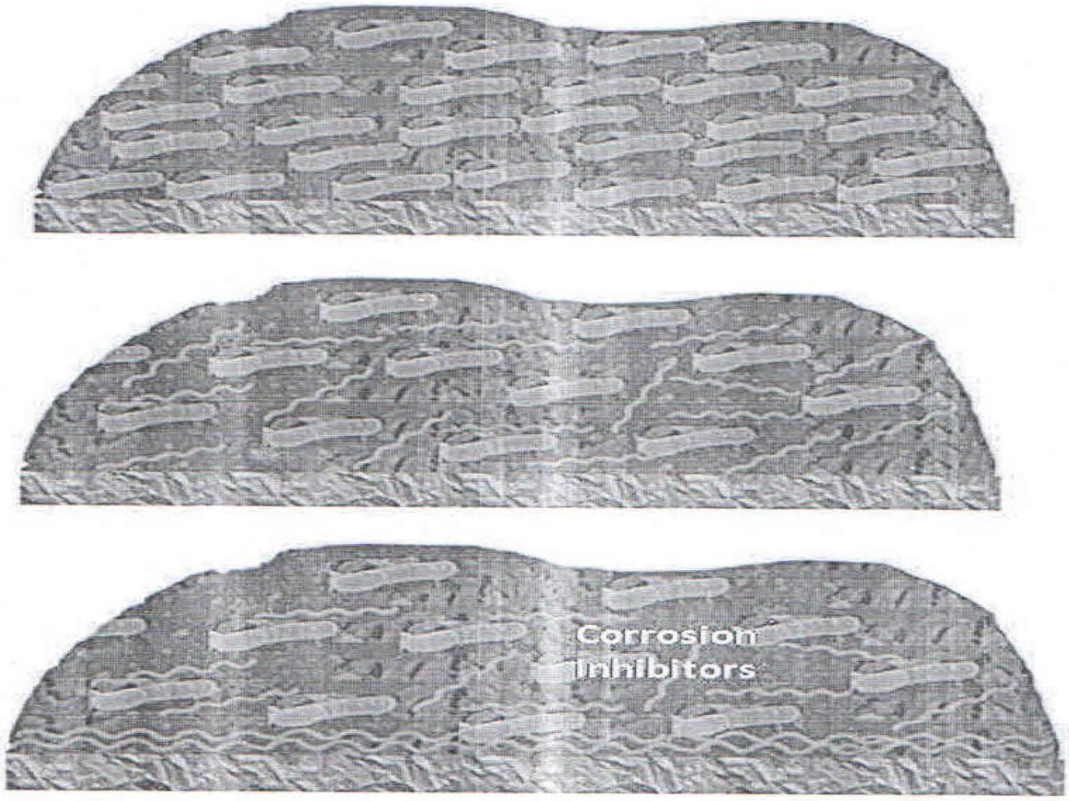

Figure 2.10: Corrosion Resistance by the Formation of Biofilm

The mechanism involves the removal of corrodents (such as oxygen) by aerobic respiration of biofilms, elimination of corrosion-causing bacteria by biofilms generated antimicrobials, biofilm secreted corrosion inhibitors from passive layer, decreasing contact of metal corrodents. Such corrosion inhibiting microbes include *Pseudomonas cichorii, Bacillus mycoides, Bacillus licheniformis*, and several others. The use of biofilms as anti-corrosion agents requires extensive research to be focused mainly on interactions between bacteria within the microbial community and interactions between certain bacteria and metal. This requires the collaboration of microbiologists and corrosion chemists for further fruitful results in the field.

2.2.9 Cashew nut shell liquid (CNSL)

CNSL is obtained as a by-product of the cashew nut industry, mainly containing anardic acid- *80.9%*, cardol- *10-15%*, cardanol, and 2-methyl cardol. The chemical structure of CNSL, as contained in Bierwagen (2011) is represented in Fig. 2.11. The substance occurs as a brown viscous fluid in the shell of cashew nut, a plantation product obtained from the cashew tree- *Anacardium oxidentale*. CNSL modified phenolic resins are suitable for many applications, and they perform improved corrosion and insulation resistance. Considering its corrosion resistance applications, CNSL has excellent combination of functional groups viz: hydroxyls, double bonds, long aliphatic chain and aromatic ring. It can impart good adhesion to coating material due its structural attributes. Aggarwal *et al* (2007) prepared epoxy-cardanol resin based paints from epichlorohydrin, bisphenol-A and cardanol, in the presence of zinc powder, zinc phosphate, micaceous iron oxide and synthetic iron oxide as pigments, fillers, additives and hardener (aromatic polyamine). The coated panels were subjected to immersion test in water (5% NaCl), urea and di-

ammonium phosphate for 180 days and humidity cabinet test at 100% RH at 42-48ºC. The coating showed good SH, adhesion, FL; coatings with micaceous iron oxide showed minimum blistering in immersion and humidity cabinet test. According to Menon *et al* (2002), CNSL can also be used as a modifier for phenolformaldehyde (PF) resin. CNSL-PF modified natural rubber has shown improved physiomechanical performance compared to pure CNSL.

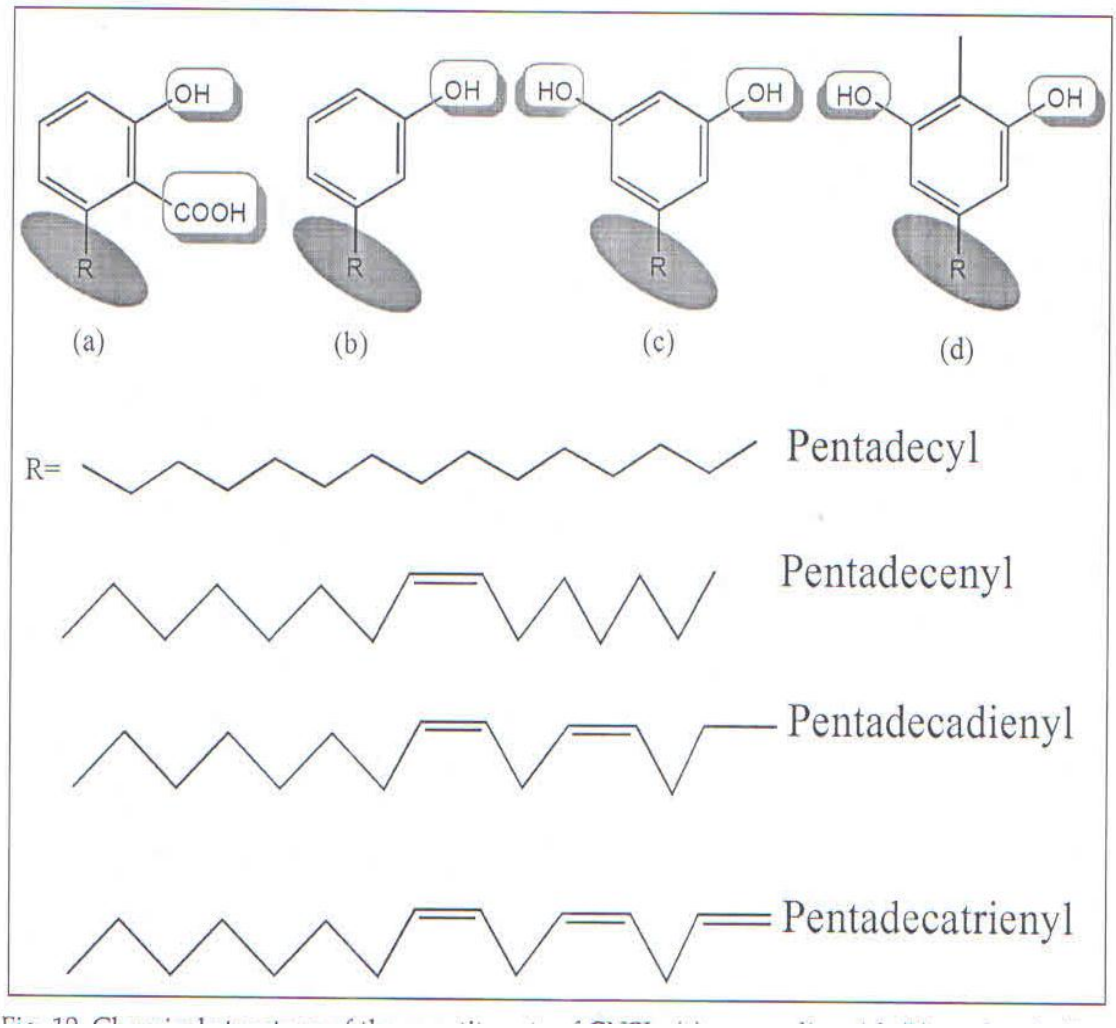

Figure 2.11: Chemical structure of CNSL constituents [(a) anacardic acid; (b) cardanol; (c) cardol; (d) 2-methylcardol

Generally, other examples of renewable resources in corrosion inhibition/control, as reported by Hussain *et al* (2002), Fabbri *et al* (2005), Sugama (1995), Abdallah (2014) and Obot *et al* (2009) include furan, polycaprolactone, glycerol, gums, proteins, pectins and drugs. The role of antibacterial and antifungal drugs (like clotrimazole, fluconazole, cefixime, ampicillin, ampiclox, cloxacillin, tetracycline, methocarbamol, orphnadrine, penicillin G, azithromycin, and others) in corrosion resistance is basically as corrosion inhibitors. Also, the inhibition mechanism is based mainly on adsorption, and is significantly influenced by the presence of the functional groups: -CHO, -N=N, R-OH, steric factors, aromaticity, electron density and molecular weight of inhibitor; this is contained in the works of Naqvi *et al* (2011) and Eddy *et al* (2010). The report further stated that drugs may often compete with green corrosion inhibitors. Similarly, Umoren (2008) and Umoren *et al* (2009) reported that gums (Raphia hookeri gum and gum Arabic) also exert their anticorrosion effect as corrosion inhibitors through the formation of films on metal surfaces via adsorption, thus blocking off the corrodents present in the environment.

In an excellent review by Shchukin and Mchwald (2007), the nanoreservoirs containing active materials (corrosion inhibitors) for self-repairing coatings and surfaces were extensively discussed. According to the study, such an approach can be employed on renewable resources in corrosion. In another review by Athawale and Nimbalkar (2011), they elaborated the use of VO in *WB*-coatings. In another report, Raja and Sethuraman (2008) described the use of plant extracts as natural corrosion inhibitors. The target of corrosion engineers and chemists, beyond the boundaries, is to achieve and come to a

cost effective, environmental friendly, user- friendly and long term solution to the menace of corrosion.

2.3 The Castor Plant *(Ricinus Communis)*

The castor-oil plant is a member of the *Euphorbiaceae* family, which is a kind of perennial woody herbaceous plant. It originated from Egypt, Ethiopia and India. Subsequently, it was spread to Brazil, Thailand, Argentina and United States of America. Belgacem and Gandini (2008) reviewed that the castor tree planted in China came from India, and has a history of more than 1400 years. Castor planting was very universal in China before 1980's, but it was given up gradually in many regions because of the low yield, low benefit, small cultivation scale and difficult selling of previous conventional varieties. Since 1990's, castor yield has increased substantially as the appearing of hybrids has gradually increased the benefits. Some experts, in Athawale and Nimbalkar (2011), predicted that the conventional varieties of the product will wholly be replaced by the hybrids in several years in the future, and the developing trend of the castor industry will be improved varieties, large scale production, high efficiency and industrialization.

In China, the distribution of castor-derived products has no boundaries obviously. Castor is planted in large regions, from southern Hainan island to northan Heilongjiang province. Castor hybrids have many outstanding characteristics such as drought-enduring, barrenness-enduring, saline-alkali-enduring, strong adaptability, simple management, low investment and high economic benefits. In this direction, castor can be planted in fertile farmland, hilly land, mountain slope, saline-alkali soil (even on the edge of the field), as well as around the houses.

Zibo Academy of Agricultural Sciences (*Zibo Brach of Shandong Academy of Agricultural Sciences*) conducted the research of castor crossbreeding firstly in China. In 1984, the plant without male flowers was discovered for the first time and a series of castor gynoecy inbred lines were developed by inducing of agronomic techniques. Using the gynoecy lines as female parent, the Zibo academy bred castor hybrid varieties (Zibo Castor *No.1 - No.9*) in progression, among which 6 varieties passed the evaluation of the Provincial Variety Evaluation Committee (PVEC), and four varieties were released by the National Variety Appraisal Committee (NVAC).

Identification by the experts show that the academy's cross breeding results reached (stand at) the international advance level of similar researches by Solomon (2012) and Derksen (2010). According to the report, zibocastor series hybrids have been popularized to more than 20 provinces and autonomous regions in China, such as Jilin, Neimeng, Xinjiang, Shanxi, Heilongjiang, Hunan, Hubei, Guangxi, Sichuan, Yunnan, Hebei, Henan and Shadong. It, also, extended to more than 10 countries such as Indonesia, Malaysia, Pakistan, Laos, Thailand, Viet Nam, Ethiopia, Nigeria and Netherlands.

2.3.1 The castor oil generation

Castor oil is derived from the seed of *Ricinus communis L.* (the castor plant), which grows in tropical or subtropical regions such as Asia, Tanzania, Brazil and Southern Kazakhstan. It occurs as a perennial or annual plant, and is a drought resistant crop (especially in India). Unfortunately in 1972, economic pressures created circumstances which led to the United States losing its domestic supply of the oil and as such became dependent on foreign countries for supply of both the seed and the oil, as contained in Mutlu and Meier

(2010). According to the report, the U.S. became many years behind in the oil expression technology. However, the expression from the castor seed is done in a similar manner to most other oil seeds. The seeds are collected when ripe, and then opened and discharged. The seeds are cleaned, decorticated, cooked and dried prior to extraction. Cooking is done in order to coagulate the protein, which is necessary to permit efficient extraction, and to free the oil after efficient pressing. After cooking, the material is dried at 100^{o}C, to remove the moisture content of approximately 4 percent.

The first stage of extraction is pre-pressing using high pressure continuous screw press-expeller. The expeller consists of a barrel containing a stainless steel helical screw. The pitch of the screw fights gradually decreases at the discharge end, to increase the pressure on the pulp as it is carried through the barrel. Extracted oil is filtered and collected in a settling tank. The material removed from the oil (called foot) is then fed back into the stream of fresh materials discharged from the press (called cake), which contains 8-10% of the oil. It is crushed into coarse meal, and subjected to solvent extraction using hexane, heptane or any effective solvent. Continuous pressing is used, based on the principle of counter-current of the solvent and oil bearing material. The oil is removed, effectively, as the material comes into contact with increase purer form of the solvent. After extraction, solvent is removed by distillation, and the resulting oil is processed in similar manner as oil from the pressing step.

Once the oil has been expressed from the seed, it is necessary to remove any impurities from the oil that may distort its performance efficiency. The oil is essentially a pure triglyceride, and contains almost 90% of glyceryl tricinoleate and tricinoleic triglyceride that is needed to produce high quality

performance. Some of the important features that characterize the castor oil include high density, viscosity and reactivity, compared to the triglycerides and other similar vegetable oils. These properties are exploited when refining the oil from the impurities. The steps involved in the refining process include settling and degumming, bleaching, neutralization and decolourization of the oil. The settling and degumming (as applied to every crude) is to remove the aqueous phase from the lipid, and to remove phospholipids from the oil. Bleaching removes the colouring materials and also the phospholipids and products due to the absorption of the impurities. Care must be taken in this case because a high acid activation can initiate reaction with the oil, which can cause an undesirable dehydration reaction. Neutralization can be done using alkali (chemical) or steam stripping means. In case of the alkali, caustic soda is mixed in the proper amounts, and the soapstock is removed from the oil, leaving it in a purer form.

Unfortunately, the use of alkali to neutralize the oil results in poor soapstock separation, leading to high neutral oil losses. This is why steam stripping is preferable. Steam stripping is done under vacuum to remove moisture, free fatty acids, odour bodies and other impurities from the oil. Because it is performed under vacuum conditions, the oil can be kept at a low temperature, preserving its chemical structure and not subjecting it to conditions that will warrant undesirable dehydration reactions. Castor oil affords a wide range of reaction in the oleochemical industry, and unique chemicals are derivable from it. These derivates are on par with petrochemical products for use in several industrial applications. In fact, they are considerably superior since they are from renewable sources, biodegradable and eco-friendly.

Castor oil is regarded as one of the most applicable vegetable oils in the field of medicine; it forms clean, light-coloured soap, which dries and hardens well. It is an excellent solvent of pure alkaloid in such solutions of atropin, cocaine, and so on, as are used in ophthalmic surgery. It could also be dropped into the eyes to remove after-irritation caused by the removal of foreign bodies. The oil also finds increasing uses in the industrial applications such as in the manufacture of artificial leather used in upholstery, and also furnishes the colouring for butter; this was reported by Micha et al (2006). The report went further to state that the oil is an essential component in artificial rubber-making, in various descriptions of celluloid, and in making of certain waterproof preparations, as well as in the manufacture of transparent soaps.

2.3.2 The composition and benefits of castor seed oil

Castor oil is a vegetable oil obtained by pressing the seeds of the castor oil plant. The oil is a colourless-to-very pale yellow liquid, with a distinct taste and odour once first digested. It is a triglyceride in which approximately 90 percent of fatty acid chains are ricinoleates. It is a monounsaturated, 18-carbon fatty acid. Among all the fatty acids, ricinoleic acid is unusual, in that it has a hydroxyl functional group on the 12th carbon. This functional group causes ricinoleic acid (and castor oil) to be more polar than most fats. Because of its ricinoleic acid content, castor oil is a valuable chemical in feedstock, commanding a higher price than other seed oils. Thomas (2005) and Fromtling (1988) reorted that castor oil, over the century, was a stuff of nightmares for many children, and there were sufficient reasons for this. It was extensively used as a purgative, and most peculiarly, as a medicine for almost all ailments in both children and adults. The idea behind such a treatment was that malfunctions in the stomach were the root of all other

diseases/problems. So, whenever you have a problem, you need a thorough cleansing of your digestive system, and the problem would disappear.

Castor seed oil has a number of benefits to humanity, but these benefits are significantly felt through its health and industrial usages. The health benefits, as documented by Wilson *et al* (1998), include the following:

(a) Rheumatism**:** The Ricinoleic Acid, Oleic Acid, Linoleic

Acid and other fatty acids found in castor oil are very effective in the treatment of rheumatism, arthritis and gout. They easily penetrate the skin, and can be mixed with other medicines (for rheumatism) to facilitate their penetration power and to enhance the effects.

(b) Birth Control**:** Castor seed oil contains a toxin called ricin (a protein) which, if administered in very low dosages, acts as a germicidal substance. Due to this property, it is also used as a spermicide in spermicidal gels and lotions. If administered to pregnant women in high dosages, it may cause abortions.

(c) Menstrual Disorders**:** Ricinoleic acid, present in castor seed oil, is naturally emmenagogue and helps to open menstruation in cases of delayed painful or obstructed menstruation. It also helps to relieve pain during the menstrual period.

(d) Skin Care**:** Castor seed oil contains undecylenic acid, which (due to its germicidal and disinfectant properties) is useful for treating skin ulcers, particularly those that are caused by bacterial or fungal infections.

(e) Constipation**:** Castor oil most widely used as a laxative (and/or purgative). It is, thus, a very effective treatment for constipation, even at extreme cases where bulk laxatives do not work.

(f) Lactation**:** Most of the substances, which are considered as emmenagogues, also are galactagogues in nature. This means that they stimulate the secretion of milk; castor oil does this as well. Apart from easing and enhancing milk flow, castor oil also increase the quantity of milk due to the presence of fatty acids in the oil. However, its compressed form only should be taken in low doses to avoid any adverse effect on the infant.

(g) Hair Care**:** The germicidal, insecticidal and fungicidal properties of Ricin and Ricinoleic acid that is present in castor oil protects the scalp and hair from microbial and fungal infections, the two prime causes of hair loss. In addition to this, the fatty acids in the oil nourish hair and prevent the scalp from drying through moisture retention powers.

On the other hand, the industrial benefits of castor seed oil, as reported by Wilson *et al* (1998) include the following;

(a) Food and Preservative**:** In the food industry, castor oil (food grade) is used in food additives, flavourings and candy (such as polyglycerol polyricinoleate in chocolate). It is also used as a mold inhibitor, and in packaging; polyoxyethylated castor oil is also used in the food processing industries (Busso and Castro-Prado, 2004).

(b) Medicine and Pharmaceuticals**:** The United States Food and Drug Administration (FDA) has categorized castor oil as "generally recognized as safe and effective" GRASE for over-the-counter use as a laxative, with its

major action sited on the small intestine where it is digested into ricinoleic acid. Therapeutically, several researches (Kelly *et al*, 2013; Zhang and Wu, 2001; Marmion *et al*, 2010) have proven that modern drugs are rarely given in a pure chemical state; so most active ingredients are combined with excipients or additives. Castor oil, or a castor oil derivative (such as Kolliphor-EL, that is polyethoxylated castor oil- a nonionic surfactant) is added to many modern drugs including miconazole (an antifungal agent), paclitaxel (a mitotic inhibitor used in cancer chemotherapy), sandimmune (cyclosporine injection USP- an immunosuppressant drug widely used in connection with organ transplant to reduce the activity of the patients immune system), nelifinavir mesylate (a HIV protease inhibitor), tacrolimus (an immunosuppressive drug), xenaderm ointment (a topical treatment for skin ulcers) and so on.

(c) Coatings**:** Castor oil is used as bio-based polyol in the polyurethane industry. The average functionality (number of hydroxyl groups per triglyceride molecule) of castor oil is 2.7; so it is widely used as rigid polyol and coating (Thomas, 2011). Also, castor oil is not a drying oil, meaning that it has a low reactivity toward air, compared to other oils (such as linseed and tung oils). Dehydration of castor oil gives linoleic acids, which have drying properties (Mohammed *et al*, 2015; Mutlu and Meier, 2010).

(d) Precursor to Industrial Chemicals: Castor oil can be broken down into other chemicals that have numerous applications, as reviewed by Beitz, (2005) and Ogunniyi (2006). Also, Kelly *et al* (2013) reported that transesterification, followed by steam cracking gives undecylenic acid, a precursor to specialized polymer nylon. Breakdown of castor oil in strong base gives 2-octanol, both a fragrance component and a specialized solvent. Hydrogenation of castor oil saturates the alkenes, giving rise to a waxy lubricant. The production of

lithium grease consumes a significant amount of castor oil. Brady *et al* (2007) has it that hydrogenation and saponification of castor oil yields 1,2-hydroxystearic acid, which is then reacted with lithium hydroxide or lithium carbonate to give high performance lubricant grease. Since it has a relatively high dielectric constant (of 4.7), highly refined and dried castor oil is sometimes used as a dielectric fluid within high performance, high voltage capacitors.

(e) Lubrication**:** Vegetable oils (like castor oil) are typically unattractive alternatives to petroleum-derived lubricants, because of their poor oxidative stability. Castor oil has better low-temperature viscosity properties and high-temperature lubrication ability than most vegetable oils, making it useful as a lubricant in jet, diesel and racing engines. McGuire (2012) stated that the viscosity of castor oil, at 10^{o}C, is 2,420 Centipoise. However, castor oil tends to form gums in a short time, and thus its usefulness is limited to engines that are regularly rebuilt (such as racing engines). The lubricants company, *Castrol* took its name from castor oil. Castor oil has, also, been suggested as a lubricant for bicycle pumps, as it does not degrade natural rubber seal. Castor oil was the preferred lubricant for rotary engines, such as the Gnome engine after that engine's widespread adoption for aviation in Europe in 1909. It was used, in rotary engine allied aircraft in World War I, almost universally. Germany had to make do with inferior *ersatz oil* its rotary engines, which resulted in poor reliability (Guilmartin, 1994; Fisher, 2009; US Tariff Commission, 2011). The methanol-fueled two-cycle glow plug engines used for aero-modeling, since their adoption by model airplane hobbyists in the 1940s, have used varying percentages of castor oil as their lubricant. Gummy residues can, still, be a problem for aero-modeling power-plants, lubricated

with castor oil, even though an eventual replacement of ball bearings is required when the residue accumulates within the engine's bearing races. Also, Older (2000) reported that Turkey red oil (a sulphonated castor oil) is made by adding sulfuric acid to vegetable oils, most notably castor oil.

(f) Biodiesel**:** Castor oil, like other currently less expensive vegetable oils, can be used as feedstock in the production of biodiesel. The resulting fuel, according to Wood (2001) and Boel *et al* (2009), is superior for cold winters, because of its exceptionally low cloud and pour points. Initiatives to grow more castors for energy production, in preference to other oil crops, are motivated by social considerations.

2.4 The Rubber Plant (*Hevea Brasiliensis*)

Natural rubber, also called India rubber, (as initially produced) consists of polymers of the organic compound called isoprene, with minor impurities of other organic compounds plus water. It has vegetable origin, and is created by enzymatic process in many plants; these are contained in the works of Kang *et al* (2000), Xie *et al* (2008) and Heinz-Hermman (2008). The rubber seed (from which the rubber seed oil is derived) is industrially achieved from the rubber tree-*Hevea Brasiliensis*, belonging to the Euphorbiacea family. It is grown in a plantation way in warm (average monthly temperature of 25-28^{o}C) and humid (about 80% humidity) climate of South-Eastern Asia (Malaysia, India, China, Sri Lanka and Vietnam), in Western Africa (Nigeria and Cambodia) and in Northern part of South America (Brazil and Guatemala).

Koyama and Steinbuchel (2011) reported that annual production of rubber is presently varying around 3000-3500kg per 1ha, and it depends on weather, soil quality, used stimulation means, age of the trees and other external factors. The first source of rubber is sucrose that is created from carbon oxides

and water during photosynthesis process. In the first biosynthesis stage, the acetyl-coenzyme is created from it, and this is changed into iso-pentyl-pyrophoshate through mevalone acid, and the rubber (in form of latex) is generated by polymerization. The rubber is achieved from it by means of coagulation.

At the ends of its macromolecules, there may be bonds of non-isoprene structural units, mainly proteins, amino acids and phospholipids, in macromolecules backbone (that may be epoxides, ester, aldehyde and lactone groups). Also, part of non-rubber additives that are present in latex is remaining in the rubber. Though their contents may differ, they generally vary just within the range of 5-10% (Kang *et al*, 2000). Even in small amount of these contents in the rubber, they have significant influence on its properties, and they represent one reason of different properties of natural rubber and its synthetic equivalence (IR). A typical chemical structure of poly-cis-1.4 isoprene is represented in fig. 2.12.

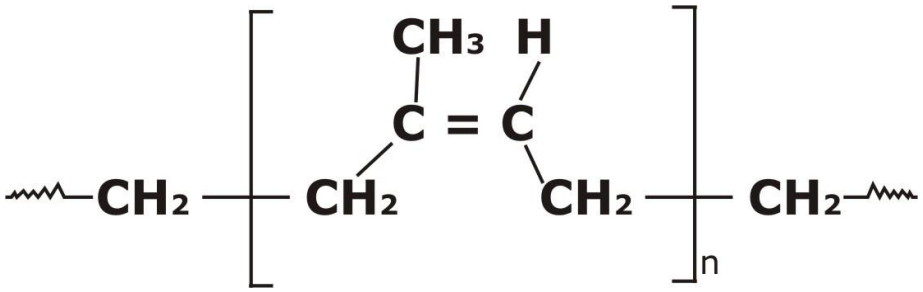

Figure 2.12: Poly-Cis-1.4-isoprene structure

Natural rubber from fresh latex that is immediately dried-out after coagulation contains small portion of gel too. Gel-rubber has higher nitrogen and mineral contents in comparison with sol-rubber, which leads to the vision that rubber

chains are more branched in gel-rubber, and they are mutually connected with proteins through hydrogen bridges.

This assumption is approved also by discovery that the content of gel-rubber in deproteinized rubber is much lower. Rook (1995) reported that average amount of side branches per one rubber macromolecule is varying approximately between 1 and 6, and it is higher in macromolecules with higher molecular weight, compared to those of low molecular weight. The report also revealed that accompaniment of the natural rubber storing is the gradual increase of its viscosity that is externally shown by its hardening. The reason for this phenomenon is not well known, but it is accredited to cross-linking reactions of non-rubber groups present in its macromolecules. Natural rubber belongs to highly non-saturated rubbers as a result the double bond contained in the structural units (as could be observed in Fig. 2.12). Also, reactive α-methylene hydrogens are related with its presence.

Both types of these functional groups may take part in different addition or substitution polymeranalogical reactions that can run also as parallel reactions (e.g. during hydrogenation). They are utilized for chemical modification of the rubber itself, as well as for its vulcanization. In general, natural rubbers are vulcanized by means of sulfur systems, even though other vulcanizing agents (such as phenol formaldehyde resins, urethanes, peroxides, and so on) could be used. Ozone and oxygen react very easily with natural rubber functional group, which causes its very low aging resistance.

2.4.1 Rubber seed oil

Rubber seed, from which the rubber seed oil is extracted, is obtained in high yield as a by-product of *Hevea brasiliensis*, cultivated primarily for its latex

Various reports by Aigbodion *et al* (2003), Kim (1994) and George *et al*, (2014) have stated that rubber seed is abundant in Nigeria, and is found to contain 42% of the oil. However, Aigbodion and Pillai (2007) reported that rubber seed is a rich source of oil that is comparable in quality to dry oils, even though its yield (with n-hexane) is relatively not high. Also, Patel *et al* (2010) and Okieimen and Okieimen (2000) reported that the industrial value of vegetable oils generally depends on their constituents' fatty acids and the ease at which it can be modified or combined with other chemicals.

Several physical and chemical modifications of rubber seed oil, to enhance its initial quality, have been evolved over the years. Examples of such modification techniques include acrylation, catalytic and thermocatalytic polymerization, inter-esterification and epoxidation, as documented in a number of research works (Ebelewe *et* al, 2010; Pryde and Rothfus, 2011; Solomon, 2012; Akintayo and Adebowale, 2004; Trumbo *et al*, 2001; Athawale and Joshi, 2012; Zhong *et al*, 2001). Chemical transformation of vegetable oil to fatty acid alkyl ester (trans-esterification) is one of the methods of modifying the quality of vegetable oils. Raw vegetable oils are composed of glycerol, esters of fatty acids and various amounts of solubilized impurities, such as pigments, vitamins, sterols, phospholipids and so on. These impurities may compromise the quality of the finished alkyde resins. Bun *et al* (2006) reported that rubber seeds can be used to feed livestock in many manufacturing areas (such as Cambodia). Undiandeye *et al* (2014) reviewed that phytochemical properties of an oil sample (such as flavonoid, phenol, cardiac glycosides and saponin) are responsible for its corrosion inhibition properties. But in spite of these industrial importance, rubber seeds contain cyanogenic glycosides, which will release prussic acid in the presence

of enzymes or in slightly acidic conditions, as contained in Mallika *et al* (1991) and Jumat *et al* (2012).

Rubber seed oil is also of commercial importance. Uzu *et al* (1985) and Thomas *et al* (1998) reviewed that rubber seed has, in the past, largely been allowed to waste, with very small quantity used for raising root stock seedlings for propagation purposes. The useful properties of the rubber seed oil make it similar to well-known linseed and soyabean oil; this is contained in Anon (2009), Aigbodion (1994) and Achmad, *et al* (2012). Yordanov and Petkov (2008a) reported that rubber seed oils represent an embodiment of carbonyl attachment to its ester linkage, as contained in rubber seed oil, also, could be used for the paint industry as semi-drying oil, in the manufacturing of soap, for production of linoleum and alkyd resin. It could also serve as core binder for factice preparation, and the cake left after extraction of the oil could be used in fertilizer preparation and as feed for cattle and poultry (Anon, 1950; Vimal, 2010). Sakhri *et al* (2011), also, documented that rubber seed oil has been, recently, widely utilized for inhibition of metallic corrosion through varying applications.

2.5 Basis for Corrosion Measurements

The mixed potential theory consists of two simple hypotheses. The first hypothesis states that any electrochemical reaction can be divided into two or more partial oxidation and reduction (redox) reactions; the second is that there can be no net accumulation of electric charge during an electrochemical reaction. The second hypothesis is a restatement of the law of conservation of charge. It follows that during the corrosion of an electrically isolated metal sample, the total rate of oxidation must be equal to the total rate of reduction. Corrosion involves the destructive attack of metal material by chemical or

electrochemical reaction with its environment. Usually, corrosion consists of a set of redox reactions that are electrochemical in nature. The metal is oxidized to corrosion products at anodic sites as shown in equation (2.1).

$$M \rightleftharpoons M^{2+} + 2e^{-} \qquad (2.1)$$

and hydrogen is reduced at the cathodic sites (in acidic medium), as shown in equation (2.2).

$$2H^{+} + 2e^{-} \rightleftharpoons H_2 \qquad (2.2)$$

Because of the electrochemical nature of most corrosion processes, electrochemical methods are useful tools for studying corrosion. More specifically, electrochemical techniques can be used to measure the kinetics of electrochemical processes (such as corrosion rates) in specific environment, and also to measure and control the oxidizing power of the environment. Undiandeye *et al* (2011) and Ostovari (2009), also revealed that increase in temterature of corrosion reaction leads to increase in entropy, as well the heat change of the reaction.

2.5.1 Calculation of corrosion rate from the corrosion current

According to Faraday's law, as contained in equation (2.3),

$$Q = \frac{nFW}{M} \qquad (2.3)$$

Where:

Q = Charge passed (coulombs)

N = Number of electrons involved in the electrochemical reaction

W = Weight of electroactive species (gr)

M = Molecular weight (gr)

Then, *'W'* can be obtained as shown in equation (2.4).

$$W = \frac{QM}{\mathrm{nF}} \qquad (2.4)$$

The utilization of mixed-potential theory can be best demonstrated by considering mixed electrodes. A mixed electrode is a metal sample that is in contact with two or more oxidation-reduction systems. For instance, in the case when zinc is immersed in hydrochloride acid, the metal is rapidly corroded, and the electrochemical reactions are very pertinent. If zinc electrode is considered (in equilibrium with its ions), it would be represented by a reversible potential, corresponding to the zinc-zinc-ion electrode reaction and a corresponding exchange current density. This new potential is achieved when the second hypothesis of the mixed-potential theory is satisfied, that is the total rate of oxidation must be equal to the total rate of reduction. At the point of intersection of the total rates of oxidation and reduction, the rate of zinc dissolution is equal to the rate of hydrogen evolution (expressed in terms of current density).

2.5.2 Potentiodynamic polarization measurements

The potentiodynamic polarization technique is generally used to produce a qualitative picture or fingerprint of a substance in a given solution. It, also, detects important information such as the potential region over which the specimen remains passive, the corrosion rate in the passive region and the ability of the material to spontaneously passivate in the particular medium. The corrosion of the material begins in a particular region, in which the applied potential is made more positive.

This, subsequently, initiates the passivation process. Various works (Dhoke and Khanna, 2009; Behzadnasab et al, 2011; Alam and Al-Aandis, 2012;

Zafar *et al*, 2004; Alam *et al*, 2013) have shown that passivation is probable due to the formation of a film on the surface of the metal. This point is characterized by two values - the primary passive potential (E_{pp}) and the critical current density (i_o). In a third region, the current decreases rapidly as the passivating film forms on the specimen. Finally, the passivating film begins to break down in the region where the oxygen evolution starts to occur (the transpassive region).

When the anodic current is interrupted, passivity decays within a short time in a specific pattern. Ahmad *et al* (2012) reported that if the displacement in $\mathbf{E_{corr}}$ is greater than 85mV, the inhibitor could be classified as being anodic or cathodic, and if the displacement is less than 85mV, the inhibitor is seen as a mixed type. The potential first changes quickly to a value still noble on the hydrogen scale, and then changes slowly for a matter of seconds to several minutes.

2.6 Summary of Previous Work and the Research Gap

The findings of previous works, related to the present study and the limitations are presented in Table 2.1.

Table 2.1: Summary of findings and limitations of previous works

Author (s)	Title of work	Finding	Limitation
Aigbodion and Pillai (2007)	Preparation, analysis and applications of rubber seed oil and its derivatives in surface coatings	Rubber seed oil and its derivative, such as esterified rubber seed oil were found to mitigate corrosion in metal surfaces	Normal hexane was used for the extraction of oil; the oil yield was found to be low
Eddy and Odoemelam (2008)	Inhibition of the corrosion of mildsteel in acidic medium by penicillin-V potassium	Effect of temperature increases the degree of randomness in adsorbed molecular layer	The inhibitor used was synthetic, not green; and the study was in static system, not flow system.
Udiandeye, *et al* (2011)	Investigation of the use of ethyl esters of castor seed oil and rubber Seed	Inhibitors were able to inhibit mildsteel corrosion; inhibition efficiency	The oils were purchased (not extracted for the research purpose, and were of unknown

	oil as corrosion inhibitors	increases with increase in inhibitor concentration	phytochemical properties; study considered inhibition in static system only (not flow)
Hui, *et al* (2013)	Corrosion inhibition of mildsteel by aloes extract in HCl solution medium	Inhibition efficiency decreases with increase in temperature, and the adsorption process obeys Langmuir isotherm	The mildsteel used was a surface platform (not pipe), and the system is static (not flow)
Eddy *et al* (2010)	Fluoroquinolones as corrosion inhibitors for mildsteel in acidic medium- experimental and theoretical studies	Inhibitor was able to inhibit mildsteel corrosion at lower temperature and specific concentration.	Study used synthetic inhibitors (not green sources); considered one concentration condition, in a static system
Mohammed *et al* (2015)	Development of castor oil based Poly (urethane-esteramide) /TiO_2 nanocomposites as anticorrosive and antimicrobial coatings	Refined castor oil possessed anticorrosive properties for mildsteel corrosion control	Data fitness to adsorption models was not tested; basic inhibition properties of the inhibitor were not assessed
Satapathy *et al* (2009)	corrosion inhibition by justicia gendarussa plant extract in hydrochloric acid solution	Inhibition of up to 93% was achieved with the study sample	The study employed only Langmuir isotherm for assessment of data fitness, and the study considered static sytaem, not flow.
Ostovari *et al* (2009)	Corrosion inhibition of mildsteel in 1M HCl solution by henna extract: A comparative study of the inhibition by henna and its constituents (lawsone, gallic acid, a-D-glucose and tannic acid)	Polarization measurements gave up to 92.06% inhibition efficiency	FTIR technique was not assessed, to determine the active homologous series in the study samples.
Asuquo *et al* (2012)	Extraction and characterization of rubber seed oil	Low yield (< 10%) of the rubber seed oil was witnessed	Better choice of solvent (such as organic solvent) was not employed
Eddy *et al* (2008)	Ethanol extract of musa acuminate peel as an eco-friendly inhibitor for the corrosion of mild steel in H_2SO_4	Extract was able to 35.4% inhibition efficiency in the acidic medium	Oil sample was not refined for better performance; and mildsteel was in plate, not pipe.
Bello *et al* (2010)	Modified cassava starches as corrosion inhibitors of carbon steel: An electrochemical and morphological approach	Sample was identified as possessing the capacity to inhibit mildsteel corrosion.	Study sample was assessed using results of SEM images, wiyhout considering the homologous series that play important role in the inhibition process
Nwabanne and Okafor (2012)	Adsorption and thermodynamics study	The extract was found	Again, the system was

	of the inhibition of corrosion of mildsteel in H_2SO_4 medium using *vernonia amygdalina*	to be a good inhibitor of mildsteel corrosion in H_2SO_4 medium; inhibition efficiency of 38.59% was achieved.	static, not flow. Only gravimetric aspect of the stuady was considered.
Eddy *et al* (2009)	Inhibitive, adsorption and synergistic studies on ethanol extract of *gnetum africana* as green corrosion inhibitor for mild steel in H_2SO_4	Extract was found to possess milsteel corrosion inhibition properties	Investigation was done in static system, not flow system.
Obot *et al* (2009)	Inhibitive properties of clotrimazole for aluminium corrosion in hydrochloric acid	Inhibition efficiency was foun to increase with increase in concentration, but decreased with rise in temtearture	Initial characteristics of the study sample were not assessed, and the inhibitor was of synthetic origin.
Jiali *et al* (2013)	Environmental friendly inhibitor for mildsteel by *artemisia halodendron*	Study sample was found to be devoid of toxins and by-products that could harmful to the environment	Phytochemistry of the sample was not studied, and the study was in a static system.
Naqvi *et al* (2011)	Cefixime: A drug as efficient corrosion inhibitor for mild steel in acidic media-electrochemical and thermodynamic studies	Cefixime was found to be a good inhibitor of mildsteel corrosion in acid medium; inhibition efficiency of 37% was achieved in the study.	The study considered static system, not flow. The stuady did not also assess the process using isotherm (kinetic) models.
Okafor *et al* (2010)	*Azadirachta indica* etract as corrosion inhibitor for mildsteel in acid medium	Extracts of leave, root and seed of *A.indica* were found to inhibit metallic corrosion.	Only one model (Freunlich) was tested for data fitness.

A number of research works, such as contained in table 2.1, have been conducted in the study area of corrosion science and its applications. Vegetable oils and other notable agents have continuously made substantive impacts in the inhibition of mildsteel corrosion, as well as those of other corrodible materials. However, almost (if not) all the studies reviewed considered static systems, and this has left a large gap in the assessment of what the corrosion situations would be in flow systems (such as flow pipes). The present study considered a flow system for a better appreciation of the corrosion inhibition process. Also, amongst the works reviewed that considered the use of rubber seed oil as inhibitor, only a few number (such as Aigbodion and Pillai, 2007) tried to extract the oil from the seed using the normal hexane; this, as usual, yielded very low, possibly due to the herbaceous nature of the seed. But this work would seek to try an alternative solvent (petroleum ether) for a possible better yield.

CHAPTER THREE

MATERIALS AND METHODS

3.1 Materials

The materials used in this study include the following:

(i) Castor seed (bought at Ekwulobia market, Aguata)

(ii) Rubber seed (acquired from the Imo rubber estate, Ohaji)

(iii) Mildsteel pipe (97.6% Fe, 0.26% C, 1.03% Mn)

(iv) Thermostat waterbath (model: *TT-6*)

(v) Plastic container (bought at Owerri main market)

(vi) pH meter (model: *PHS-3C*)

(vii) Dozing pump (model: *JM-15774-C07*)

(viii) Viscometer (model: *NDJ-5S*)

(ix) Beakers/conical flasks (100ml, 200ml, 250ml, 500ml and 1000ml)

(x) Analytical weighing balance (model: *FA-2104*)

(xi) Pipette

(xii) Glass stopper

(xiii) Graduated cylinder

(xiv) Burette

(xv) Glass rod

(xvi) Mechanical press (locally made)

(xvii) Soxhlet extractor

(xviii) Heating mantle

(xix) Centrifuge

(xx) Constant-temperature stirrer

(xxi) 263-Potentiostat/galvanostat workstation

(xxii) Gravite rod

(xxiii) Saturated calomel electrode

(xxix) XL-30 FEG scanning electron microscope

(xxx) FTIR spectrophotometer (IR-560 model)

(xxxi) 99% n-hexane (industrial grade)

(xxxii) Petroleum ether

(xxxiii) Acetic acid

(xxxiv) Chloroform

(xxxv) De-ionized water

(xxxvi) Potassium iodide

(xxxvii) Sodium thiosulfate

(xxxviii) Starch indicator

(xxxix) 98% diethyl ether (with 2% ethanol)

(xL) Ethanol

(xLi) Phenolphthalein

(xLii) Potassium hydroxide

(xLiii) Hydrochloric acid

(xLiv) Carbon tetrachloride

(xLv) Dam's reagent (Wig's iodine)

(xLvi) Potassium mecuric iodide (Dragendroff's reagent)

(xLvii) Olive oil

(xLviii) Ammonia (NH_3) solution

(xLix) Methyl red indicator

(L) Tetraoxosulphate (vi) acid

(Li) Ammonium hydroxide (NH_4OH) solution

(Lii) Aqueous methanol

(Liii) Sodium hydroxide

(Liv) Pentanol

(Lv) Ethanoic acid

(Lvi) Methanol

(Lvii) Dinitro salicylic acid (DNS)

(Lviii) Ammonium thiocyanate solution

(Lix) Calcium chloride ($CaCl_2$) solution

(LX) Potassium permanganate ($KMnO_4$) solution

(LXi) Anti-bumping chips

(Lxii) Potassium bromide

3.2 Methods

3.2.1 Preparation of the Castor Seed Oil

The castor seeds, from which the oil sample was extracted, were bought at a local market in Ekwulobia-Aguata in Anambra State of Nigeria. The seeds were sun-dried, deshelled and ground into fine powder.

3.2.1.1 Oil extraction

1446.12g of ground (powdered) castor seed was impregnated with 2.5litres of n-hexane for 24hours, and the mixture was subjected to mechanical pressure. The mass of seed used was informed by the need to get a reasonable quantity of the oil for the required slated investigations. The 'solvent-solute' mixture was then fed to a soxhlet extractor for 8hours at 60^{o}C; the heating mantle was used to supply the required heat content. The solvent was afterwards recovered from the mixture as a condensate.

3.2.1.2 Water degumming

The water degumming was intended to remove hydratable gums, as well as other hydrophilic substances (such as carbohydrates). During the process, 3.7ml of hot water (2%-volume of total oil) was added to the oil at a temperature of 60^{o}C, such that the water and the oil were mixed for 10minutes. While the phospholipids absorbed the water (thus becoming insoluble in the oil), the insoluble phospholipids inter-combined to form the gum. The gum was then separated through centrifugation, giving rise to a pure sample of the oil.

3.2.2 Preparation of the rubber seed oil

The rubber seeds used for this study were collected (picked) from the Imo Rubber Estate, Obiti-Ohaji in the Ohaji/Egbema L.G.A. of Imo State, Nigeria.

The seeds were de-shelled and sun-dried for forty-eight (48) hours, after which they were collected and ground to finer forms.

3.2.2.1 Oil extraction

1418.20g of the ground rubber seed was impregnated with 2litres of petroleum ether solution for 18hours, after which the mixture was subjected to mechanical pressure. The solvent was sequentially recovered from the mixture (of oil and petroleum ether), through a controlled heat application (by means of a heating mantle) at the temperature of 60^{o}C, using a soxhlet extractor; the oil was then collected as a reflux.

3.2.2.2 Degumming

Hot water method of degumming was used in this regard, as this stands to be the best way of dealing with any possible traces of the used solvent present in the mixture. 1ml of the hot water was added to 50ml of the oil sample, and the mixture was placed in a water bath at 60^{o}C for 10minutes. At the elapse of the time, the mixture was then centrifuged at 80rpm for 5minutes. The process tactically separates the formed gums from the pure sample of the oil, which was isolated by simple decantation.

3.2.3 Acid esterification of the oils

The oil samples were converted to esters for better performance as inhibitors of mildsteel corrosion. The esterification of oil samples was achieved following the procedure reported in Yordanov and Petkov (2008b).

The esterification process of the samples was performed in two different 1litre-beakers (one for each oil), using 50ml of each of castor seed oil and rubber seed oil. The measured volume of the samples were poured in the flasks differently and heated up to 60^{o}C. Then 45% volume per volume (v/v)

methanol was added to the preheated samples and stirred for 3minutes with the magnetic stirrer. 0.5% diluted sulphuric acid was added to the mixture and heating and stirring continued for 45minutes at atmospheric pressure. After completion of the reaction (within this specified time), the mixture was poured into a separatory funnel, to separate the excess alcohol, impurities and sulphuric acid. The alcohol, impurities and sulphuric acid formed the top phase, while the esterified oil (that is denser) settled below. The esterified oil was then carefully collected from the separatory funnel.

3.2.4 Samples characterization

Characterization of the esterified oil samples was conducted in order to determine the physicochemical characteristics. The method developed by Association of Official Analytical Chemist (AOAC, 1997), as reported in Pearson (2008), was used during the processes. The same procedure was used for both esterified oil samples during the characterization process, and the results are presented in Table 4.1.

3.2.4.1 Percentage yield

The percentage yield of the oil and esterified oil samples was obtained by simple evaluation of the total mass of the oil extracted, and expressed as the percentage of the mass of the ground solid sample, as stated in equation (3.1). The masses (of both oil and seed) were obtained using the analytical weighing balance (model: *FA-2104*).

$$Y = \frac{\mathrm{Mo}}{\mathrm{Ms}} \mathrm{X} \frac{100}{1} \qquad (3.1)$$

Where: Y = Yield of the sample

M_O = Mass of sample

M_S = Mass of solid

3.2.4.2 Potential hydrogen (pH)

This was done using the digital pH meter (model: *PHS-3C*) at the ratio of 1:10 sample-to-water measurement, that is, 10g each of the oils (CSO and RSO), and those of etser of castor seed oil (ECSO) and ester of rubber seed oil (ERSO) was weighed into a beaker and 100g of distilled water was added to it. Then the pH and conductivity electrodes were dipped into the solution, and the readings were taken.

3.2.4.3 Viscosity

The clean dry digital viscometer (of model: NDJ-5S) was used for this purpose. 0.5g of each of the samples was, differently, filtered through a sintered glass (fine mesh screen) to eliminate dust and other solid materials in the liquid sample. The viscometer was charged with the sample by inverting the tube's thinner arm into the sample, and suction force was drawn up to the upper timing mark of the viscometer, after which the instrument was turned to its vertical position. The viscometer was then placed into a holder and inverted to a constant-temperature bath set at 29^{o}C and allowed for about 10minutes to enable the sample assume the bath temperature. The suction force was then applied to the thinner arm to draw the sample slightly above the upper timing mark. The afflux time (that is the timing as the sample flows freely from the upper mark to the lower mark) was read and recorded.

3.2.4.4 Refractive index

The refractometer (model: ATC-Range 44-891) was used for this purpose. Three drops of each of the samples were transferred into the glass slide of the refractometer. Water, at 30^{o}C, was circulated round the glass slide to keep its temperature uniform. The dark portion, viewed through the eye piece of the

refractometer, was adjusted to be in line with the intersection of the cross. At no parallax error, the pointer on the scale was read and recorded; the process was repeated, and the mean value was evaluated and recorded as the refractive index.

3.2.4.5 Specific gravity

The density bottle was used to determine the density of the samples at ambient temperature of 26ºC. A clean and dry bottle of 25ml capacity was weighed empty (W_O) by means of analytical weighing balance (model: FA-2104), and then filled with each of the samples. The sample-in-bottle was then reweighed to obtain W_1. The bottle was filled again with water after washing and drying, and weighed to obtain W_2. The results were used to evaluate the specific gravity as stated in equation (3.2)

$$S.G. = \frac{W_1 - W_O}{W_2 - W_O} = \frac{\text{Mass of Substance}}{\text{Mass of equal Vol. of Water}} \qquad (3.2)$$

3.2.4.6 Saponification value

Saponification value was determined by weighing 0.5g of the sample into a conical flask. 25ml of potassium hydroxide was then added with 5 granules of anti-bumping chips. The system was attached to reflux air condenser, and was refluxed for 30min until saponification was complete.

1ml of phenolphthalein indicator was added into the hot soap solution and slowly titrated against 0.5NHCl until the pink colour of the indicator disappears; the same procedure was used for the blank. The saponification value (S.V.) is given by equation (3.3).

$$S.V. = \frac{56.1\ \text{N}(V_0 - V_1)}{\text{M}} \qquad (3.3)$$

Where V_O = Vol. of acid used in blank solution

V_1 = Vol. of acid used in the sample

N = Actual normality of the HCl used

M = Mass of the sample.

3.2.4.7 Iodine value

0.4g of the test sample was weighed into a conical flask and 20ml of carbon tetrachloride was added to it. 25ml of Dam's reagent (Wig's iodine) was then added using a safety pipette. The stopper was inserted and the content of the flask was vigorously swirled. The flask was then placed in the dark for 2hours 30mins. At the lapse of the time, 20ml of 10% aqueous potassium iodide and 125ml of water were added using a measuring cylinder. The content was then titrated with 0.1N of sodium thiosulphate solution until the yellow colour almost disappeared. At this point, few drops of 1% starch indicator were added and the titration continued by drop-wise addition of more sodium thiosulphate until the blue colour formed disappeared (after vigorous shaking). The same procedure was used for the blank test, and the iodine value (I.V.) is given by equation (3.4).

$$I.V. = \frac{12.69\ \mathrm{C}\ (\mathrm{V_1} - \mathrm{V_2})}{\mathrm{M}} \qquad (3.4)$$

Where, C = concentration of sodium thiosulphate used

V_1 = Vol. of sodium thiosulphate used for blank

V_2 = Vol. of sodium thiosulphate used for the determination.

M = Mass of sample.

3.2.4.8 Peroxide value

5.0g of the sample was weighed into a 250ml glass-stopperred flask, containing a chloroform solution. Using a graduated cylinder, 3ml of acetic acid was added to the mixture. The flask was stoppered, and then swirled gently for 1minute, after which 30ml of distilled water was then added and stopperred. The mixture was swirled vigorously to liberate the iodine from the chloroform layer. The mixture was then titrated against 0.1N sodium thiosulphate, in the presence of starch indicator, until blue-gray colour disappeared in aqueous upper layer. The peroxide value was evaluated as presented in equation (3.5).

$$P.V. = \frac{100(V_1 - V_2)\mathrm{N}}{\mathrm{M}} \qquad (3.5)$$

Where: V_1 = titre value of sample

V_2 = titre value of blank

N = normality of the thiosulphate

M = Mass of oil used

3.2.2.9 Acid value determination

25ml of diethyl ether and 25ml ethanol were mixed together in a beaker. The resulting mixture was added to 10g of the esterified oil in a 250ml conical flask, with the addition of few drops of phenolphthalein. The mixture was then titrated against 0.1M of sodium hydroxide and shaken vigorously. The end point was indicated by a dark-pink coloration. According to Pearson (2008), the Acid Value is given as stated in equation (3.6).

$$Acid\ Value = \frac{56.9\ \mathrm{M\ V}}{\mathrm{m}} \qquad (3.6)$$

Where: m = mass of sample used

M = Molarity of the Base (NaOH)

V = titre volume

From the result of equation (3.6), the free fatty acid value was evaluated using equation (3.7).

$$\text{Free Fatty } Acid\ Value = \frac{\text{Acid value}}{2} \qquad (3.7)$$

3.2.5 Qualitatative analysis of phytochemical characteristics

The esterified oil samples were, also, subjected to screening of phytochemical features in order to assess their viability for effective corrosion inhibition. The procedures adopted in the phytochemical analysis were as contained in Harbone (1998).

3.2.5.1 Test for alkaloid

0.5g of each of the test samples was treated with four (4) drops of potassium mercuric iodide solution (Dragendroff's reagent), and a cream colouration was observed, which indicated the presence of alkaloid.

3.2.5.2 Test for tannin

0.5g of the sample was boiled in 20ml of distilled water in a test tube, after which it was removed and filtered into a conical flask by means of a filter paper. 0.1% $FeCl_3$ was then added to the filtrate and a reddish colour change was observed, which indicated the presence of tannin.

3.2.5.3 Test for saponin

0.5g of the sample was boiled with 20ml of distilled water (in a water bath), and was removed and then filtered. 10ml of the filtrate was mixed with 5ml of distilled water and shaken vigorously, to obtain stable persistent froth. The

frothing was then mixed with 3drops of olive oil and observed for the formation of emulsion; the formation of emulsion indicated the presence of saponin.

3.2.5.4 Test for flavonoid

3drops of 1%-ammonia (NH_3) solution was added to the sample (etserified oil extract) in a test tube, and a pale-yellow precipitate was observed, which indicated the presence of flavonoid.

3.2.5.5 Test for phenol

5g of the test sample was boiled with 2ml of phenol in a water bath, and then filtered. 2ml of the filtrate was pipetted into a conical flask, and 10ml of distilled water was added. A brownish colour was observed in each case, and this indicated the presence of phenol.

3.2.5.6 Test for cardiac glycosides

1ml of concentrated H_2SO_4 was prepared in a test tube. Then 5ml of the sample was mixed with 2ml of glacial acetic acid (CH_3CO_2H), containing 1drop of $FeCl_3$. The mixture was carefully added to the 1ml of concentrated H_2SO_4 so that the concentrated H_2SO_4 was underneath the mixture; observation for a brick-red precipitate was made, which indicated the presence of cardiac glycoscides.

3.2.5.7 Test for phytate

5ml of the test sample was soaked in 100ml of 2% concentrated HCl for 2hrs, after which the sample was filtered. 5ml of the filtrate was then put into a 250ml beaker, and 100ml of distilled water was added to it. A brownish colour was observed, and this indicated the presence of phytate.

3.2.5.8 Test for oxalate

Four drops of methyl red indicator were added to 125ml of the oil, and calcium chloride solution was added to the mixture drop-wise until a clear change in the salmon-pink colour was observed and noted accordingly; the colour change indicated the presence of oxalate.

3.2.6 Quantitative analysis of phytochemical characteristics

3.2.6.1 Determination of alkaloid content

5.0g of each of the sample was weighed into a beaker, and 200ml of 10% acetic acid (in ethanol) was added to the beaker. The mixture was covered and allowed to stay for 4hrs, after which it was filtered; the filtrate was concentrated by means of water bath to one-quarter of the original volume. Then concentrated ammonium hydroxide solution (NH_4OH) was added drop-wise until precipitation was completed. The whole solution was allowed to settle and the precipitate was collected, washed with dilute NH_4OH and then filtered. The residue was the alkaloid, which was dried in an oven, weighed and recorded.

3.2.6.2 Determination of tannin content

The quantity of tannin was determined using Follins Denn's titration method as reported in Solomon (2012). 20g of the samples (ECSO and ERSO) were, respectively, put into a conical flask, and 100ml of petroleum ether was added and was covered for 24hrs. The mixture was then filtered and exposed for 15minutes to allow traces of the petroleum ether to evaporate. It was then soaked in 100ml of 10%-acetic acid in ethanol for 4hrs, after which it was filtered. 25ml of NH_4OH solution was added to the filtrate to precipitate the alkaloids, which were heated in electric hot plate to remove any traces of

NH_4OH still in the solution. The remaining volume was measured to be 32.5ml, from which 5ml of it was taken and combined with 20ml of ethanol. The mixture was titrated with 0.1M solution of sodium hydroxide (NaOH), using phenolphthalein as indicator. Appearance of pink colour indicated the end point. The tannin content is given by equation (3.8).

$$\text{The tannin content, } C_1 = \frac{C_2 V_2}{V_1} \qquad (3.8)$$

Where, C_2 = Molar Conc. of NaOH = 0.1M

V_1 = Vol. of Ethanol = 5ml

V_2 = Vol. of NaOH = Titre value; and equation (3.8) was used to obtain the percentage tannic acid content as contained in equation (3.9).

$$\%\ \text{Tannic Acid Content} = \frac{C_1\ X\ 100}{m} \qquad (3.9)$$

Where m = mass of sample analysed.

3.2.6.3 Determination of saponin content

The procedure employed here is as described by Solomon (2012). 5g of the study sample was weighed into a beaker containing 20%-acetic acid (in ethanol) and allowed to stand in a water bath at 50^{o}C, for 24hrs. This was filtered, and the filtrate was concentrated using a water bath to one-quarter of its original volume. Concentrated NH_4OH was then added drop-wise to the mixture until precipitation was completed. The whole solution was allowed to settle, and the precipitate was collected (through filtration) and weighed. The saponin content (expressed in percentage) is given by equation (3.10)

$$\%\ \text{Saponin Content} = \frac{m_2\ X\ 100}{m_1} \qquad (3.10)$$

Where m_1 = mass of Sample analsed

m_2 = mass of residue (after filtration)

3.2.6.4 Determination of flavonoid content

10g of each of the samples (ECSO and ERSO) was put into a beaker, containing 100ml of 80% aqueous methanol at room temperature. The whole solution was filtered (by means of filter paper), and the filtrate was transferred to a water bath and evaporated to dryness. The residue was then weighed and noted accordingly. The flavonoid content (expressed in percentage) is given by equation (3.11).

$$\% \text{ Flavonoid content } = \frac{m_2 \text{ X } 100}{m_1} \qquad (3.11)$$

Where m_1 = mass of sample analysed

m_2 = mass of residue (after evaporation)

3.2.6.5 Determination of Phenol Content

The quantity of phenol in the sample was determined using the spectrophotometric method. 2g of the test sample was combined with 50ml of ethanoic acid and allowed to boil for 15minutes. Then 5ml of the boiled sample was pipetted (after cooling) into a 50ml conical flask, and 10ml of distilled water was added to it. Also 2ml of NH_4OH and 5ml of concentrated pentanol were added to the mixture. After insuring thorough mixing of the reagents, the sample was made up to the reference mark of the flask and allowed for 30minutes for possible colour change; it was then collected and viewed in a U.V. spectrophotometer (at 505nm wavelength). The reading represents the phenol content, and was noted accordingly (in mg of solution per 100g of sample).

3.2.6.6 Determination of cardiac glycoside content

The procedure described by Osagie (1998) was adopted.1ml of the test sample was added to 1ml of 2%-solution of 3,5-dinitro salicylic acid (DNS) in

methanol and 1ml of 5%-aqueous NaOH. It was boiled for about 2minutes (until a brick-red colour was observed), and the boiled sample was filtered (having taken note of the weight of the filter paper used). The absorbed residue was then dried to dryness in an oven at 50^{o}C. The weight of the dried residue was evaluated and noted accordingly. The percentage cardiac glycoside content is given by equation (3.12).

$$\% \text{ Cardiac glycoside content} = \frac{m_2 \text{ X } 100}{m_1} \qquad (3.12)$$

Where m_1 = mass of sample analysed

m_2 = mass of residue (after drying to dryness)

3.2.6.7 Determination of phytate content

The procedure adopted is as described by Osagie (1998). 2g of the study sample was introduced into a flask, and was soaked in 100ml of 2% hydrochloric acid (HCl) for 3hrs, after which the mixture was filtered. 50ml of the filtrate was placed in a 250ml beaker and 100ml of distilled water was added. Also 10ml of 0.3% ammonium thiocyanate solution was added as indicator, and the mixture was titrated with iron(III) chloride solution which contained 0.00195g of iron per ml. The percentage phytic acid content (Phytate) is given by equation (3.13).

$$\% \text{ Phytic acid content} = \frac{V\ C\ (0.00195) \text{ X } 100}{m} \qquad (3.13)$$

Where V = titre value

C = molar conc. of Fe_3Cl_3 = 1.19M

m = mass of sample analysed

3.2.6.8 Determination of oxalate content

This was determined using the procedure reported in Osagie (1998). The procedure involves three major steps, namely: digestion, precipitation and

permanganate titration. For the digestion, 2g of the sample was suspended in 190ml of distilled water in a 250ml volumetric flask. 10ml of 6% HCl was added, and the suspension digested at 100^{o}C for 1hr. At the lapse of the time, the mixture was cooled, and then made up to the 250ml mark before filtration.

Oxalate precipitation involved the measurement of duplicates of 125ml of the filtrate into beakers, and four drops of methyl red indicator were added. This was followed by the addition of NH_4OH solution (drop-wise) until the test solution changed from salmon-pink colour to a faint-yellow colour. Each portion was then heated to 90^{o}C, cooled and filtered (to remove precipitate containing ferrous ion). The filtrate was, again, heated to 90^{o}C, and 10ml of 5% $CaCl_2$ solution was then added while being stirred constantly. After heating for about 5minutes, it was allowed to cool overnight. By the next day, the solution was then centrifuged at 250rpm for 5minutes, after which the supernatant was decanted while the precipitate was completely dissolved in 10ml of 20% H_2SO_4 solution.

Finally, in permanganate titration, the total filtration resulting from digestion of 2g of the sample was made up to 300ml. Aliquots of 125ml of the filtrate was heated until it was near boiling, before it was removed and titrated against 0.05M of standardized potassium permanganate ($KMnO_4$) solution to faint pink colour, which persisted for 30sec. The oxalate content is given (in mg of solution per 100g of sample) by equation (3.14).

$$\text{Oxalate content} = \frac{(\mathrm{T})(\mathrm{V}_{me})(\mathrm{D}_f) \times 10^5}{\mathrm{M}_E \times \mathrm{M}_F} \qquad (3.14)$$

Where T = titre value

V_{me} = molar mass/equivalent of $KMnO_4$ *(0.00225g)*

M_E = molarity/equivalent of $KMnO_4$ *(0.5)*

M_F = mass of sample analyzed *(2g)*

D_f = oxalate factor *(125)*

3.2.7 Flow system setup:

The seven (7) main components (water bath, dozing pump, mildsteel pipe, reservoir, electric power source, retort stand and platform) shown in Figure 3.1 played major roles in the flow system design used for the corrosion inhibition assessment.

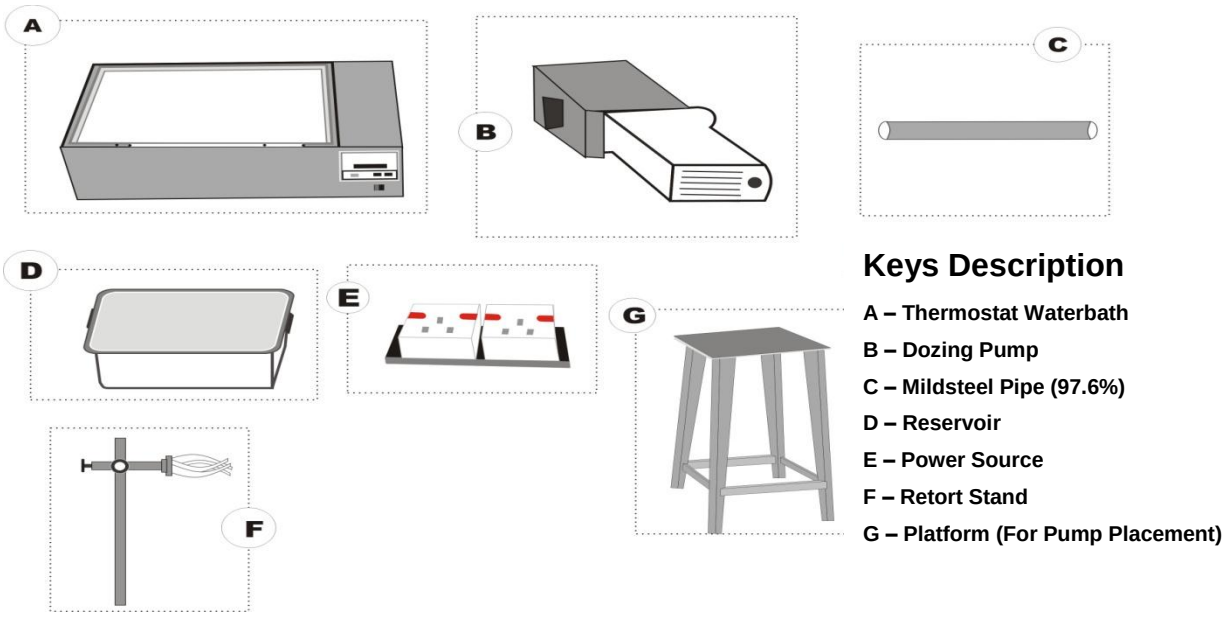

Figure 3.1: Major components of the flow system studied

The dozing pump (of model: *JM-15774-C07*) was firmly fixed on the wooden platform by means of screws. The inlet hose was then cut at the middle, and the ends of steel pipe firmly connected to each of the points (of the cut) using clips. The lower end of the pipe was passed through a sizeable opening made on the plastic reservoir (containing a given concentration of the inhibitor-in-acid), while the other end was connected to the pump inlet. Another hose connected the outlet of the pump to the reservoir, which served as a recycle stream. The reservoir was already securely placed in the thermostat water bath (of model: TT-6), which contained about 4-litres of water, and both the pump and water bath were connected to a source of electric power. These gave rise to the composite flow system presented in Figure 3.2.

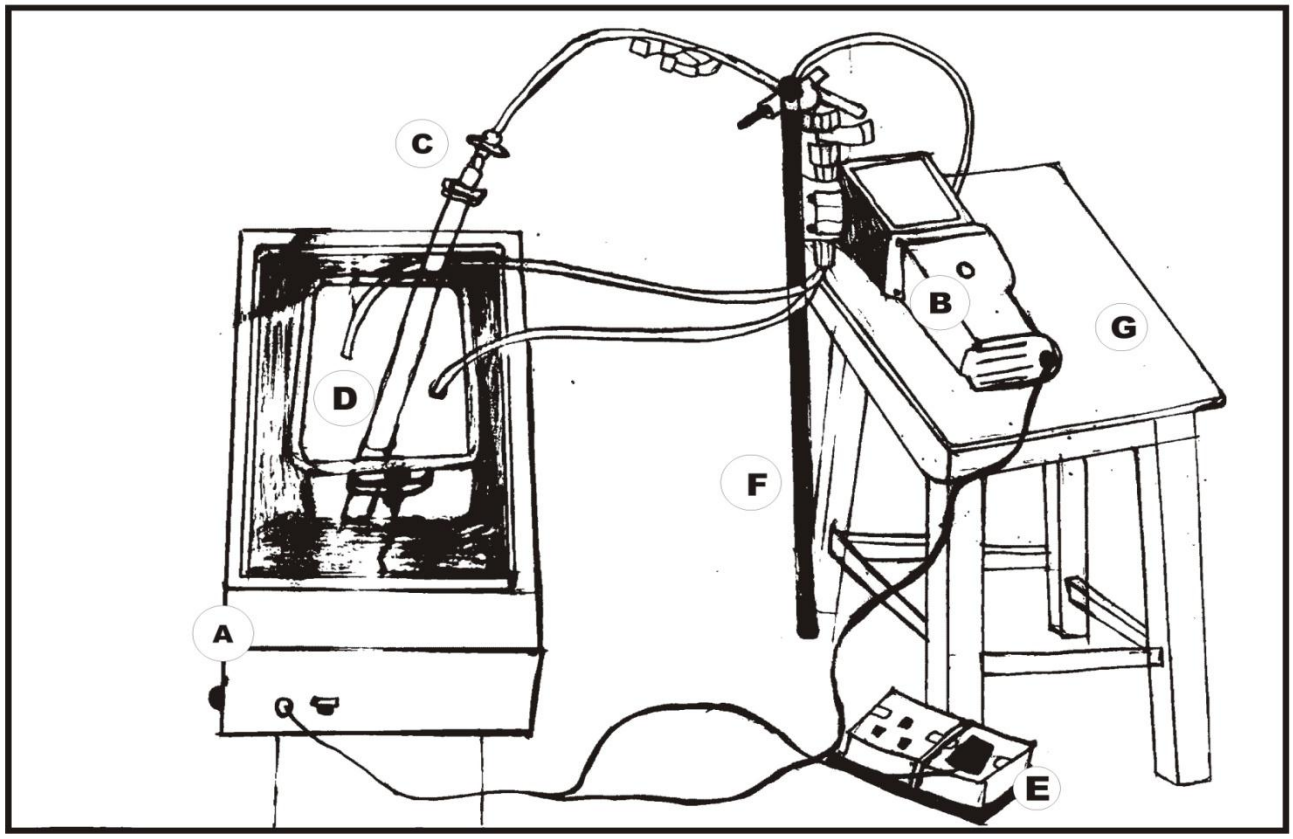

Figure 3.2: Composite flow system setup for the study

3.2.8 Corrosion inhibition assessment

Electric power was supplied to the pump and water bath, and the temperature of the water bath was set at 40^{o}C and the pump set at 50% stroke; the inhibitor concentration was 10g/*l*. The inhibitor-in-acid mixture in the reservoir was then transmitted in a continuous flow pattern, through the steel pipe for various time intervals of 4, 8, 16, 24 and 32hours and dosages of 50, 60 and 70% stroke. At the lapse of the time, the steel sample was removed, and placed in an oven dryer (model: DHG-9101-1SA) for 5minutes. With the initial weight of the steel pipe (W_1) already measured, the final weight (W_2) was then measured, and the weight difference ($W_1 - W_2$) was obtained and recorded. The procedure was repeated in the absence of inhibitor, and the results recorded as well.

These procedures were repeated at different temperature (of 50^{o}C and 60^{o}C) and concentration (of 15g/*l* and 20g/*l*) sequentially, using different steel pipes, and their results were duly collated as contained in Appendix 1; the experiments were conducted using the flow system set-up, presented in Figure 3.2.

3.2.9 Electrochemical Study

As an electrochemical process, corrosion reactions usually employ electrochemical measurements for obtaining detailed mechanistic insights into corrosion studies. Experiments were conducted to determine the effect of various concentrations of **ECSO** and **ERSO** inhibitors on the electrochemical corrosion behaviour of the mildsteel pipe in H_2SO_4 solutions. The method considered in this work is the potentiodynamic polarization (PDP). However, scanning electron microscopy (SEM) and Fourier transform infrared

spectroscopy (FTIR) were, respectively, used to show the effect of the acid medium and the inhibitors on the midsteel pictorially, and to identify the functional groups present in the inhibitors.

3.2.9.1 Potentiodynamic polarization measurements

The mildsteel sample for electrochemical experiment was fixed in polytetrafluoroethylene (PTFE) rods by epoxy resin in such a way that only one surface area of $1cm^2$ was left uncovered. The electrodes used (graphite rod, calomel electrode and mildsteel) were, sequentially, polished with emery papers (600, 1000 and 1200 numbers), rinsed thoroughly with distilled water, degreased with ethanol and then with acetone.

Electrochemical experiments were carried out in a three-electrode corrosion cell using a 263-Potentiostat/Gavalnostat electrochemical work station, with Powersuit software. The corrosion data were obtained in a three-electrode mode (as stated ealier). Graphite rod and saturated calomel electrodes were used as counter and reference electrodes respectively, while the mild steel material served as the working electrode. Measurements of the corrosion potential and those of corrosion current were performed in aerated and unstirred solutions at the end of 1hour of immersion at 303K. The potentiodynamic polarization studies were conducted in a potential range of ±250 mV (that is the initial potential was –250 mV, while the final potential was +250 mV), at a scan rate of 0.333mV/s. Each test was run in triplicate to verify the reproducibility of the system.

3.2.9.2 Scanning Electron Microscope

The mildsteel specimen was cleaned (with emery papers and degreased accordingly) and immersed for 24hr in the blank solutions (0.2M H_2SO_4) in the absence and presence of the respective inhibitors under study, at 30±1 ^oC.

The blank serves as a reference to the examination of the inhibitors. It was then washed with acetone, dried in warm air, and affixed firmly on the specimen chamber of the scanning electron microscope (XL-30FEG model). The electron beam of the equipment was then directed towards the specimen under examination. Electron guns (thermionic and field-emission guns), located at the top of the device, shot out beams of highly concentrated electrons on the mildsteel specimen. The first, thermionic guns, continued to heat the filament (that was directed on the specimen) until electrons streamed away, while the second one, field emission guns, ripped electrons away from their atoms by generating a strong electrical field. When the specimen was hit with the beam of the electrons (known as the incident beam), it emits x-rays and three kinds of electrons (primary backscattered electrons, secondary electrons and Auger electrons). An electron recorder picked up the rebounding electrons and recorded their imprint. This information was translated onto a screen which allowed three-dimensional images to be presented clearly.

3.2.9.3 Fourier transform infrared spectroscopy

This method was used to identify the functional groups present in the inhibitors. Two coupons of the mildsteel were dipped into the inhibitor-in-acid medium (20mg/l concentration) for 24hrs to form an adsorbed layer, after which it was removed for examination, in the Nicolet Magna-IR 560 FTIR spectrophotometer, at a frequency of 4000 to 400 cm^{-1}. The monochrometer of the machine (a salt prism, with finely spaced etched lines) separated the source of radiation into its different wavelengths. A slit selected the collection of wavelengths that shine through the mildsteel sample. In double beam operation, a beam splitter separates the incident beam into two; half went to the sample (mildsteel material), and the other half goes to a reference

(embedded in the machine). The sample absorbed light according to its chemical properties. A detector collected the radiation that passed through the sample, and in double-beam operation, compared its energy to that going through the reference. The detector put out an electrical signal, which was normally sent directly to an analogue recorder. A link between the monochrometer and the recorder, then, allowed the energy to be recorded as a function of wavelength.

The spectra for the inhibitors under investigation, as well as the protective film formed on the mild steel surface were recorded by carefully removing the film, mixing it with KBr, and making the pellets.

3.2.10 Thermodynamic Study

The thermodynamics of the process was studied at inhibitor concentration of 20g/l and pressure of 70% stroke for both samples at varying temperatures of 40, 50 and 60^{o}C. The heat energy requirement for corrosion reaction on the mildsteel, in the presence and absence of the inhibitor samples, at varying times, was evaluated using the Arrhenius formulation of equation (3.15) as contained in Eastop and McConkey (1993):

$$\%\mathbf{w}_{\boldsymbol{c}} = A\,\frac{-\Delta H}{\mathrm{RT}} \qquad (3.15)$$

Where:

$\%w_C$ = percentage weight loss at a given inhibitor concentration in a given time.

A = pre-exponential factor (*2.1 exp.9 sec* $^{-1}$)

ΔH = change in heat energy content

R = general gas constant (*8.31KJmol*$^{-1}$*K*$^{-1}$)

T = reaction temperature

The percent weight loss, $\mathbf{W_c}$ was evaluated using equation (3.16), as presented in Apendix 5.

$$w_c = \frac{(W_1 - W_2)}{W_1} X\ 100 \qquad (3.16)$$

Where: W_1 = initial mass of the material (before corrosion)

W_2 = final mass of material (after corrosion)

And the enthalpy change of the reaction, *ΔH* is given by equation (3.17).

$$\Delta H = \frac{1}{A} . (\boldsymbol{RT}) . (w_c) \qquad (3.17)$$

The values of the *ΔH* at the respective conditions were duly computed. Also, the corresponding Entropy changes (*ΔS)* and Free Energy changes (*ΔG)* were respectively evaluated using equations (3.19) and (3.20) as contained in Philip (2003), and presented in Table 4.5.

$$\Delta S = \frac{\Delta H}{\Delta T} \qquad 3.18$$

$$\Delta G = \Delta \boldsymbol{H} - \boldsymbol{T}\Delta \boldsymbol{S} \qquad 3.19$$

3.2.11 Adsorption isotherm study

Adsorption isotherm of the process was studied to assess the equilibrium relationship between the concentration in the fluid phase and the concentration of the study samples, which is to assess the relationship between the quantity of fluid (inhibitor) sample adsorbed and the bulk (mildsteel) surface, under equillibrum conditions at constant temeperature. Four forms of isotherm were considered in the study: the Langmuir, Freundlich, Temkin and El-Awady isotherms. The assumptions of the Langmuir isotherm relates with the provisions of equation (3.21a), as reported by Offurum *et al* (2011).

$$\frac{x}{m} = \frac{abC_e}{1 + bC_e} \qquad (3.20a)$$

Where:

x/m = mass of adsorbate (medium) per unit mass of adsorbent (mildsteel)

a,b = empirical constants

C_e = concentration of adsorbate in solution after adsorption.

Equation 3.20(a) could be rearranged to another form as stated in equation (3.20b)

$$\frac{C_e}{(\frac{x}{m})} = \frac{1}{ab} + \frac{1}{a} C_e \qquad (3.20b)$$

The constants of Langmuir Isotherm were determined by plotting log[C_e/(x/m)**]** against log$\mathbf{C_e}$, at different conditions, with considerations of the presence and absence of inhibitor. The slope of the plot is equivalent to log(1/a), from which 'a' was evaluated. Also, the intercept is equivalent to (1/ab), and 'b' was evaluated (with 'a'already computed).

On the other hand, the Freundlich isotherm is mostly applicable to adsorption processes that occur on heterogenous surfaces (Metcalf and Eddy, 2006). The isotherm gives an expression which defines the surface heterogeneity and the exponential distribution of the active sites. The empirical model of Freundlich Isotherm, as reported in Offurum *et al* (2011) is given by equation (3.21).

$$\frac{x}{m} = K_f C_e^{\,1/n} \qquad (3.21)$$

Where:

x/m = mass of adsorbate per unit mass of adsorbent

K_f = Freundlich capacity factor

C_e = concentration of adsorbate in solution after adsorption

1/n = Freundlich intensity parameter

Taking logarithm of both sides of equation (3.21) gives its linear form, as presented equation (3.22).

$$\log\left(\frac{\mathrm{x}}{\mathrm{m}}\right) = \log K_f + \frac{1}{\mathrm{n}}\log C_e \qquad (3.22)$$

The constants of the Freundlich Isotherm were then determined by plotting log (x/m) against log C_e. The slope of the graph is equivalent to '1/n', while the intercept is equivalent to log K_f. With the known values of the slope and intercept, the Freundlich factors were successively evaluated.

Similarly, the Temkin and El-Awady models, as reported in Nwabanne and Nwoye (2012), Nnaji *et al* (2011), Obi-Egbedi *et al* (2011) and Obot *et al* (2009b), are given by equations (3.23) and (3.24) respectively.

$$Log\theta = LogK + \frac{1}{\mathrm{f}}LogC \qquad (3.23)$$

$$Log\left(\frac{\theta}{1-\theta}\right) = Log\mathrm{K}^1 + yLogC \qquad (3.24)$$

Where: θ = degree of coverage of the mildsteel surface by adsorbed inhibitor.

K^1 = binding constant.

f = factor of energetic homogeneity.

C = inhibitor concentration

y = number of inhibitor molecules occupying one active site.

(1/y) = number of surface active sites occupied by one inhibitor molecule.

The factor of energetic homogeneity (f), contained in equation (3.23), is related to the lateral interaction factor (a) as given by equation (3.25).

$$\mathrm{a} = \frac{\mathrm{f}}{-2} \qquad (3.25)$$

Also, the value of the degree of surface coverage (Θ) was obtained using equation (3.26) (Adejo *et al*, 2014).

$$\theta = \left(\frac{CR_{abs} - CR_{\mathrm{pre}}}{CR_{abs}}\right) \qquad (3.26)$$

Where CR_{abs} and CR_{pre} are mildsteel corrosion rates, in the absence and presence of the inhibitor sample respectively. The binding constant (K) of the El-Awady model is given by equation (3.27).

$$K = K^1\left(\frac{1}{y}\right) \qquad (3.27)$$

The plot of logϴ versus logC will give logK and (1/f) as intercept and slope respectively, from which the Temkin parameters are computed. In the same vein, plot of equation (3.24) will give $logK^1$ and 'y' as intercept and slope respectively, from which the El-Awady parameters are evaluated.

3.2.12 Effect of Time on Weight Loss

In order to appreciate the effect of time on weight loss, the linear relationship between the weight loss and the process time (at varying reaction conditions) were plotted, using MS-Excel software. Also, the corrosion rate, CR (in millimeter per year, mm/y) was evaluated using the relationship presented in equation 3.28 as reported by Nwabanne and Okafor (2012), and the graph of corrosion rate was plotted against time as shown in figures. 4.73 - 4.84.

$$CR(in\ mm/y) = \frac{87.6(W)}{DAT} \qquad 3.28$$

Where: W = weight loss (g); D = metal density(g/cm^3); A = surface area of Pipe(cm^2); T = time of exposure of metal sample(hr)

CHAPTER FOUR

RESULTS AND DISCUSSION

4.1 RESULTS

4.1.1 Results of Characterization and Phytochemistry of Samples

The results obtained from the characterization of the study samples (esterified oils) are presented in table 4.1, while those of the qualitative and quantitative analysis are presented in tables 4.2 and 4.3 respectively.

Table 4.1: Characterization Results of the Samples

S/N	Parameter	Result for CSO	Result for RSO	Result for ECSO	Result for ERSO
1	pH	6.28	1.90	3.00	1.76
2	Viscosity (*mPoise*)	75.00	61.20	215.20	208.30
3	Moisture Content *(%)*	10.40	2.60	18.86	11.78
4	Specific Gravity	0.9600	0.9000	0.9222	0.9189
5	Conductivity (µS/cm*)*	83.18	148.80	150.00	610.00
6	Mass *(g)*	398.50	283.40	365.02	312.57
7	Volume *(ml)*	411.10	308.00	354.00	350.00
8	Density *(g/ml)*	0.96	0.92	1.03	0.89
9	Yield (%)	19.90	8.00	25.24	22.04
10	Acid Value *(gNaOH/g)*	3.72	26.80	14.40	16.40
11	Free Fatty Acid *(%)*	1.86	13.40	7.20	8.20
12	Saponification Value *(mg/ml)*	177.00	83.60	49.09	28.65
13	Iodine value*(mg/ml)*	87.80	131.70	4.12	4.83
14	Peroxide Value*(mg/ml)*	15.52	16.30	2.00	4.00

Table 4.2: Qualitative analysis of phytochemicals in samples A and B

S/N	Parameter	Result for sample A (ECSO)	Result for sample B (ERSO)
1	Akaloid	++	++
2	Flavonoid	+	+++
3	Tannin	++	+++
4	Cardiac Glycocides	++	+++
5	Phenol Content	+	+++
6	Phytate	++	++
7	Saponin	+	+++
8	Oxalate Content	++	++
9	Terpernoid		+
10	Steroids	++	++

Table 4.3: Quantitative analysis of phytochemicals in samples A and B

S/N	Parameter	Sample A (EECSO)	sample B (EERSO)
1	% Akaloid	0.083	0.083
2	Flavonoid Content *(µg/ml)*	364.71	379.41
3	% Tannins	85.76	85.76
4	% Cardiac Glycocides	51.64	39.31
5	Phenol Content (mg/100g)	0.0404	0.0422
6	% Phytate	3.02	3.25
7	% Saponins	3.198	21.99
8	Oxalate Content (mg/100g)	12937.5	59062.5
9	Steroid Content (mg/100g)	2.03	5.21
10	Terpernoids (mg/100g)	3.00	4.50
11	Hydrogen Cyanide (mg/kg)	0.0288	0.0512

4.1.2 Effect of time on weight loss

The results of the effect of time on corrosion rate, for cases with inhibitors and those without inhibitors, (at varying reaction conditions) are presented in Figures 4.1-4.3 for ECSO, while those for ERSO are presented in Figures 4.4-4.6. Also, the corrosion rate, CR (in millimeter per year, mm/y) was evaluated using the relationship presented in equation 3.28, and the graph of corrosion rate was plotted against time, as presented in figures 4.7-4.9 and figures 4.10-4.12 for ECSO and ERSO respectively.

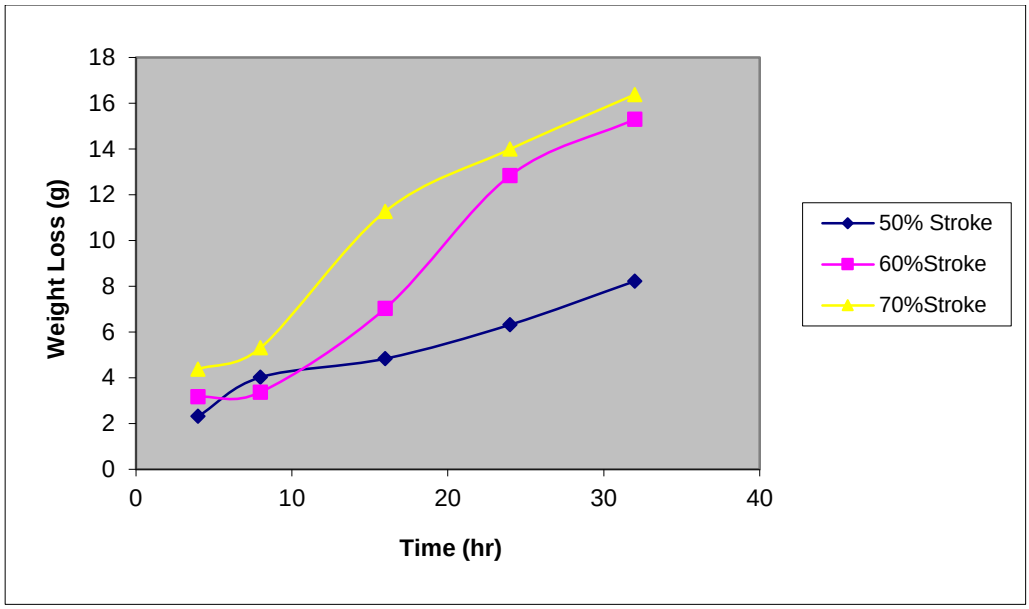

Figure. 4.1(a): Weight loss vs time at various pump pressure, with ECSO (at 10g/*l* and 40^{o}C Conditions)

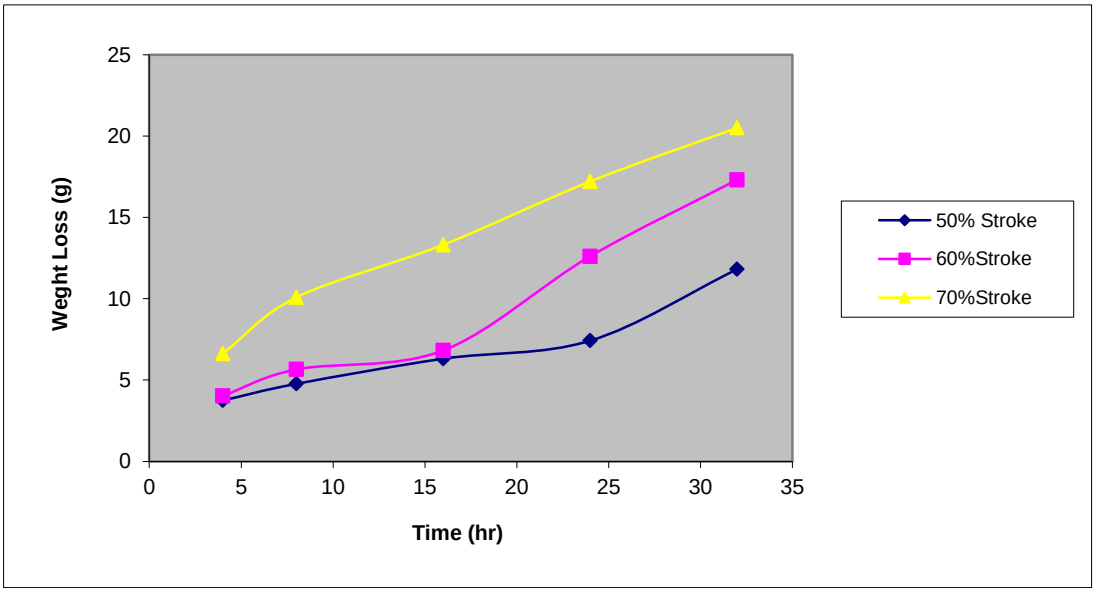

Figure 4.1(b): Weight loss vs time at various pump pressure**,** without ECSO (at 10g/*l* and 40^{o}C Conditions)

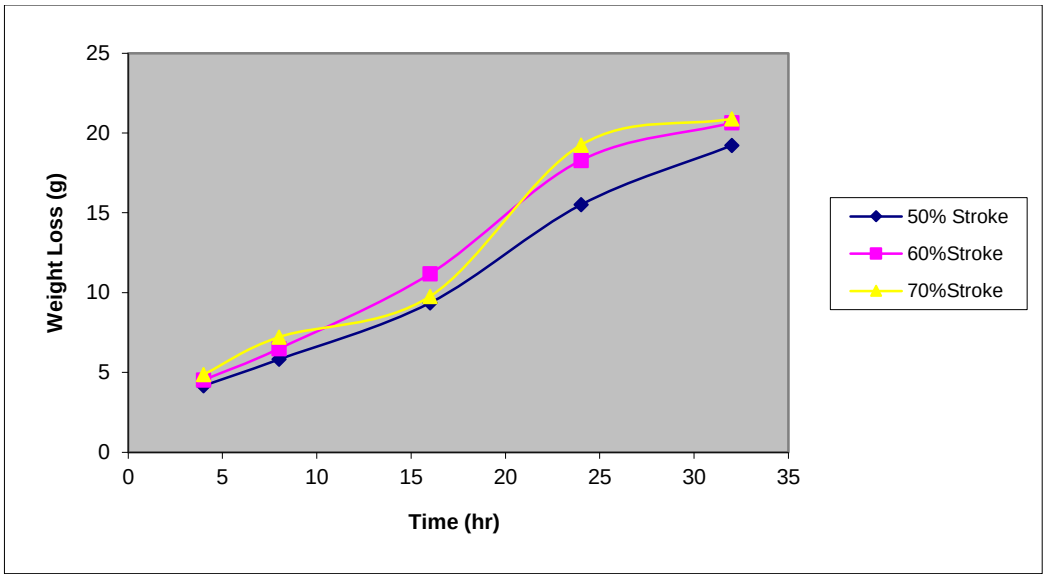

Figure 4.2(a): Weight loss vs time at various pump pressure, with ECSO (at 15g/*l* and 50ºC Conditions)

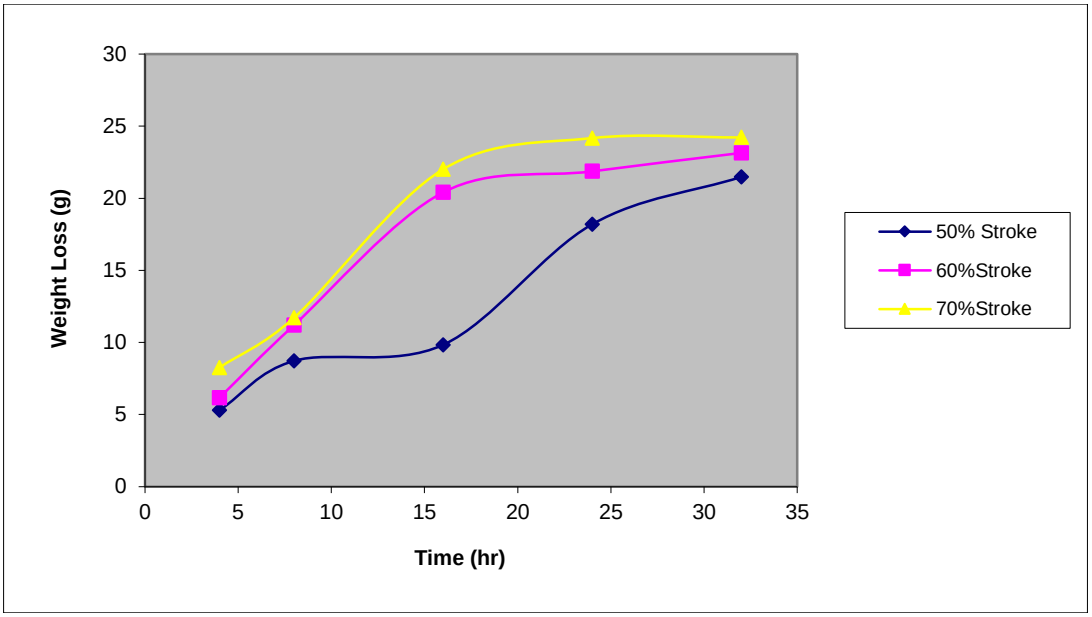

Figure 4.2(b): Weight loss vs time at various pump pressure, without ECSO (at 15g/*l* and 50ºC Conditions)

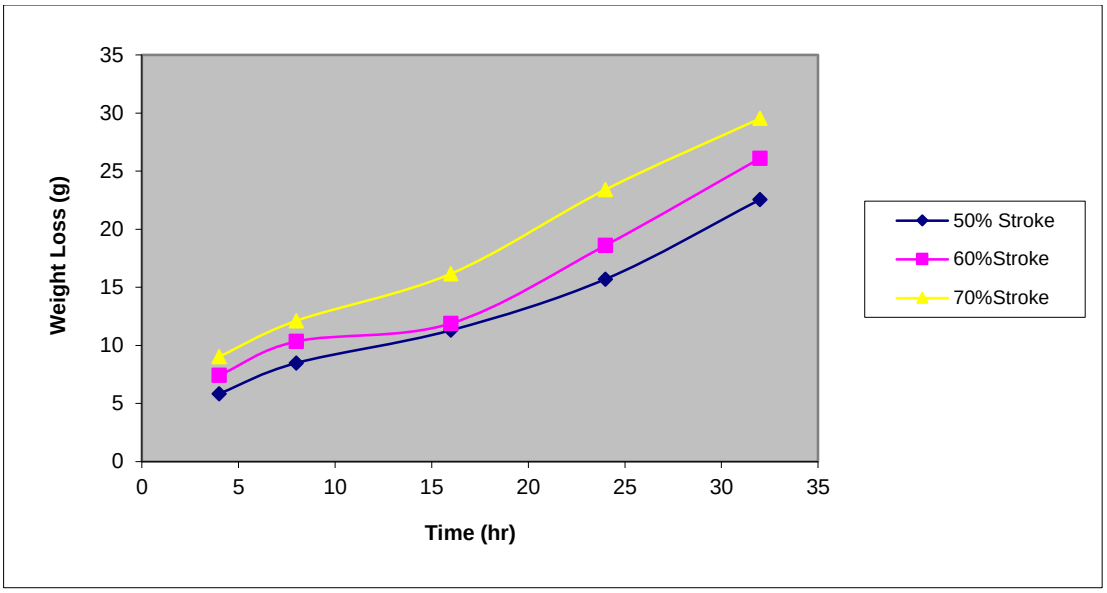

Figure 4.3(a): Weight loss vs time at various pump pressure, with ECSO (at 20g/*l* and 60^{o}C Conditions)

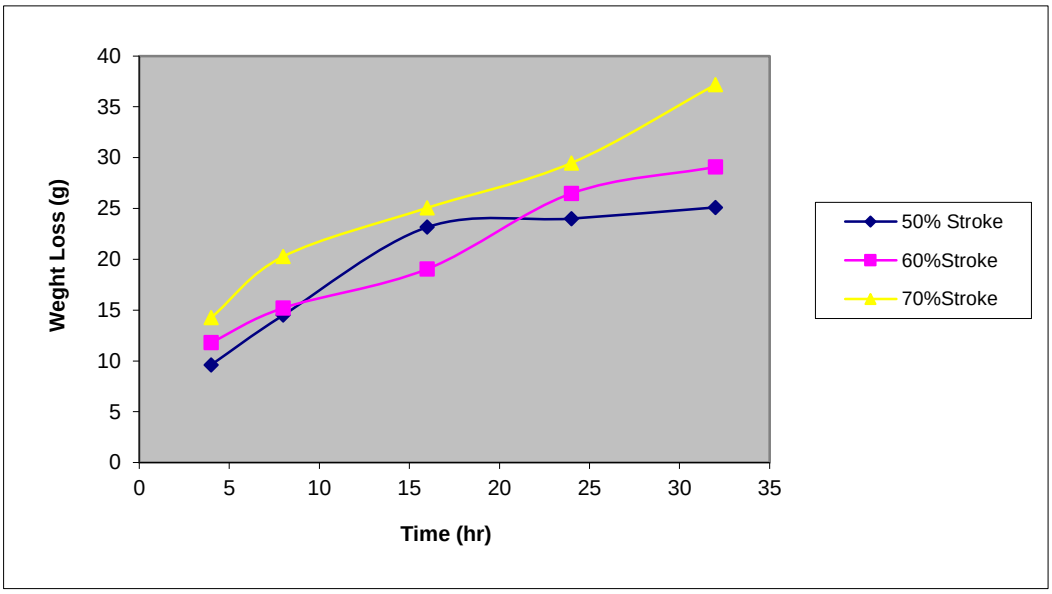

Figure 4.3(b): Weight loss vs time at various pump pressure, without ECSO (at 20g/*l* and 60^{o}C Conditions)

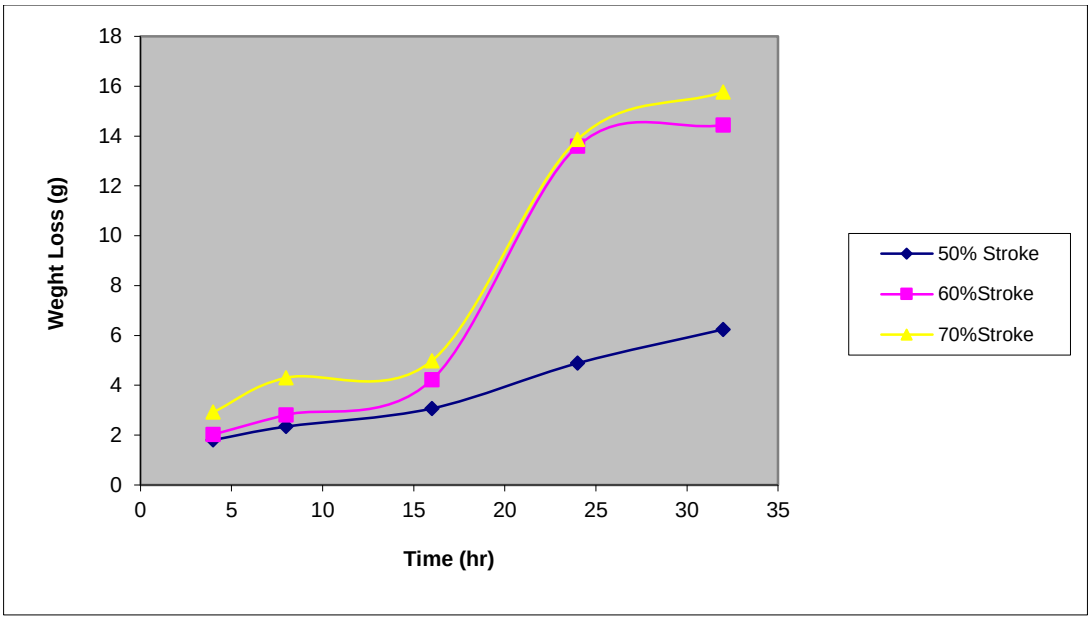

Figure 4.4(a): Weight loss vs time at various pump pressure, with ERSO (at 10g/*l* and 40°C Conditions)

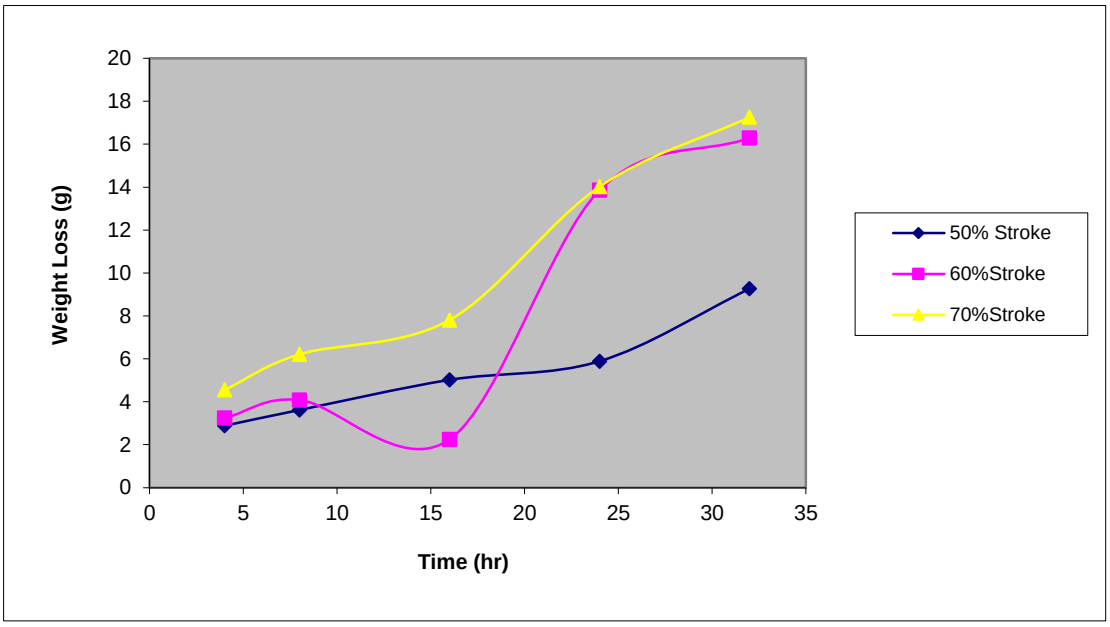

Figure 4.4(b): Weight loss vs time at various pump pressure, without ERSO (at 10g/*l* and 40°C Conditions)

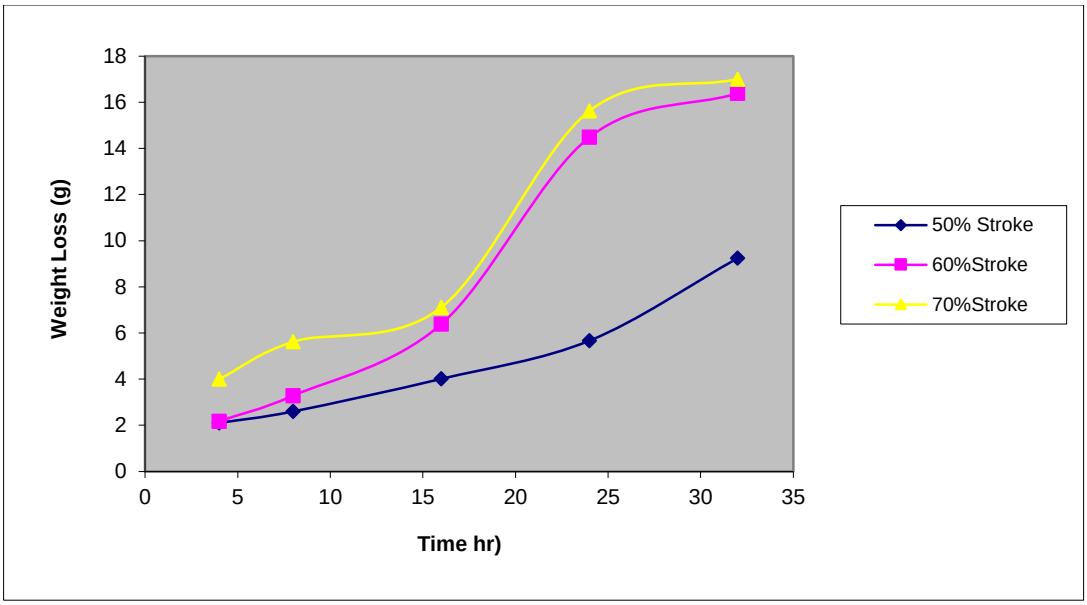

Figure 4.5(a): Weight loss vs time at various pump pressure, with ERSO (at 15g/*l* and 50°C Conditions)

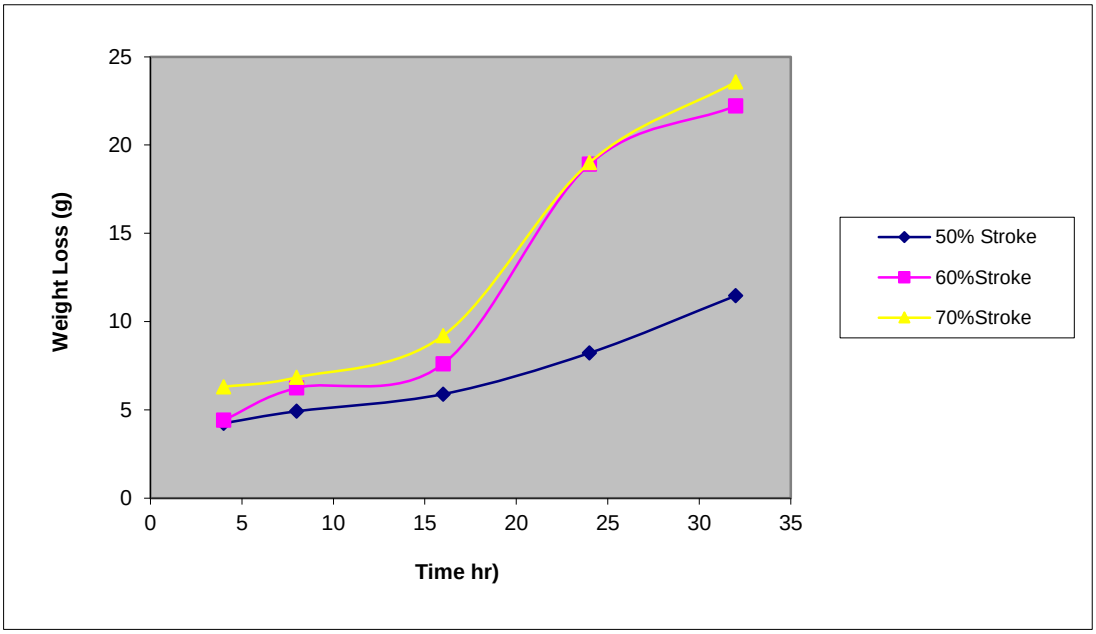

Figure 4.5(b): Weight loss vs time at various pump pressure, without ERSO (at 15g/*l* and 50°C Conditions)

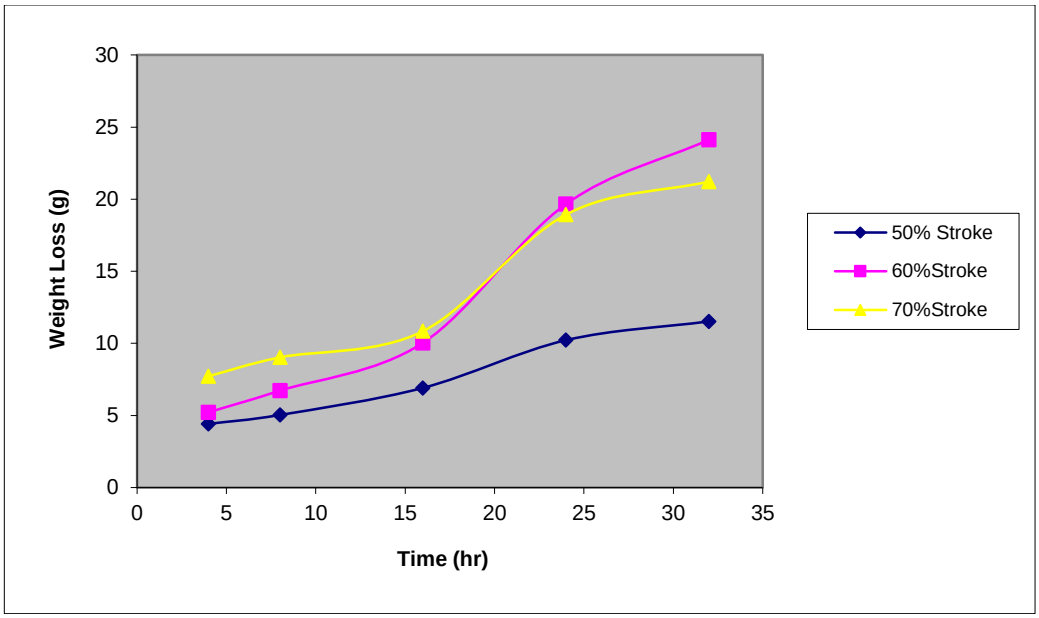

Figure 4.6(a): Weight loss vs time at various pump pressure, with ERSO (at 20g/*l* and 60°C Conditions)

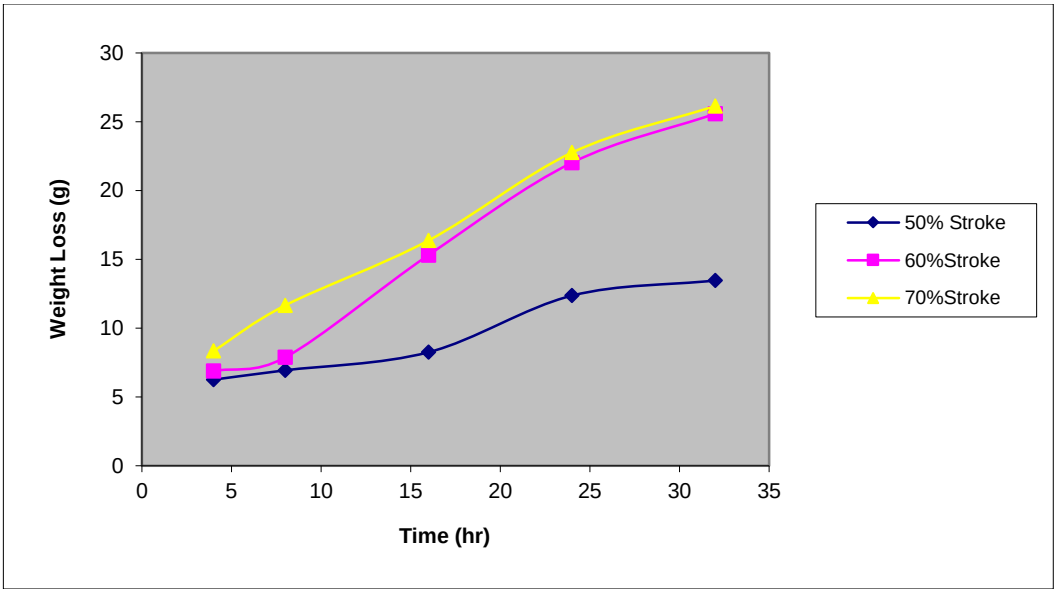

Figure 4.6(b): Weight loss vs time at various pump pressure, without ERSO (at 20g/*l* and 60°C Conditions)

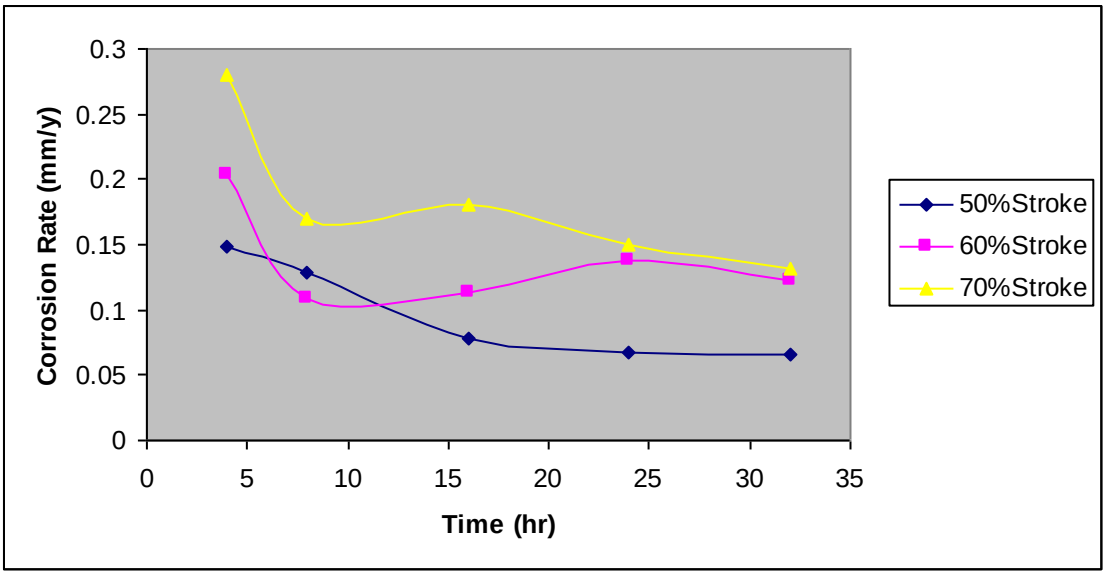

Figure 4.7(a): Corrosion rate vs time at various pump pressure, with ECSO (at 10g/*l* and 40°C Conditions)

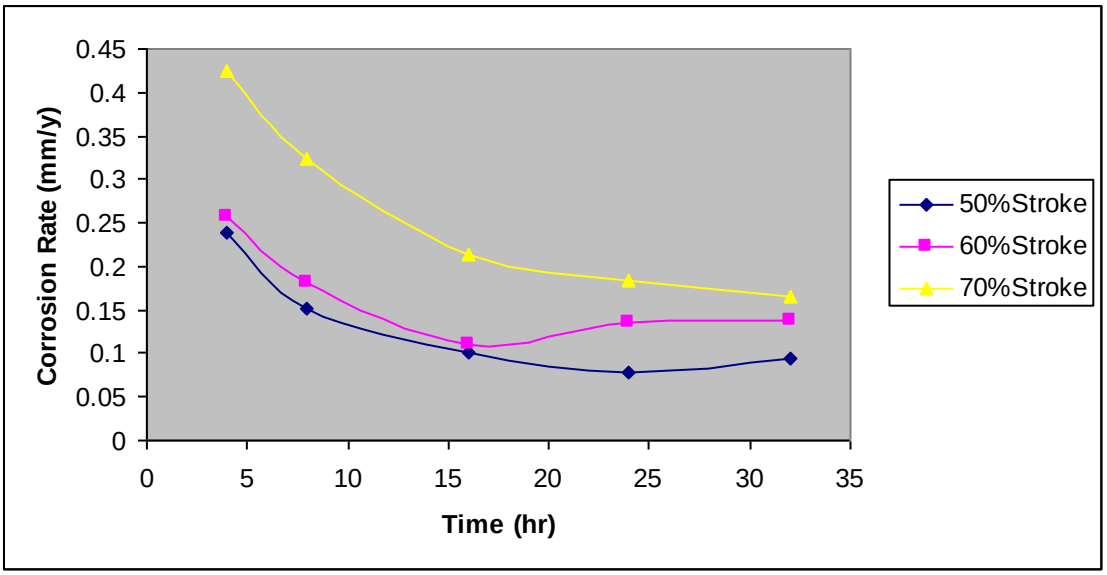

Figure 4.7(b): Corrosion rate vs time at various pump pressure, without ECSO (at 10g/*l* and 40°C Conditions)

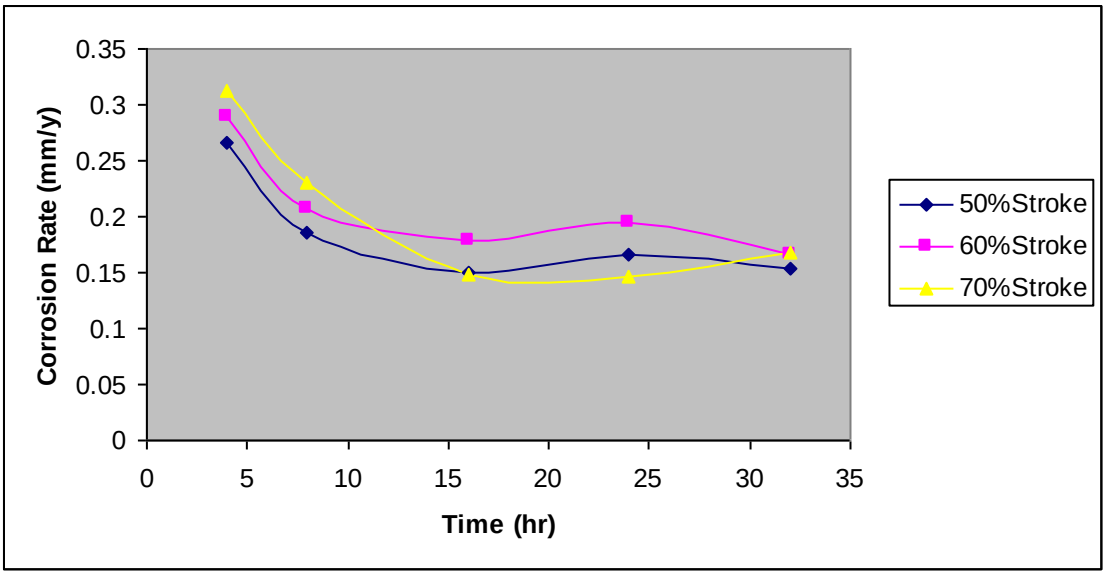

Figure 4.8(a): Corrosion rate vs time at various pump pressure, with ECSO (at 15g/*l* and 50^{o}C Conditions)

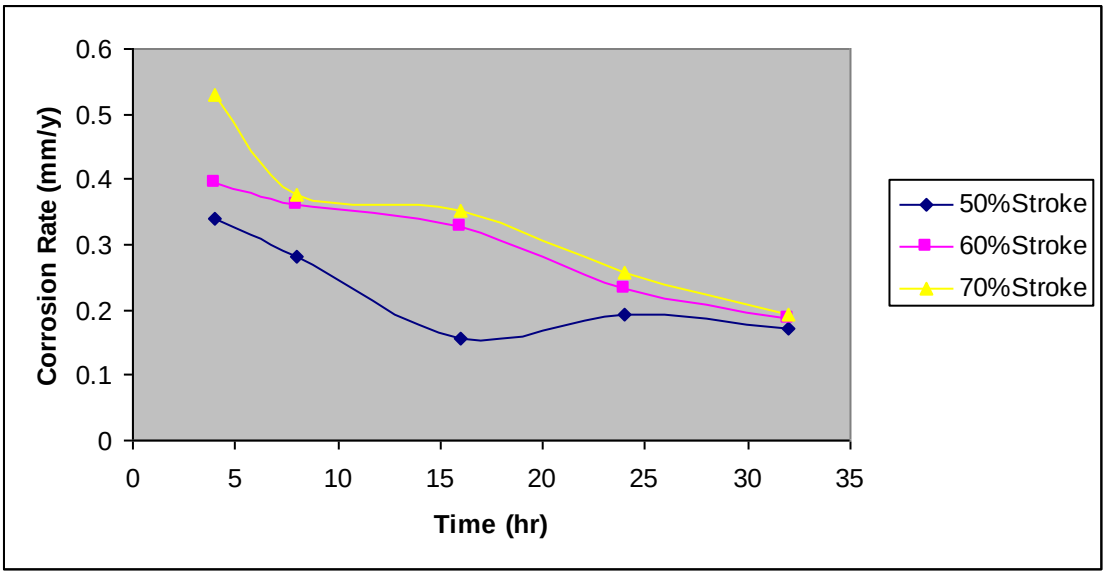

Figure 4.8(b): Corrosion rate vs time at various pump pressure, without ECSO (at 15g/*l* and 50^{o}C Conditions)

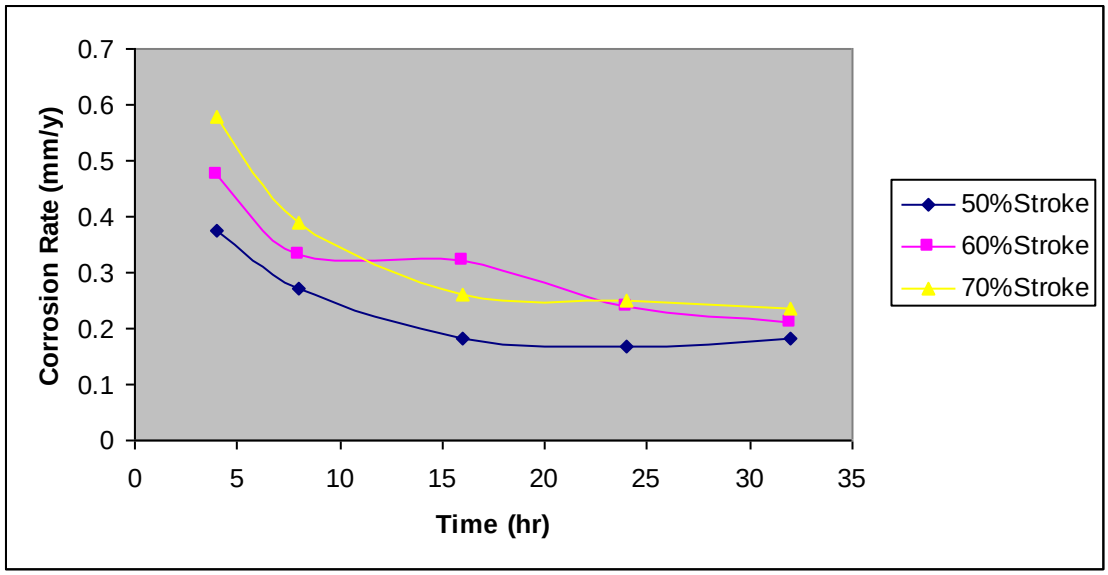

Figure 4.9(a): Corrosion rate vs time at various pump pressure, with ECSO (at 20g/*l* and 60^{o}C Conditions)

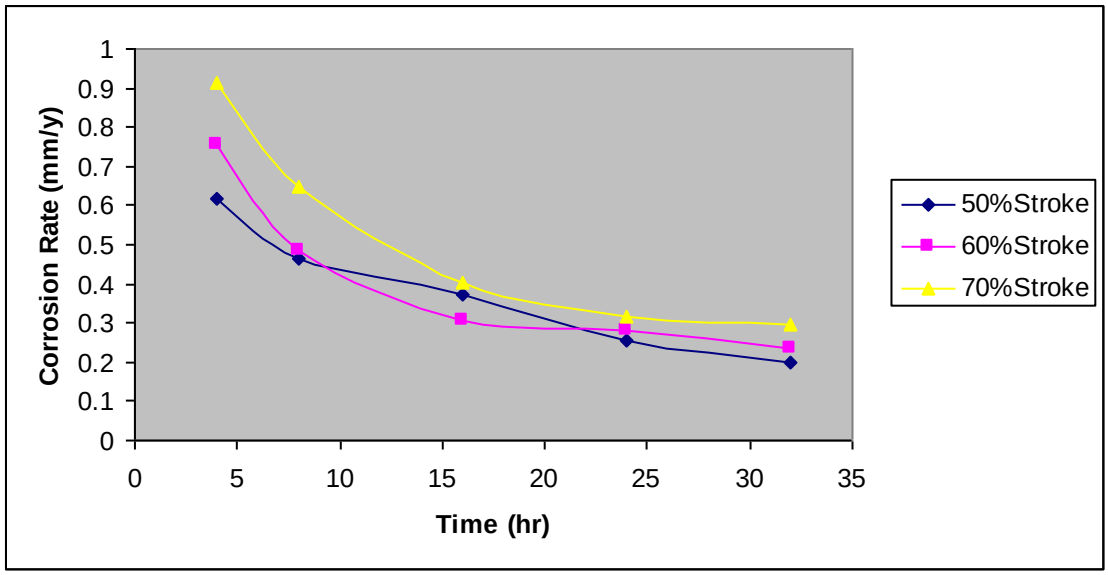

Figure 4.9(b): Corrosion rate vs time at various pump pressure, without ECSO (at 20g/*l* and 60^{o}C Conditions)

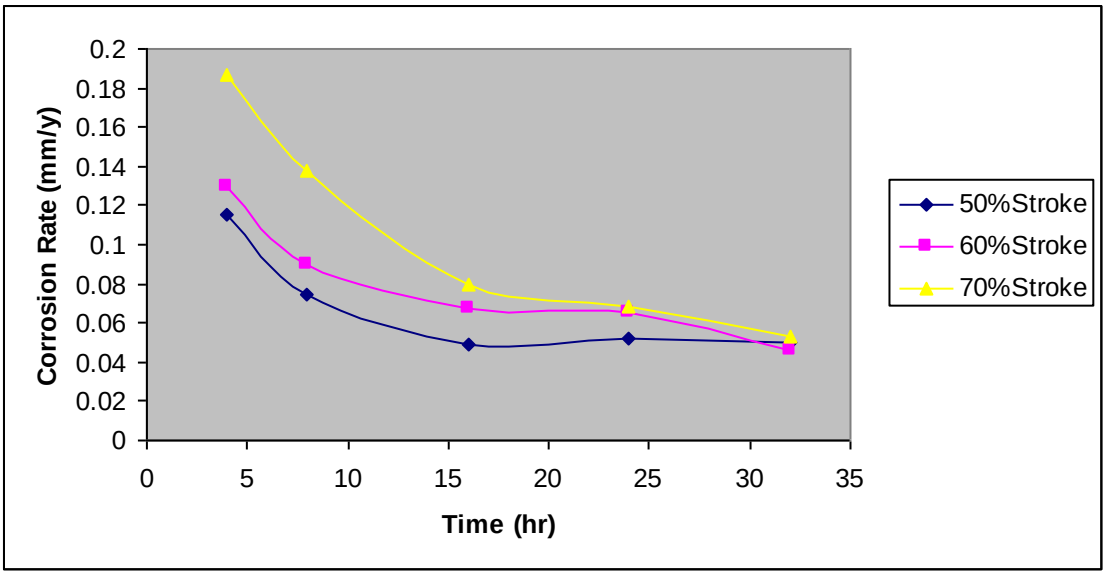

Figure 4.10(a): Corrosion rate vs time at various pump pressure, with ERSO (at 10g/*l* and 40^{o}C Conditions)

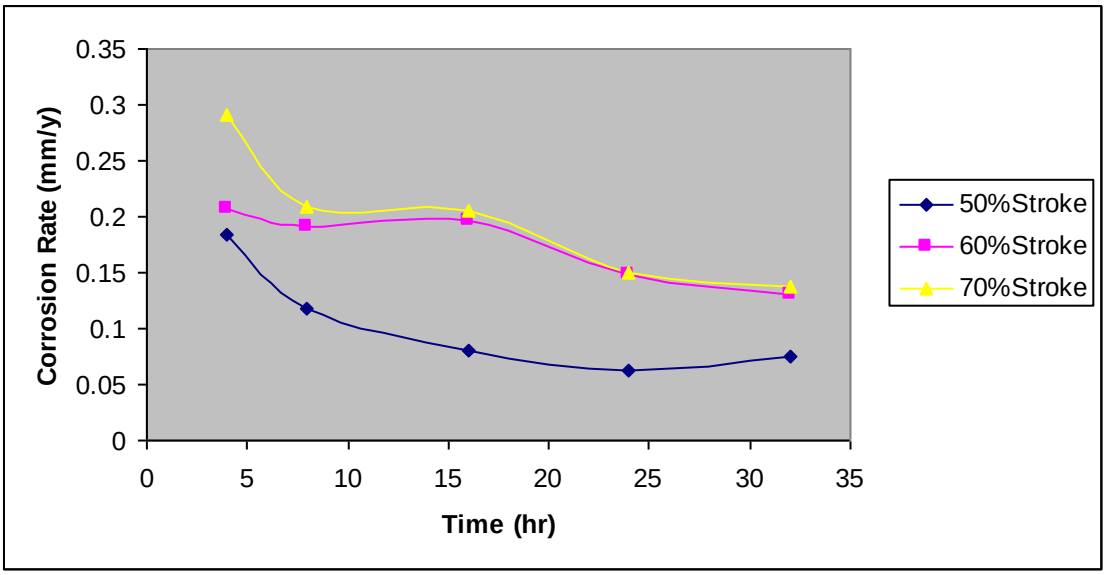

Figure 4.10(b): Corrosion rate vs time at various pump pressure, without ERSO (at 10g/*l* and 40^{o}C Conditions)

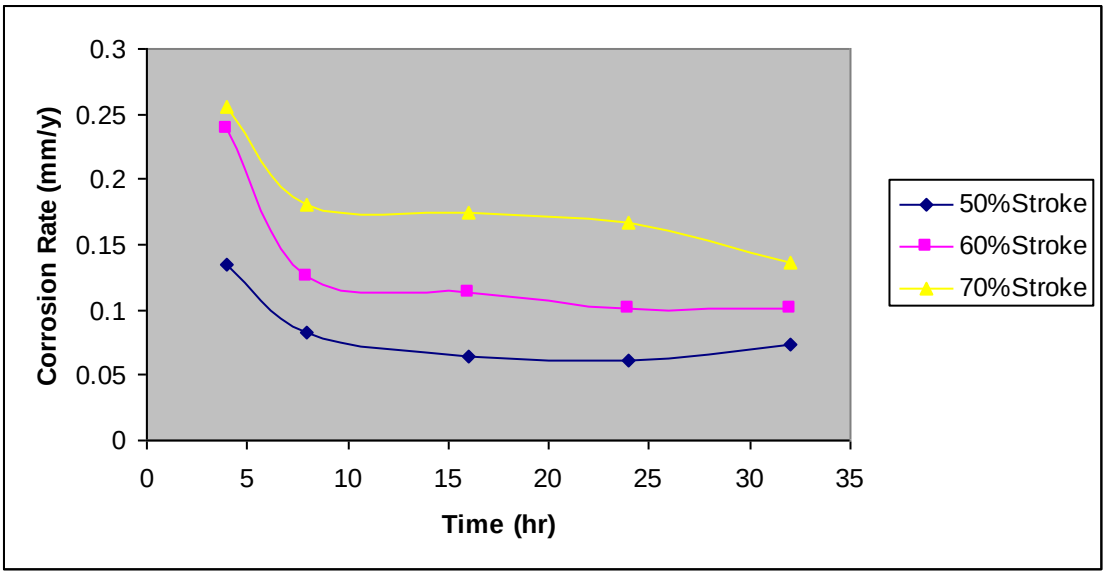

Figure 4.11(a): Corrosion rate vs time at various pump pressure, with ERSO (at 15g/*l* and 50^{o}C Conditions)

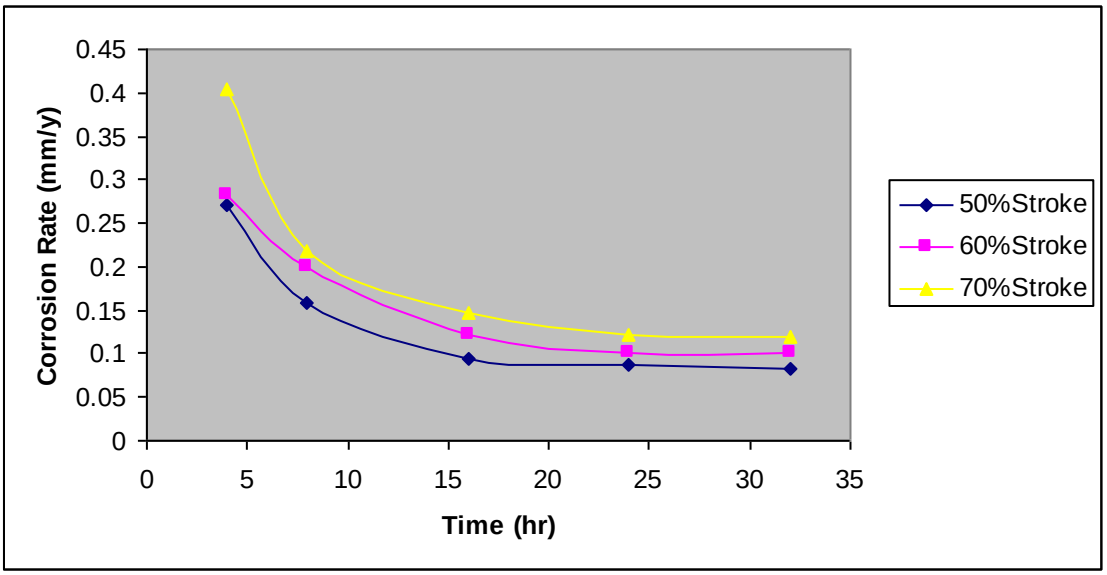

Figure 4.11(b): Corrosion rate vs time at various pump pressure, without ERSO (at 15g/*l* and 50^{o}C Conditions)

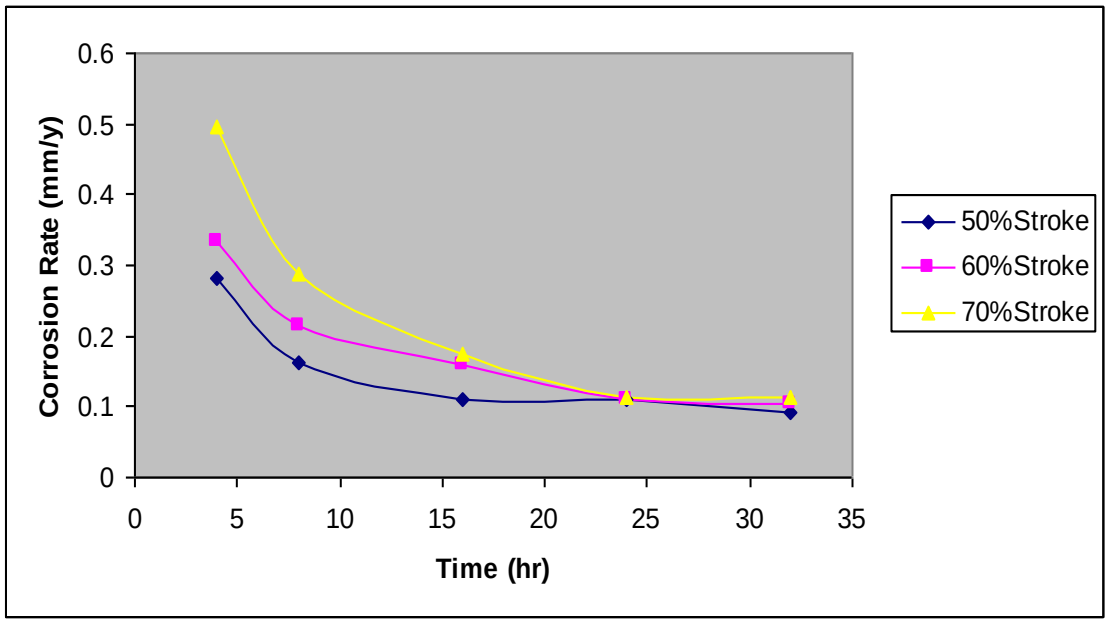

Figure 4.12(a): Corrosion rate vs time at various pump pressure, with ERSO (at 20g/*l* and 60^{o}C Conditions)

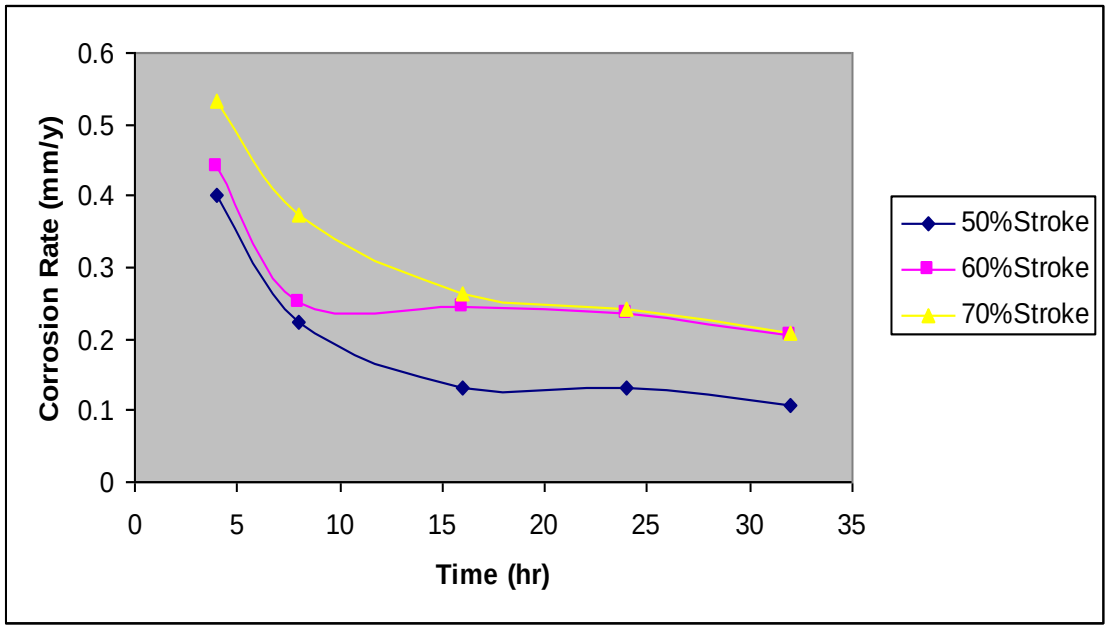

Figure 4.12(b): Corrosion rate vs time at various pump pressure, without ERSO (at 20g/*l* and 60^{o}C Conditions)

4.1.3 Results of electrochemical studies

The results of the potentiodynamic polarization are presented in figures 4.13 and 4.14, while the inhibition efficiencies for the samples are shown inTable 4.4. Also shown in figures 4.15 and 4.16 are the SEM images, while figures 4.17 and 4.18 show the FTIR spectra of the inhibitors.

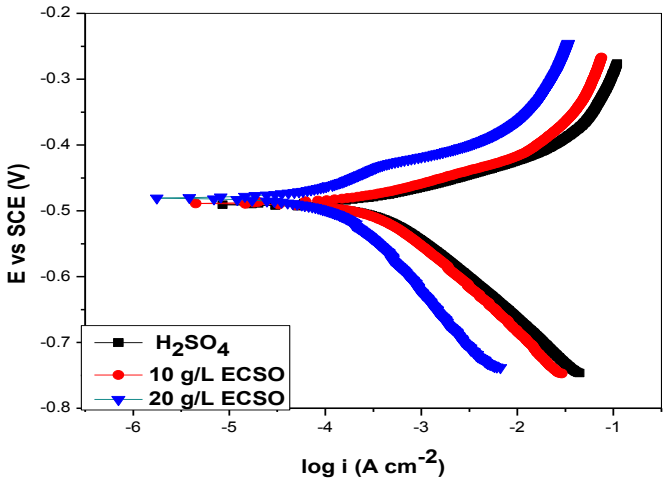

Figure 4.13: Potentiodynamic polarization curves of mildsteel in H_2SO_4 in the absence and presence of ECSO.

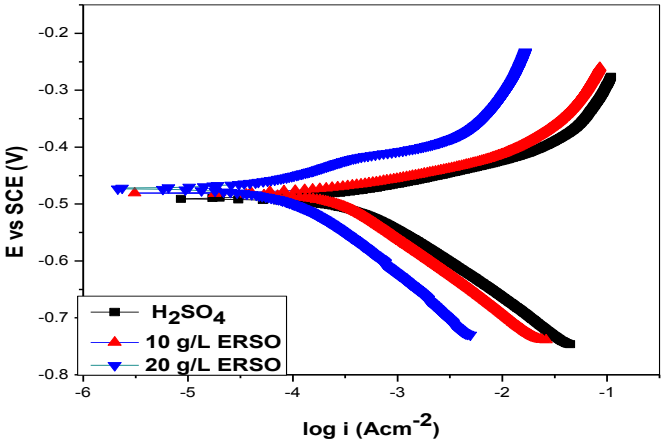

Figure 4.14: Potentiodynamic polarization curves of mildsteel in H_2SO_4 in the absence and presence of ERSO.

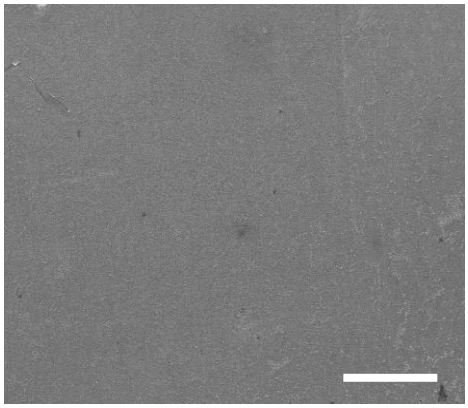

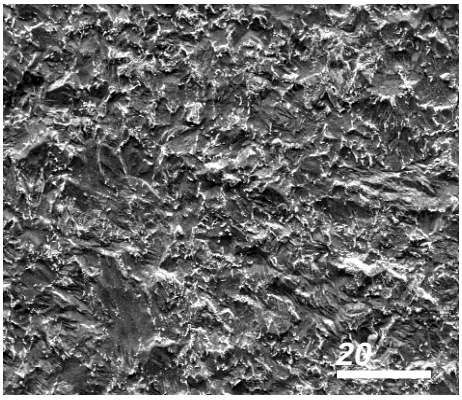

(a) As received (b) Without Inhibitor

Figure 4.15: SEM images in the absence of inhibitor

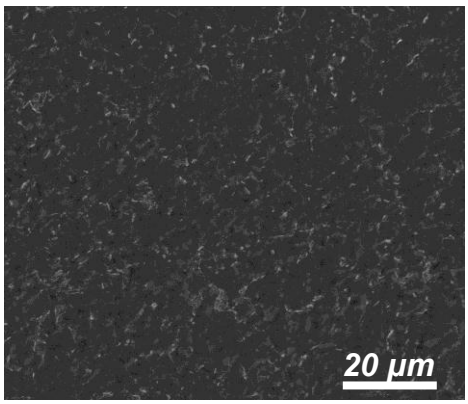

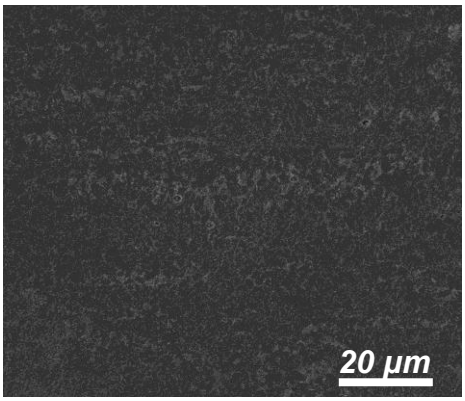

(a) ECSO (b) ERSO

Figure 4.16: SEM images in the presence of inhibitor

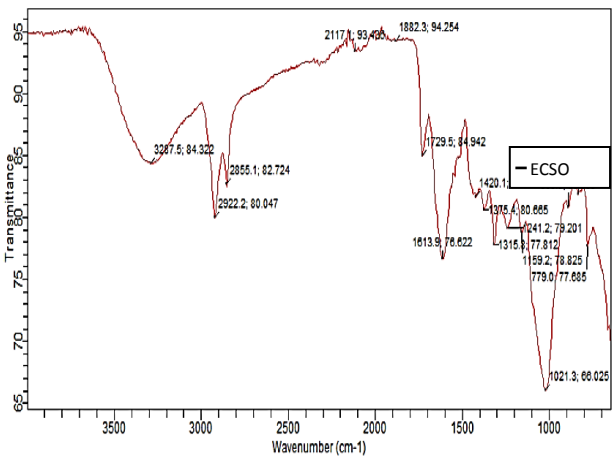

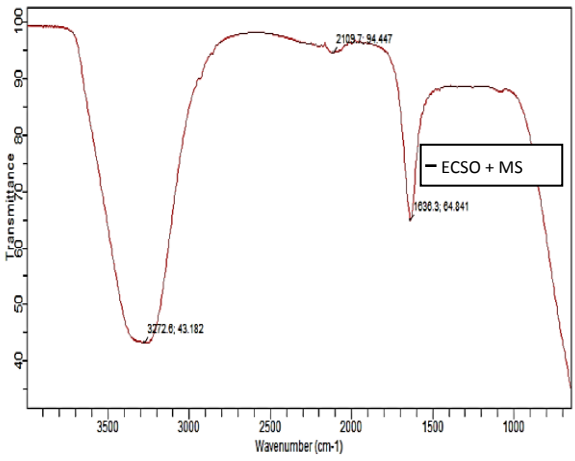

(a) ECSO (b) ECSO + MS

Figure 4.17: FTIR spectra of ECSO and surface film on mildsteel

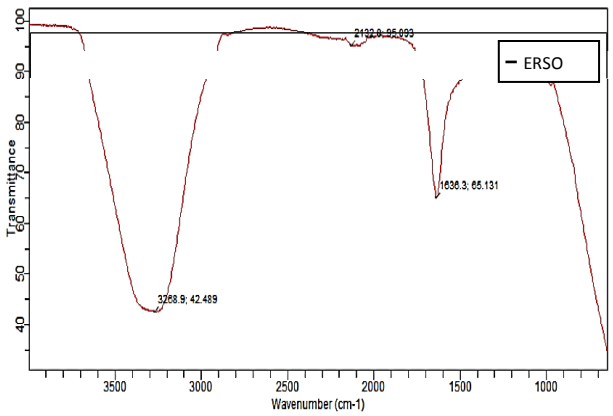

(a) ERSO

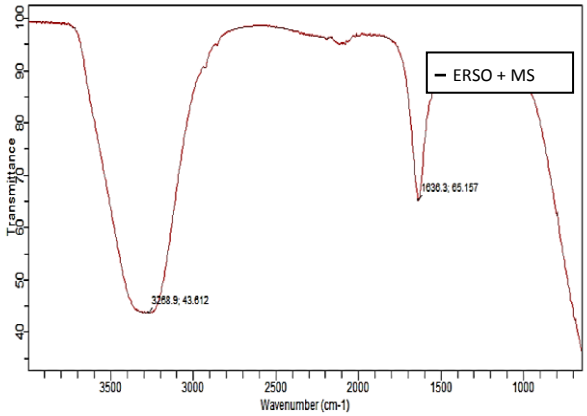

(b) ERSO + MS

Figure 4.18: FTIR spectra of ERSO and surface film on mildsteel

Table 4.4: Polarization parameters for mildsteel in H_2SO_4 environment in the absence and presence of ECSO and ERSO.

System	E_{corr}(mV)	I_{corr}(mAcm^{-2})	Θ	IE (%)
0.5M H_2SO_4	-496.40	1340		
10g/*l* ECSO	-491.30	698.20	0.434	47.90
20g/*l* ECSO	-456.40	329.70	0.909	75.40
10g/*l* ERSO	-478.60	678.90	0.419	49.30
20g/*l* ERSO	-489.20	245.40	0.890	81.70

4.1.4 Results of Thermodynamic Study

The results of thermodynamic study are presented in Table 4.5.

Table 4.5: thermodynamic parameters

Sample	**Time (hr)**	**ΔH (KJ/mol)**			**ΔS (KJ/mol/K)**			**– ΔG (KJ/mol)**		
		313K	***323K***	***333K***	***313K***	***323K***	***333K***	***313K***	***323K***	***333K***
A (ECSO)	***4.00***	2.00	2.06	2.12	0.200	0.206	0.212	60.600	64.478	68.476
	8.00	2.68	2.76	2.85	0.268	0.276	0.285	81.204	86.388	92.055
	16.00	3.57	3.69	3.80	0.357	0.369	0.380	108.171	115.497	122.740
	24.00	5.17	5.34	5.50	0.517	0.534	0.550	156.651	167.142	177.650
	32.00	6.52	6.73	6.94	0.652	0.673	0.694	197.556	210.649	224.162
B (ERSO)	***4.00***	1.70	1.76	1.81	0.170	0.176	0.181	51.510	55.088	58.463
	8.00	1.99	2.06	2.12	0.199	0.206	0.212	60.297	64.478	68.476
	16.00	2.39	2.47	2.55	0.239	0.247	0.255	72.417	77.311	82.365
	24.00	4.18	4.31	4.45	0.418	0.431	0.445	126.654	134.903	143.735
	32.00	4.69	4.84	4.99	0.469	0.484	0.499	142.107	151.492	161.177

4.1.5 Results of adsorption isotherm study

The results of isotherm study of the two conditions (with and without inhibitor) are placed side-by-side for proper comparison, and are presented in Figures 4.19-4.27 and Figures 4.28-4.36 for ECSO and ERSO respectively. The Langmuir constants generated are presented in Tables 4.6-4.8 for ECSO and Tables 4.9-4.11 for ERSO.

Also, results of Freundlich isotherm for ECSO and ERSO are presented in figures 4.37-4.45 and 4.46-4.54 respectively, and the values of the Freundlich factors are successively evaluated, and the results are presented in Tables 4.12-4.14 and Tables 4.15-4.17 for ECSO and ERSO accordingly.

Similarly, the results of Tempkin isotherm are presented in figures 4.55-4.56, while those of El-Awady isotherm are presented in figures 4.57-4.58. The Temkin and El-Awady parameters were computed and presented in Table 4.18. However, details of the preliminary isotherm data are presented in Appendix 5.

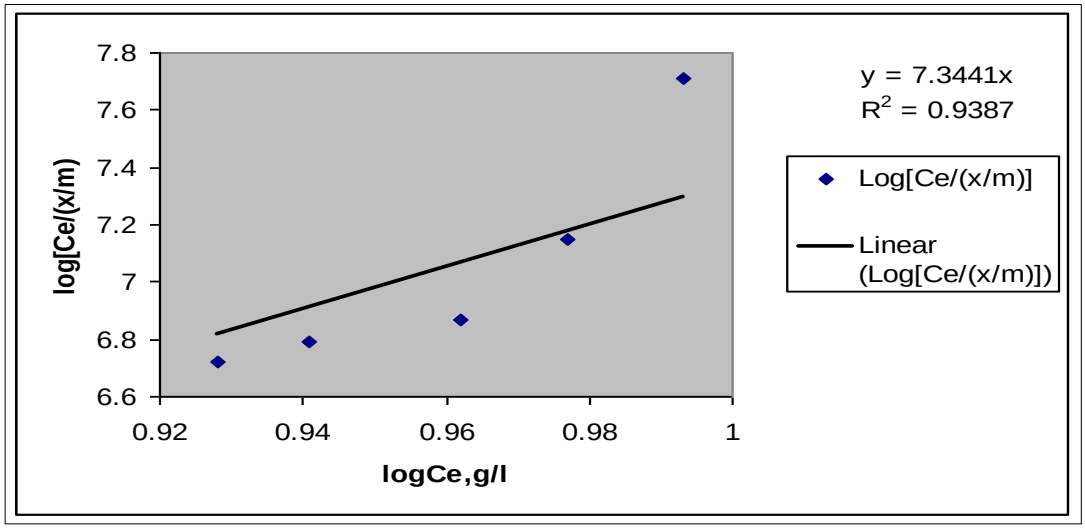

Figure 4.19(a): Langmuir plot for C_o=10g/*l* at 40^{o}C, 50% stroke with ECSO

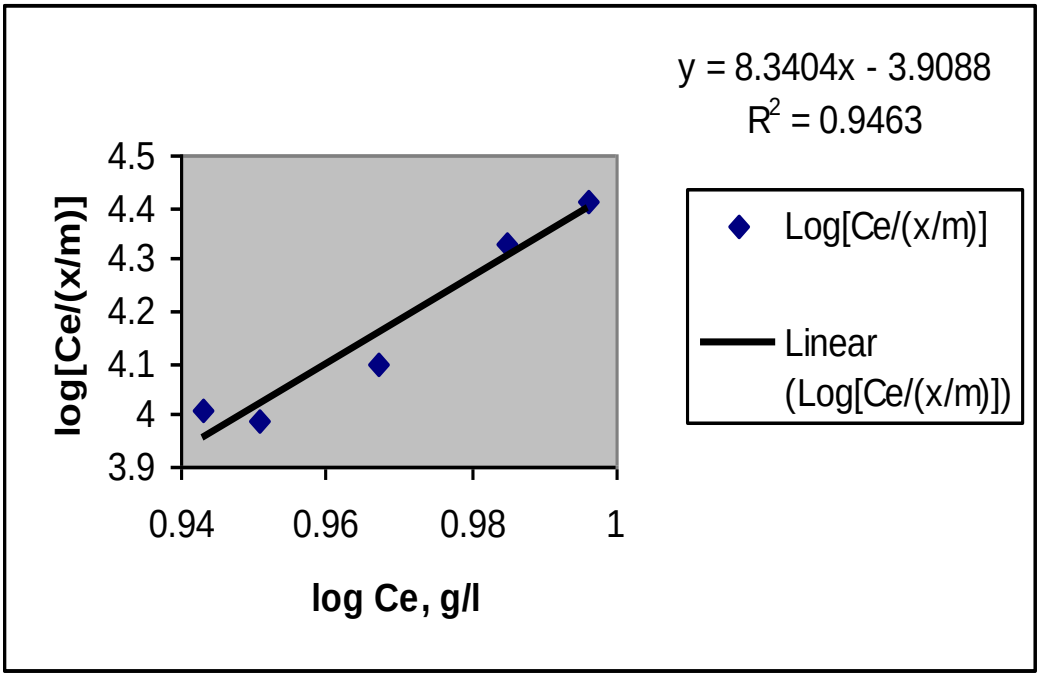

Figure 4.19(b): Langmuir plot for C_o=10g/*l* at 40°C, 50% stroke without ECSO

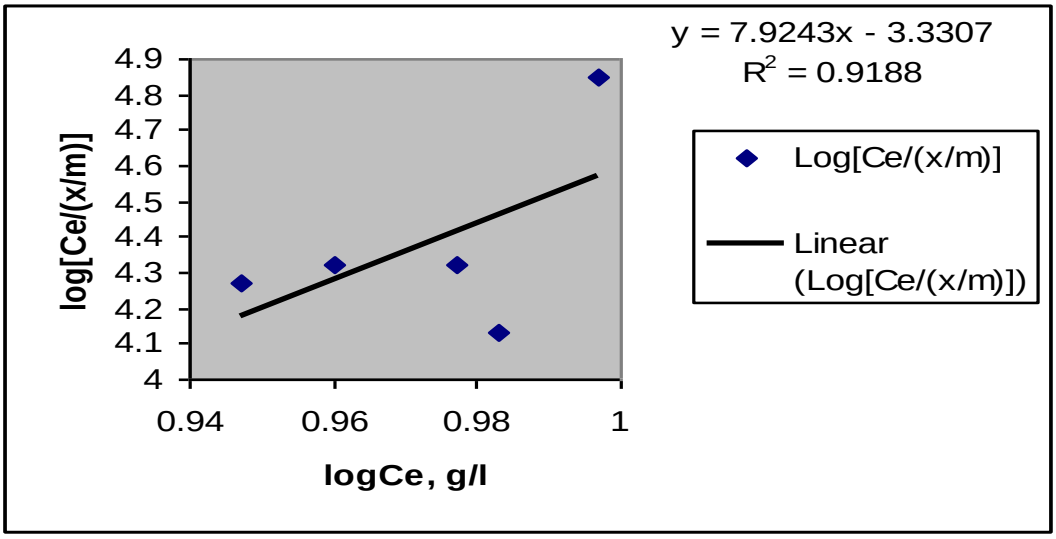

Figure 4.20(a): Langmuir plot for C_o=10g/*l* at 40°C, 60% stroke with ECSO

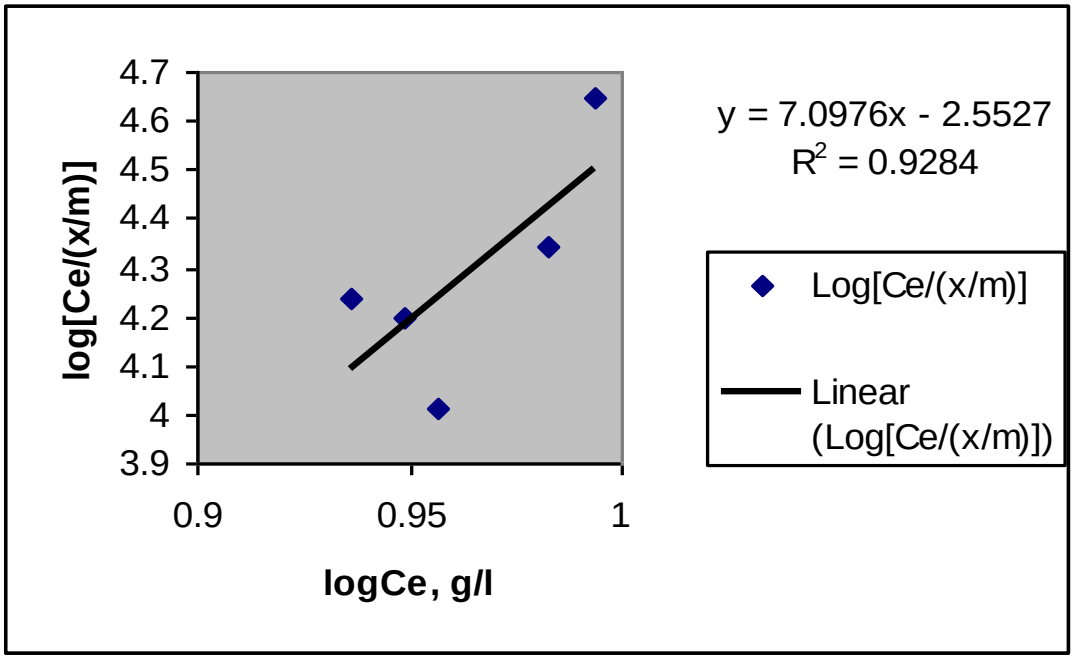

Figure 4.20(b): Langmuir plot for C_o=10g/*l* at 40°C, 60% stroke without ECSO

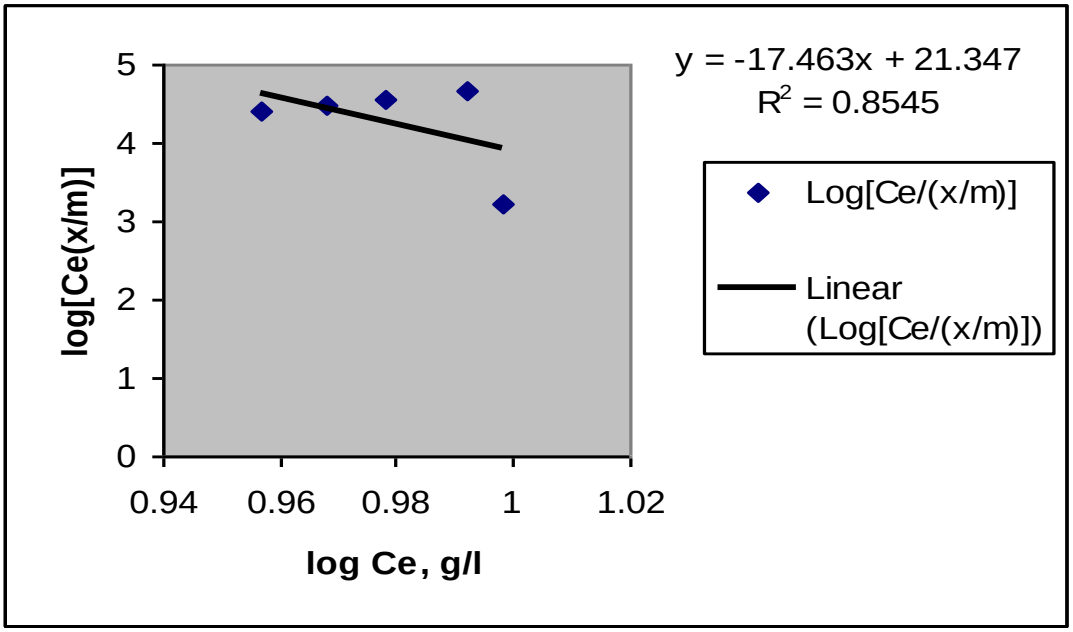

Figure 4.21(a): Langmuir plot for C_o=10g/*l* at 40°C, 70% stroke with ECSO

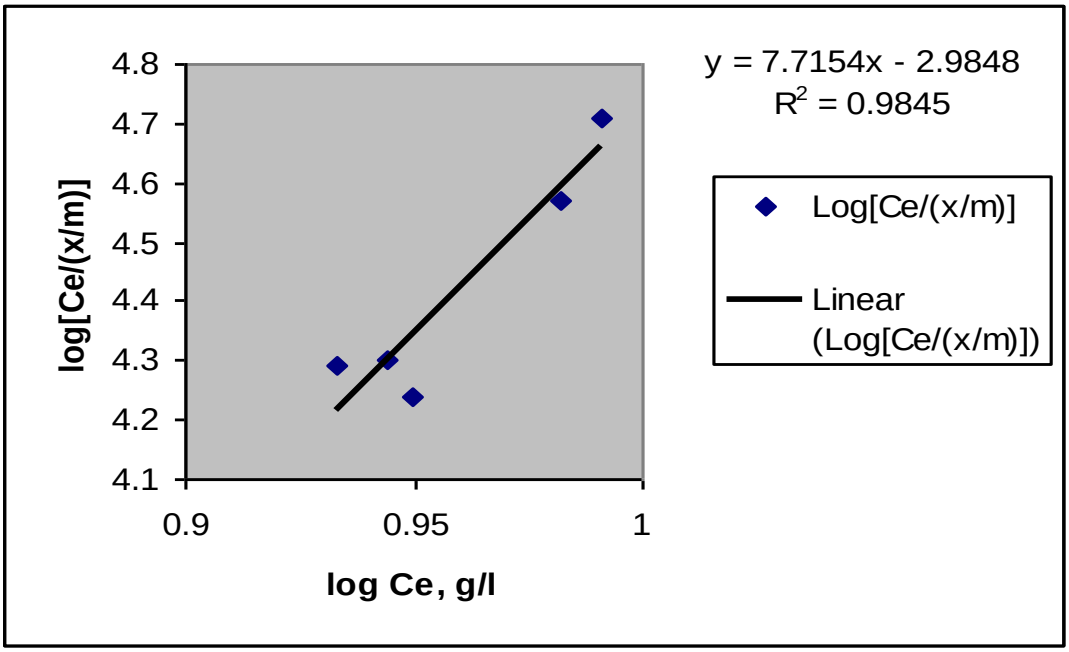

Figure 4.21(b): Langmuir plot for C_o=10g/*l* at 40°C, 70% stroke without ECSO

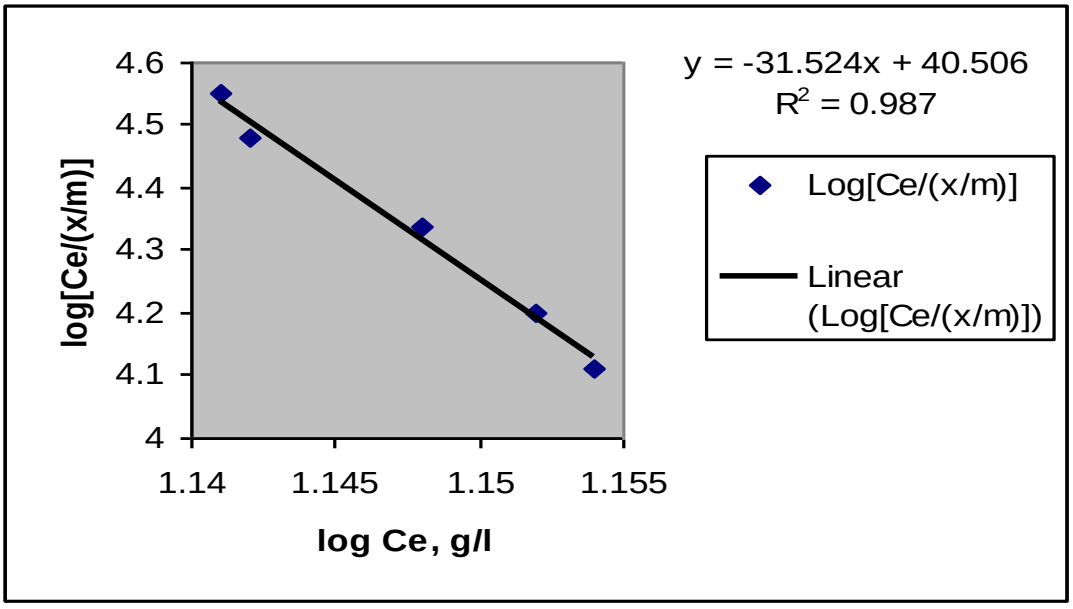

Figure 4.22(a): Langmuir plot for C_o=15g/*l* at 50°C, 50% stroke with ECSO

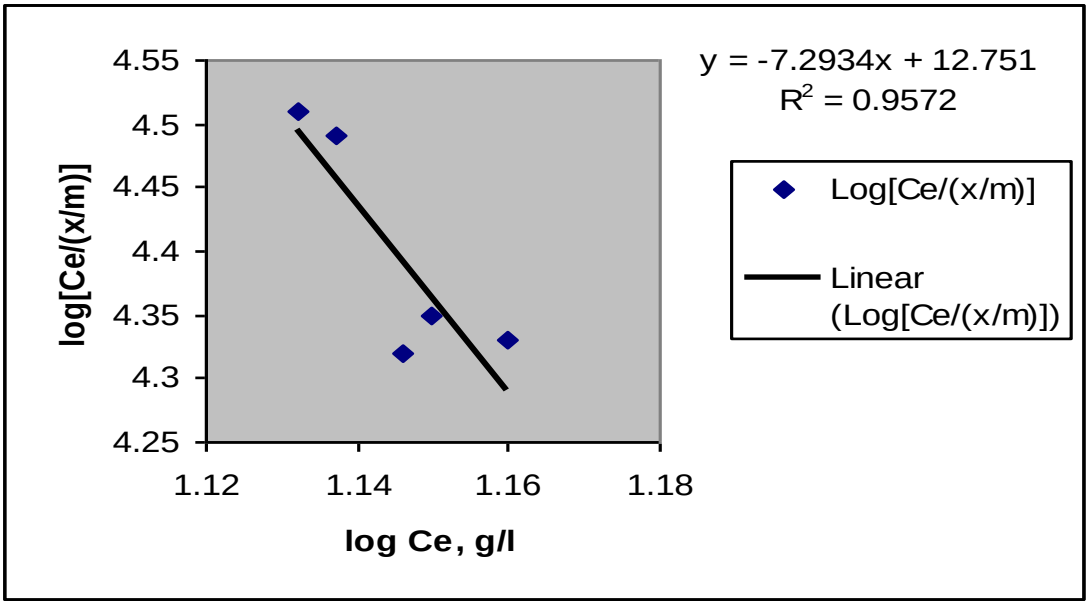

Figure 4.22(b): Langmuir plot for C_o=15g/*l* at 50°C, 50% stroke without ECSO

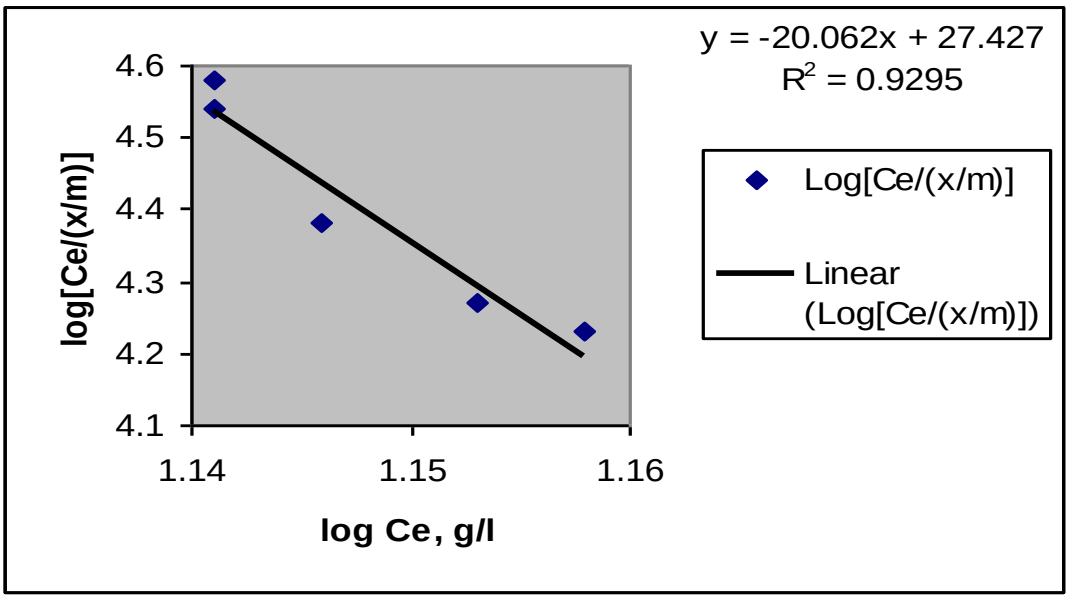

Figure 4.23(a): Langmuir plot for C_o=15g/*l* at 50°C, 60% stroke with ECSO

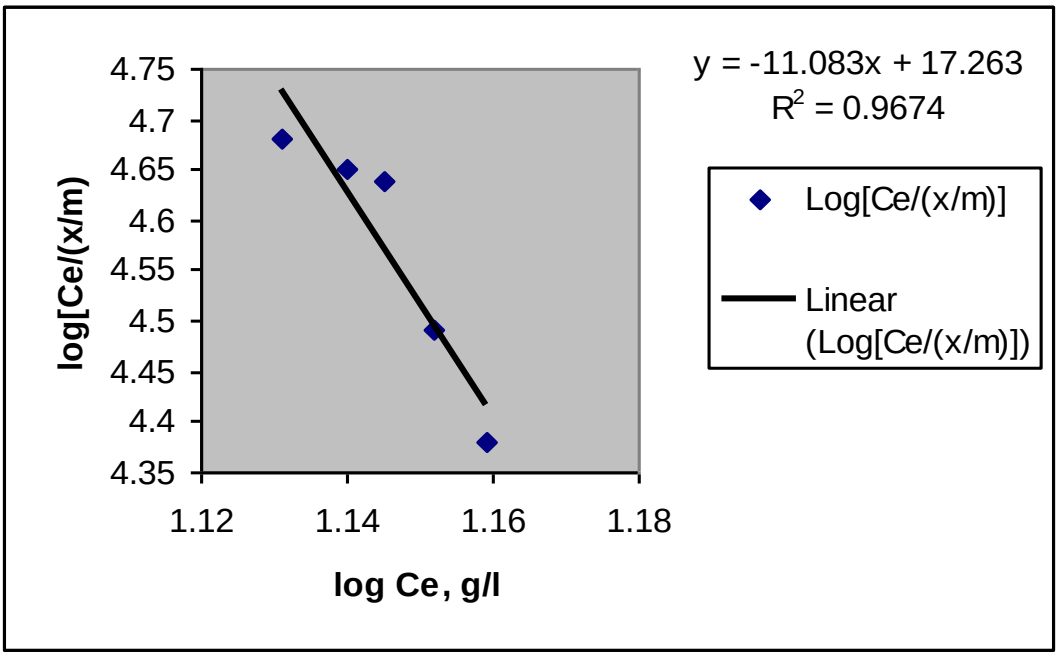

Figure 4.23(b): Langmuir plot for C_o=15g/*l* at 50°C, 60% stroke without ECSO

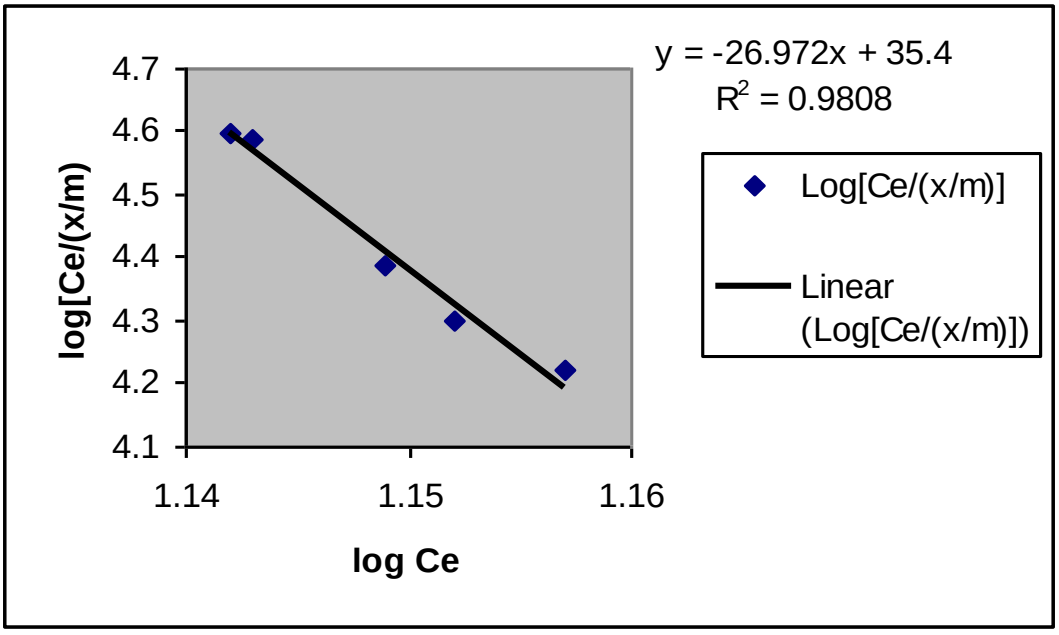

Figure 4.24(a): Langmuir plot for C_o=15g/*l* at 50°C, 70% stroke with ECSO

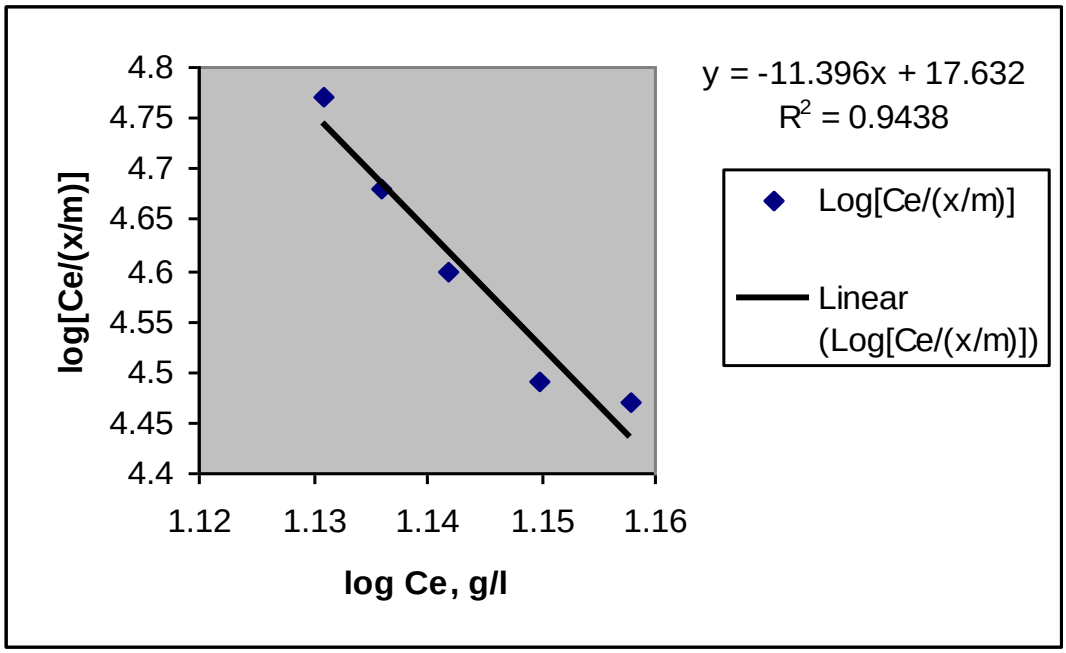

Figure 4.24(b): Langmuir plot for C_o=15g/*l* at 50°C, 70% stroke without ECSO

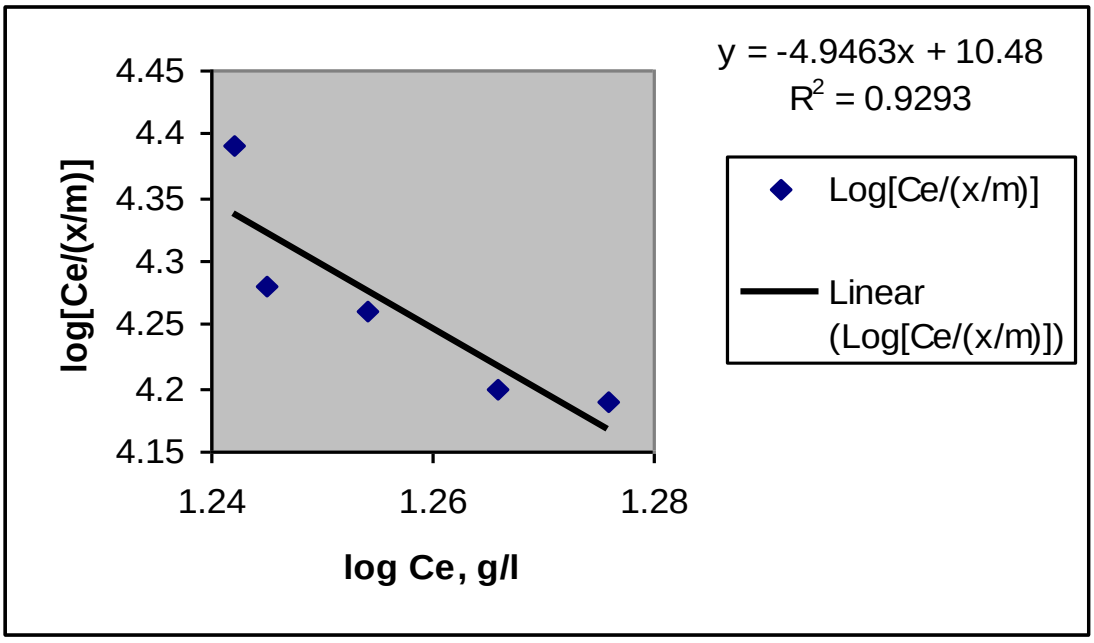

Figure 4.25(a): Langmuir plot for C_o=20g/*l* at 60°C, 50% stroke with ECSO

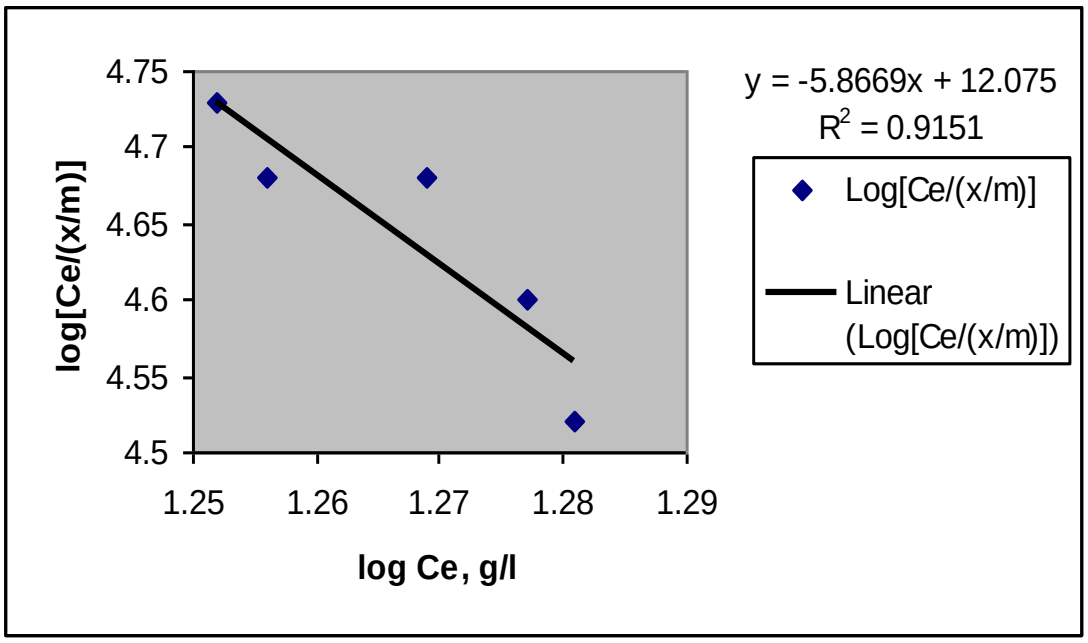

Figure 4.25(b): Langmuir plot for C_o=20g/*l* at 60°C, 50% stroke without ECSO

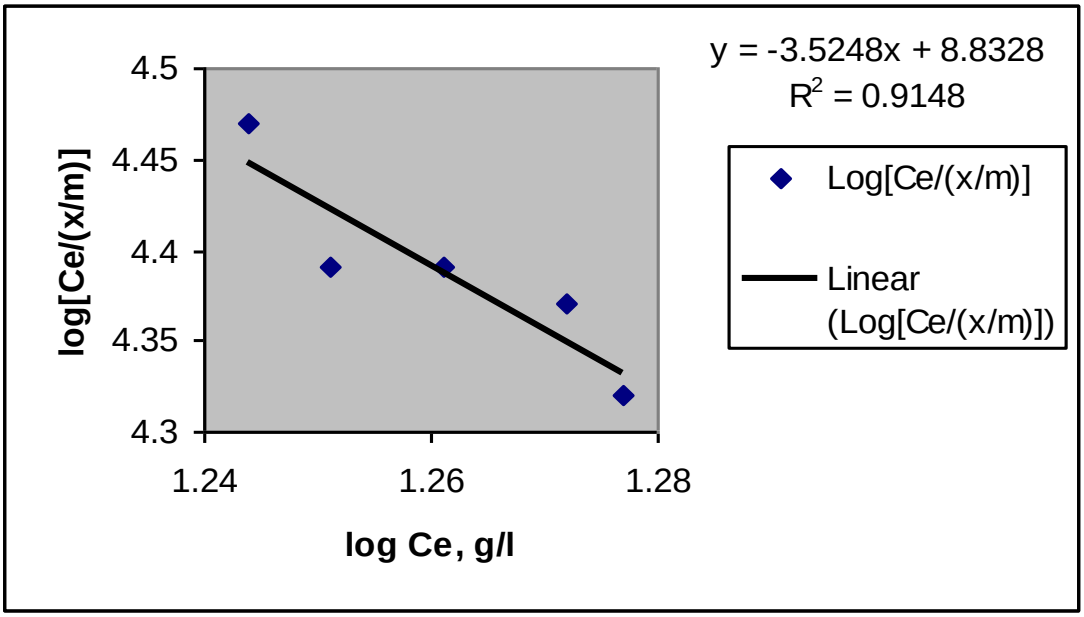

Figure 4.26(a): Langmuir plot for C_o=20g/*l* at 60°C, 60% stroke with ECSO

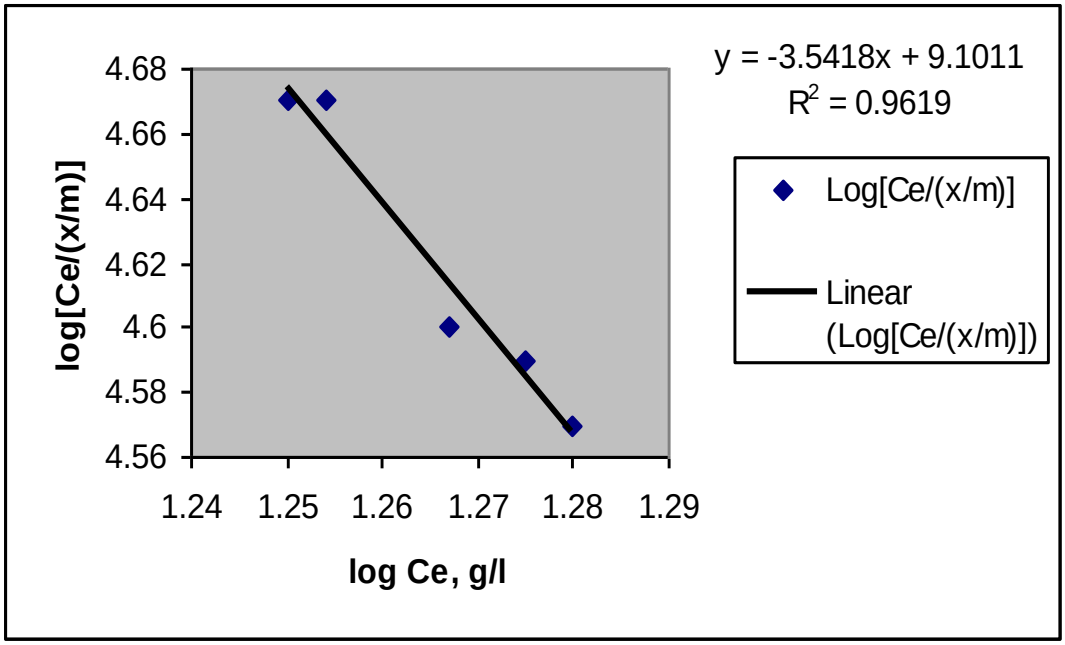

Figure 4.26(b): Langmuir plot for C_o=20g/*l* at 60°C, 60% stroke without ECSO

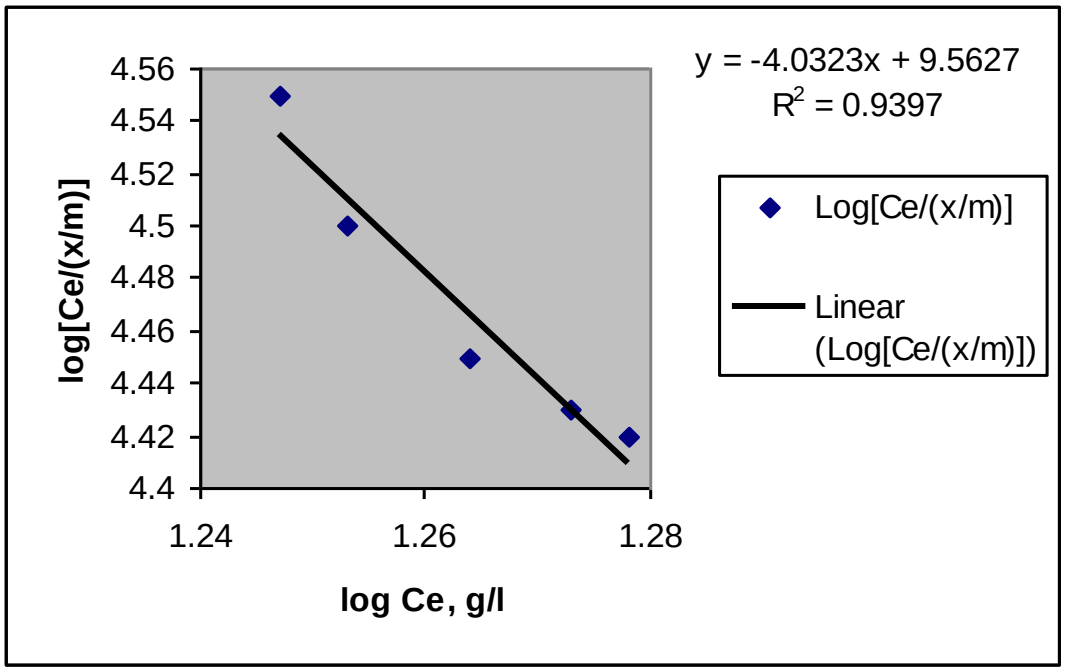

Figure 4.27(a): Langmuir plot for C_o=20g/*l* at 60°C, 70% stroke with ECSO

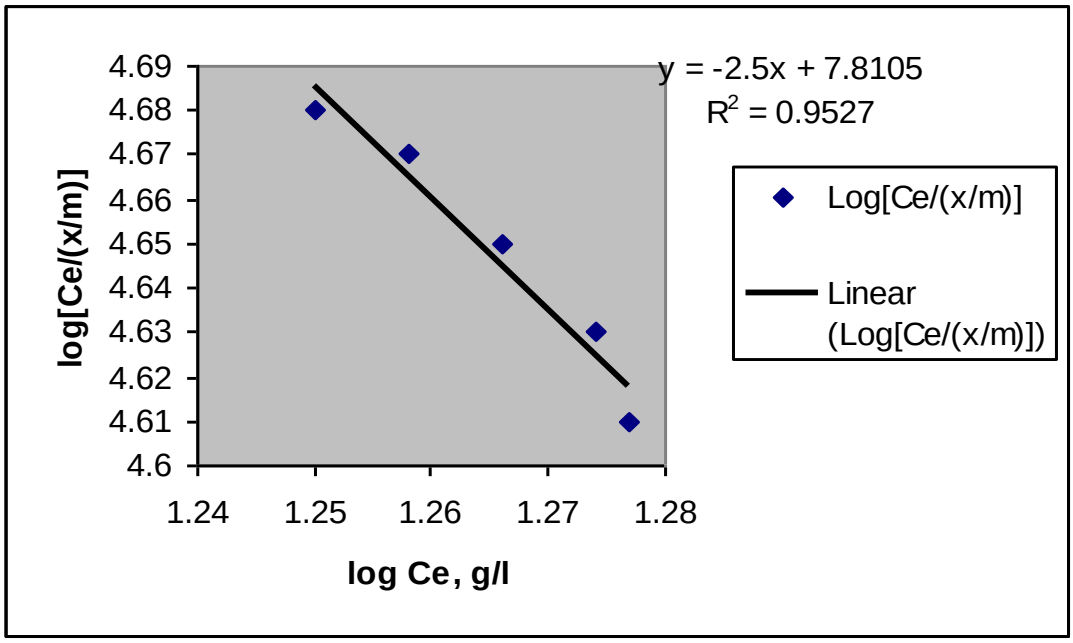

Figure 4.27(b): Langmuir plot for C_o=20g/*l* at 60°C, 70% stroke without ECSO

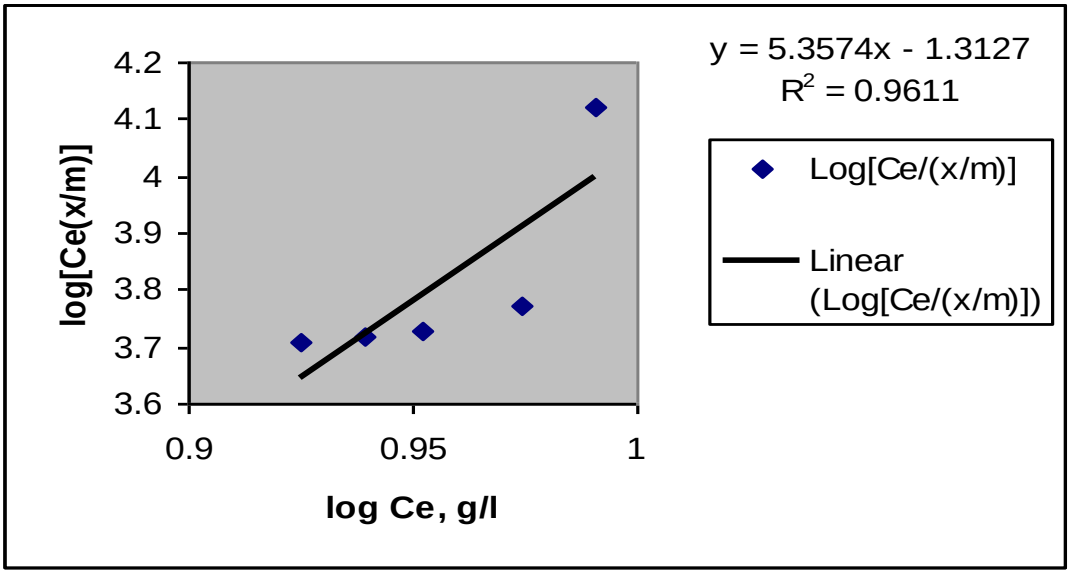

Fig. 4.28(a): Langmuir plot for C_o=10g/*l* at 40°C, 50% stroke with ERSO

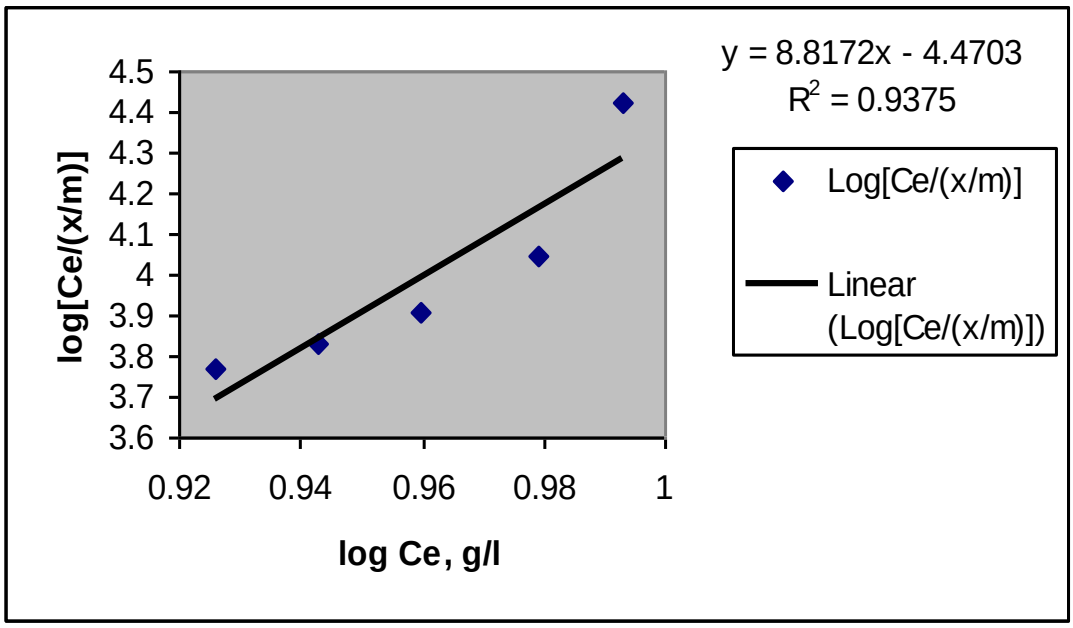

Figure 4.28(b): Langmuir plot for C_o=10g/*l* at 40°C, 50% stroke without ERSO

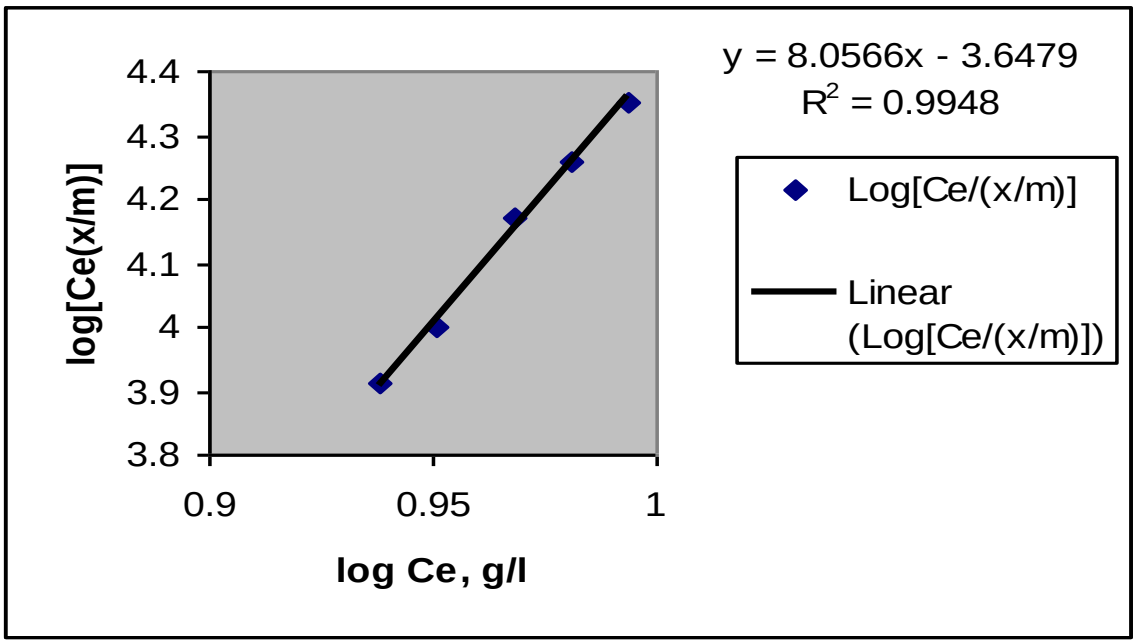

Figure 4.29(a): Langmuir plot for C_o=10g/*l* at 40°C, 60% stroke with ERSO

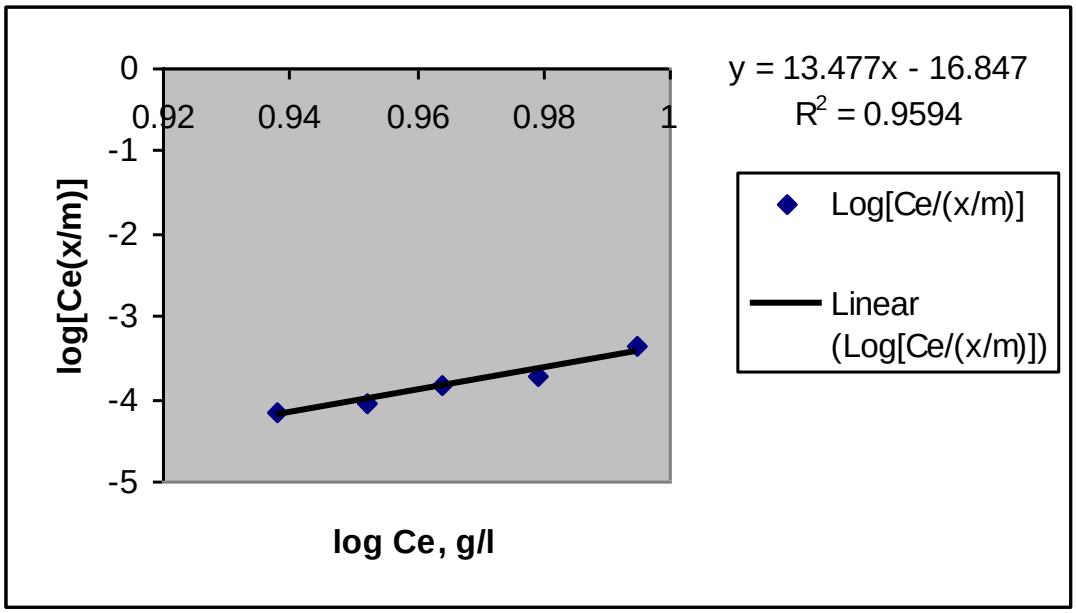

Figure 4.29(b): Langmuir plot for C_o=10g/*l* at 40°C, 60% stroke without ERSO

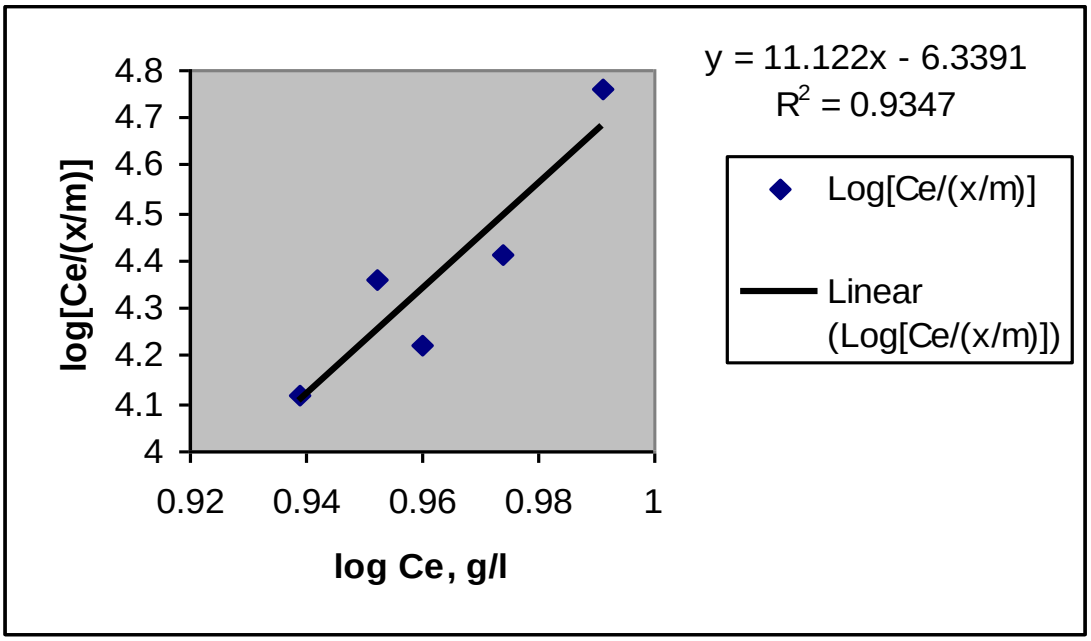

Figure 4.30(a): Langmuir plot for C_o=10g/*l* at 40°C, 70% stroke with ERSO

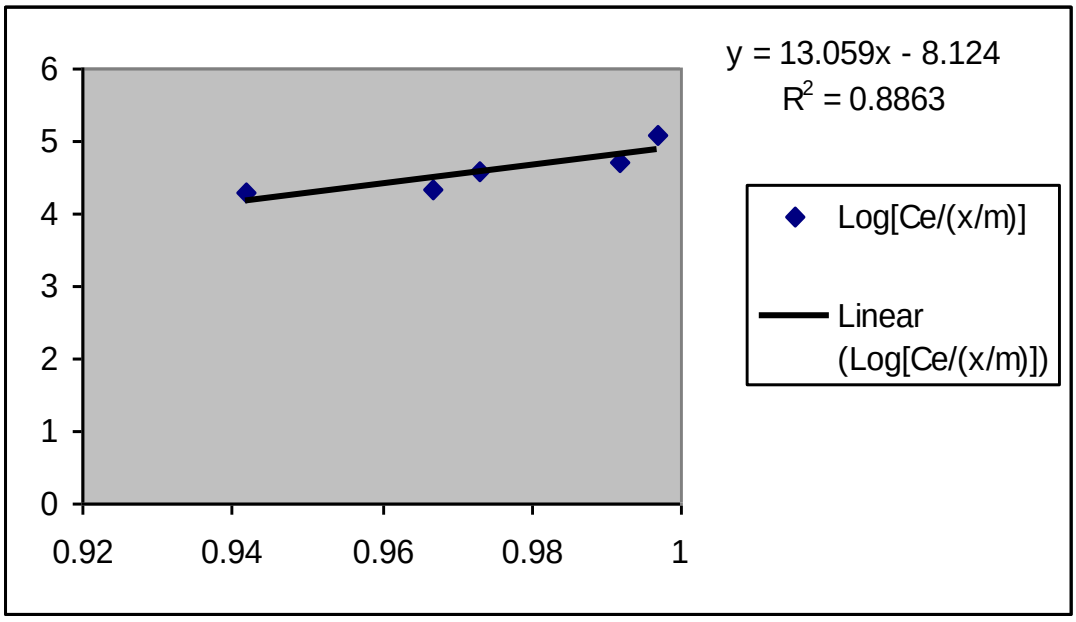

Figure 4.30(b): Langmuir plot for C_o=10g/*l* at 40°C, 70% stroke without ERSO

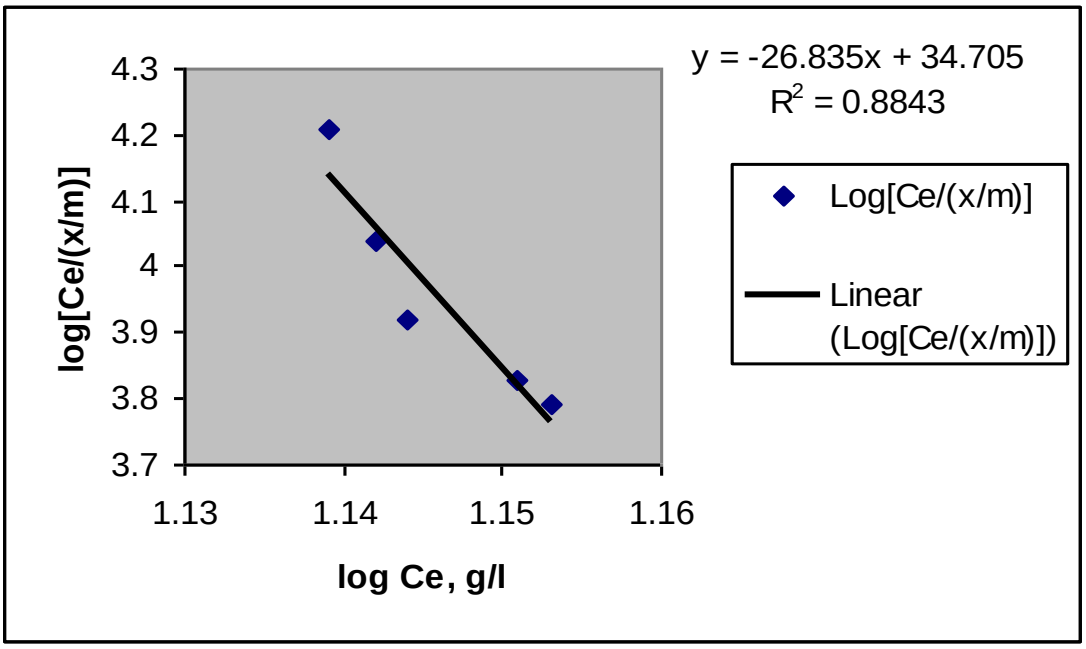

Figure 4.31(a): Langmuir plot for C_o=15g/*l* at 50°C, 50% stroke with ERSO

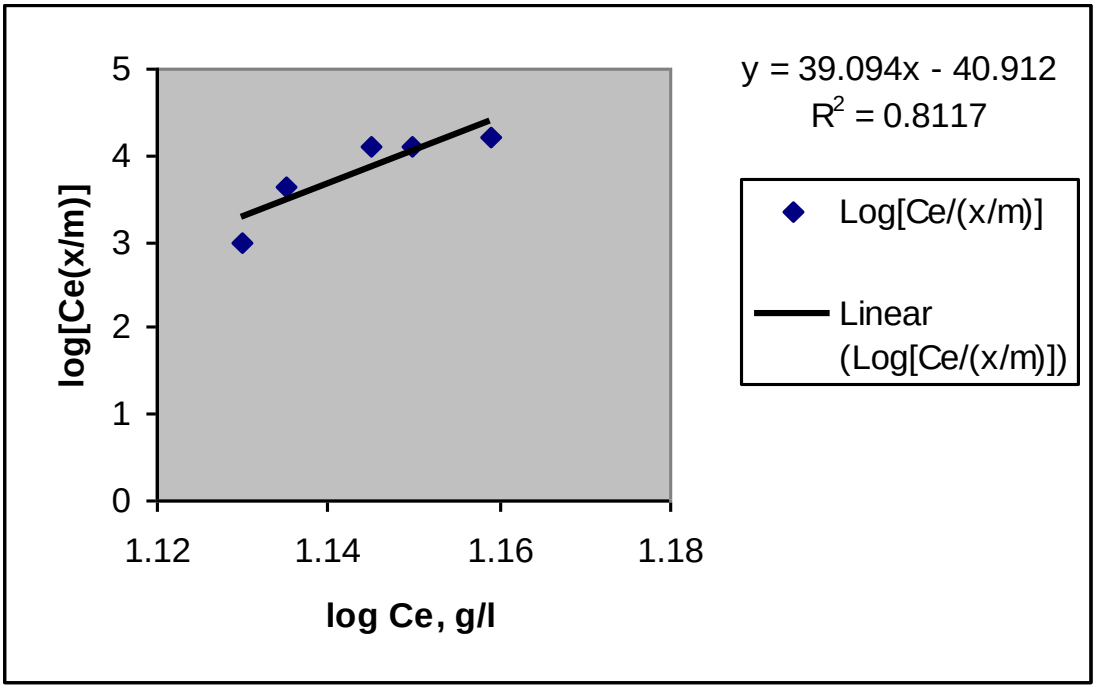

Figure 4.31(b): Langmuir plot for C_o=15g/*l* at 50°C, 50% stroke without ERSO

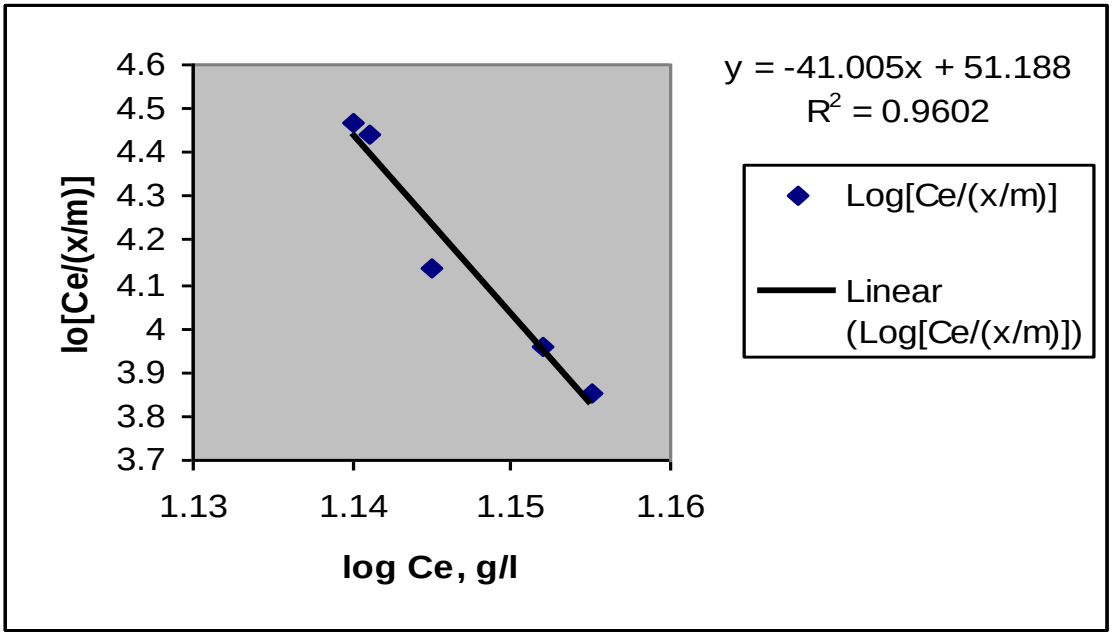

Figure 4.32(a): Langmuir plot for C_o=15g/*l* at 50°C, 60% stroke with ERSO

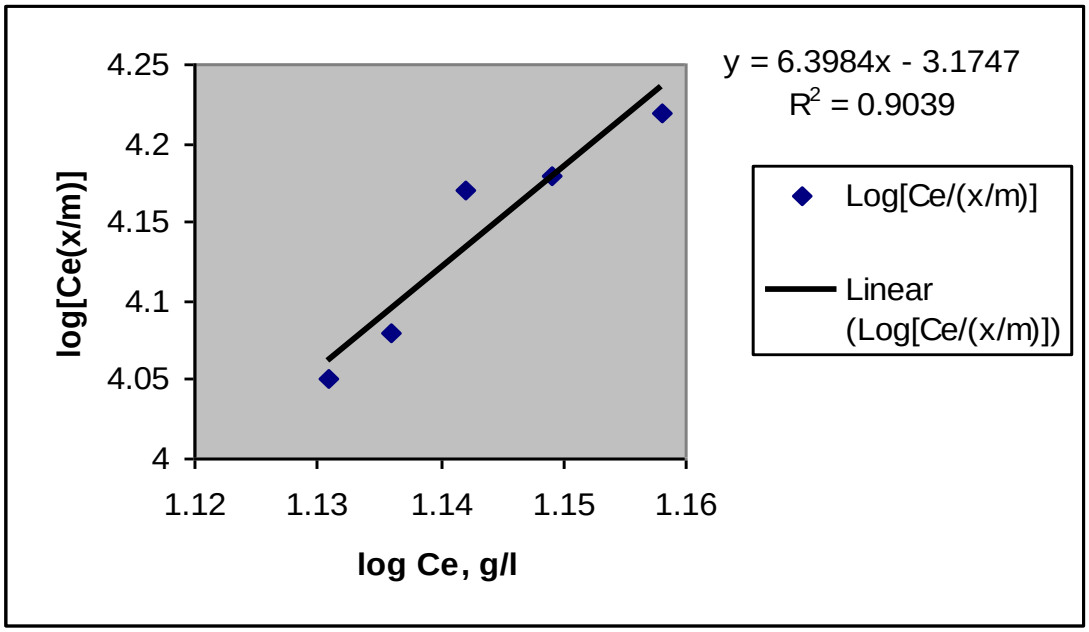

Figure 4.32(b): Langmuir plot for C_o=15g/*l* at 50°C, 60% stroke without ERSO

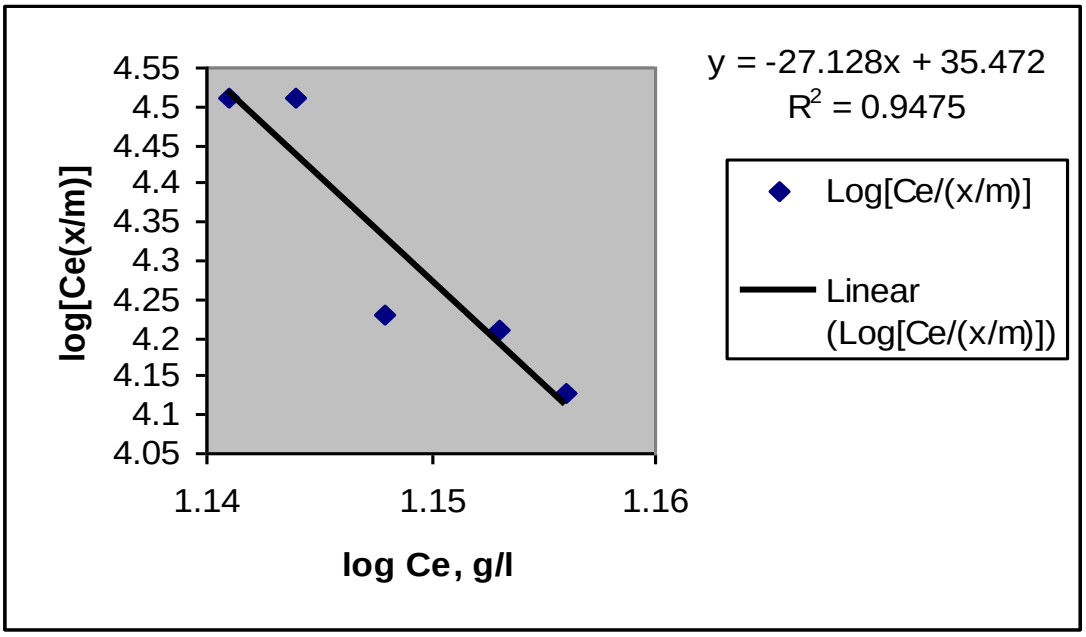

Figure 4.33(a): Langmuir plot for C_o=15g/*l* at 50°C, 70% stroke with ERSO

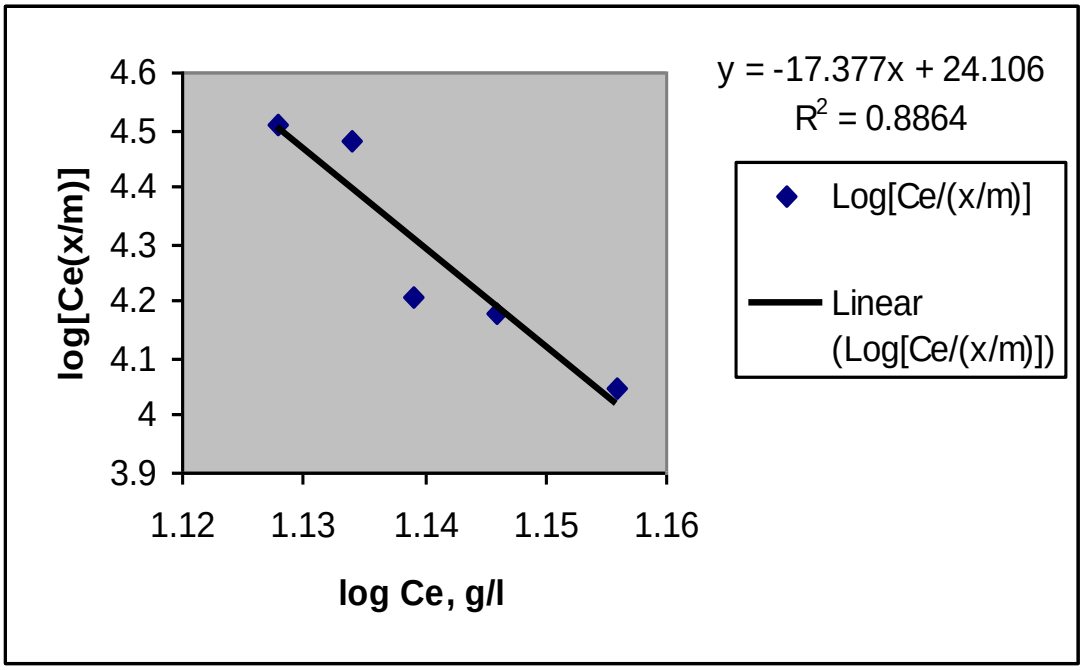

Figure 4.33(b): Langmuir plot for C_o=15g/*l* at 50°C, 70% stroke without ERSO

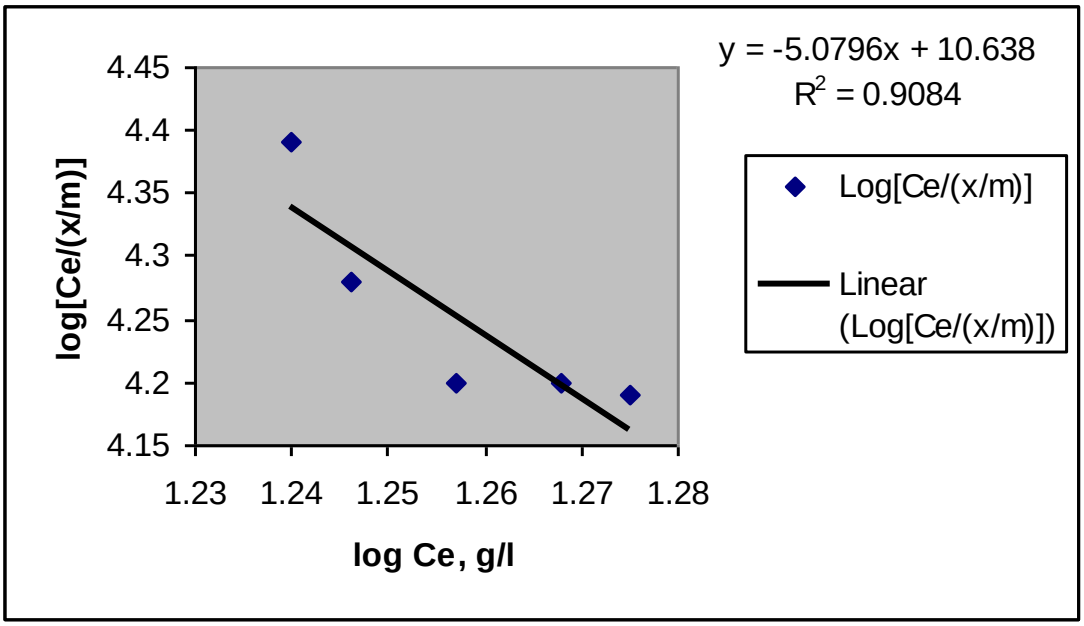

Figure 4.34(a): Langmuir plot for C_o=20g/*l* at 60°C, 50% stroke with ERSO

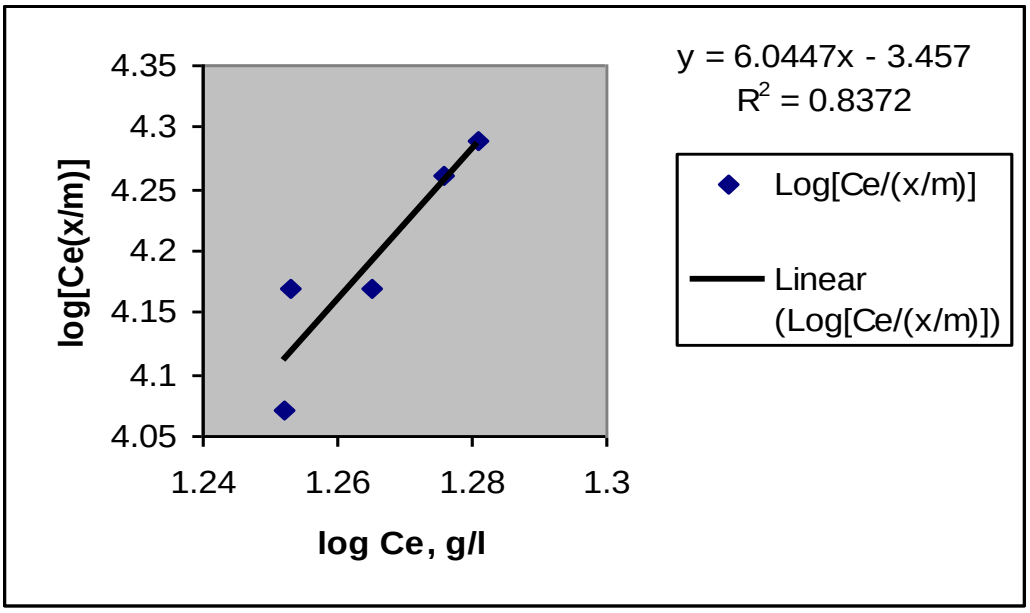

Figure 4.34(b): Langmuir plot for C_o=20g/*l* at 60°C, 50% stroke without ERSO

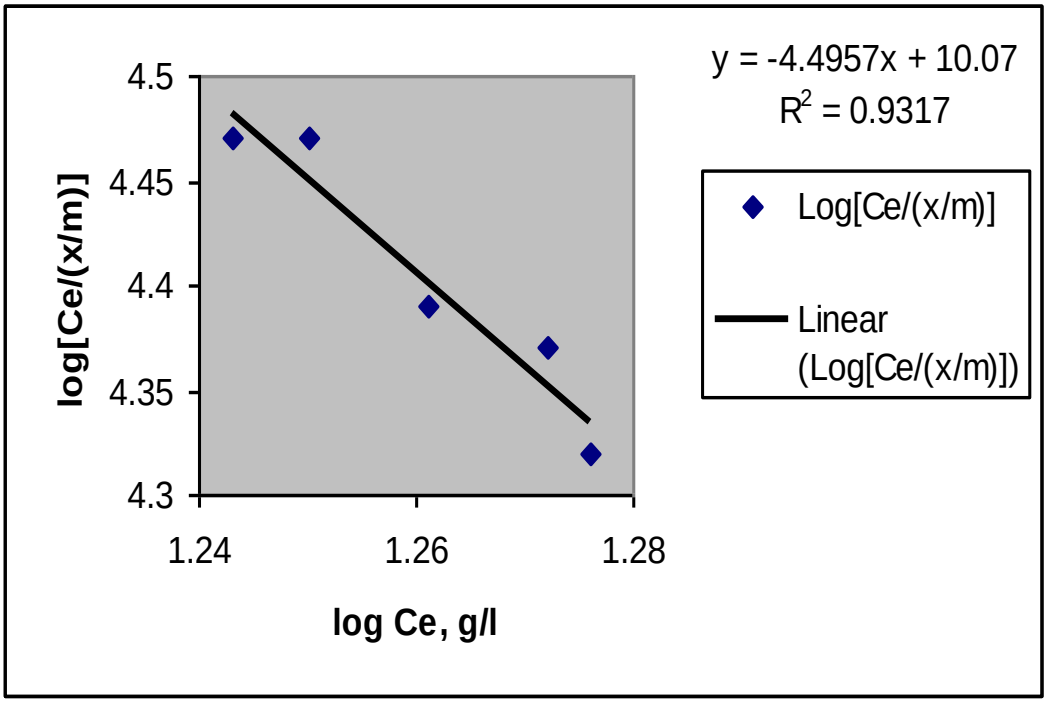

Figure 4.35(a): Langmuir plot for C_o=20g/*l* at 60°C, 60% stroke with ERSO

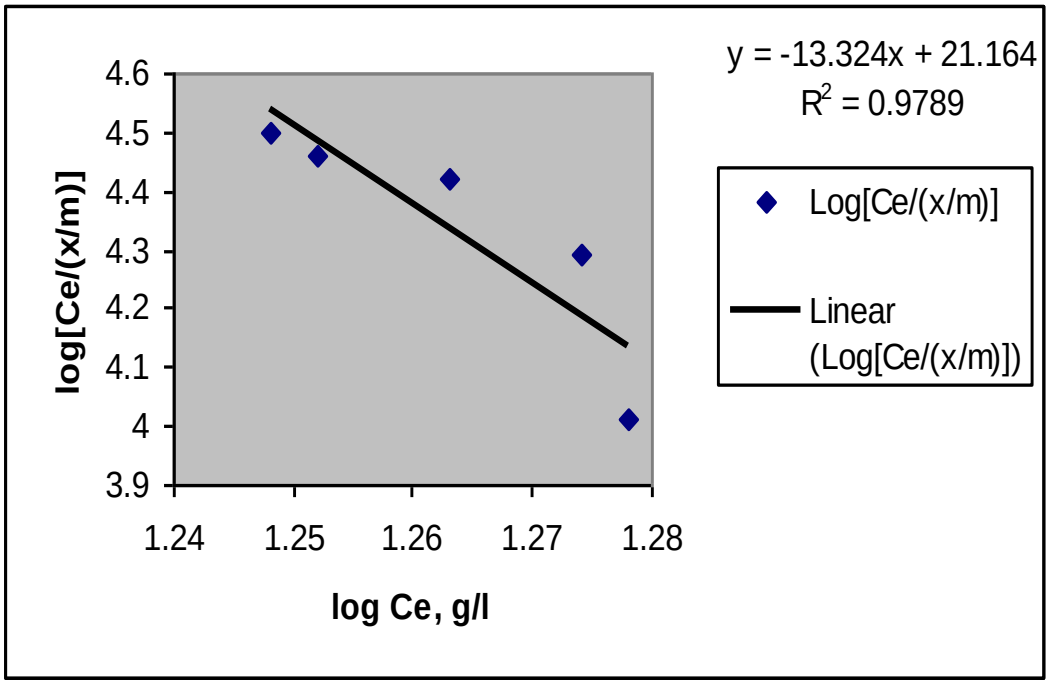

Figure 4.35(b): Langmuir plot for C_o=20g/*l* at 60°C, 60% stroke without ERSO

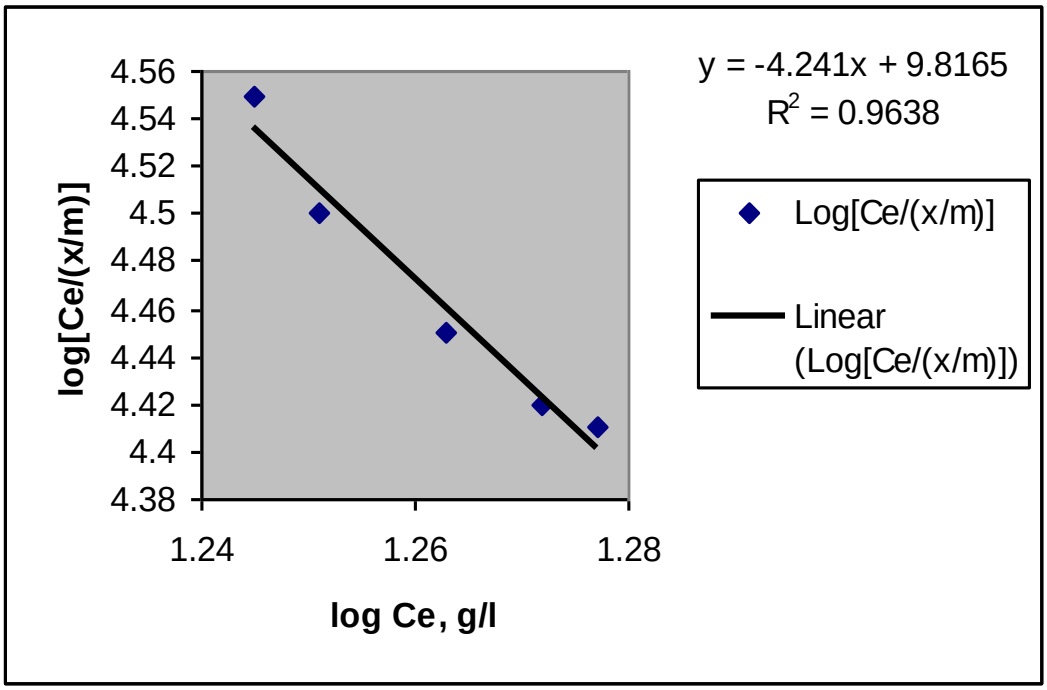

Figure 4.36(a): Langmuir plot for C_o=20g/*l* at 60°C, 70% stroke with ERSO

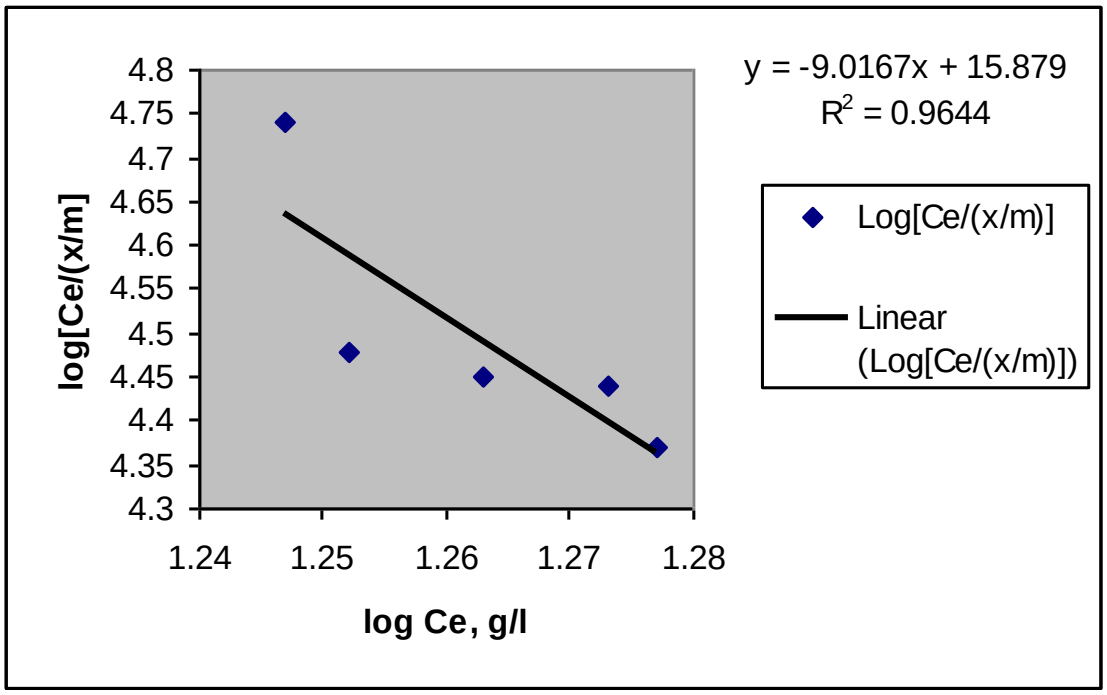

Figure 4.36(b): Langmuir plot for C_o=20g/*l* at 60°C, 70% stroke without ERSO

Table 4.6: Langmuir Isotherm Parameters for ECSO at 10g/*l* and 40°C

Dosage (%Stroke)	With inhibitor			Without inhibitor		
	a ($x10^4$)	b	R^2	a ($x10^4$)	b	R^2
50	0.14	-0.125	0.9387	0.14	-0.129	0.9284
60	0.12	-0.129	0.9463	0.06	-0.118	0.8545
70	1.08	-0.143	0.9188	0.13	-0.143	0.9845

Table 4.7: Langmuir Isotherm Parameters for ECSO at 15g/*l* and 50°C

Dosage (%Stroke)	With Inhibitor			Without Inhibitor		
	a ($x10^4$)	b	R^2	a ($x10^4$)	b	R^2
50	0.03	-0.069	0.9870	-0.09	-0.048	0.9674
60	-0.14	-0.074	0.9572	-0.04	-0.045	0.9808
70	0.05	-0.064	0.9295	-0.09	-0.364	0.9438

Table 4.8: Langmuir isotherm parameters for ECSO at 20g/*l* and 60ºC

Dosage (%Stroke)	With inhibitor			Without inhibitor		
	a ($x10^4$)	b	R^2	a ($x10^4$)	b	R^2
50	-0.20	-0.042	0.9293	-1.00	-0.28	0.9619
60	-0.17	-0.036	0.9195	-10.00	-0.25	0.9397
70	-0.28	-0.044	0.9148	-5.50	-0.40	0.9527

Table 4.9: Langmuir isotherm parameters for ERSO at 10g/*l* and 40ºC

Dosage (%Stroke)	With inhibitor			Without inhibitor		
	a ($x10^4$)	b	R^2	a ($x10^4$)	b	R^2
50	0.19	-0.125	0.9611	0.07	-0.111	0.9594
60	0.11	-0.400	0.9375	0.09	-0.167	0.9347
70	0.12	-0.143	0.9948	0.08	-0.121	0.8863

Table 4.10: Langmuir isotherm parameters for ERSO at 15g/*l* and 50ºC

Dosage (%Stroke)	With inhibitor			Without inhibitor		
	a ($x10^4$)	b	R^2	a ($x10^4$)	b	R^2
50	-0.04	-0.071	0.8843	0.16	-0.200	0.9039
60	0.03	-0.062	0.8117	-0.04	-0.067	0.9475
70	-0.02	-0.069	0.9602	-0.06	-0.045	0.8864

Table 4.11: Langmuir isotherm parameters for ERSO at 20g/*l* and 60ºC

Dosage (%Stroke)	With Inhibitor			Without Inhibitor		
	a ($x10^4$)	b	R^2	a ($x10^4$)	b	R^2
50	-0.20	-0.050	0.9084	-0.08	-0.200	0.9789
60	0.17	-0.040	0.8372	-0.24	-0.034	0.9638
70	-0.22	-0.044	0.9317	-0.11	-0.056	0.9644

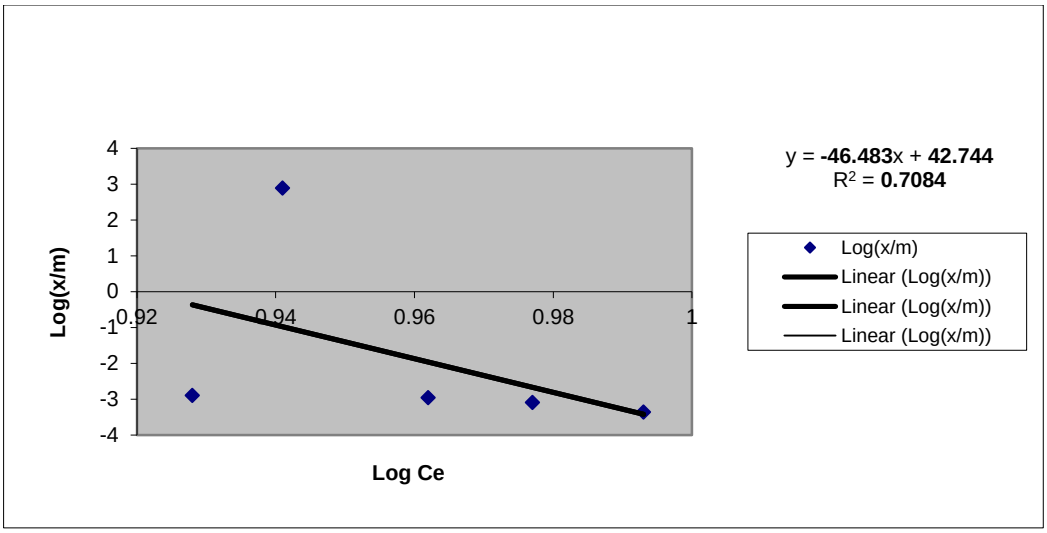

Figure 4.37(a): Linearized Freundlich plot for C_o=10g/*l* at 40°C, 50% stroke with ECSO

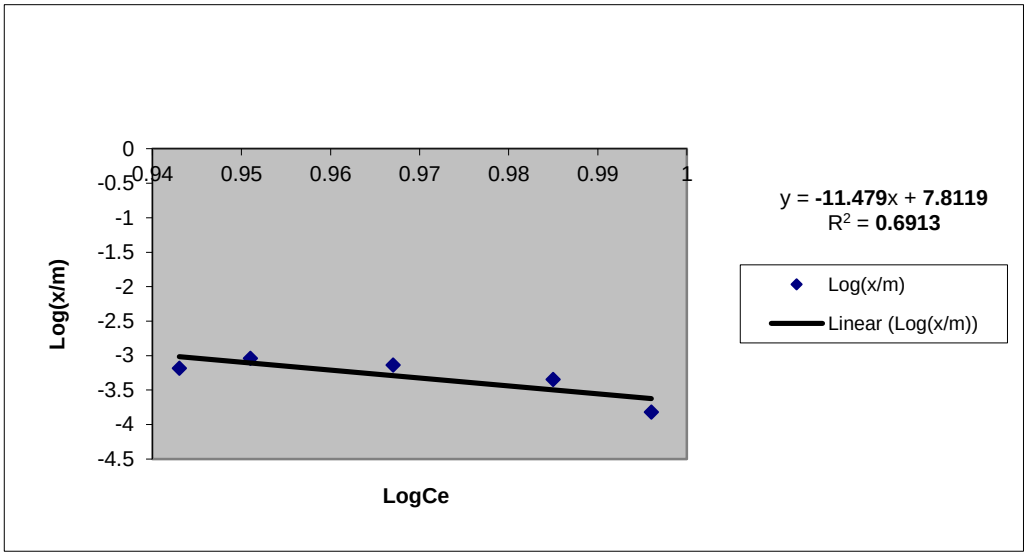

Figure 4.37(b): Linearized Freundlich plot for C_o=10g/*l* at 40°C, 50% stroke without ECSO

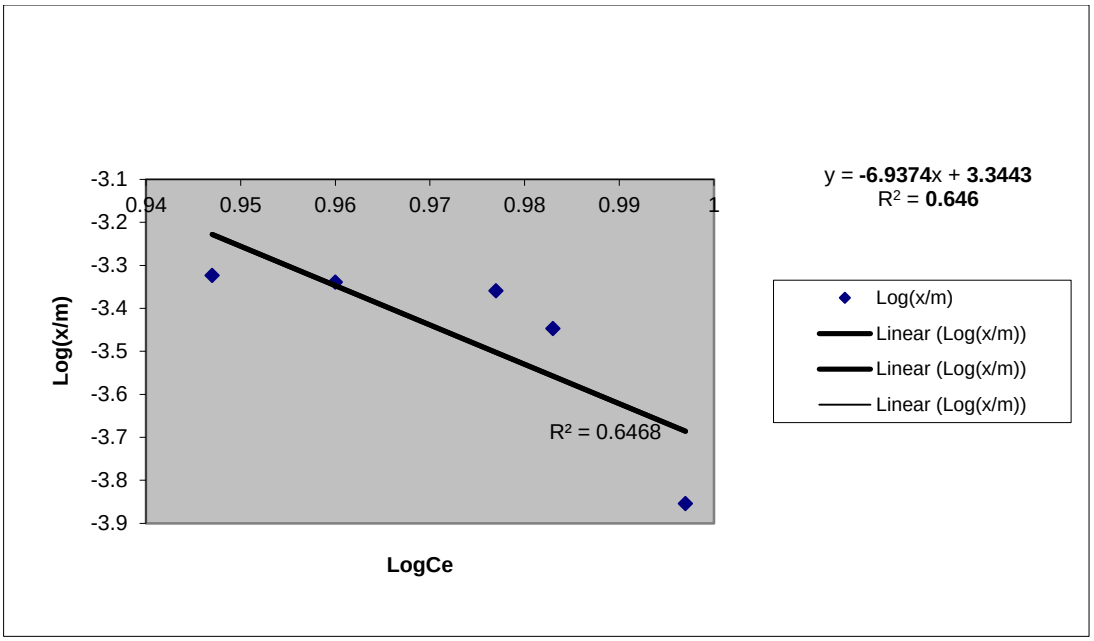

Figure 4.38(a): Linearized Freundlich plot for C_o=10g/*l* at 40°C, 60% stroke with ECSO

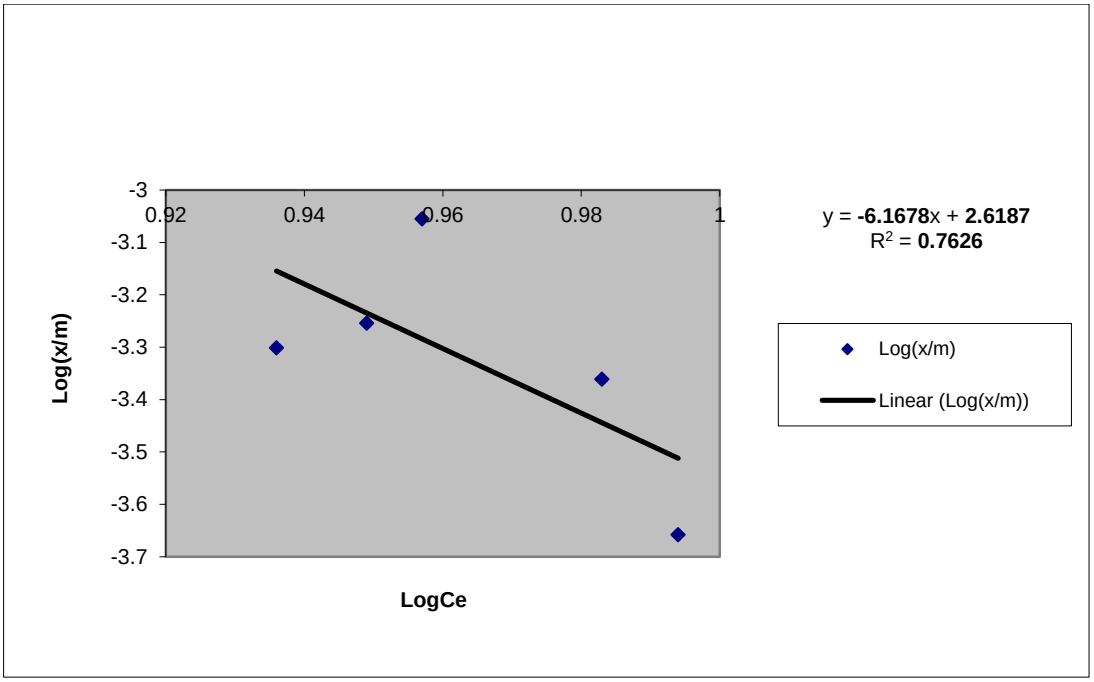

Figure 4.38(b): Linearized Freundlich plot for C_o=10g/*l* at 40°C, 60% stroke without ECSO

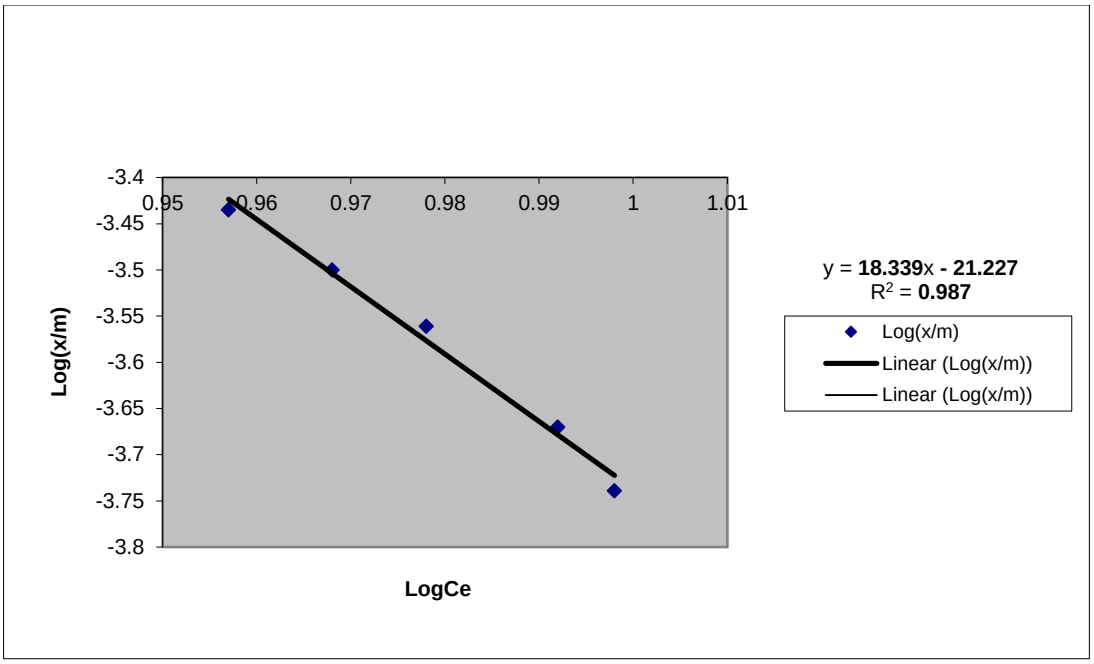

Figure 4.39(a): Linearized Freundlich plot for C_o=10g/*l* at 40ºC, 70% stroke with ECSO

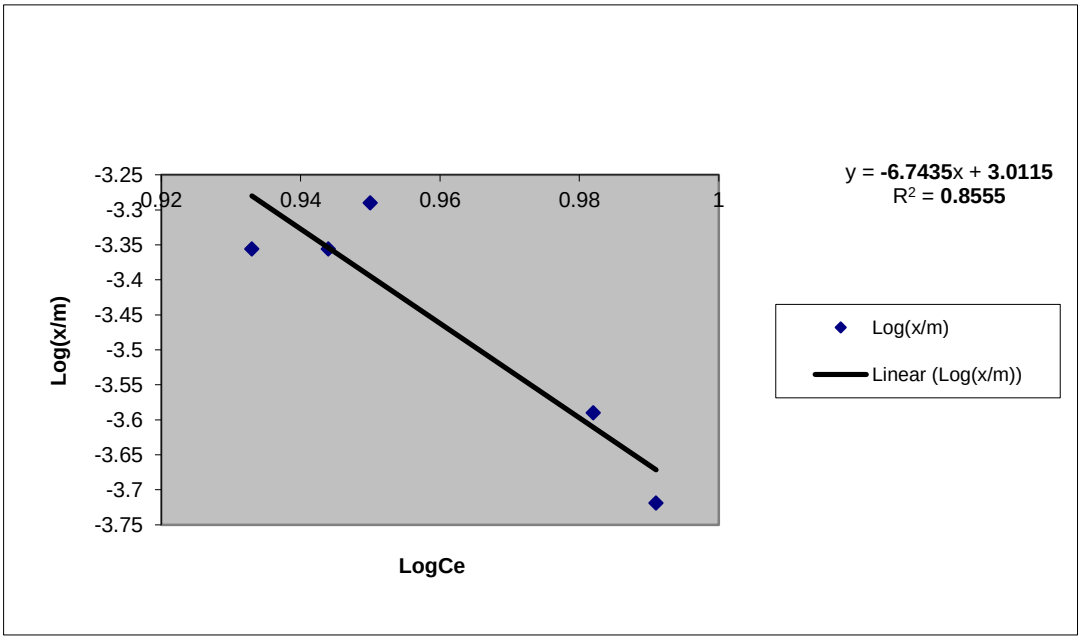

Figure 4.39(b): Linearized Freundlich plot for C_o=10g/*l* at 40ºC, 70% stroke without ECSO

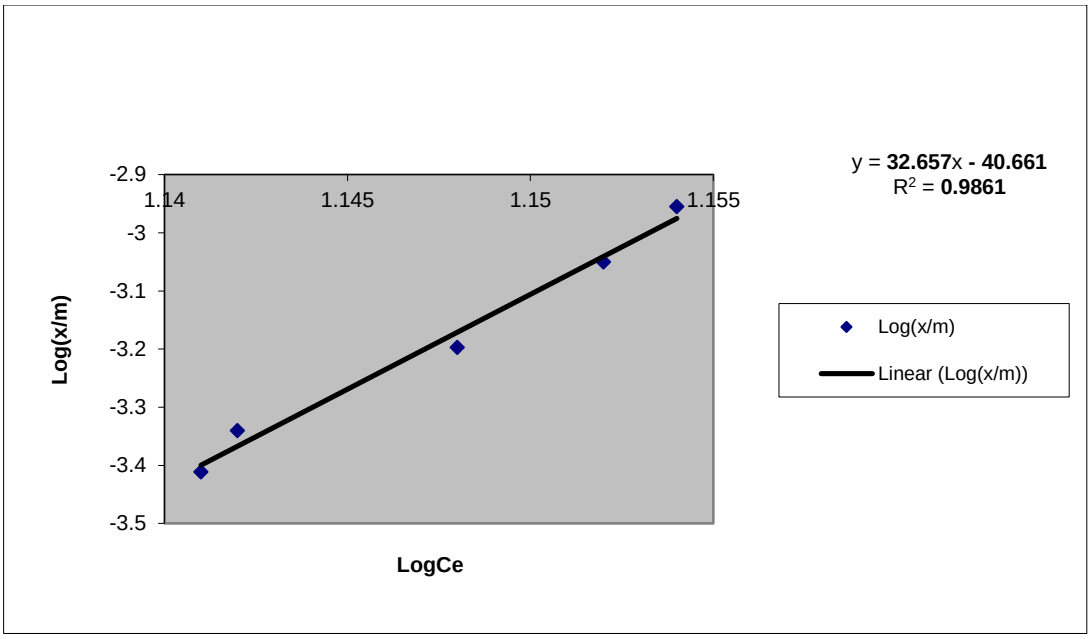

Figure 4.40(a): Linearized Freundlich plot for C_o=15g/*l* at 50°C, 50% stroke with ECSO

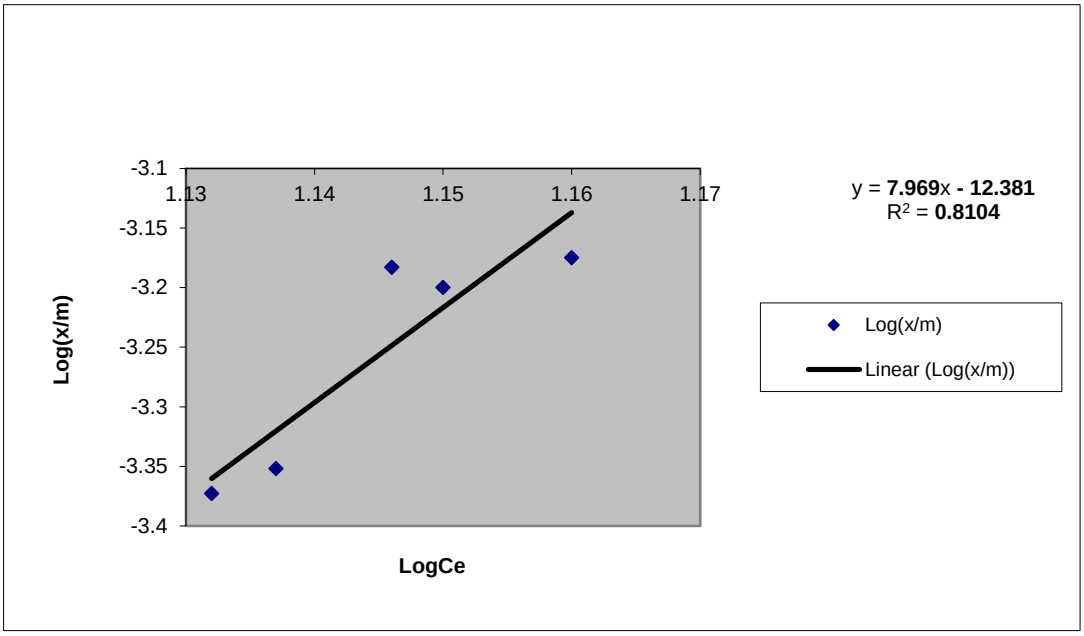

Figure 4.40(b): Linearized Freundlich plot for C_o=15g/*l* at 50°C, 50% stroke without ECSO

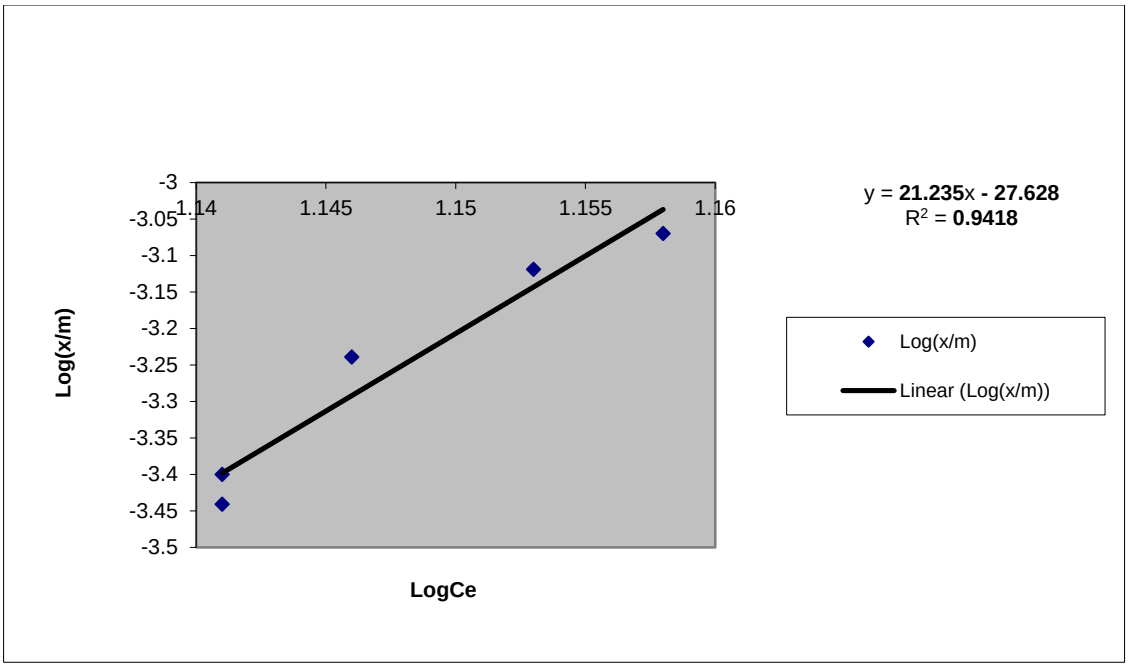

Figure 4.41(a): Linearized Freundlich plot for C_o=15g/*l* at 50ºC, 60% stroke with ECSO

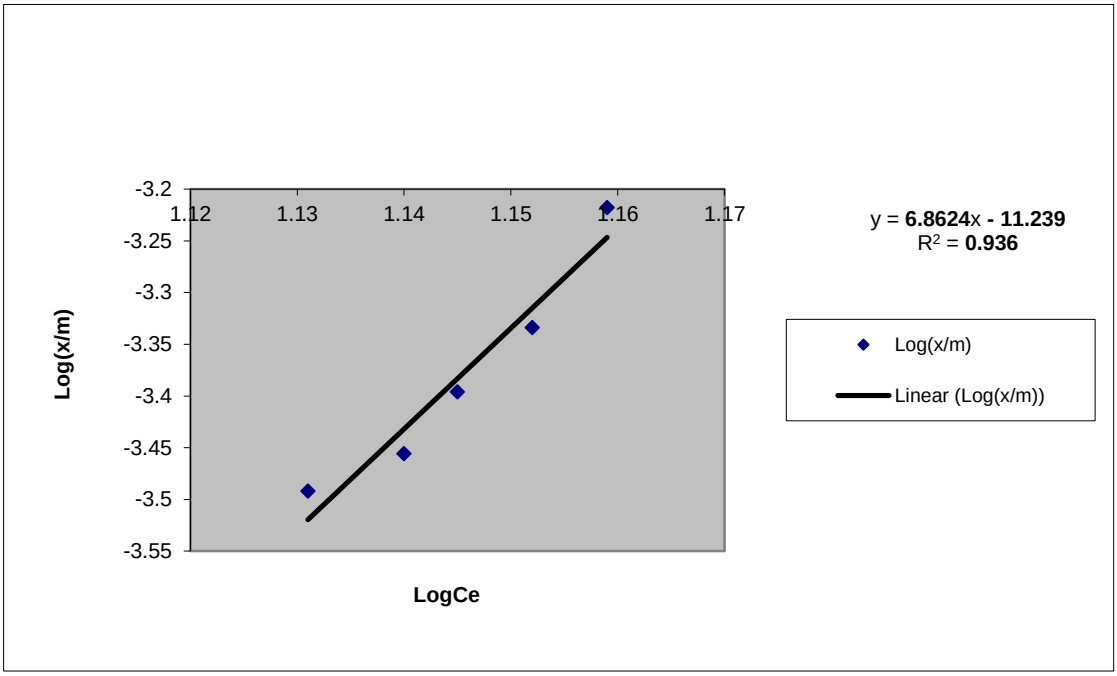

Figure 4.41(b): Linearized Freundlich plot for C_o=15g/*l* at 50ºC, 60% stroke without ECSO

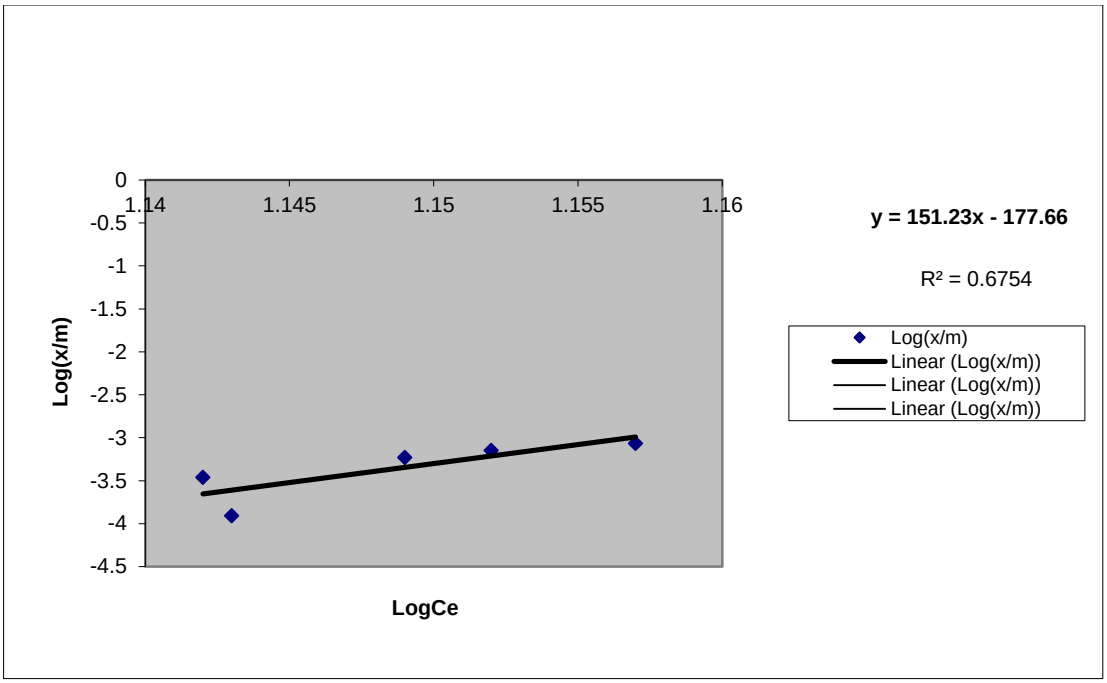

Figure 4.42(a): Linearized Freundlich plot for C_o=15g/*l* at 50ºC, 70% stroke with ECSO

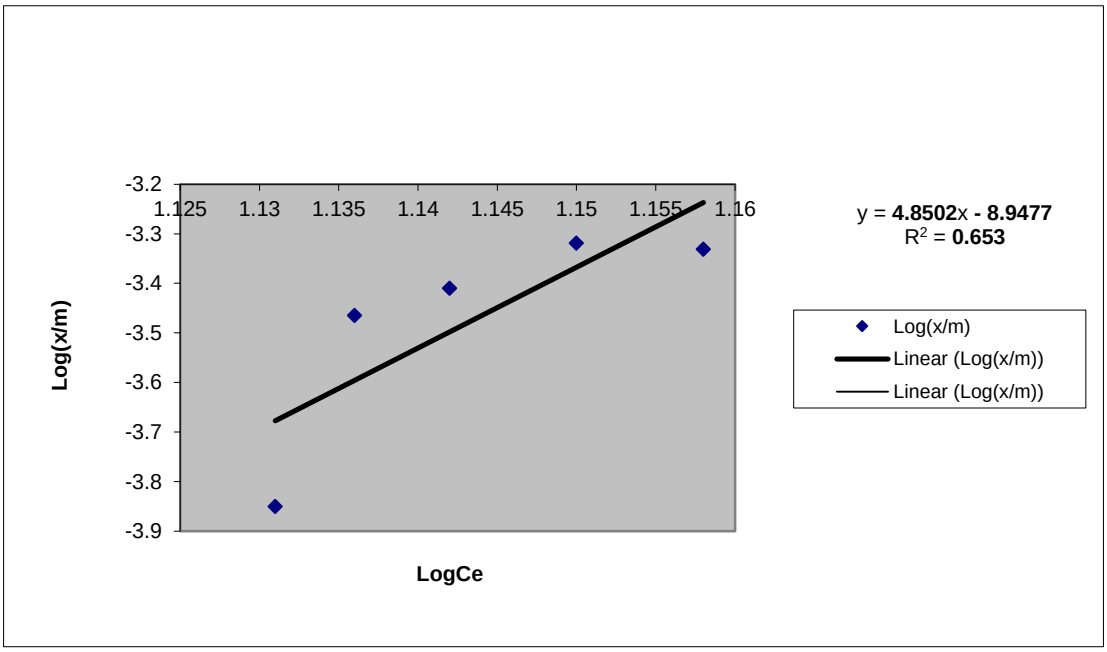

Figure 4.42(b): Linearized Freundlich plot for C_o=15g/*l* at 50ºC, 70% stroke without ECSO

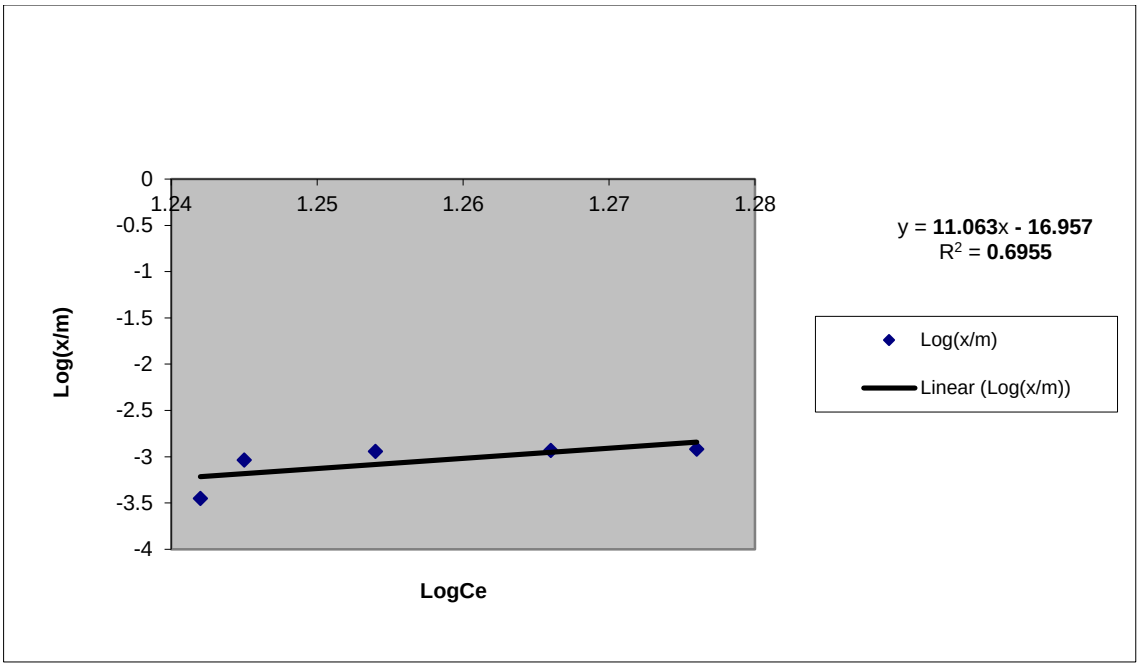

Figure 4.43(a): Linearized Freundlich plot for C_o=20g/*l* at 60ºC, 50% stroke with ECSO

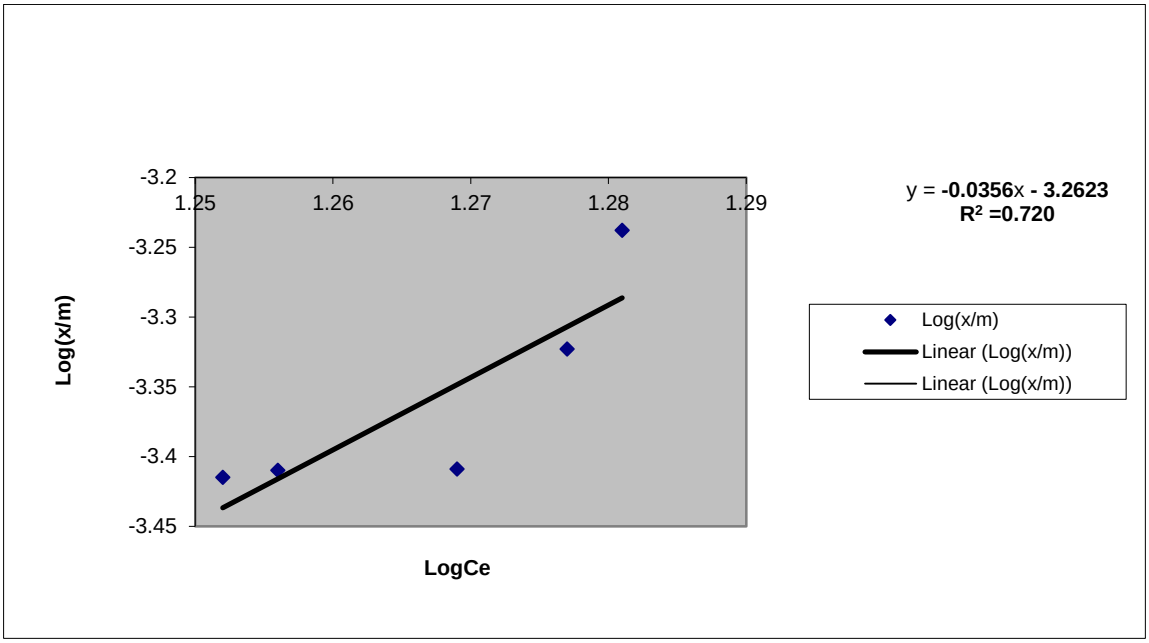

Figure 4.43(b): Linearized Freundlich plot for C_o=20g/*l* at 60ºC, 50% stroke without ECSO

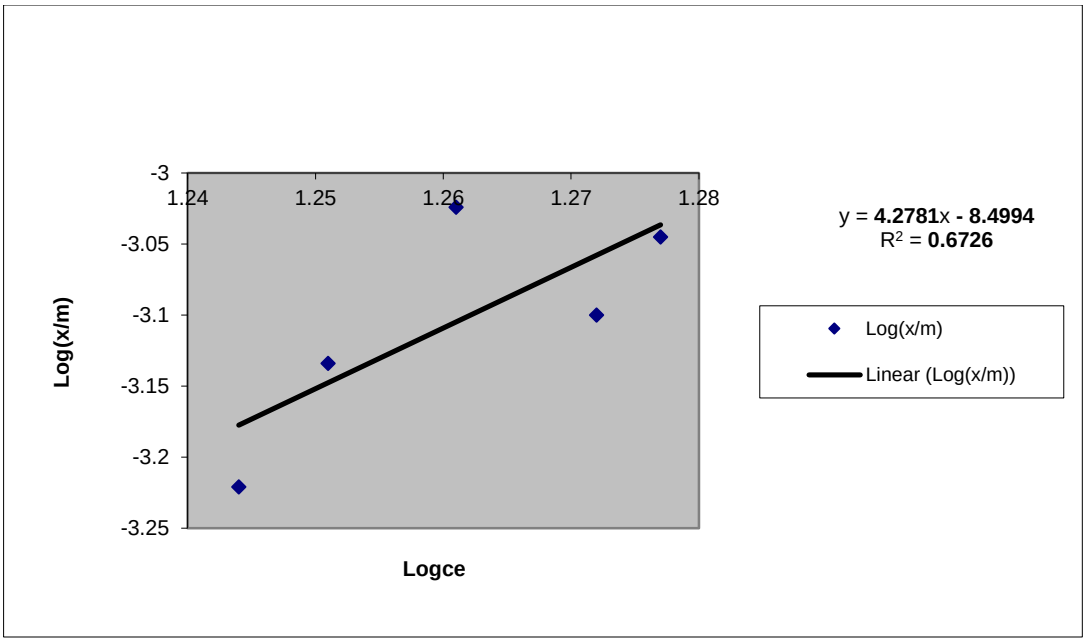

Figure 4.44(a): Linearized Freundlich plot for C_o=20g/*l* at 60°C, 60% stroke with ECSO

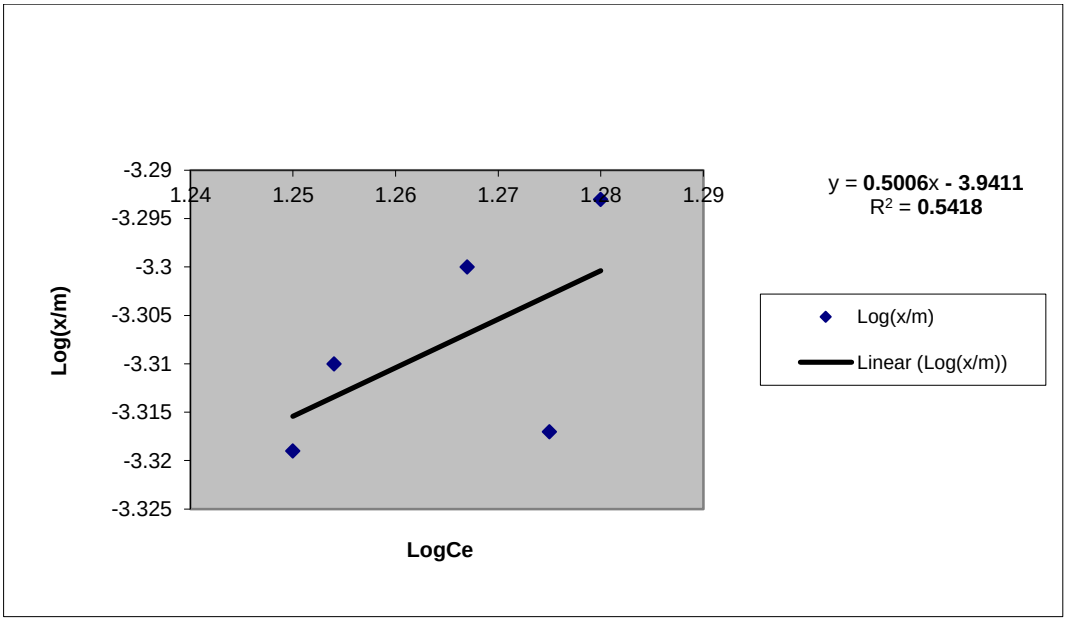

Figure 4.44(b): Linearized Freundlich plot for C_o=20g/*l* at 60°C, 60% stroke without ECSO

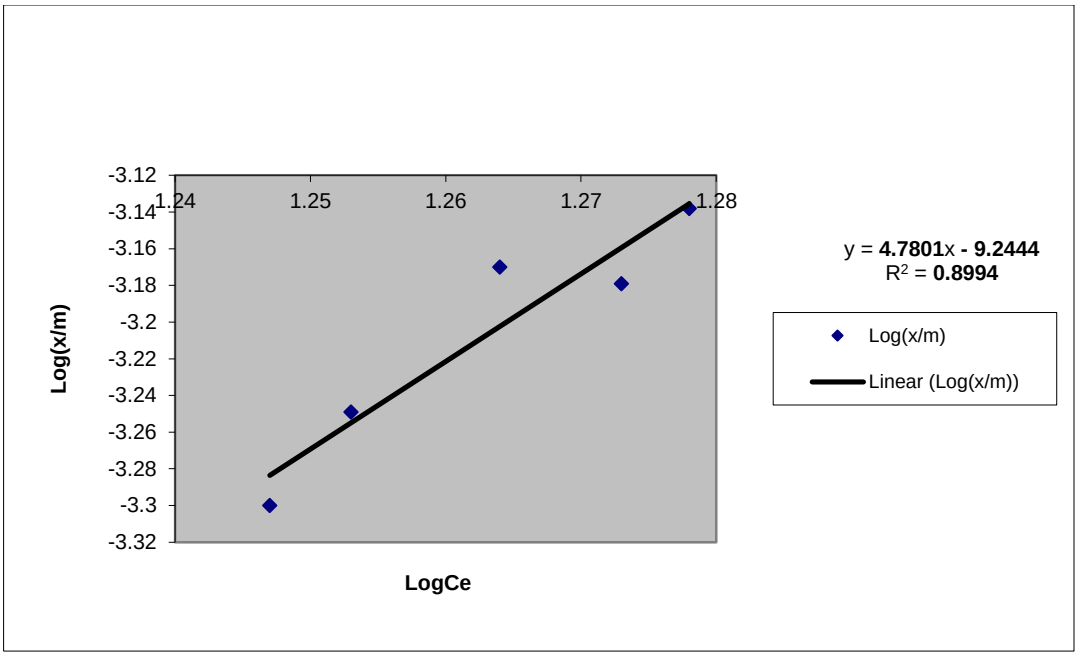

Figure 4.45(a): Linearized Freundlich plot for C_o=20g/*l* at 60°C, 70% stroke with ECSO

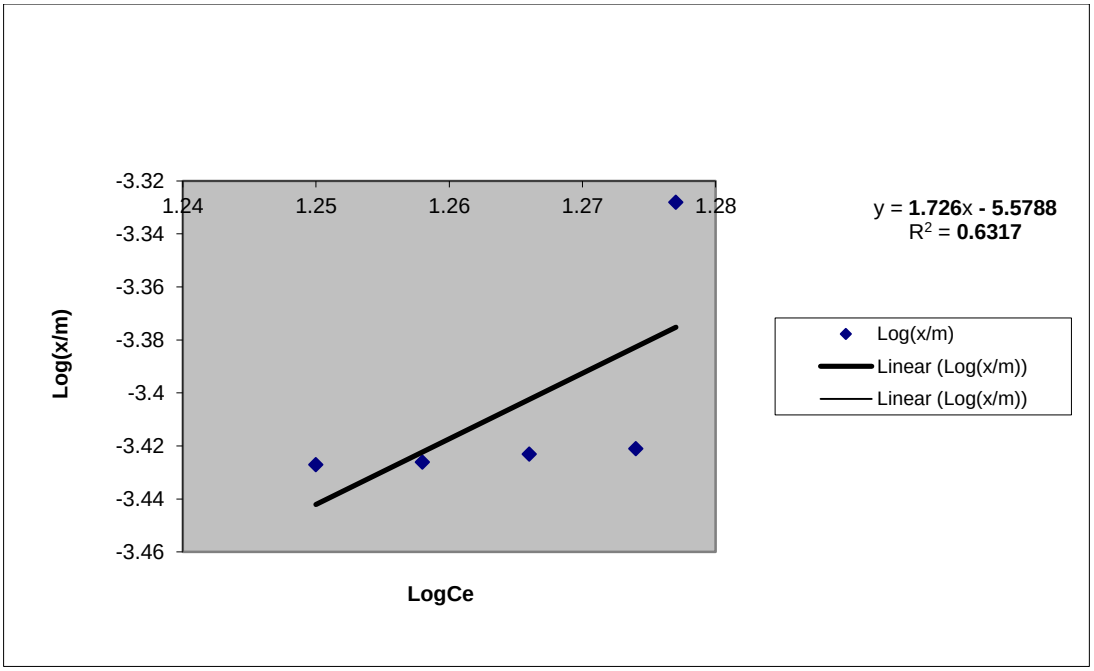

Figure 4.45(b): Linearized Freundlich plot for C_o=20g/*l* at 60°C, 70% stroke without ECSO

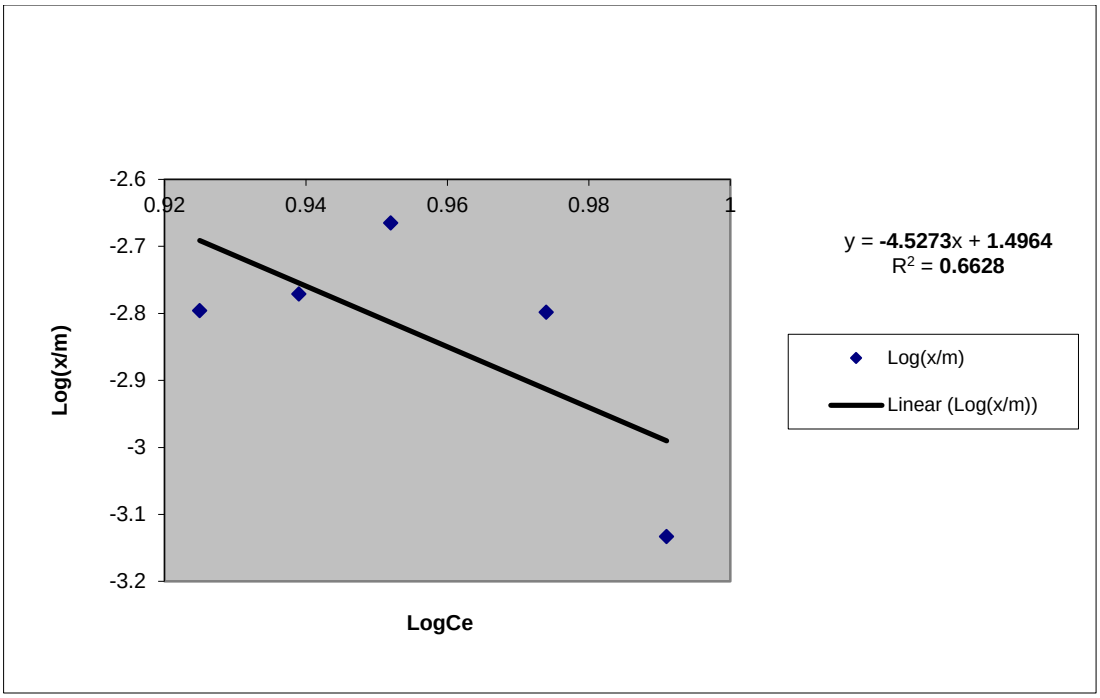

Figure 4.46(a): Linearized Freundlich plot for C_o=10g/*l* at 40ºC, 50% stroke with ERSO

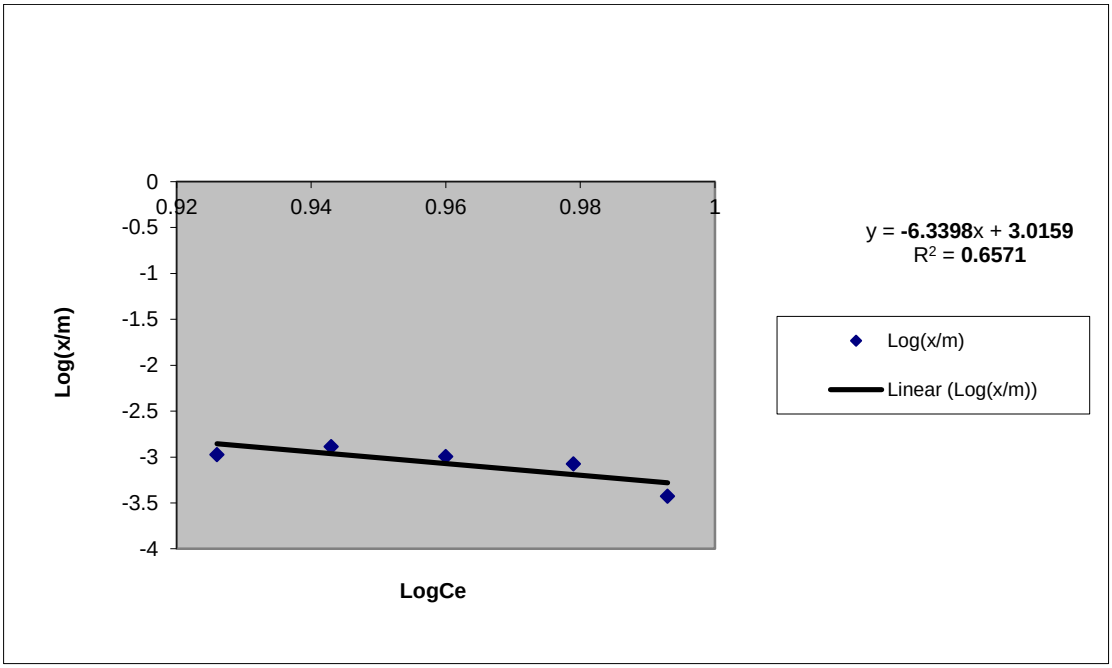

Figure 4.46(b): Linearized Freundlich plot for C_o=10g/*l* at 40ºC, 50% stroke without ERSO

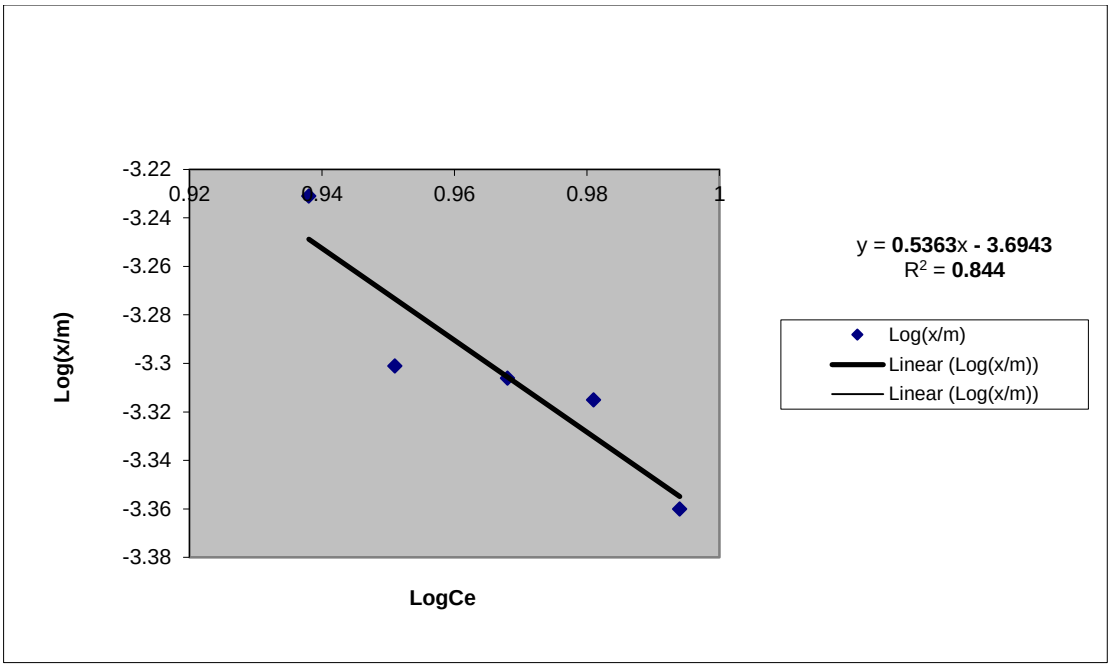

Figure 4.47(a): Linearized Freundlich plot for C_o=10g/*l* at 40°C, 60% stroke with ERSO

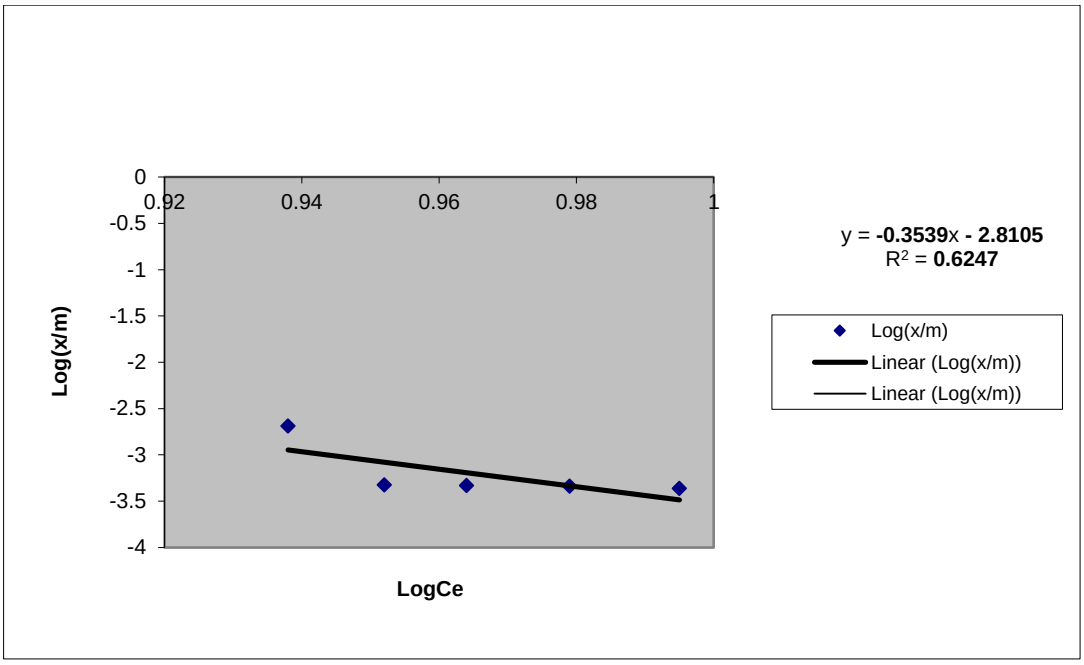

Figure 4.47(b): Linearized Freundlich Plot for C_o=10g/*l* at 40°C, 60% stroke without ERSO

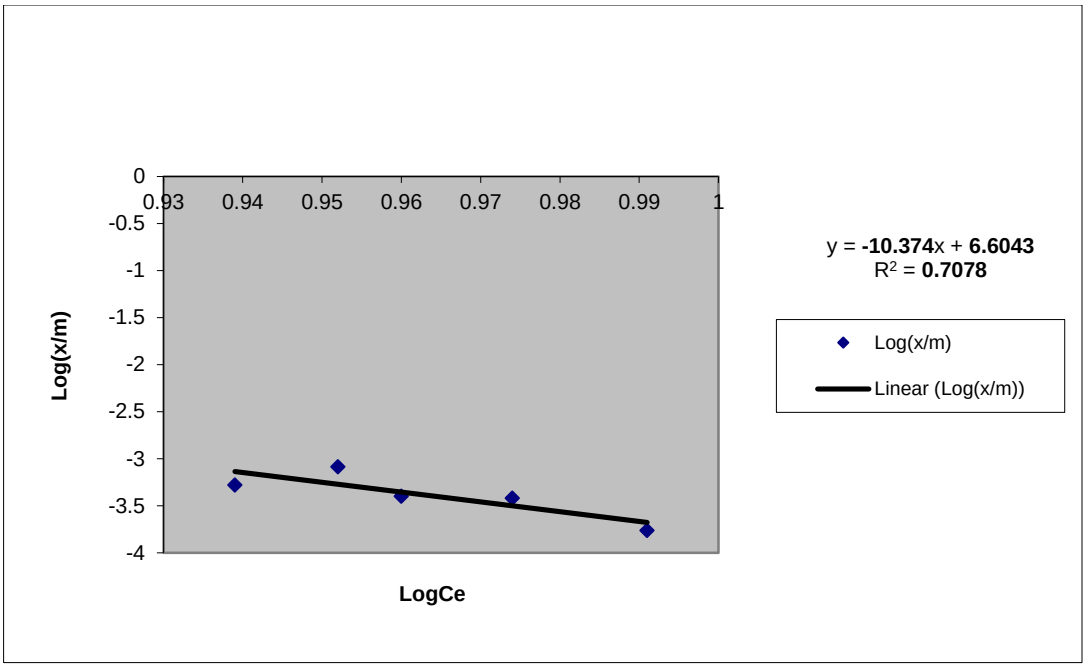

Figure 4.48(a): Linearized Freundlich plot for C_o=10g/*l* at 40°C, 70% stroke with ERSO

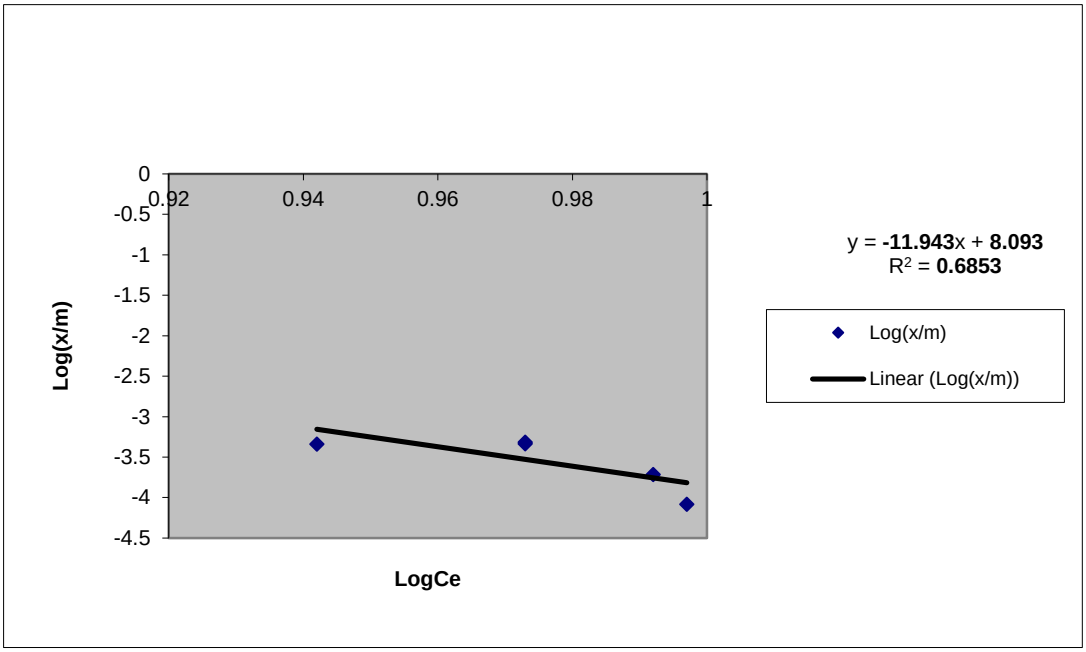

Figure 4.48(b): Linearized Freundlich plot for C_o=10g/*l* at 40°C, 70% stroke without ERSO

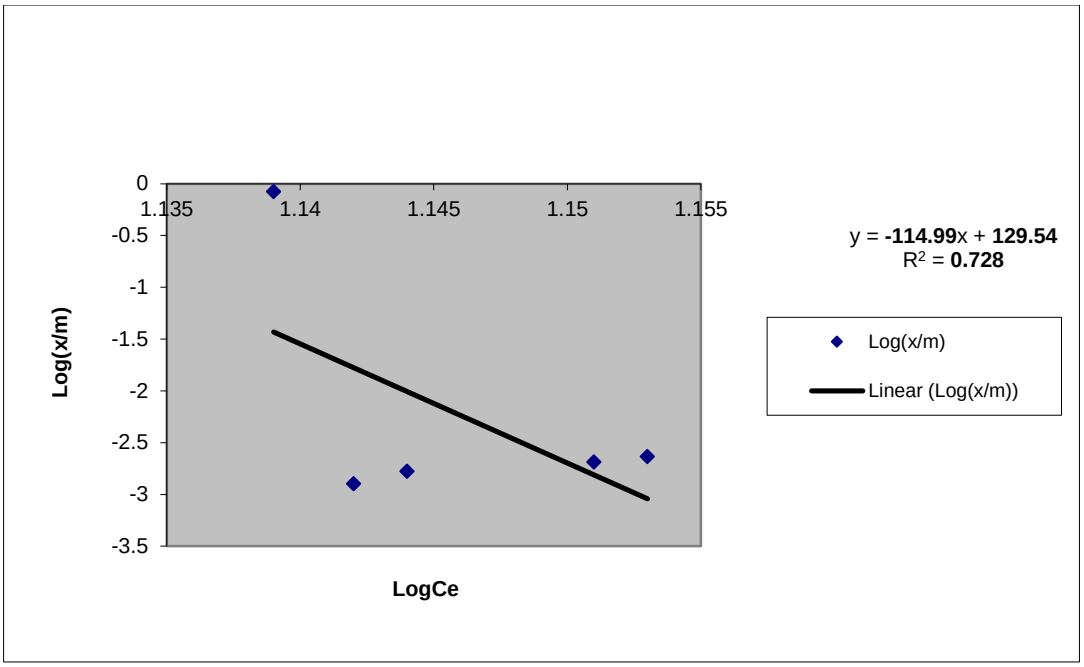

Figure 4.49(a): Linearized Freundlich plot for C_o=15g/*l* at 50ºC, 50% stroke with ERSO

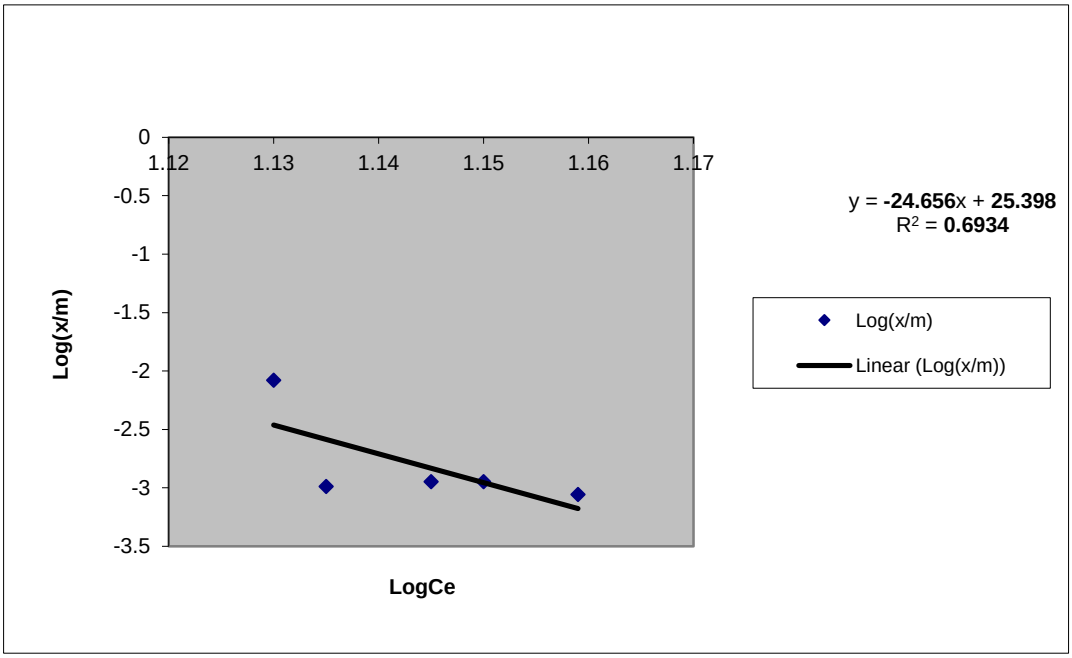

Figure 4.49(b): Linearized Freundlich plot for C_o=15g/*l* at 50ºC, 50% stroke without ERSO

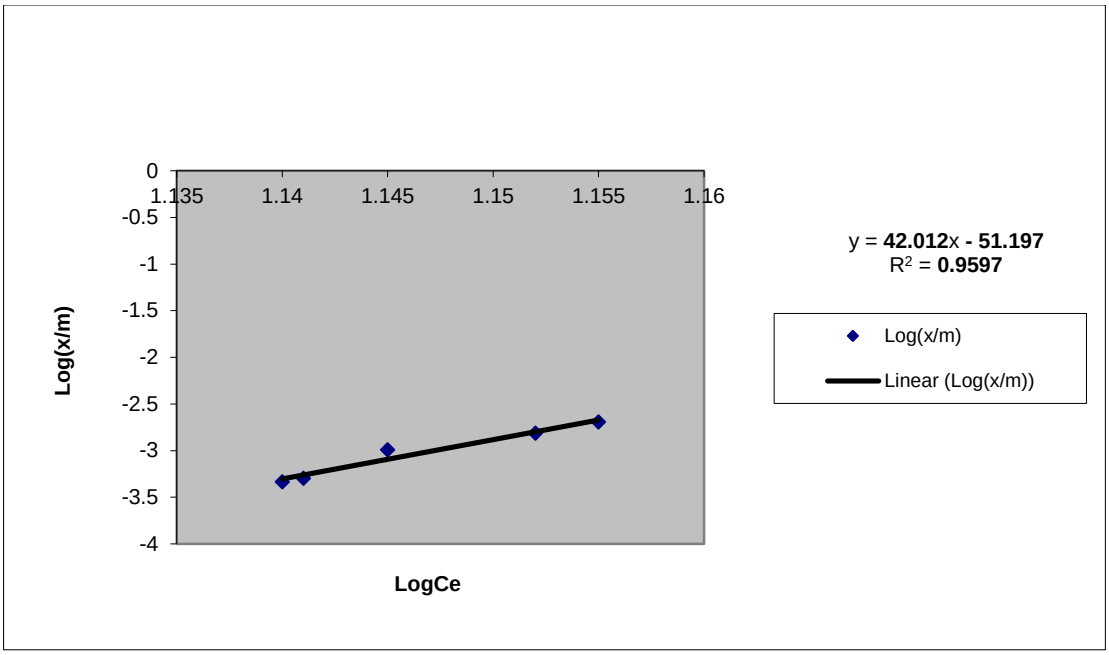

Figure 4.50(a): Linearized Freundlich plot for C_o=15g/*l* at 50°C, 60% stroke with ERSO

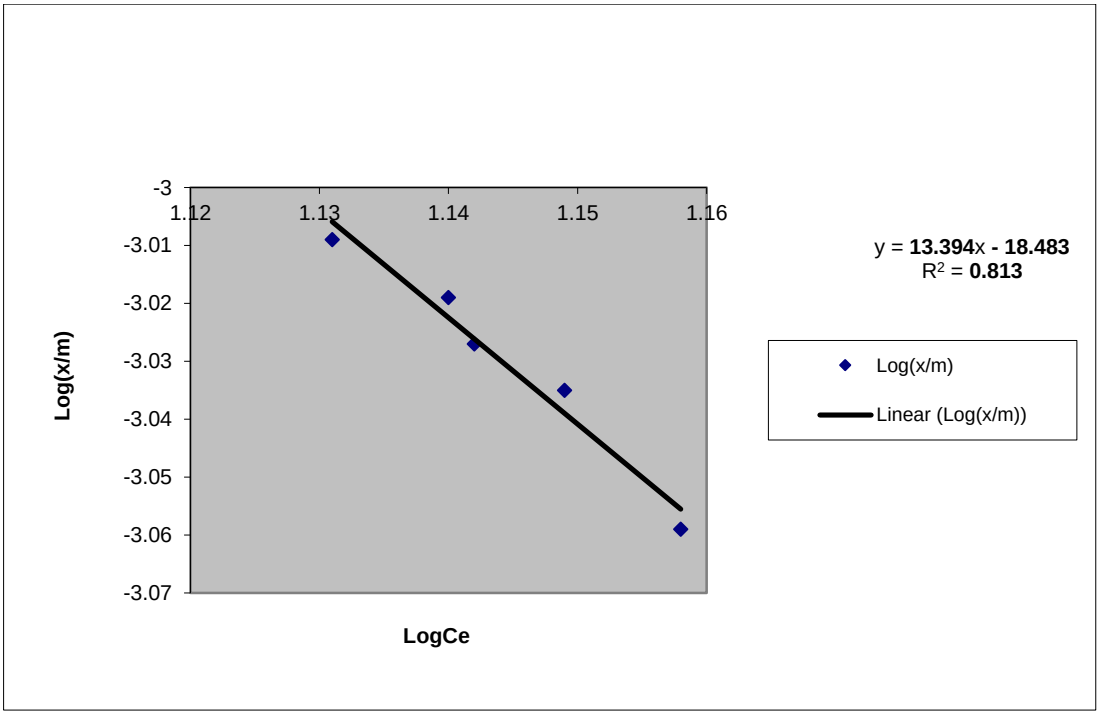

Figure 4.50(b): Linearized Freundlich plot for C_o=15g/*l* at 50°C, 60% stroke without ERSO

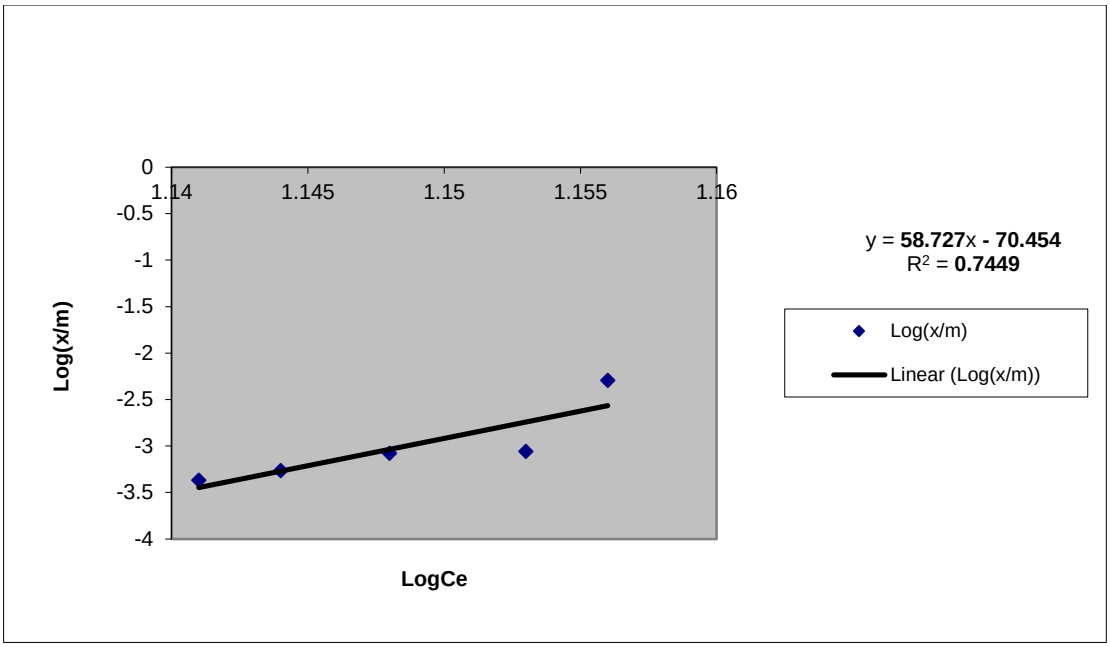

Figure 4.51(a): Linearized Freundlich plot for C_o=15g/*l* at 50ºC, 70% stroke with ERSO

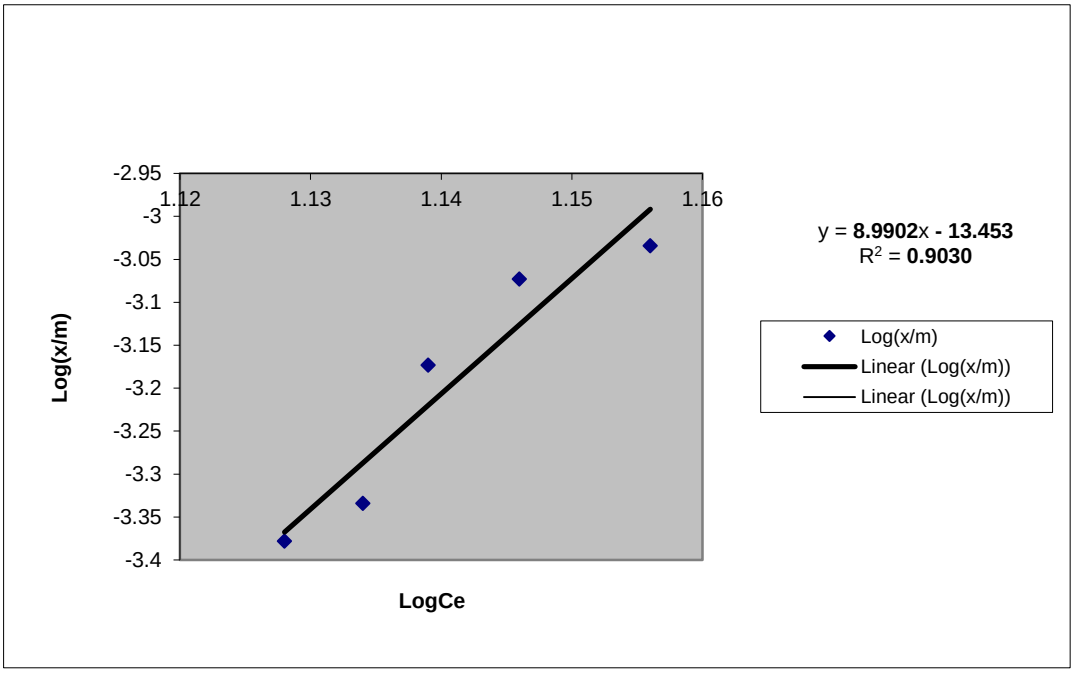

Figure 4.51(b): Linearized Freundlich plot for C_o=15g/*l* at 50ºC, 70% stroke without ERSO

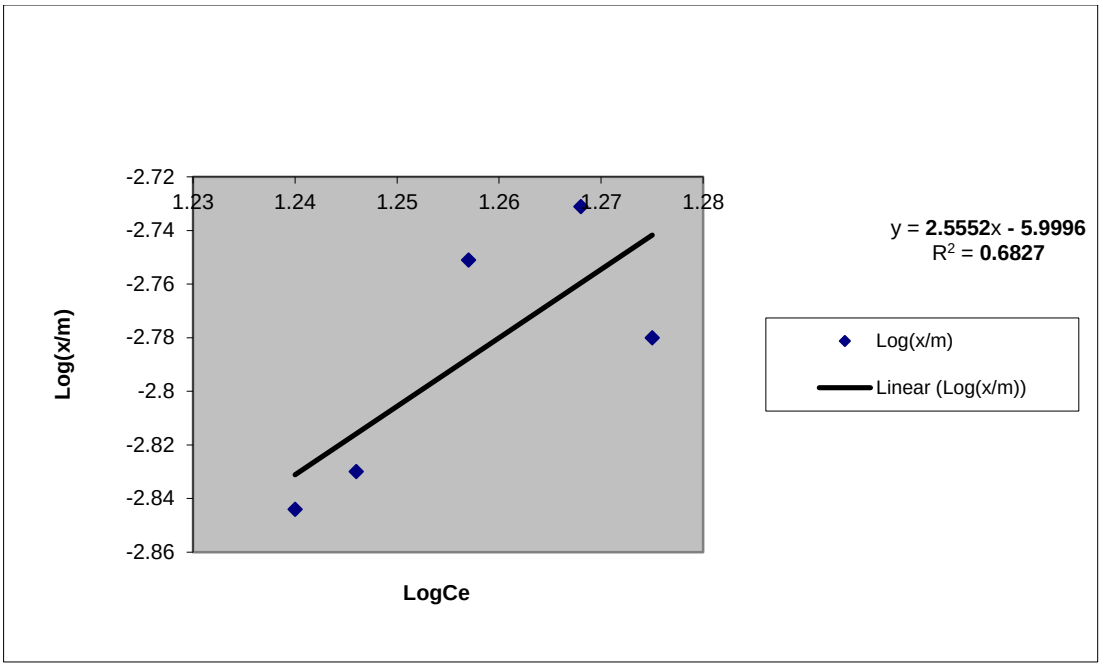

Figure 4.52(a): Linearized Freundlich plot for C_o=20g/*l* at 60ºC, 50% stroke with ERSO

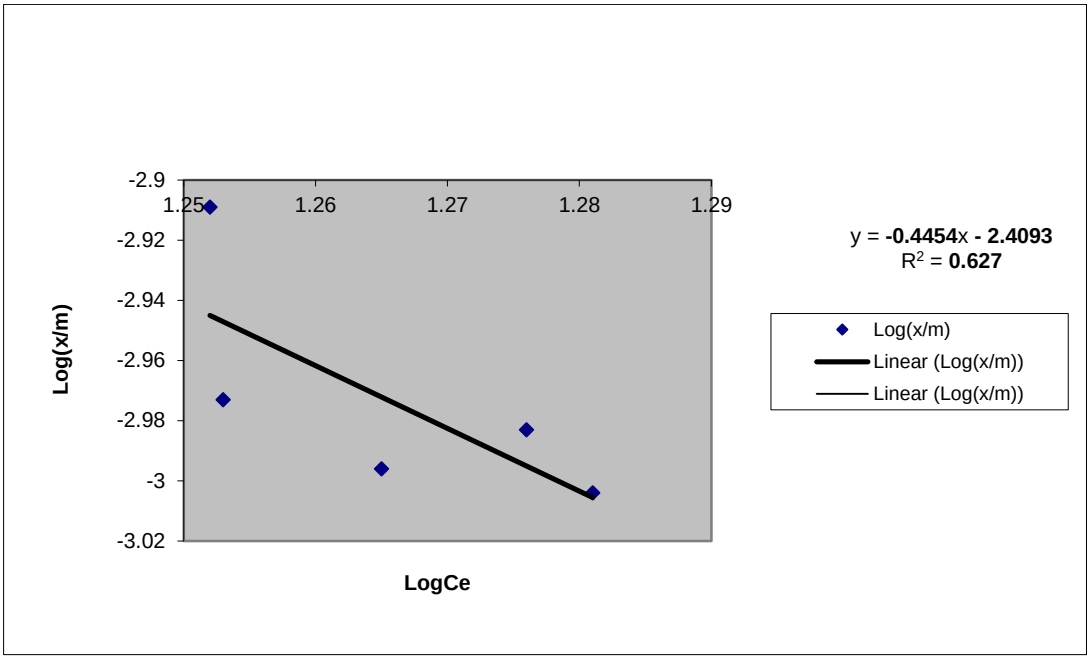

Figure 4.52(b): Linearized Freundlich plot for C_o=20g/*l* at 60ºC, 50% stroke without ERSO

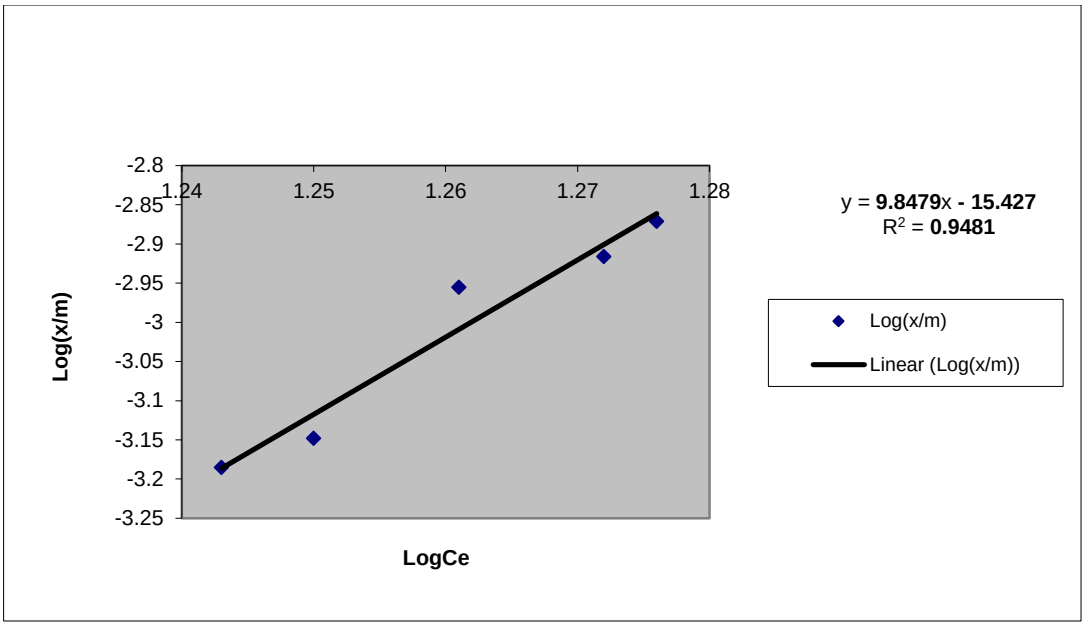

Figure 4.53(a): Linearized Freundlich plot for C_o=20g/*l* at 60ºC, 60% stroke with ERSO

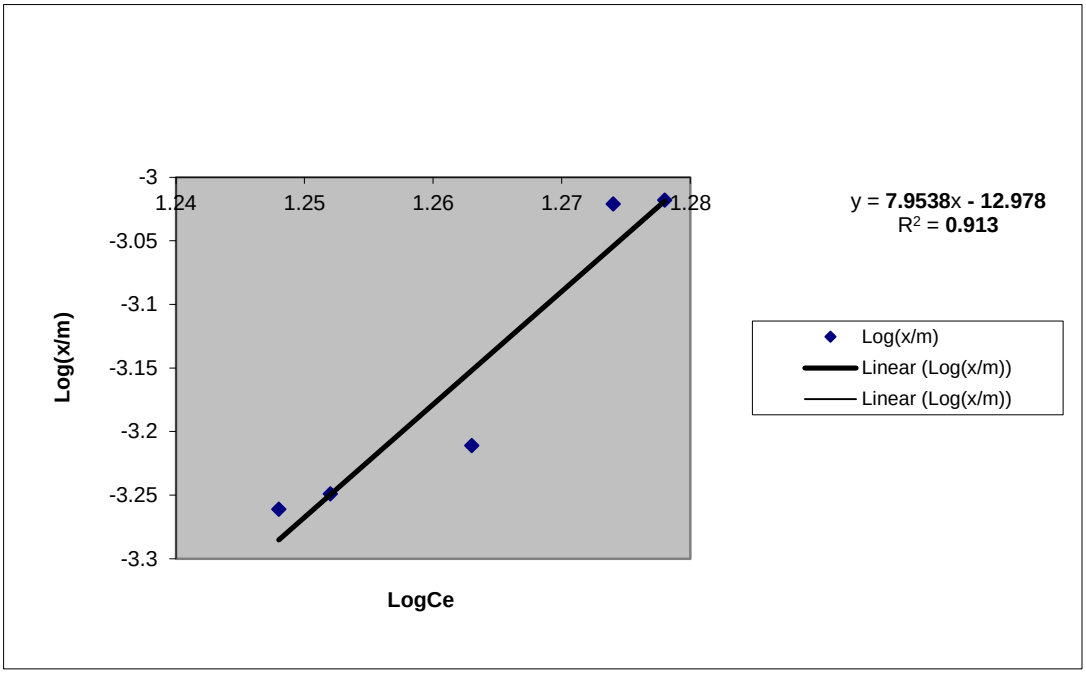

Figure 4.53(b): Linearized Freundlich plot for C_o=20g/*l* at 60ºC, 60% stroke without ERSO

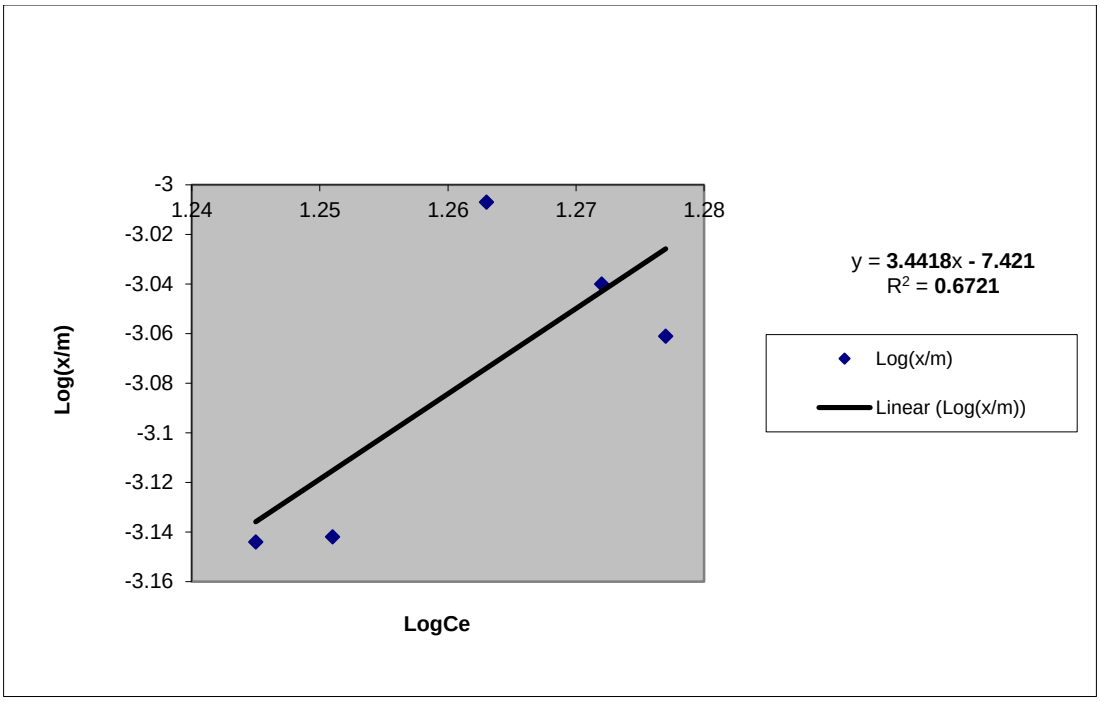

Figure 4.54(a): Linearized Freundlich plot for C_o=20g/*l* at 60ºC, 70% stroke with ERSO

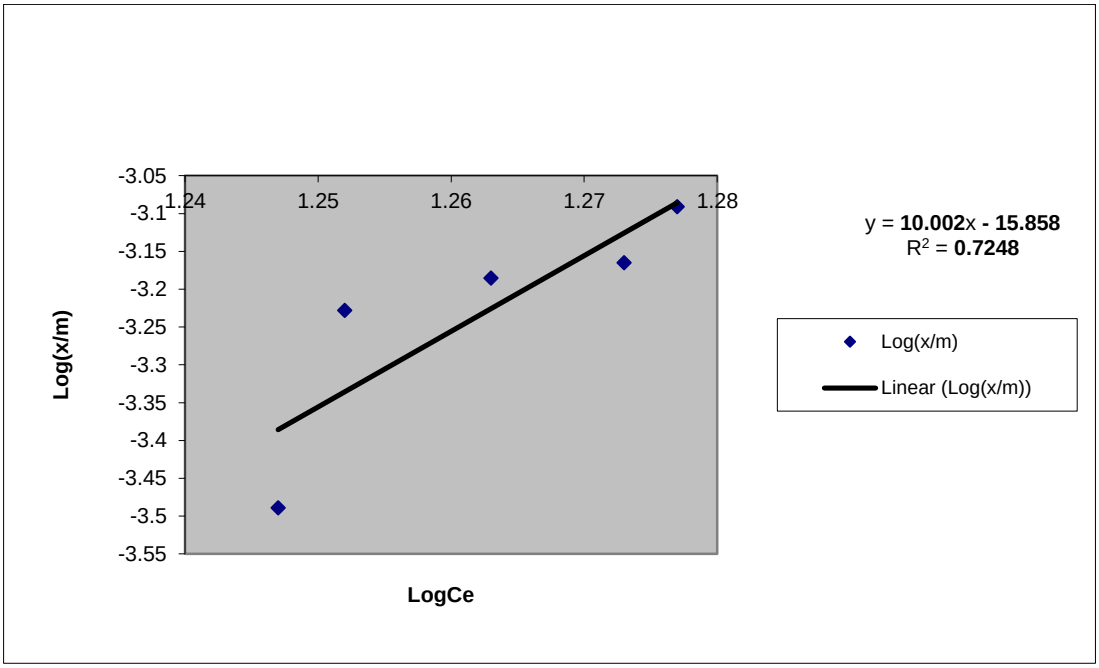

Figure 4.54(b): Linearized Freundlich plot for C_o=20g/*l* at 60ºC, 70% stroke without ERSO

Table 4.12: Freundlich isotherm parameters for ECSO at 10g/*l* and 40^{o}C

Dosage (%Stroke)	With inhibitor			Without inhibitor		
	K_f	n	R^2	K_f	n	R^2
50	$5.6x10^{42}$	-0.022	0.7084	$6.5x10^{7}$	-0.087	0.6913
60	$2.2x10^{3}$	-0.144	0.6460	$4.2x10^{2}$	0.162	0.7626
70	$5.9x10^{-22}$	-0.055	0.9870	$1.0x10^{3}$	0.148	0.8555

Table 4.13: Freundlich isotherm parameters for ECSO at 15g/*l* and 50^{o}C

Dosage (%Stroke)	With inhibitor			Without inhibitor		
	K_f	n	R^2	K_f	n	R^2
50	$2.2x10^{-41}$	0.031	0.9861	$4.2x10^{-13}$	0.125	0.8104
60	$2.4x10^{-28}$	0.047	0.9418	$5.8x10^{-12}$	0.146	0.9360
70	0.0000	0.007	0.6750	$1.1x10^{-9}$	0.206	0.6530

Table 4.14: Freundlich isotherm parameters for ECSO at 20g/*l* and 60^{o}C

Dosage (%Stroke)	With inhibitor			Without inhibitor		
	K_f	n	R^2	K_f	n	R^2
50	$1.1x10^{-17}$	0.090	0.6955	$5.5x10^{-4}$	-28.09	0.7200
60	$3.2x10^{-9}$	0.234	0.6726	$1.2x10^{-4}$	1.998	0.5418
70	$5.7x10^{-10}$	0.209	0.8994	$2.6x10^{-6}$	0.579	0.6317

Table 4.15: Freundlich isotherm parameters for ERSO at 10g/*l* and 40^{o}C

Dosage (%Stroke)	With inhibitor			Without inhibitor		
	K_f	n	R^2	K_f	n	R^2
50	31.36	-0.221	0.6628	$2.5x10^{25}$	-0.041	0.6571
60	$2.0x10^{-4}$	1.865	0.8440	$3.3x10^{-19}$	0.075	0.6247
70	$4.0x10^{6}$	-0.096	0.7078	$3.5x10^{-14}$	0.111	0.6853

Table 4.16: Freundlich isotherm parameters for ERSO at 15g/*l* and 50^{o}C

Dosage (%Stroke)	With inhibitor			Without inhibitor		
	K_f	n	R^2	K_f	n	R^2
50	0.0000	-0.009	0.7280	$2.5x10^{25}$	-0.041	0.6934
60	$6.4x10^{-52}$	0.024	0.9597	$3.3x10^{-19}$	0.075	0.6378
70	$3.5x10^{-71}$	0.017	0.7449	$3.5x10^{-14}$	0.111	0.9030

Table 4.17: Freundlich isotherm parameters for ERSO at 10g/*l* and 40°C

Dosage (%Stroke)	With inhibitor			Without inhibitor		
	K_f	n	R^2	K_f	n	R^2
50	$1.0x10^{-6}$	0.391	0.6827	$3.9x10^{-3}$	-2.245	0.6270
60	$3.7x10^{-16}$	0.102	0.9481	$1.1x10^{-13}$	0.126	0.9130
70	$3.8x10^{-8}$	0.291	0.6721	$1.4x10^{-16}$	0.100	0.7248

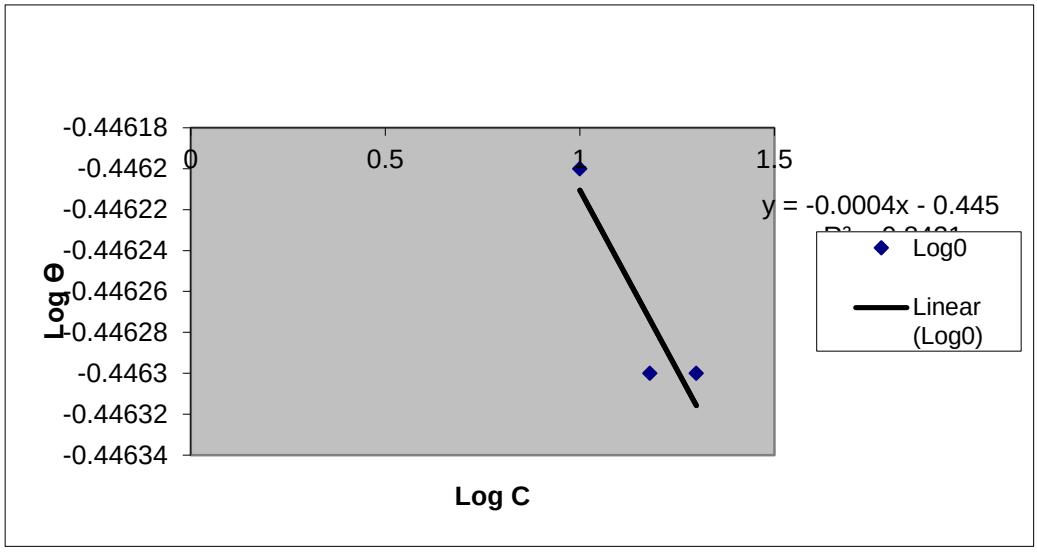

Figure 4.55: Temkin isotherm plot for ECSO

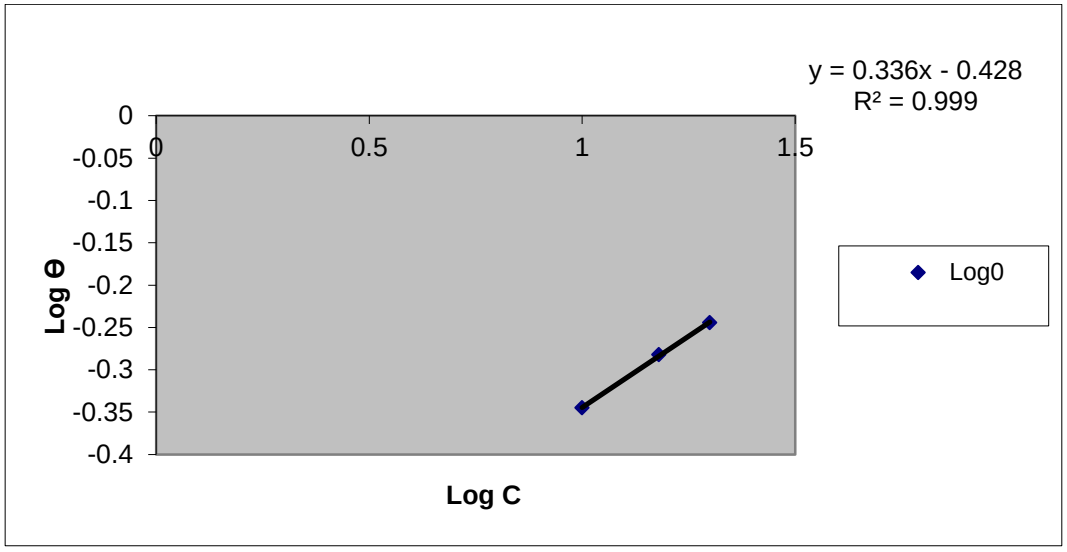

Figure 4.56: Temkin isotherm plot for ERSO

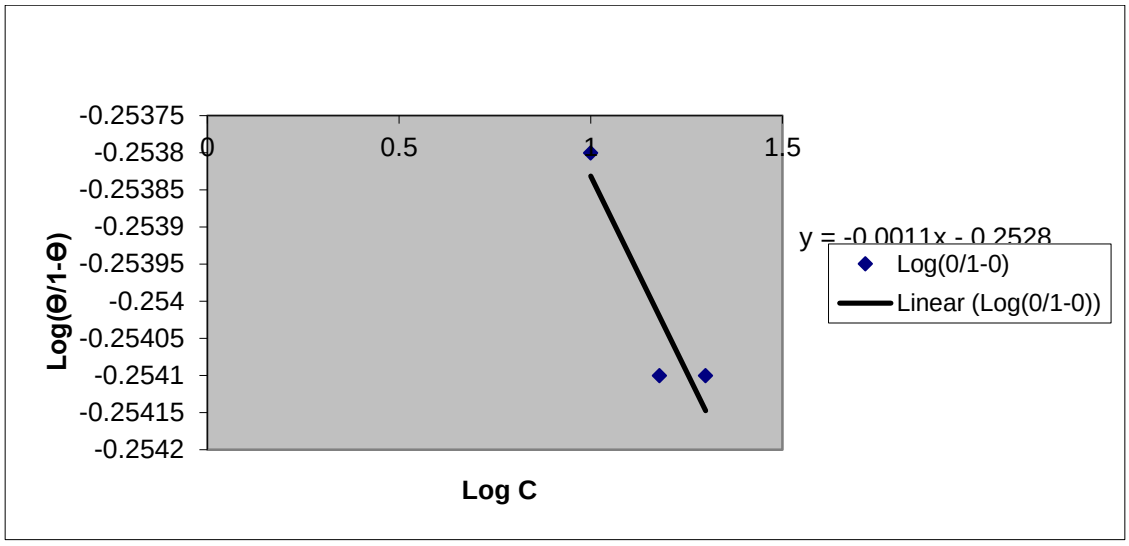

Figure 4.57: El-Awady isotherm plot for ECSO

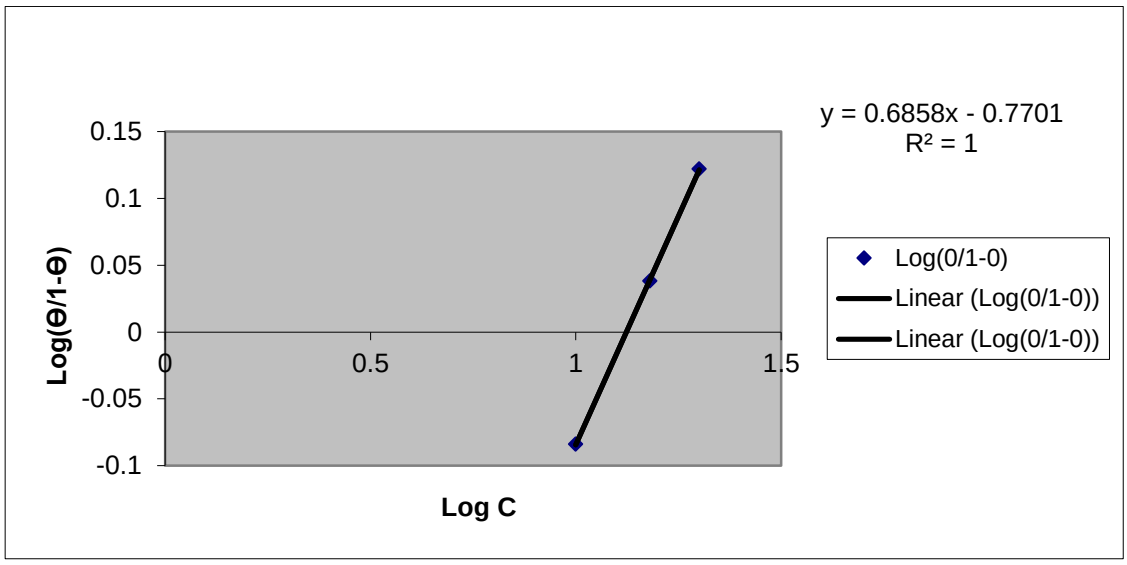

Figure 4.58: El-Awady isotherm plot for ERSO

Table 4.18: Temkin and El-Awady Isotherm Parameters

Sample	Temkin parameters				El-Awady parameters				
	K	f	a	R^2	K^1	K	y	1/y	R^2
ECSO	0.3589	-2500	1250	0.8421	0.5587	-505.91	-0.0011	-909.09	0.8420
ERSO	0.3733	2.9727	-1.4863	0.9993	0.1698	0.2476	0.6858	1.4582	1.0000

4.2 DISCUSSION

In line with the organization of the result sub-section, the discussion of the results is systematically arranged to allow a better flow of information.

4.2.1 Characterization and phytochemistry of samples

The results of the sample characterization indicate that ester of castor seed oil (ECSO) is less acidic (pH=3.0), than that of rubber seed oil (ERSO**),** which has pH of 1.76. This feature, no doubt, gave sample A a better saponifying characteristic (with saponification value of 49.09) as against its counterpart (ECSO) that has saponification value of 26.65, even though both oils are rarely utilized for soap production. According to Asuquo *et al* (2012a), the lower the saponification value of an oil sample, the lower its lauric acid content. As the lauric acid content and the saponification value of oil samples serve as important parameters in determining the suitability of the oil for soap making, the study samples are not very suitable for soap making. The moisture content of ECSO (18.86%) was found to be higher than that of ERSO (11.78%). This is traceable to the fact that the rubber seed is more woody (or herbaceous) in nature than the castor seed, and this has the capacity of lowering the triglyceride properties (Asuquo *et al*, 2012a; Asuquo *et al*, 2010). ECSO was, also, found to be denser (density=1.03g/ml) than ERSO (density=0.89g/ml). The moisture content, also, played important role in the specific gravity values of the samples (0.9222 for ECSO and 0.9189 for ERSO). However, both results fall within the standard specifications of these properties for vegetable oils as documented by Alam *et al* (2013). The viscosity of ECSO was found to be 215.20mPoise, while that of ERSO is 208.30mPoise, and these are all within the viscosity range (70.00-280.00mPoise) of organic oils such as shear butter oil and crambe oil (Asuquo

et al, 2012a; Asuquo *et al*, 2010). The iodine value of ECSO (4.12g/100g) is lower than that obtained for ERSO (4.83g/100g); this indicates that the ester of castor seed oil is less unsaturated than that of rubber seed oil. According to (Asuquo *et al*, 2012b), the iodine value measures the degree of unsaturation in a vegetable oil sample, which determines the stability of the oil to oxidation, and allows the overall unsaturation of the fat/oil to be determined qualitatively. Generally, other characteristics of the study samples (such as refractive index, free fatty acid value and peroxide value) all fall within the FAO/WHO standard specifications of 1993 for vegetable oils, as reported in Ngassapa and Othman (2001).

On the other hand, it can be observed, from Table 4.2, that there was little presence of flavonoid, phenol and saponin contents (+) in ECSO, when compared with those of ERSO (+++). This has the ability of giving ERSO "upper hand'' in the inhibition of mildsteel corrosion, in agreement with the respective documentations of Harbon (1998) and Undiandeye *et al* (2014) that the phytochemical properties of an oil sample (such as flavonoid, phenol, cardiac glycosides and saponin) dispose it better for corrosion inhibition. It could, also, be observed that there is no presence of terpernoid in ECSO, while it appears only slightly in ERSO, and irrespective of the heavy presence of the phenol content in ERSO (+++), the quantitative value was very little (0.0422%). This, categorically, demonstrates that qualitative assessment of a research data is not always enough to deduce the degree of the presence of a given phytochemical characteristic of the study sample. However, the rubber seed oil sample indicated greater presence of most of the phytochemicals investigated (Table 4.3). This represents an embodiment of carbonyl attachment to its ester linkage (Yordanov and Petkov, 2008a). The results of

phytochemical analysis of the study samples (ECSO and ERSO) show that phytochemical characteristics are more established in ERSO than in ECSO. This feature, thus, increases the chances of ERSO being more effective in corrosion inhibition applications.

4.2.2 Effect of Time on Weight Loss

The linear plots considered the effect of the most significant factor (time) on the response factor (weight loss). Figures 4.1-4.6 show that weight loss increases with increase in time at all reaction conditions for both study samples. Also, Figures 4.7-4.12 show that the rate of corrosion increases in the direction of increasing pressure. In other words, as the flow rate increases (from 40% stroke through 70% stroke) due to the increase in pump pressure which increases intermolecular collision of the particles, the metal sample experiences more degradation. This, of course, is partially dependent on the time of reaction as well.

4.2.3 Discussion on Electrochemical study

4.2.3.1 Potentiodynamic polarization measurements

In the potentiodynamic polarization curves of mildsteel-in-H_2SO_4, containing different concentrations of the inhibitors, the mildsteel specimen was seen to exhibit active dissolution, with no distinctive transition to passivation within the studied potential range in the absence and presence of both inhibitors-in-H_2SO_4. In Figure 4.13, the influence of castor-derived inhibitor on the corrosion potential (E_{corr}) was not very significant; the same thing was applicable in Figure 4.14 (where rubber-derived inhibitor was involved). Furthermore, a reduction in the cathodic and anodic half reactions was observed at both low and high concentrations. For ECSO (Figure 4.13),

however, no significant shift on $\mathbf{E_{corr}}$ was observed at lower concentration, unlike the case of ERSO (where a little shift was observed in $\mathbf{E_{corr}}$). But Ahmad *et al* (2012) reported that if the displacement in $\mathbf{E_{corr}}$ is greater than 85mV, the inhibitor could be classified as being anodic or cathodic, and if the displacement is less than 85mV, the inhibitor may be seen as a mixed type. In line with this, the results presented in Table 4.4 indicate that the maximum displacements in E_{corr} value (within the sulphuric acid environment) are less than 85mV; thus, the inhibitor samples used in this study (ECSO and ERSO) are regarded as mixed-type of inhibitors. However, the inhibiting effect became more pronounced at higher concentrations. The values of inhibition efficiency show that ethyl esters of rubber seed oil were better inhibitors than those of castor seed oil. In other words, the results obtained using this technique followed the same trend with those of gravimetric study.

4.2.3.2 Scanning electron microscope

The images show that the surface of mildsteel in Figure 4.15a (as received) appears smooth, but when dipped in the aggressive (acid) solution in the absence of the inhibitor (Figure 4.15b), the surface was very rough due to active dissolution of the metal. However, the roughness reduced significantly on addition of ECSO (Figure 4.16a) and ERSO (Figure 4.16b) to the acidic environment. The result reveals that the introduction of the inhibitors reduced the active dissolution of mildsteel by forming a protective layer on its surface. Careful examination of the metal surfaces dipped in the presence of the inhibitors revealed the existence of adsorbate species.

However, close scrutiny of the images in figures 4.16a and 4.16b reveals that the mildsteel surface was more protected in ERSO, compared to ECSO. This

suggests the presence of a more compact/stronger protective layer formed on metal surface in the presence of ERSO; this is in agreement with the higher inhibition efficiency obtained therein.

4.2.3.3 Fourier transform infrared spectroscopy

Close examination of the FTIR spectra of ECSO (Fig. 4.17a) and ERSO (Fig. 4.18a) and those of their protective layers formed on the metal surfaces (Figs. 4.17b and 4.18b respectively), shows the presence of some peaks, which could be attributed to the existence of functional groups (chemical bonds). Almost all the peaks in ECSO and ERSO are identifiable in the protective layers adsorbed on the metal surfaces in each case, confirming the existence of these functional groups in the inhibitor film. However, some of the peaks deviated, while some vanished. Also observed was a shift from 1648cm^{-1} to 1604cm $^{-1}$, probably due to the C=O stretching; the bonds related to O-H/N-H (at 3320cm^{-1}) shifts to 3209cm^{-1}, while those associated with C-N at 1002cm^{-1} vanished. The shift of C=C and C-O stretching frequencies, from 1650cm^{-1} to 1636cm $^{-1}$ and from 1250cm $^{-1}$ to 1083cm^{-1}, respectively suggests the rapid adsorption of the inhibitor molecules on the corroding metal surface. The shift due to O-H/N-H and C=O stretching frequencies, from 3386cm^{-1} to 3209cm^{-1} and from 1743cm^{-1} to 1203cm^{-1}, also confirm the adsorption of the inhibitor species on the metal surface (Jiali *et al*, 2013).

4.2.4 Thermodynamic study

From the thermodynamic parameters (Table 4.5), it can be observed that enthalpy change (ΔG) increases with increase in time of the corrosion reaction. This demonstrates the continuous heat energy demand for the sorption process. The positive values of the entropy change (ΔS), also

increases down the table, showing that the reaction at the solid-liquid interface occurs in the direction of increasing randomness. Also, the free energy values, at all cases, were negative; the negativity of the values deepened with increase in temperature of the reaction. This is traceable to the fact that effect of temperature tends to increase the degree of randomness in adsorbed molecular layer (Eddy and Odoemelam, 2008). In other words, there are higher collisions at higher temperatures, which result in higher kinetic energy (as well as the overall energy demand) of the reaction. The result, thus, confirms that the reaction is more spontaneous in the direction of increasing temperature change, and it is entropy-driven; any reaction that has a positive enthalpy change must be entropy-driven if it is spontaneous (Philip, 2003). This is because the combination of a rise in temperature and a large ΔS value has the ability to make $T\Delta S$ a large positive value, hence $-T\Delta S$ becomes a large negative number that overcomes ΔH.

However, the results were in agreement with the ones obtained in related works done by Undiandeye *et al* (2011) and Ostovari (2009).

4.2.5 Adsorption isotherm study

The data presented in Tables 4.6-4.11 indicate all-negative values of the empirical constant of the Langmuir model, *b* for both study samples, and the R^2 values all tend to unity. This demonstrates the heat loss during the adsorption process of a given concentration of the medium at constant temperature; this suggests that the number of available active sites increases with continuous increase in energy demand, which results to reduced competition for adsorption sites, and the adsorption process readily increases; a similar observation was reported by Offurum *et al* (2011). However, the

Langmuir model (by these features) fits the research data for both study samples. (Metcalf and Eddy, 2006). Also, most of the $\boldsymbol{R^2}$ values were tending towards unity, which indicate a good curve fit of the data points.

On the other hand, it can be observed that the Freundlich Intensity Factor, $\boldsymbol{K_f}$ for both study samples (ECSO and ERSO), as presented in Tables 4.12-4.17, are extremely wide (between $3.5x10^{-71}$ - $5.6x10^{42}$). This wide variation in the Freundlich capacity factor demonstrates that the model does not fit the data for both study samples (Metcalf and Eddy, 2003).

The factor of energy homogeneity, f (as contained in Table 4.18) of the Temkin model was found to be less than zero for ECSO, but greater than zero for ERSO. This indicates that mutual attraction occurred in the use of ECSO, while mutual repulsion took place in the case of ERSO (Nnaji *et al*, 2011). From the Temkin's assertion, therefore, it is evident that positive values of 'f' suggest negative values of the attractive parameter (a), which indicates that repulsion occurs in adsorption layers (Nwabanne *et al*, 2012; Shukla *et al*, 2011). Following from this, it was deduced that the Temkin model fits the data for ERSO, but does not fit those for ECSO.

Also, the numerical values of the inhibitors' binding constant (K) were found to be higher for ERSO than for ECSO in both Temkin and El-Awady isotherms. This indicates that the inhibition efficiency is better when using the ERSO, compared with ECSO as mildsteel corrosion inhibitors. Though the

data for both inhibitors fit the El-Awady model (as suggested by the positive values ofd K^1), the R^2 values show that it best fits the ERSO data.

4.2.6 Flow system for the corrosion inhibition study

The innovation made in the development of a proto-type flow system set-up (as contained in figure 3.2) is a promising one. The system was used effectively as corrosion study kit in the corrosion inhibition study conducted herein. The efficiency of the system was achieved because the components of of kit, such as dozing pump (of model: *JM-15774-C07*) and thermostat water bath (of model: *TT-6*), were standard equipment. Also, stringent care was taking during the assemblage and usage of the set-up, to avoid unwarranted systematic errors.

CHAPTER FIVE

CONCLUSION AND RECOMMENDATION

5.1 CONCLUSION

It is important to draw attention to a number of conclusions that follow the realization of the goals of this study. The Ester of Castor seed oil (ECSO) is less acidic than that of Rubber seed oil (ERSO), and as such saponifies better. ERSO is better enriched with phytochemical properties (such as flavonoid, saponins, oxalate and steroid) than ECSO; this, thus, disposes the ERSO more than the ECSO for corrosion inhibition applications.

Inhibition efficiencies of ERSO-treated dynamic runs, at all concentrations and treatment temperatures, were higher than those of ECSO; maximum inhibition efficiencies for ERSO and ECSO applications were respectively 64.4% and 34.4% at 50% stroke, 10g/*l* dosage and 40^{o}C. Further more, increase in treatment temperatures and pressures drastically lowered the inhibition efficiency. Also increase in dosage of the corrosion medium per unit time of the flow system leads to increase in the rate of corrosion of the mildsteel.

Inhibition efficiencies of ERSO-reacted static runs, obtained from potentiodynamic polarization measurements were also higher than those of ECSO, peaking at 81.70% whereas that of ECSO peaked at 75.40%, both for 20g/*l* treatments at ambient temperature. SEM pictures of the mildsteel immersed in ECSO and ERSO showed the existence of absorbate species, while FTIR spectra revealed that there were shifts due to O-H/N-H and C=O stretching frequencies from 3386cm^{-1} to 3209cm^{-1} and from 1743cm^{-1} to 1203cm^{-1}.

Thermodynamic study of process showed that the corrosion reaction is endothermic, and is influenced by process parameters such as pressure, temperature and time. The data for both samples were found to fit the Langmuir model, but do not fit the Freundlich model. Temkin and El-Awady isotherms favoured ERSO data better than those of ECSO. The inhibitor samples studied, generally, proved to be good for mildsteel corrosion inhibition, even though the Rubber-derived one was more effective.

5.2 RECOMMENDATION

Sequel to the observations and consequent inferences from this research work, the following recommendations are essential:

(a) Soxhlet extraction, at suitable temperature (about 60^{o}C) is recommended for purer and better oil yield and quality.

(b) For corrosion inhibition purposes, assessment of phytochemical properties of the proposed inhibitor is necessary in determining its inhibition suitability.

(c) Inhibitor samples of higher phytochemical composition are recommended for mildsteel corrosion inhibition purposes.

(d) Langmuir isotherm is recommended for assessment of data fit for corrosion reaction, because of its better fits.

(e) As the inhibitor samples assessed in this research work made very reasonable impacts in the protection of the mildsteel, they are both recommended for wider and regular corrosion inhibition applications.

(f) In further studies, methods of electronic impedance spectroscopy (EIS) and quantum chemicals should be adopted for better results.

5.3 CONTRIBUTION TO KNOWLEDGE

In recognition of very vast existing knowledge in corrosion studies, the present work was able make the following contributions:

1. Development of corrosion study kit used for the corrosion inhibition study in flow system, which could serve as a road-map for the study of corrosion inhibition in flow pipes.
2. It established a reasonable guidance on the utilization of esters of rubber and castor seed oils for corrosion inhibition in flow pipes, especially in oil and gas industries (that use corrodible materials).
3. The present study offers a relevant guide on the extraction of rubber seed oil, using petroleum ether as alternative solvent to normal hexane.
4. The study was able establish that maximum inhibition efficiencies of 64.4% and 34.4% for ERSO and ECSO applications respectively are obtainable at 50% stroke, 10g/*l* dosage and 40^{o}C conditions for the flow system, while those of the static runs (from potentiodynamic polarization) were obtained at 81.70% and 75.40% ERSO and ECSO respectively at 20g/*l* treatments and ambient temperature conditions.

REFERENCES

Abdallah M. (2014). Antibacterial Drugs as Corrosion Inhibitors for Corrosion of Aluminum in Hydrochloric Solution; *Corrosion Science*; 46(8): 1981-1996.

Achmad W., Devina I.A. and Indah H. (2012). Oil Extraction Process from Solid Waste Rubber Seed by Soxhletation and Extraction Solvent by Stirring Methods; *Proceeding of International Conference of the Department of Chemical Engineering on 'Chemical and Material Engineering'*; Diponegoro University, Indonesia; September 12-13.

Adejo S., Ekwenchi M.M., Gbertyo J. and Ogbodo J.O. (2014). Determination of Adsorption Isotherm Model Best Fit for Methanol Leaf Extract of Securinega Virosa as Corrosion Inhibitor for Corrosion of Mildsteel in HCl; *Journal of Corrosion Science and Control*; 5(8): 1-17.

Aggarwal L.K., Thapliyal P.C. and Karade S.R. (2007). Anticorrosive Properties of the Epoxy-Cardanol Resin Based Paints; *Progress in Organic Coatings*; 59(1):76-80.

Ahamad I, Prasad R., Ebenso E.E. and Quraishi M.A. (2012). Electrochemical and Quantum Chemical Study of Albendazole as Corrosion Inhibitor for Mildsteel in Hydrochloric Acid Solution; *International Journal of Electrochemical Science*; 7(3): 3436-3452.

Ahmed S. (2007). Polymer Science, Coatings and Adhesives, Safety Aspects of Coatings in Coatings and Adhesives; *National Science Digital Library*, India.

Ahmad S., Zafar F., Sharmin. E., Garg N. and Kashif M. (2012). Synthesis and Characterization of Corrosion Protective Polyurethanefattyamide/ Silica Hybrid Coating Material; *Progress in Organic Coatings*; 73(1): 112- 117

Aigbodion A.I. (1994). Effect of Storage of Seeds on Quality of Rubber Seed Oil; *India Journal of Natural Rubber*; 9(2): 141-143.

Aigbodion A.I. and Pillai C.K.S. (2007). Preparation, Analysis and Applications of Rubber Seed Oil and its Derivatives in Surface Coatings; *Progress in Organic Coatings*; 3(8):187-192.

Aigbodion A.I. and Pillai C.K.S. (2001). Synthesis and Molecular Weight Characterization of Rubber Seed Oil-Modified Alkyd Resins; *Journal of Applied Polymer Science*; 79(10): 2431-2438.

Aigbodion A.I., Okieimen F.E., Ikhuoria E.U., Bakare I.O. and Obazee E.O. (2003). Rubber Seed Oil Modified with Maleic Anhydride and Fumaric Acid and their Alkyd Resins as Binders in Water-Reducible Coatings, *Journal of Applied Polymer Science*; 89(12): 3256-3259.

Aigbodion A.I., Okiemien F.E., Ikhuoria E.U., Bakare I.O. and Obazaa E.O. (2010). Rubberseed Oil Modified with Maleic Anhydride and Fumaric Acid and their Alkyd Resins as Binders in Water Reducible Coatings; *Journal of Applied Polymer Science*; 89(8): 3256-3259.

Aigbodion A.I., Okiemien F.E., Obaza E.O. and Bakare I.O. (2003). Utilization of Rubber Seed Oil and its Alkyd Resin as Binders in Water Borne Coatings; *Progress in Organic Coating*; 46(1): 28-31.

AI-Mayouf A.M. (1999). Inhibitors For Chemical Cleaning Of Iron With Tannic Acid; *Desalination*; 121(2): 173-182.

Akintayo C.O. and Adebowale K.O. (2004). Synthesis and Characterization of Acrylated Albizia Senth Medium Oil Alkyds; *Progress in Organic Coatings*; 50: 207-12.

Alam J., Riaz U. and Ahmad S. (2009). High Performance Corrosion Resistant Polyaniline/Alkyd Eco-friendly Coatings; *Current Applied Physics*; 9(1): 80-86.

Alam M., and Al-Aandis N. (2012). Synthesis and Characterization of Poly(Styrene-Co-Maleic Anhydride) Modified Pyridine Polyesteramide Coating from Sustainable Resource; *Pigment & Resin Technology*; 41(1): 20-24.

Alam M., Shaik M.R. and Alandis N.M. (2013). Vegetable-Oil-Based Hyperbranched Polyester-Styrene Copolymer Containing Silver Nanoparticle as Antimicrobial and Corrosion-Resistant Coating Materials; *Journal of Chemistry*; 20(3): 211-218.

Altwaiq A, Khouri S. J., Al-luaibi S., Lehmann R, Drucker H. and Vogt C. (2011). The Role of Extracted Alkali Lignin as Corrosion Inhibitor; *Journal of Materials and Environmental Science*; 2(3): 259-270.

Amadi, S.A. (2006). Corrosion Failure Analysis of Oil and Gas Flowlines in the Niger Delta Region of Nigeria. *Journal of the Nigerian Society of Chemical Engineers*, 21(4), 132-134.

Anon C.E. (1950). Drying Oil for the Paint Industry; *Board of Trade Journal*; 15(4): 771-773.

Anon A.C. (2009). Para-Rubber Seed as a Source of Oil and Feeding Cake; *Bulletin of Imperial Institute*; Vol.17: 543-571.

Araujo W.S, Margarit I.C.P., Mattos O.R, Fragata F.L. and de Lima-Neto P. (2010). Corrosion Aspects of Alkyd Paints Modified with Linseed and Soy Oils; Electrochimica Acta, 55(12): 6204-6211.

Association of Official Analytical Chemist, AOAC (1997). Official Method of Analysis; Alpha Books Inc.; Washington D.C.

Asuquo J.E., Anusiem A.C.I., and Etim E.E. (2012a). Comparative Study of the Effect of Temperature on Adsorption of Metallic Soaps of Shear Butter, Castor and Rubber Seed Oils onto Hematite; *International Journal of Modern Chemistry*; 3(1): 39-50.

Asuquo J.E., Anusiem A.C.I., and Etim E.E. (2012b). Extraction and Characterization of Rubber Seed Oil; *International Journal of Modern Chemistry*; 3(1): 109-115.

Asuquo J.E., Anusiem A.C.I., and Etim E.E. (2010). Extraction and Characterization of Shear Butter Oil; *World Journal of Applied Science Technology;* 2(1): 282-288.

Athawale V.D. and Joshi K.R. (2012). A Comparative Study on Coating Properties of Chemoenzymatically Synthesized and Conventional Alkyd Resins; *Paintindia*, India; 47-51.

Athawale V.D. and Nimbalkar R.V. (2011). Waterborne Coatings Based on Renewable Oil Resources: an Overview; *Journal of American Oil Chemists' Society*; 88(2): 159-185.

Ayotunde E.O., Offem B.O. and Bekah A.F. (2011). Toxicity of Carica Papaya Linn: Haematological and Piscidal Effect on Adult Catfish; *Journal of Fisheries and Aquatic Science; 6*(3): 291-308.

Baker J.M. (1971). Seasonal Effect, In: Cowell E.B. (ed.); *The Environmental Effects of Oil Pollution on Littoral Community*; Institute of Petroleum, London.

Bautista-Banos S., Hernandez-Lauzardo A.N., Velazquez-del Valle M.G., Hernandez-Lopez M., Ait Barka E., Bosquez-Molina E. and Wilson C.L. (2006). Chitosan as a Potential Natural Compound to Control Pre and Postharvest Diseases of Horticultural Commodities; *Crop Protection*; 25(2): 108-118.

Baycan N. (2005). Advanced Oxidative Treatment of Chlorinated Hydrocarbons; *Dokuz Eylul University: Graduate School Natural and Applied Sciences, PhD Thesis* Izmir.

Behzadnasab M., Mirabcdini S.M., Kabir K. and Jamali S. (2011). Corrosion Performance of Epoxy Coatings Containing Silane Treated ZrO_2 Nanoparticles on Mild Steel in 3.5% Nacl Solution; *Corrosion Science*; 53(1): 89-98.

Beitz J.M. (2005). Heparin-induced Thrombocytopenia Syndrome Bullous Lesions Treated with Trypsin-Balsam of Peru-Castor Oil Ointment: A Case Study; *Ostomy Wound Manage*; 51(6): 52-58.

Belgacem M.N. and Gandini A. (2008). Materials from Vegetable Oils: Major Sources, Properties and Applications, in Monomers, Polymers and Composites from Renewable Resources; *Elsevier*, Amsterdam; pp.39-66.

Belgacem M.N., Blayo A. and Gandini A. (2003). Organosolv Lignin as a Filler in Inks, Varnishes and Paints; *Industrial Crop and Products*; 18(2): 145-153.

Bello M., Ochoa N., Balsamo V., Lopez-Carrasquero F., Coli S., Monsalved A. and Gonzalezd G. (2010). Modified Cassava Starches as Corrosion Inhibitors of Carbon Steel: An Electrochemical and Morphological Approach; *Carbohydrate Polymers*; 82(3): 561-568.

Bierwagen G.P. (2011). Reflections on Corrosion Control by Organic Coatings; *Progress in Organic Coatings*; 28(1): 43-48.

Boel M.E., Lee S.J., Rijken M.J., Paw M.K., Pimanpanarak M., Tan S.O., Singhasivanon P., Nosten F. and McGready R. (2009). **Castor Oil for induction of labour: not harmful not helpful**; *Australia and New Zealand Journal of Obstetrics and Gynaecology*; 49(5): 499-503.

Brady George S., Clauser Henry R. and Vaccari John (2007). Materials Handbook (14th ed.); McGraw-Hill, New York.

Bruning H.H. (1992). Utilization of Vegetable Oils in Coatings; *Industrial Crops and Products*; 1(2): 89-99.

Brydson J.A. (2009). Rubbery Materials and their Compounds; *Hob House*; Washington D.C.

Bun Tean, Sath E.O., Pok Samkol and Ly J. (2006). Utilization by Pigs of Diets Containing Cambodian Rubber Seed Meal; *Journal of Natural and Applied Science*; 84(13): 101-110.

Burkill H.M. (2007). Useful Plants of West Tropical Africa; *Kew Publishing Company*, United Kindom.

Busso C. and Castro-Prado M.A. (2014). Cremophor El Stimulates Mitotic Recombination in UVSH//UVSH Diploid Strain of Aspergillus Nidulans; *Anais da Academia Brasileira de Ciencias*; 76(1):49-55.

Byron R.B., Warren E.S. and Edwin N.L.(2002). Transport Phenomena; *John Wiley & Sons Inc.*; New-Delhi.

Kusefoglu C. and Wool R.P (2002). Rigid Thermosetting Liquid Molding Resins from Renewable Resources II; Copolymers of Soybean Oil Monoglyceride Maleates with Neopentyl Glycol and Bisphenol a Maleates; *Journal of Applied Polymer Science*; 83(5):972-980.

Casey P.J. and Seabra, M.C. (1996). Prenyltransferases Protein; *Journal of Biological Chemistry*; 271(10): 5289-5292.

Catalkaya C.E. and Kargi F. (2007). Color, Toc and Aox Removals from Pulp Mill Effluent in Advanced Oxidation Processes: A Comparative Study; *Journal of Hazardous Materials*; 139(16): 244-253.

Chen X., Li G., Lian J. and Jiang Q. (2008). Study of the Formation and Growth of Tannic Acid Based Conversion Coating on AZ91D Magnesium Alloy; *Surface and Coatings Technology*; 204(5): 736-747.

Chen X., Li G., Lian J. and Jiang Q. (2009). An Organic Chromium-Free Conversion Coating on AZ91D Magnesium Alloy; *Applied Surface Science*; 255(5): 2322-2328.

Chen Z., Wu Jennifer F., Fernando S. and Jagodzinski K. (2011). Soy-Based, High Biorenewable Content UV Curable Coatings; *Progress in Organic Coatings*; 71(1): 98-109.

Cheng S., Chen S., Liu T., Chang X. and Yin Y. (2007). Carboxymethylchitosan + Cu^{2+} Mixture as an Inhibitor used for Mild Steel in 1M HCl; *Electrochimical Acta*; 52(19): 5932-5938.

Chin H.C. (2012). Methods of Measuring the Dry Rubber Content of Field Latex; *RRIM Training Manual on Analytical Chemistry*, Revised Edition; Kuala Lumpar.

Dahmani M., Et-Touhami A, AI-Deyab S.S., Hammouti B. and Bouyanzer A. (2010). Corrosion Inhibition of C38 Steel in 1M HCl: A Comparative Study of Black Pepper Extract and Its Isolated Piperine; *International Journal of Electrochemical Sciences*; 5(1):1060-1069.

Derksen J.T.P., Cuperus F.P. and Kolster P. (2010). Paints and Coatings from Renewable Resources; *John-Willy and Sons*; London.

Derksen J.T.P., Cuperus F.P. and Kolster P. (1996). Renewable Resources in Coatings Technology: a Review; *Progress in Organic Coatings*; 27(1): 45-53.

Devan S., Sangaula H. and Kumar V. (2000). Preliminary Studies on the Analgestic Activity of Latex of Calotropis Procera; *Journal of Ethnopharmacology*; 7(3): 307-311.

Dhoke S.K. and Khanna A.S. (2009). Effect of Nano-Fe_2O_3 Particles on the Corrosion Behavior of Alkyd Based Waterborne Coatings; *Corrosion Science*; 51(1): 6-20.

Eastop T. D. and McConkey A. (1993). Applied Thermodynamics for Engineering Technologists; *Pearson Education Ltd*; New Delhi.

Ebelewe R.O., Iyayi A.F. and Hymore F.K. (2010). De-acidification of High Acidic Rubber Seed Oil by Re-esterification with Glycerol; *International Journal of Physical Sciences*, 5(6): 841-846.

Eddy N. O. and Odoemelam S. A. (2008). Inhibition of the Corrosion of Mild Steel in Acidic Medium by Penicillin V Potassium; *Advances in Natural and Applied Sciences*; 2(3): 225-232.

Eddy N. O., Odoemelam S. A. and Odiongenyi, A. O. (2008). Ethanol Extract of Musa acuminate peel as an eco-friendly inhibitor for the corrosion of mild steel in H_2SO_4; *Advances in Natural and Applied Sciences*; 2(1): 35-42.

Eddy N. O., Odoemelam S. A. and Odiongenyi A. O. (2009). Inhibitive, adsorption and synergistic studies on ethanol extract of Gnetum Africana as green corrosion inhibitor for mild steel in H_2SO_4; *Green Chemistry Letters and Reviews*; 2(2): 111-119.

Eddy N.O., Stoyanov S.R. and Ebenso E. (2010). Fluoroquinolones as Corrosion Inhibitors for Mild Steel in Acidic Medium- Experimental and Theoretical Studies; *International Journal of Electrochemical Science*; 5(8): 1127-1150.

Eram Sharmin, Sharif Ahmed and Fahmina Zafar (2011). Renewable Resources in Corrosion Resistance; PG-Lecture Note; Department of

Chemistry, Jamia Millia Islamia Central University, New Delhi-India.

Fabbri P., Singh B., Leterrier Y., Manson J.A.E., Messori M. and Pilati F. (2006). Cohesive and Adhesive Properties of Polvcaprolactone/Silica Hybrid Coatings on Poly(Methyl Methacrylate) Substrates; *Surface and Coatings Technology*; 200(24): 6706-6712.

Fafioye O.O., Adebisi A.A. and Fagade S.O. (2004). Toxicity of Parkia Biglossa and Raphia Vinfera Extracts on Clarias Gariepinus Juveniles; *African Journal of Biotechnology*; 3(6): 627-630.

Fekry A.M. and Mohamed R.R. (2010). Acetyl Thiourea Chitosan as an Eco-friendly Inhibitor for Mild Steel in Sulphuric Acid Medium; *Electrochimica Acta*; 55(6): 1933-1939.

Fisher Suzanne Hayes (2009). Aircraft, Production during the War; In Tucker Spencer C., Wood Laura Matysek and Murphy Justin D.(ed.): ***The European Powers in the First World War: An Encyclopedia***. *Taylor & Francis*; U.K.

Fromtling R.A. (1988). Overview of Medically Important Antifungal Azole Derivatives; *Clinical Microbiological Reviews*; 1(2): 187-217.

Galvan, Jr. I.C, Simancas J., Morcillo M., Bastidas J.M., Almeida E. and Feliua S. (2012). Effect of Treatment with Tannic, Gallic and Phosphoric Acids on the Electrochemical Behaviour of Rusted Steel; *Electrochimica Acta*; 37(11): 1983-1985.

Gandini A. and Belgacem M.N. (2002). Recent Contributions to the Preparation of Polymers Derived from Renewable Resources; *Journal of Polymers and Environment*; 10(3): 105-114.

George U.U., Andy J.A. and Joseph A. (2014). Biochemical and Phytochemical Characteristics of Rubber Latex (Hevea Brasiliensis) obtained from a Tropical Environment in Nigeria; *International Journal of Scientific and Technology Research*; 3(8): 377-380.

Ghali E., Sashtri V.S. and Elboujdaini M. (2011). Corrosion Prevention and Protection, Practical Solutions, Seiten, Hardcover; *John Wiley & Sons*, United Kingdom.

Gomez J.B., and Moir G.F. (2009). The Ultracytology of Latex Vessels in Hevea Brasiliensis; *Malaysia Rubber Research Development*, Kuala Lumpar.

Grassino S.B., Strumia M.C., Couve J. and Abadie M.J.M. (1999). Photoactive Films Obtained from Methacrylo-Urethanes Tannic Acid-based with Potential Usage as Coating Materials: Analytic and Kinetic Studies; *Progress in Organic Coatings*; 37(2): 39-48.

Guilmartin John F., Jr. (1994). Technology and strategy: What are the limits; *United States Army War College, Strategic Studies Institute*, U.S.A.

Harbone J.B. (1998). Phytochemical Methods: A Guide to Modern Techniques of Plant Analysis; *Chapman and Hall*, New York.

Ha-Won S. and Velu S. (2007). Corrosion Monitoring of Reinforced Concrete Structures- A Review; *International Journal of Electrochemical Science*; 2(2): 1-28.

Heidariani M., Shishesaz M.R., Kassiriha S.M. and Nematollahi M. (2010). Characterization of Structure and Corrosion Resistivity of Polyurethane/Organoclay Nanocomposite Coatings Prepared through an Ultrasonication Assisted Process; *Progress in Organic Coatings*; 68(3): 180-188.

Heinz-Hermann Greve (2008). Rubber-2-Natural, In: *Ulmann's Encyclopedia of Industrial Chemistry*; *Wiley-VCH*; Weinheim.

Heisey R.M. and Papadatos S. (1995). Isolation of Microorganisms Able to Metabolize Puriced Natural Rubber; *Applied Environmental Microbiology,* 61(1): 3092-3097.

Hobhouse Henry (2005). Seeds of Wealth: Farm Plants that made Men Rich; *Shoemaker and Hoard*; Delhi.

Hubert G., Elmar-Manfred H., Hartmut S. and Helmut S. (2002). Corrosion: Ullmann's Encyclopedia of Industrial Chemistry; *Wiley-VCH*; Weinheim.

Finsgarand M. and Milosev I. (2010). Inhibition of Copper Corrosion by 1,2,3-Benzotriazol: a Review; *Journal of Corrosion Science*; 52(1): 2737-2749.

Hui C., Zhenghao F., Jingling S., Wenyan S. and Qi X. (2013). Corrosion Inhibition of Mildsteel by Aloes Extract in HCl Solution Medium; *International Journal of Electrochemical Science*; 8(2): 720-734.

Hussain S., Fawcett A.H. and Taylor P. (2002). Use of Polymers from Biomass in Paints; *Progress in Organic Coatings*; 5(4): 435-439.

Institut de Recherche sur le Caoutchouc en Afrique (2007). L'hevea Cultures En France: Les Stations ; *I.R.C.A. des Caraibes* ; Caoutchouc et Plastiques.

Jaen J.A, De Obaldia J. and Rodriguez M.V. (2011). Application of Mossbauer Spectroscopy to the Study of Tannins Inhibition of Iron and Steel Corrosion; *Hyperfine Interactions*; 751-011-0337-1Online First.

Jendroseck D., Tomasi G. and Kroppenstedt R.M. (2015). Bacterial Degradation of Natural Rubber: A Privilege of Antinomycetes; *FEMS Microbiology Letters*; Vol. 150: 179-188.

Jiali H., Hui C., Quianwei L. and Jingling S. (2013). Environmental Friendly Inhibitor for Mildsteel by Artemisia Halodendron; *International Journal of Electrochemical Science*; 8(2): 8592-8602.

John Mitchell Peter, Diemer Per and Griffee Peter (2013). Processing Of Natural Rubber, Manufacture Of Latex-Grade Crepe Rubber; *Agricultural and Food Engineering Technology Service*; Vol. 19.

Jumat S., Bashar M.A. and Nadia S. (2012). Rubber (*Hevea Brasiliensi*) Seed Oil Toxicity Effect and Linamarin Compound Analysis; *Biomed Central Ltd,* Malaysia.

Kang H., Kang M.Y. and Han K.H. (2000). Identification of Natural Rubber and Characterization of Biosynthetic Activity; *Plant Physiolology*; 123(3): 1133-1142.

Kelly A.J., Kavanagh J. and Thomas J. (2013). Castor Oil, Bath and/or Enema for Cervical Priming and Induction of Labour; *Cochrane Database of Systematic Reviews*, Vol. 7.

Khalid K.B.(1982). Determination of Dry Rubber Content of Hevea Latex by Microwave Technique; *Pertenika;* 5(2): 192-195.

Kim H.B. and Winnink N.A. (1994). Effect of Surface Acid Group Neutralization on Rubber Latex Films; *Macromolecules;* 2(7):1007-1012.

Konwar U., Karak N. and Mandal M. (2010). Vegetable Oil Based Highly Branched Polyester/Clay Silver Nanocomposites as Antimicrobial Surface Coating Materials; *Progress in Organic Coatings*; 60(4): 265-273.

Koyama, Tanetoshi and Steinbuchel, Alexander (2011). Biosynthesis of Natural Rubber and Other Natural Polyisoprenoids; *Wiley-Blackwell*, London.

Kroon G. (1993). Associative Behavior of Hydrophobically Modified Hydroxyethyl Celluloses (HMHECs) in Waterborne Coatings; *Progress in Organic Coatings*; 22(4): 245-260.

Kumar G., Buchheit R.G. (2005). Development and Characterization of Corrosion Resistant Coatings using Natural Biopolymer Chitosan; *Electrochemical Society Transactions*; 1(9): 101-117.

Larshin, M. Bousaid, Lazrek H.B., Jana M. and Amarouch H. (2007). Evaluation of Antifungal and Molluscidal Properties of Extract of Calotropis Procera; *Fitoterapia;* 6(8): 371-373.

Leeang, K.W.H (1993). Microbiologic Degradation of Rubber; *Journal of Amalgamated Water Works Association*, 5(3): 1523-1535.

Legrini O., Oliveros E., and Braun A.M. (1993). Photochemical Processes for Water Treatment; *Chemical Reviews*; 93(5): 671-698.

Linos A. and Steinbuchel A. (1998). Microbial Degradation of Natural and Synthetic Rubbers by Novel Bacteria Belonging to the Genus Gordona; *Kautsch Gummi Kunstst*; 5(1): 496-499.

Linos Alexandros, Reichelt Rodulf Keller Ulrike and Steinbuchel Alexander (1998). A Gram-Negative Bacterium, Identified as Pseudomonas Aeruginosa- Al98, is a Potent Degrader of Natural Rubber and Synthetic Cis-L, 4-Polyisoprene; *FEMS Microbiology Letters*, Vol. 182: 155-161.

Linos Alexandros, Steinbuchel Alexander, Sproer Cathrin and Kropenstedt Reiner M. (1999). Species of Gordonia Polyisoprenivorans, a Rubber Degrading Actinomycete Isolated from Automobile Tire; *International Journal of System Bacterial*; 4(9): 1785-1791.

Liu X., Xu K., Liu H, Cai H, Su J., Fu Z., Guo Y. and Chen M. (2011). Preparation and Properties of Waterborne Polyurethanes with Natural Dimer Fatty Acids Based Polyester Polyol as Soft Segment; *Progress in Organic Coatings*; 16(7): 22-30.

Lopes F.A, Morin P., Oliveira R. and Melo L.F. (2006). Interaction of Desulfovibrio Desulfuricans Biofilms with Stainless Steel Surface and its Impact on Bacterial Metabolism; *Journal of Applied Microbiology*; 101(3): 1087-1095.

Lu Y., Zhan, L. and Xiao P. (2004). Structure, Properties and Biodegradability of Water Resistant Regenerated Cellulose Films Coated with Polyurethane/Benzyl Konjac Glucomannan Semi-IPN Coating; *Polymer Degradation and Stability*; 86(1): 51-57.

Lundvall O., Gulppi M., Paez M.A, Gonzalez E., Zagal J.H, Pavez J. and Thompson G.E. (2007). Copper Modified Chitosan for Protection of AA-2024. Surface and Coatings Technology; 201(12): 5973-5978.

Mallika G.V., Jansz E.R. and Nirmala M. Pieris (1991). Cyanogenic Glucosides and Glucosidases of Rubber Seed Kernel; *Journal of Natural Sciences*; 6(8): 24-32.

Marmion L.C., Desser K.B., Lilly R.B. and Stevens D.A. (2010). Reversible Thrombocytosis And Anemia Due to Miconazole Therapy; *Antimicrobial Agents and Chemotherapy*; 10(3): 447-449.

McGuire Nancy (2012). Taming the Bean; *The American Chemical Society*; Vol. 6.

Meir M.A, Metzger J.O., Scubert U.S. (2007). Plant Oil Renewable Resources as Green Alternatives in Polymer Science; *Chemical Society Review*; 36(11): 1788-1802.

Menon A.R.R., Aigbodion A.I., Pillai C.K.S., Mathew N.M. and Bhagawans S.S. (2002). Processibility Characteristics and Phsyco-Mechanical Properties of Natural Rubber Modified with Cashew Nut Shell Liquid and Cashew Nut Shell Liquid-Formaldehyde Resin; *European Polymer Journal*; 38(1): 163-168.

Metcalf A. and Eddy C. (2006). Wastewater Engineering: Treatment and Reuse; *McGraw-Hill*, New York.

Metzger J.O. (2001). Organic Reactions without Organic Solvents and Oils and Fats as Renewable Raw Materials for the Chemical Industry; *Chemosphere*; 43(1): 83-87.

Micha J.P., Goldstein B.H. and Birk C.L. (2006). Abraxane in the Treatment of Ovarian Cancer: the Absence of Hypersensitivity Reactions; *Gynecologic Oncology*; 100(2): 437-448.

Mohammed R.S., Manawwer A. and Nasar M.A. (2015). Development of Castor Oil Based Poly (Urethane-esteramide)/TiO_2 Nanocomposites as Anticorrosive and Antimicrobial Coatings; *Journal of Nanomaterials*; 7(4): 1-10.

Morcillo M., Feliu S., Simancas J., Bastidas J.M., Galvan J.C., Feliu, Jr S., and Almeida E.M. (1992). Corrosion of Rusted Steel in Aqueous Solutions of Tannic Acid; *Corrosion*; 48(1032): 1-8.

Mulder W.J., Gosselink R.J.A, Vingerhoeds M.H, Harmsen P.F.H and Eastham D. (2011). Lignin Based Controlled Release Coatings; *Industrial Crops and Products*; 34(1): 915-920.

Muller F. (2010). Current Rubber Industries Situation in Thailand; *Rubber International Magazine*; Vol.2, pg.71-78.

Musa A.Y., Kadhum A.H., Mohamad A.B., Rahoma A.B. and Mesmari H. (2010). Electrochemical and Quantum Chemical Calculations on 4,4-dimethyloxazolidine-2-thione as Inhibitor for Mildsteel Corrosion in Hydrochloric Acid; *Journal of Molecular Structure*, 9(6): 233-237.

Mutlu H., Meier M.A.R. (2010). Castor Oil as A Renewable Resource For The Chemical Industry; *European Journal of Lipid Science and Technology*; 112(1): 10-30.

Naqvi I., Saleemi A.R. and Naveed S. (2011). Cefixime: A drug as Efficient Corrosion Inhibitor for Mild Steel in Acidic Media- Electrochemical and Thermodynamic Studies; *International Journal of Electrochemical Science*; 6(1): 146-161.

Nasrazadani S. (1997). The Application of Infrared Spectroscopy to a Study of Phosphoric and Tannic Acids Interactions with Magnetite ($Fe3O_4$), Goethite (a-FEOOH) and Lepidocrocite (y-FeOOH); *Corrosion Science*; 39(11): 1845-1859.

Ngassapa F.N. and Othman O.C (2001). Physicochemical Characteristics of Some Locally Manufactured Edible Vegetable Oils Marketed Dar Es Salam; *Tanzanian Journal of Science*; 27(1): 49-58.

Nnaji N.J.N., Obi-Egbedi N.O. and Ani J.U. (2011). Leaf Extract of Anthodeista Djalonensis as Corrosion Inhibitor of Aluminium in HCl Solution; *Journal of Scientific and Industrial Research*; 9(1): 26-32.

Nwabanne J.T. and Okafor V.N. (2012). Adsorption and Thermodynamics Study of the Inhibition of Corrosion of Mildsteel in H_2SO_4 Medium Using Vernonia Amygdalina; *Journal of Minerals Characterization and Engineering*; 11(3): 885-890.

O'Toole G., Kaplan H.B. and Kolter R. (2000). Biofilm Formation as Microbial Development. *Annual Review of Microbiology*; 54(1): 49-79.

Obi-Egbedi N.O., Essien K.E., Obot I.B. and Ebenso E.E. (2011). 1,2-diaminoanthraquinone as Corrosion Inhibitor for Mildsteel in HCl; *International Journal of Electrochemical Science*; 6(2): 913-930.

Obot I.B., Obi-Egbedi N.O. and Umoren S.A. (2009a). Antifungal Drugs as Corrosion Inhibitors for Aluminum in 0.1M HCl; *Journal of Corrosion Science and Control*; 51(8): 1868-1875.

Obot I.B., Obi-Egbedi N.O. and Umoren S.A. (2009b). Inhibitive Properties of Clotrimazole for Aluminium Corrosion in Hydrochloric Acid; *International Journal of Electrochemical Science*; 4(1): 863-877.

Ocampo L.M., Margarit I.C.P., Mattos O.R., Cordoba-de-Torresi S.I and Fragata F.L. (2004). Performance of Rust Converter based in Phosphoric and Tannic Acids; *Corrosion Science*; 46(6): 1515-1525.

Offurum J.C., Iheme C. and Chikaire A.J. (2011). Isotherm and thermodynamics Studies for Adsorption of Dissolved Solid Particles on Cow Bone Granule; Continental Journal of Engineering Science; 6(1): 31-36.

Offurum J.C. (2011). Surface Response Methodology for the Coagulation of Solid Particles in Coal Effluent using Chitin-derived Coagulant; Continental Journal of Engineering Science; 6(2): 7-14.

Ogunniyi D.S. (2006). Castor Oil: a Vital Industrial Raw Material Bioresource Technology; 97(9): 1086-1091.

Okafor P.C., Ebenso E.E. and Ekpe U.J. (2010). Azadirachta Indica Extractas Corrosion Inhibitor for Mildsteel in Acid Medium; *InternationalJournal of Electrochemical Science*; 5(1): 978-993.

Okieimen F.E. (2000). Effect of Rubber Seed Oil Derivatives on the Thermal Degradation of the PVC; *Journal of Scientific Industrial Research*; 5(9): 563-568.

Okieimen F.E. and Okieimen C.O. (2000). Utilization of Vegetable Oils as an Alternative Diesel Fuel: A review; *Nigerian Journal of Applied Science*; 1(8):102-108.

Older Jules (2010). Back-road and Off-road Biking; *Stackpole Books*, Mechanicsburg.

Oluwadare G.O., Akindahunsi A.A., Oluwole O. and Agbaje A.I. (2009). Effects of Cassava Juice on Corrosion of Mild and High Yield Steel Bars in Concrete Structures; *NSE Technical Transaction, 44(1)*; January-March.

Onyeike E.N. and Acheru G.N. (2002). Chemical Composition Composition of Selected Nigerian Oil Seeds and Phytochemical Properties of the Oil Extracts; *Journal of Food Chemistry*; 7(6): 431-437.

Osagie A.U. (1998). Anti-nutritional Factors; In: *Nutritional Quality of Plant Foods*; *Ambik Press*, Benin City-Nigeria.

Ostovari A, Hoseinieh S.M., Peikari M., Shadizadeh S.R.and Hashemi S.J. (2009). Corrosion Inhibition of Mild Steel in 1M HCl Solution by Henna Extract: A Comparative Study of the Inhibition by Henna and its Constituents (Lawsone, Gallic acid, a-D-Glucose and Tannic acid); *Corrosion Science*; 51(9): 1935-1949.

Ozcan M. and Dehri I. (2004). Electrochemical and Quantum Chemical Studies of Some Sulphur-containing Organic Compounds as Inhibitors for the Acid Corrosion of Mildsteel; *Progress in Organic Coatings*; 51: 181-187.

Pagella C, Spigno G., De Faveri D.M. (2002). Characterization of Starch based Edible Coatings; *Food and Bioproducts Processing*; 80(3): 193-198.

Park Y., Doherty W.O.S. and Halley P.J. (2008). Developing Lignin-Based Resin Coatings and Composites; *Industrial Crops and Products*; 27(2): 163-167.

Patel R.P., Patel P.C. and Raval D.A. (2010). Alkyd Resins from Acylated Prepolymerized Rubber Seed Oil; *Inter Polym Matter*; 4(8):49-61.

Paterson-Jones J.C., Gilliland M.G. and Van Staden J. (1990). The Biosynthesis of Natural Rubber; *Journal of Plant Physiology*; 136(3): 257-263.

Pearson (2008). Pearson's Chemical Analytical Methods- General Methods; In: Young Jnr A.V. (ed); ***Laboratory Handbook of Methods of Food and Analysis***; *Leonard Hall*, U.K.

Petringa Maria (2013). Brazza, a life for Africa; *Author House*; Bloomington.

Petsonk E.L. (2009). Couriers of Asthma: Antigenic Proteins in Natural Rubber Latex; *Occupational Medicine*; Philadelphia; Vol.15, pg. 421-430.

Philip Matthews (2003). Advanced Chemistry: Physical and Industrial; *Cambridge University Press*; Delhi.

Pryde E.H. and Rothfus J.A. (2011). Industrial and Non-Food Users of Vegetable Oils; In: Robbelen G., Downey R.K. and Ashri A. (ed). ***Oil crops of the world***; *McGraw-Hill;* New York; pp 87-117.

Raja P.B. and Sethuraman M.G. (2008). Natural Products as Corrosion Inhibitor for Metals in Corrosive Media - A review; *Materials Letters*; 62(1): 113-116.

Rinaudo M. (2006). Chitin and Chitosan: Properties and Applications; *Progress in Polymer Science*; 31(7): 603-632.

Rook, J.J. (1995). Microbiological Deterioration of Vulcanized Rubber; *Applied Microbiology*; 3(7): 302-309.

Sakhir A, Perrin F.X., Benaboura A, Aragon E. and Lamouric S. (2011). Corrosion Protection of Steel by Sulfo-Doped Polyaniline-Pigmented Coating; *Progress in Organic Coatings*; 72(3):473-479.

Satapathy A.K., Gunasekaran G., Sahoo S.C, Amit K. and Rodrigues P.V. (2009). Corrosion Inhibition by Justicia Gendarussa Plant Extract in Hydrochloric Acid Solution; *Corrosion Science*; 51(12): 2848-2856.

Schulze Gronover Christian, Wahler Daniela and Prufer, Dirk (2011). Natural Rubber Biosynthesis and Physic-Chemical Studies on Plant Derived Latex; In: Magdy Elnashar (ed). *Biotechnology of Biopolymer*; 97(8); 179-184.

Sena-Martins G., Almeida-Vara E. and Duarte J.C. (2008). Eco-friendly New Products from Enzymatically Modified Industrial Lignins; *Industrial Crops and Products*; 27(2): 189-195.

Sharmin E., Akram D., Zafar F., Ashraf S.J. and Ahmed S. (2012). Plant Oil Polyol Based Poly (Ester Urethane) Metallohybrid Coatings; *Progress in Organic Coatings*; 73(1): 118-122.

Shchukin D.G. and Mchwald H. (2007). Self-Repairing Coatings Containing Active Nanoreservoirs; *Small*; 3(6): 926-943.

Shiwkar Y.M. and Kumar V.L. (2003). Histamine Mediates the Pro-inflammatory Effect of Latex of Calotropis Procera in Rats; *Mediators Inflammation*; Vol.12: 299-302.

Shukla S.K. and Ebenso E.E. (2011). Corrosion Inhibition, Adsorption Behaviour and Thermodynamic Properties of Streptomycin on Mildsteel in Hydrochloric Acid Medium; *International Journal of Electrochemical Science*; 6(1): 3277-3291.

Singh D.D.N. and Yadav S. (2008). Role of Tannic Acid based Rust Converter on Formation of Passive Film on Zinc Rich Coating Exposed in Simulated Concrete Pore Solution; *Surface & Coatings Technology*; 202(5): 1526-1542.

Solomon D.H. (2012). The Chemistry of Organic Film Formers; *R.E. Krieger Publishing Co.*; New York; pp 60.

Sorensen P.A, Kiil S., Johansen K.D. and Weinell C.E. (2009). Anticorrosive Coatings: A Review; *Journal of Coatings Technology Research*; 6(2): 135-176.

Standards and Industrial Research Institute of Malaysia (1995). Methods of Sampling and Testing; *Concentrated Natural Rubber Lattices*; MS-3, Vol.18.

Stewart D. (200S). Lignin as a Base Material for Materials Applications: Chemistry, Application and Economics; *Industrial Crops and Products*; 27(2): 202-207.

Stosic D.D. and KayKay J.M. (2006). Rubber Seed as Animal Feed in Liberia; *World Animal Review*; Vol.39, pp 29-39.

Subramaniam A. (2008). The Chemistry of Natural Rubber Latex; *Immunology and Allergy Clinic of North-America*; Vol.15: 1-20.

Sugama T.I. (1995). Pectin Copolymers with Organosiloxane Grafts as Corrosion-protective Coatings for Aluminum; *Materials Letters*; 25(6): 291-299.

Sugama T.I. (1997). Oxidized Potato-starch Films as Primer Coatings of Aluminum; *Journal of Materials Science*; 32(15) 3995-4003.

Sugama T.I. and DuVall J.E. (1996). Polyorganosiloxane-grafted Potato Starch Coatings for Protecting Aluminum from Corrosion; *Thin Solid Films*; 289(2): 39-48.

Sugama T.I. and Milian-Jimenez S. (1999). Dextrine-modified Chitosan Marine Polymer Coatings; *Journal of Materials Science*; 34(9): 2003-2014.

Tanaka, Y. and Sakdapipanich J.T. (2008). Chemical Structure and Occurrence of Natural Polyisoprenes In: *T. Koyama and Steinbuchel (ed.)*; Biopolymers Isoprenoids Volumes; *Wiley-VCH;* Weinheim-Germany.

Tangestanian P., Papini M. and Spelta J.K (2001). Starch Media Blast Cleaning of Artificially Aged Paint Films; *Wear*; 248(2): 128-139.

Tarnborim S.M., Dias S.L.P., Silva S.N, Dick L.F.P. and Azambuja N.S. (2011). Preparation and Electrochemical Characterization of Amoxicillin-Doped Cellulose Acetate Films for AA2024-T3 Aluminum Alloy Coatings; *Corrosion Science*; 53(4): 1571-1580.

Tarvainena M., Sutinen R., Peltonen S., Mikkonen H., Maunusa J., Vaha-Heikkilad K, Lehtod V.P, and Paronena P. (2003). Enhanced Film-Forming Properties for Ethyl Cellulose and Starch Acetate using N-Alkenyl Succinic Anhydrides as Novel Plasticizers; *European Journal of Pharmaceutical Sciences*; 19(5): 363-371.

Thomas V., Mercykutty V.C. and Saraswathyamma C.K. (1998). Rubber Seed: Its biological and Industrial Applications; *Planter-Malaysia*; 74(8):437-443.

Thomas, Alfred (2011). Fats and Fatty Oils; *Ulmannn's Encyclopedia of Industrial Chemistry*; Wiley-VCH, Weinheim.

Trumbo D.L., Mote B.E. and Rasoul H.A.A. (2001). Synthesis of Copolymer of a Linoleic Derivative and Properties of the Copolymer Films. *Journal of Applied Polymer Science*; 80(7): 261-67.

Tsuchii A., Suzuki T. and Takeda K. (1998). Microbial Degradation of Natural Rubber Vulcanizates; *Applied Environmental Microbiology*, 50(6): 965-970.

Udoh D.E. (2012). Influence of Rawolfa Vomitora Bark Extract and Cardiac Enzymes of Normal Wistar Albino Rats; *Recent Progress Biopharmaceoticals in Medicinal Plants;* 14(4): 273-275.

Undiandeye J.A., Usman H.T, Abubakar M. and Offurum J.C. (2014) . Kinetics of Corrosion of Mild Steel in Petroleum-Water Mixture using Ethyl Esters of Lard as Inhibitor; *International Journal of Engineering and Science*; 3(4): 18-26.

Undiandeye J.A., Okewale A.O., Etuk B.R. and Igbokwe P.K. (2011) . Investigation of the use of Ethyl Esters of Castor Seed Oil and Rubber Seed Oil as Corrosion Inhibitors; *International Journal of Basic and Applied Sciences*; 11(6): 48-54.

U.S. Trariff Commision (2011). Tariff Information Surveys on the Articles in Paragraphs 44 and 45 of the Tariff Act of 1913; *Government Printing Office*, Washington DC.

Umoren S.A (2008). Inhibition of Aluminum and Mild Steel Corrosion in Acidic Medium Using Gum Arabic; *Cellulose*; 15(5): 751-761.

Umoren S.A, Obot I.B. and Obi-Egbedi N.O. (2009). Raphia Hookeri Gum as a Potential Eco-Friendly Inhibitor for Mild Steel in Sulfuric Acid; *Journal of Materials Science*; 44(1): 274-279.

Uzu F.O., Ihenyen G.A., Chukwuma F. and Imoebe S.O. (1985). Processing, Analysis and Utilization of Rubber Seed Oil and Cake; *Paper presented at the National Conference on Industrial Utilization of Natural Rubber Seed, Latex and Wood, Rubber Research Institute of Nigeria*, Benin City, 22nd-24th Jan.; pp 7-12.

Vasconez M.B, Flores S.K., Campos C.A, Alvaradoa J. and Gerschensonb L.N. (2009). Antimicrobial Activity and Physical Properties of Chitosan-Tapioca Starch Based Edible Films And Coatings; *Food Research International*; 42(7): 762-769.

Videla H.A and Herrera L.K. (2005). Microbiologically Influenced Corrosion: Looking to the Future; *International Journal of Microbiology*; 8(3): 169-180.

Videla H.A. and Characklis W.G. (2012). Biofouling and Microbially Influenced Corrosion; *International Journal of Biodeterioration and Biodegradation*; 29(3): 195-212.

Vimal P.O. (2010). The Use of Rubber Seed; *Planer Chronicle- India*; 76(7):333-336.

Vogel S. (2010). Quantitative Chemical Analysis; *RC-Denny, New Jessy*.

Warren L. McCabe, Julian C. Smith and Peter Harriott (2005). Unit Operations of Chemical Engineering; *McGraw-Hill Company*, New York.

Weiss K.D. (2012). Paint and Coatings: a Mature Industry in Transition; *Progress in Polymer Science*; 22(2): 203-245.

Wilson R., Van Schie B.J. and Howes D. (1998). Overview of the Preparation, Use and Biological Studies on Polyglycerol Polyricinoleate (PGPR); *Food and Chemical Toxicology*; 36(9): 711-718.

Wititsuwannakul D., Sakulborirug C. and Wititsuwannakul D. (1998). A Lectin from the Bark of Rubber Tree (Hevea Brasiliensis); *Phytochemistry*; 47(9): 18-27.

Witte F., Fischer J. Nellesen. J., Crostack H.A, Kaese V., Pisch-A-Beckmann F. and Windhagen H (2006). In-vitro and In-vivo Corrosion Measurements of Magnesium Alloys; *Biomaterials*; 27(7): 1013-1018.

Wood M. (2011). High-tech Castor Plants May Open Door to Domestic Production; *Agricultural Research Magazine* 49(1): 11-13.

Xie W., McMahan C.M., Distefano A.J. and DeGraw M.D. (2008). Initiation Of Rubber Synthesis in Vitro Comparisons Of Benzophenone-Modified Diphosphate Analogues in three Rubber Producing Species; Journal of Phytochemistry; 6(9): 2539-2545.

Xu T. (2002). Chemical Modification, Properties, and Usage of Lignin, Springer; *Biochemistry*; 2(1): 91-101.

Yordanov D. and Petkov P (2008a). Investigation of Ethyl Esters of Fatty Acids as Corrosion Inhibitors; *Journal of the University of Chemical Technology and Metallurgy*; 43(4): 405-408.

Yordanov D. and Petkov P. (2008b). Synthesis of Oxygenated Ethyl Esters of Tall Oil Fatty Esters and Characterization of their Properties as Corrosion Inhibitor to Mild Steel; *Journal of the University of Chemical Technology and Metallurgy*; 43(4): 399-404.

Yordanov, D. and Petkov, P (2008c). Protective Coatings for Metal Surfaces from Ethyl Esters of Fatty Acids and Waste Products of the oil Industry; *Journal of the University of Chemical Technology and Metallurgy*; 43(3): 315-318.

Zafar F., Ashraf S.M. and Ahmad S. (2006). Cd and Zn-Incorporated Polyesteramide Coating Materials from Seed Oil- A Renewable Resource; *Progress in Organic Coatings*; 59(1): 68-75.

Zafar F., Ashraf S.M. and Ahmad S. (2007). Studies on Zinc-Containing Linseed Oil Based Polyesteramide; *Reactive and Functional Polymers*; 67(10): 928-935.

Zafar F., Mir M.H, Kashif M., Sharmin E. and Ahmad S. (2011). Microwave Assisted Synthesis of Biobased Metallopolyurethaneamide; *Journal of Inorganic and Organometallic Polymers and Materials*; 21(1): 61-68.

Zafar F., Sharmin E., Ashraf S.M. and Ahmad S. (2004). Studies on Poly (Styrene-Co-Maleic Anhydride)-Modified Polyesleramide-Based Anticorrosive Coatings Synthesized from a Sustainable Resource; *Journal of Applied Polymer Science*; 92(4): 2538-2544.

Zhang K.E and Wu E. (2001). Circulating Metabolites of the Human Immunodeficiency Virus Protease Inhibitor Nelfinavir in Humans: Structural Identification, Levels in Plasma, and Antiviral Activities; *Antimicrobial Agents and Chemotherapy*; 45(4): 1086-1093.

Zhong B., Shaw C., Rahim M. and Massingill H. (2001). Novel Coatings from Soybean Oil Phosphate Ester Polyols. *Journal of Coating Technology*; 7(3):53-57.

Zucchi F. and Omar I.H. (2008). Plant Extracts as Corrosion Inhibitors of Mild Steel in HCl Solutions; *Surface Technology*; 24(4): 391-399.

Zuo R. (2007). Biofilms: Strategies for Metal Corrosion Inhibition Employing Microorganisms; *Applied Microbiology and Biotechnology*; 76(6): 1245-1253.

APPENDICES

APPENDIX 1(a)- VALUES OF WEIGHT LOSS FOR THE RANDOM EXPERIMENTS (Corrosion Inhibition Assessment)

RECALL:

INHIBITOR A – ESTERIFIED CASTOR SEED OIL

INHIBITOR B – ESTERIFIED RUBBER SEED OIL

RESULTS OF EXPERIMENTS ON SAMPLE A

(A) 10g/*l* at 40^{o}C *(*with inhibitor*)*

S/N	TIME (hr)	PERCENT STROKE		
		50%	60%	70%
		WEIGHT LOSSES (g)		
1	4	***2.3146***	***3.1681***	***4.3813***
2	8	***4.0219***	***3.3716***	***5.3106***
3	16	***4.8346***	***7.0348***	***11.2753***
4	24	***6.3172***	***12.8365***	***13.9926***
5	32	***8.2214***	***15.3012***	***16.3827***

(B) 10g/*l* at 40^{o}C (without inhibitor)

S/N	TIME (hr)	PERCENT STROKE		
		50%	60%	70%
		WEIGHT LOSSES (g)		
1	4	***3.7453***	***4.0317***	***6.6281***
2	8	***4.7664***	***5.6551***	***10.0816***
3	16	***6.3128***	***6.8224***	***13.3188***
4	24	***7.4217***	***12.6103***	***17.2140***
5	32	***11.8161***	***17.3168***	***20.5111***

(C)15g/*l* at 50^{o}C (with inhibitor)

S/N	TIME (hr)	PERCENT STROKE		
		50%	60%	70%
		WEIGHT LOSSES (g)		
1	4	***4.1671***	***4.5263***	***4.8694***
2	8	***5.8174***	***6.4907***	***7.2153***
3	16	***9.3566***	***11.1778***	***9.7629***
4	24	***15.5027***	***18.2817***	***19.2471***
5	32	***19.2218***	***20.6418***	***20.8918***

(D) 15g/*l* at 50^{o}C (without inhibitor)

S/N	TIME (hr)	PERCENT STROKE		
		50%	60%	70%
		WEIGHT LOSSES (g)		
1	4	***5.2993***	***6.1715***	***8.2592***
2	8	***8.7232***	***11.2010***	***11.7149***
3	16	***9.8341***	***20.4134***	***22.0146***
4	24	***18.2005***	***21.8703***	***24.1755***
5	32	***21.4840***	***23.1465***	***24.2222***

(E) 20g/*l* at 60^{o}C (with inhibitor)

S/N	TIME (hr)	PERCENT STROKE		
		50%	60%	70%
		WEIGHT LOSSES (g)		
1	4	***5.8514***	***7.4317***	***9.0422***
2	8	***8.4915***	***10.3484***	***12.1285***
3	16	***11.3118***	***11.8996***	***16.1819***
4	24	***15.7144***	***18.6218***	***23.4251***
5	32	***22.5619***	***26.1153***	***29.5454***

(F) 20g/*l* at 60^{o}C (without inhibitor)

S/N	TIME (hr)	PERCENT STROKE		
		50%	60%	70%
		WEIGHT LOSSES (g)		
1	4	***9.6221***	***11.8126***	***14.2647***
2	8	***14.5052***	***15.2115***	***20.2776***
3	16	***23.1624***	***19.0473***	***25.0618***
4	24	***24.0043***	***26.4816***	***29.4751***
5	32	***25.1057***	***29.0887***	***37.1825***

RESULTS OF EXPERIMENTS ON SAMPLE B

(A)10g/*l* at 40^{o}C (with inhibitor)

S/N	TIME (hr)	PERCENT STROKE		
		50%	60%	70%
		WEIGHT LOSSES (g)		
1	4	***1.8024***	***2.0246***	***2.9221***
2	8	***2.3412***	***2.8126***	***4.3012***
3	16	***3.0681***	***4.2214***	***4.9844***
4	24	***4.8853***	***13.6010***	***13.8692***
5	32	***6.2418***	***14.4429***	***15.7724***

(B)10g/*l* at 40^{o}C (without inhibitor)

S/N	TIME (hr)	PERCENT STROKE		
		50%	60%	70%
		WEIGHT LOSSES (g)		
1	4	***2.8841***	***3.2426***	***4.5502***
2	8	***3.6182***	***4.0829***	***6.2133***
3	16	***5.0213***	***12.2438***	***12.8132***
4	24	***5.8898***	***13.8591***	***14.0234***
5	32	***9.2673***	***16.2860***	***17.2582***

(C) 15g/*l* at 50^{o}C (with inhibitor)

S/N	TIME (hr)	PERCENT STROKE		
		50%	60%	70%
		WEIGHT LOSSES (g)		
1	4	***2.1031***	***2.1775***	***4.000***
2	8	***2.6012***	***3.2876***	***5.6212***
3	16	***4.0133***	***6.3878***	***7.1121***
4	24	***5.6690***	***14.4873***	***15.6284***
5	32	***9.2419***	***16.3838***	***17.0026***

(D) 15g/*l* at 50^{o}C (without inhibitor)

S/N	TIME (hr)	PERCENT STROKE		
		50%	60%	70%
		WEIGHT LOSSES (g)		
1	4	***4.2418***	***4.4175***	***6.3024***
2	8	***4.9204***	***6.2444***	***6.8412***
3	16	***5.8916***	***7.6036***	***9.2016***
4	24	***8.2212***	***18.9128***	***19.0029***
5	32	***11.4681***	***22.2155***	***23.5816***

(E) 20g/*l* at 60^{o}C (with inhibitor)

S/N	TIME (hr)	PERCENT STROKE		
		50%	60%	70%
		WEIGHT LOSSES (g)		
1	4	***4.4161***	***5.2178***	***7.7218***
2	8	***5.0347***	***6.7234***	***9.0291***
3	16	***6.9121***	***10.0388***	***10.8469***
4	24	***10.2219***	***19.6624***	***19.9342***
5	32	***11.5263***	***24.1285***	***24.2275***

(F) 20g/*l* at 60°C (without inhibitor)

S/N	TIME (hr)	PERCENT STROKE		
		50%	60%	70%
		WEIGHT LOSSES (g)		
1	4	***6.2551***	***6.8827***	***8.3403***
2	8	***6.9359***	***7.8726***	***11.6519***
3	16	***8.2480***	***15.3102***	***16.3728***
4	24	***12.3611***	***22.0182***	***22.7536***
5	32	***13.4612***	***25.5783***	***26.1404***

APPENDIX 2 – CORROSION RATE VALUES

Mildsteel pipe radius = 0.65cm

Length of pipe = 10.00cm

Surface area of the pipe, A = $2\prod r(h + r)$

$A = 2 \times \frac{22}{7} \times 0.65\ (10.00 + 0.65) = \mathbf{43.51cm^2}$

Density of mildsteel = $\mathbf{7.86g/cm^3}$

A. CORROSION RATE DATA FOR SAMPLE A (ECSO)

(A) 10g/*l* at 40°C *(*with inhibitor*)*

TIME (hr)	PERCENT STROKE		
	50%	60%	70%
	CORROSION RATE (mm/y)		
4	***0.1482***	***0.2029***	***0.2806***
8	***0.1288***	***0.1080***	***0.1700***
16	***0.0774***	***0.1126***	***0.1805***
24	***0.0674***	***0.1370***	***0.1493***
32	***0.0658***	***0.1225***	***0.1311***

(B) 10g/*l* at 40°C (without inhibitor)

TIME (hr)	PERCENT STROKE		
	50%	60%	70%
	CORROSION RATE (mm/y)		
4	***0.2398***	***0.2582***	***0.4244***
8	***0.1526***	***0.1811***	***0.3228***
16	***0.1011***	***0.1092***	***0.2131***
24	***0.0792***	***0.1346***	***0.1837***
32	***0.0946***	***0.1386***	***0.1642***

(C)15g/*l* at 50^{o}C (with inhibitor)

TIME (hr)	PERCENT STROKE		
	50%	60%	70%
	CORROSION RATE (mm/y)		
4	***0.2668***	***0.2899***	***0.3118***
8	***0.1863***	***0.2078***	***0.2310***
16	***0.1498***	***0.1789***	***0.1480***
24	***0.1655***	***0.1951***	***0.2054***
32	***0.1539***	***0.1652***	***0.1672***

(D) 15g/*l* at 50^{o}C (without inhibitor)

TIME (hr)	PERCENT STROKE		
	50%	60%	70%
	CORROSION RATE (mm/y)		
4	***0.3394***	***0.3952***	***0.5289***
8	***0.2815***	***0.3614***	***0.3780***
16	***0.1574***	***0.3268***	***0.3524***
24	***0.1943***	***0.2334***	***0.2580***
32	***0.1720***	***0.1853***	***0.1939***

(E) 20g/*l* at 60^{o}C (with inhibitor)

TIME (hr)	PERCENT STROKE		
	50%	60%	70%
	CORROSION RATE (mm/y)		
4	***0.3747***	***0.4759***	***0.5790***
8	***0.2719***	***0.3313***	***0.3883***
16	***0.1811***	***0.5080***	***0.2591***
24	***0.1677***	***0.1987***	***0.2500***
32	***0.1806***	***0.2090***	***0.2365***

(F) 20g/*l* at 60^{o}C (without inhibitor)

TIME (hr)	PERCENT STROKE		
	50%	60%	70%
	CORROSION RATE (mm/y)		
4	***0.6162***	***0.7564***	***0.9135***
8	***0.4644***	***0.4871***	***0.6493***
16	***0.3708***	***0.3049***	***0.4012***
24	***0.2562***	***0.2826***	***0.3146***
32	***0.2010***	***0.2328***	***0.2976***

B. CORROSION RATE DATA FOR SAMPLE B (ERSO)

(A) 10g/*l* at 40^{o}C (with inhibitor)

TIME (hr)	**PERCENT STROKE**		
	50%	**60%**	**70%**
	CORROSION RATE (mm/y)		
4	***0.1154***	***0.1296***	***0.1871***
8	***0.0750***	***0.0901***	***0.1377***
16	***0.0491***	***0.0676***	***0.0798***
24	***0.0521***	***0.0652***	***0.0680***
32	***0.0500***	***0.0464***	***0.0532***

(B) 10g/*l* at 40^{o}C (without inhibitor)

TIME (hr)	**PERCENT STROKE**		
	50%	**60%**	**70%**
	CORROSION RATE (mm/y)		
4	***0.1847***	***0.2076***	***0.2914***
8	***0.1185***	***0.1907***	***0.2089***
16	***0.0804***	***0.1960***	***0.2051***
24	***0.0629***	***0.1479***	***0.1497***
32	***0.0742***	***0.1304***	***0.1381***

(C) 15g/*l* at 50^{o}C (with inhibitor)

TIME (hr)	**PERCENT STROKE**		
	50%	**60%**	**70%**
	CORROSION RATE (mm/y)		
4	***0.1347***	***0.1394***	***0.2561***
8	***0.0833***	***0.1153***	***0.1800***
16	***0.0643***	***0.1028***	***0.1739***
24	***0.0605***	***0.1016***	***0.1668***
32	***0.0740***	***0.1011***	***0.1361***

(D) 15g/*l* at 50^{o}C (without inhibitor)

TIME (hr)	**PERCENT STROKE**		
	50%	**60%**	**70%**
	CORROSION RATE (mm/y)		
4	***0.2716***	***0.2829***	***0.4036***
8	***0.1575***	***0.1999***	***0.2190***
16	***0.0943***	***0.1217***	***0.1473***
24	***0.0877***	***0.1019***	***0.1228***
32	***0.0828***	***0.1008***	***0.1188***

(E) 20g/*l* at 60°C (with inhibitor)

TIME (hr)	PERCENT STROKE		
	50%	60%	70%
	CORROSION RATE (mm/y)		
4	***0.2828***	***0.3341***	***0.4945***
8	***0.1612***	***0.2153***	***0.2891***
16	***0.1107***	***0.1607***	***0.1737***
24	***0.1091***	***0.1099***	***0.1128***
32	***0.0923***	***0.1031***	***0.1139***

(F) 20g/*l* at 60°C (without inhibitor)

TIME (hr)	PERCENT STROKE		
	50%	60%	70%
	CORROSION RATE (mm/y)		
4	***0.4006***	***0.4407***	***0.5341***
8	***0.2221***	***0.2521***	***0.3731***
16	***0.1320***	***0.2451***	***0.2621***
24	***0.1319***	***0.2350***	***0.2428***
32	***0.1078***	***0.2047***	***0.2092***

APPENDIX 3 – INHIBITION EFFICIENCY VALUES

(A) Inhibition Efficiecies at 10g/*l* and 40°C

SAMPLES	*50% Stroke*	*60% Stroke*	*70% Stroke*
ECSO	*30.4*	*21.6*	*20.2*
ERSO	*64.4*	*61.5*	*32.6*

(B) Inhibition Efficiecies at 15g/*l* and 50°C

SAMPLES	*50% Stroke*	*60% Stroke*	*70% Stroke*
ECSO	*13.8*	*10.8*	*10.5*
ERSO	*16.8*	*14.6*	*10.6*

(C) Inhibition Efficiecies at 20g/*l* and 60°C

SAMPLES	*50% Stroke*	*60% Stroke*	*70% Stroke*
ECSO	*20.5*	*10.2*	*10.1*
ERSO	*49.6*	*45.6*	*14.4*

APPENDIX 4- PRELIMINARY DATA FOR THERMODYNAMICS STUDIES

THERMODYNAMICS DATA ***(*for C_o=20g/*l)*** AT VARIOUS TIMES

Time (hour)	SAMPLE A (ECSO)		SAMPLE B (ERSO)	
	Weght Loss, *g*	**W_C**	**Weght Loss, *g***	**W_C**
4	9.0422	13.06	7.7218	11.15
8	12.1285	17.52	9.0291	13.04
16	16.1819	23.37	10.8469	15.66
24	23.4251	33.83	18.9342	27.34
32	29.5454	42.67	21.2275	30.66

APPENDIX 5- PRELIMINARY DATA FOR ISOTHERM STUDY

A. CASTOR SEED OIL **(Sample A)**

C_o (*in g/l*): **10g/*l* at 40ºC and 50% Stroke, with inhibitor**

S/N	**Ce, g/*l***	**C_o–Ce, g/*l***	**M, g**	**x/m, g/g**	**Ce/(x/m)**	**Log Ce**	**Log(x/m)**
1	9.84	0.16	2.3146	4.39×10^{-4}	2.25×10^{4}	0.993	– 3.360
2	9.48	0.52	4.0219	8.18×10^{-4}	1.16×10^{4}	0.977	– 3.087
3	9.16	0.84	4.8346	10.99×10^{-4}	0.83×10^{4}	0.962	– 2.959
4	8.72	1.28	6.3172	12.81×10^{-4}	0.68×10^{4}	0.941	– 2.892
5	8.47	1.53	8.2214	11.77×10^{-4}	0.72×10^{4}	0.928	– 2.929

C_o (*in g/l*): **10g/*l* at 40ºC and 60% Stroke, with inhibitor**

S/N	**Ce, g/*l***	**C_o–Ce, g/*l***	**M, g**	**x/m, g/g**	**Ce/(x/m)**	**Log Ce**	**Log(x/m)**
1	9.93	0.07	3.1681	1.40×10^{-4}	7.09×10^{4}	0.997	– 3.854
2	9.62	0.38	3.3716	7.13×10^{-4}	1.35×10^{4}	0.983	– 3.147
3	9.49	0.51	7.0348	4.58×10^{-4}	2.07×10^{4}	0.977	– **3**.339
4	9.11	0.89	12.8365	4.38×10^{-4}	2.08×10^{4}	0.960	– 3.359
5	8.85	1.15	15.3012	4.75×10^{-4}	1.86×10^{4}	0.947	– 3.323

C_o (*in g/l*): **10g/*l* at 40ºC and 70% Stroke, with inhibitor**

S/N	Ce, g/*l*	C_o–Ce, g/*l*	M, g	x/m, g/g	Ce/(x/m)	Log Ce	Log(x/m)
1	9.96	0.04	4.3813	57.76×10^{-4}	0.17×10^{4}	0.998	– 2.239
2	9.82	0.18	5.3106	2.14×10^{-4}	4.59×10^{4}	0.992	– 3.670
3	9.51	0.49	11.2753	2.75×10^{-4}	3.46×10^{4}	0.978	– 3.561
4	9.30	0.70	13.9926	3.16×10^{-4}	2.94×10^{4}	0.968	– 3.500
5	9.05	0.95	16.3827	3.67×10^{-4}	2.47×10^{4}	0.957	– 3.435

C_o (*in g/l*): **10g/*l* at 40ºC and 50% Stroke, without inhibitor**

S/N	Ce, g/*l*	C_o–Ce, g/*l*	M, g	x/m, g/g	Ce/(x/m)	Log Ce	Log(x/m)
1	9.91	0.09	3.7453	1.52×10^{-4}	6.52×10^{4}	0.996	– 3.818
2	9.66	0.34	4.7664	4.51×10^{-4}	2.14×10^{4}	0.985	– 3.346
3	9.27	0.73	6.3128	7.31×10^{-4}	1.27×10^{4}	0.967	– 3.136
4	8.93	1.07	7.4217	9.12×10^{-4}	0.98×10^{4}	0.951	– 3.040
5	8.70	1.23	11.8161	6.58×10^{-4}	1.33×10^{4}	0.943	– 3.182

C_o (*in g/l*): **10g/*l* at 40ºC and 60% Stroke, without inhibitor**

S/N	Ce, g/*l*	C_o–Ce, g/*l*	M, g	x/m, g/g	Ce/(x/m)	Log Ce	Log(x/m)
1	9.86	0.14	4.0317	2.20×10^{-4}	4.48×10^{4}	0.994	– 3.658
2	9.61	0.39	5.6551	4.36×10^{-4}	2.20×10^{4}	0.983	– 3.361
3	9.05	0.95	6.8224	8.81×10^{-4}	1.03×10^{4}	0.957	– 3.055
4	8.89	1.11	12.6103	5.57×10^{-4}	1.60×10^{4}	0.949	– 3.254
5	8.63	1.57	17.3168	5.00×10^{-4}	1.73×10^{4}	0.936	– 3.301

C_o (*in g/l*): **10g/*l* at 40ºC and 70% Stroke, without inhibitor**

S/N	Ce, g/*l*	C_o–Ce, g/*l*	M, g	x/m, g/g	Ce/(x/m)	Log Ce	Log(x/m)
1	9.80	0.20	6.6281	1.91×10^{-4}	5.13×10^{4}	0.991	– 3.719
2	9.59	0.41	10.0816	2.57×10^{-4}	3.73×10^{4}	0.982	– 3.590
3	8.92	1.08	13.3188	5.13×10^{-4}	1.74×10^{4}	0.950	– 3.290
4	8.80	1.20	17.2140	4.41×10^{-4}	2.00×10^{4}	0.944	– 3.356
5	8.57	1.43	20.5111	4.41×10^{-4}	1.94×10^{4}	0.933	– 3.356

C_o (*in g/l*): **15g/*l* at 50ºC and 50% Stroke with inhibitor**

S/N	Ce, g/*l*	C_o–Ce, g/*l*	M, g	x/m, g/g	Ce/(x/m)	Log Ce	Log(x/m)
1	14.27	0.73	4.1671	11.08×10^{-4}	1.29×10^{4}	1.154	– 2.955
2	14.18	0.12	5.8174	8.91×10^{-4}	1.59×10^{4}	1.152	– 3.050
3	14.06	1.18	9.3566	6.35×10^{-4}	2.21×10^{4}	1.148	– 3.197
4	13.88	1.12	16.5029	4.57×10^{-4}	3.04×10^{4}	1.142	– 3.340
5	13.82	1.18	19.2218	3.88×10^{-4}	3.56×10^{4}	1.141	– 3.411

C_o (*in g/l*): **15g/*l* at 50ºC and 60% Stroke with inhibitor**

S/N	Ce, g/*l*	C_o–Ce, g/*l*	M, g	x/m, g/g	Ce/(x/m)	Log Ce	Log(x/m)
1	14.39	0.61	4.5263	8.52×10^{-4}	1.69×10^{4}	1.158	– 3.070
2	14.22	0.78	6.4907	7.60×10^{-4}	1.87×10^{4}	1.153	– 3.119
3	13.98	1.02	11.1778	5.77×10^{-4}	2.42×10^{4}	1.146	– 3.239
4	13.85	1.15	18.2817	3.98×10^{-4}	3.48×10^{4}	1.141	– 3.400
5	13.82	1.18	20.6418	3.62×10^{-4}	3.82×10^{4}	1.141	– 3.441

C_o (*in g/l*):= **15g/*l* at 50ºC and 70% Stroke, with inhibitor**

S/N	Ce, g/*l*	C_o–Ce, g/*l*	M, g	x/m, g/g	Ce/(x/m)	Log Ce	Log(x/m)
1	14.34	0.66	4.8694	8.57×10^{-4}	1.67×10^{4}	1.157	– 3.067
2	14.17	0.81	7.2153	7.10×10^{-4}	2.00×10^{4}	1.152	– 3.149
3	14.09	0.91	9.7629	5.89×10^{-4}	2.39×10^{4}	1.149	– 3.230
4	13.91	1.09	19.2471	3.58×10^{-4}	3.89×10^{4}	1.143	– 3.446
5	13.86	1.14	20.8918	3.45×10^{-4}	4.01×10^{4}	1.142	– 3.462

C_o (*in g/l*): **15g/*l* at 50ºC and 50% Stroke, without inhibitor**

S/N	Ce, g/*l*	C_o–Ce, g/*l*	M, g	x/m, g/g	Ce/(x/m)	Log Ce	Log(x/m)
1	14.44	0.56	5.2993	6.68×10^{-4}	2.16×10^{4}	1.160	– 3.175
2	14.13	0.87	8.7232	6.31×10^{-4}	2.24×10^{4}	1.150	– 3.200
3	13.98	1.02	9.8341	6.56×10^{-4}	2.13×10^{4}	1.146	– 3.183
4	13.72	1.28	18.2005	4.45×10^{-4}	3.08×10^{4}	1.137	– 3.352
5	13.56	1.44	21.4840	4.24×10^{-4}	3.20×10^{4}	1.132	– 3.373

C_o (*in g/l*): **15g/*l* at 50ºC and 60% Stroke, without inhibitor**

S/N	Ce, g/*l*	C_o–Ce, g/*l*	M, g	x/m, g/g	Ce/(x/m)	Log Ce	Log(x/m)
1	14.41	0.59	6.1715	6.05×10^{-4}	2.38×10^{4}	1.159	– 3.218
2	14.18	0.82	11.2010	4.63×10^{-4}	3.06×10^{4}	1.152	– 3.334
3	13.96	1.04	20.4134	3.22×10^{-4}	4.34×10^{4}	1.145	– 3.492
4	13.79	1.21	21.8703	3.50×10^{-4}	3.94×10^{4}	1.140	– 3.456
5	13.53	1.47	23.1465	4.02×10^{-4}	3.37×10^{4}	1.131	– 3.396

C_o (*in g/l*): **15g/*l* at 50ºC and 70% Stroke, without inhibitor**

S/N	Ce, g/*l*	C_o–Ce, g/*l*	M, g	x/m, g/g	Ce/(x/m)	Log Ce	Log(x/m)
1	14.39	0.61	8.2592	4.69×10^{-4}	3.08×10^{4}	1.158	– 3.331
2	14.11	0.89	11.7149	4.80×10^{-4}	2.94×10^{4}	1.150	– 3.319
3	13.86	1.14	22.0146	3.27×10^{-4}	4.24×10^{4}	1.142	– 3.485
4	13.69	1.31	24.1755	3.43×10^{-4}	3.99×10^{4}	1.136	– 3.465
5	13.51	1.49	24.2222	3.89×10^{-4}	3.47×10^{4}	1.131	– 3.410

C_o (*in g/l*): **20g/*l* at 60ºC and 50% Stroke, with inhibitor**

S/N	Ce, g/*l*	C_o–Ce, g/*l*	M, g	x/m, g/g	Ce/(x/m)	Log Ce	Log(x/m)
1	18.88	1.12	5.8514	12.10×10^{-4}	1.56×10^{4}	1.276	– 2.917
2	18.43	1.57	8.4915	11.69×10^{-4}	1.58×10^{4}	1.266	– 2.932
3	17.96	2.04	11.3118	11.40×10^{-4}	1.58×10^{4}	1.254	– 2.943
4	17.71	2.29	15.7144	9.22×10^{-4}	1.92×10^{4}	1.245	– 3.035
5	17.47	2.53	22.5619	7.09×10^{-4}	2.46×10^{4}	1.242	– 3.449

C_o (*in g/l*): **20g/*l* at 60ºC and 60% Stroke, with inhibitor**

S/N	Ce, g/*l*	C_o–Ce, g/*l*	M, g	x/m, g/g	Ce/(x/m)	Log Ce	Log(x/m)
1	18.94	1.06	7.4317	9.02×10^{-4}	2.10×10^{4}	1.277	– 3.045
2	18.70	1.30	10.3484	7.94×10^{-4}	2.36×10^{4}	1.272	– 3.100
3	18.22	1.78	11.8996	9.46×10^{-4}	1.93×10^{4}	1.261	– 3.024
4	17.84	2.16	18.6218	7.34×10^{-4}	2.43×10^{4}	1.251	– 3.134
5	17.52	2.48	26.1153	6.01×10^{-4}	2.92×10^{4}	1.244	– 3.221

C_o (*in g/l*): **20g/*l* at 60ºC and 70% Stroke, with inhibitor**

S/N	Ce, g/*l*	C_o–Ce, g/L	M, g	x/m, g/g	Ce/(x/m)	Log Ce	Log(x/m)
1	18.96	1.04	9.0422	$7.27x10^{-4}$	$2.61x10^{4}$	1.278	– 3.138
2	18.73	1.27	12.1285	$6.62x10^{-4}$	$2.58x10^{4}$	1.273	– 3.179
3	18.35	1.65	16.1819	$6.45x10^{-4}$	$2.84x10^{4}$	1.264	– 3.170
4	17.91	2.09	23.4251	$5.64x10^{-4}$	$3.18x10^{4}$	1.253	– 3.249
5	17.66	2.34	29.5454	$5.01x10^{-4}$	$3.52x10^{4}$	1.247	– 3.300

C_o (*in g/l*): **20g/*l* at 60ºC and 60% Stroke, without inhibitor**

S/N	Ce, g/*l*	C_o–Ce, g/*l*	M, g	x/m, g/g	Ce/(x/m)	Log Ce	Log(x/m)
1	19.12	0.88	9.6221	$5.78x10^{-4}$	$3.31x10^{4}$	1.281	– 3.238
2	18.91	1.09	14.5052	$4.75x10^{-4}$	$3.98x10^{4}$	1.277	– 3.323
3	18.57	1.43	23.1624	$3.90x10^{-4}$	$4.76x10^{4}$	1.269	– 3.409
4	18.04	1.96	24.0043	$5.16x10^{-4}$	$3.50x10^{4}$	1.256	– 3.287
5	17.86	2.14	25.1057	$5.39x10^{-4}$	$3.31x10^{4}$	1.252	– 3.280

C_o (*in g/l*): **20g/*l* at 60ºC 60% Stroke, without inhibitor**

S/N	Ce, g/*l*	C_o–Ce, g/*l*	M, g	x/m, g/g	Ce/(x/m)	Log Ce	Log(x/m)
1	19.05	0.95	11.8126	$5.09x10^{-4}$	$3.74x10^{4}$	1.280	– 3.293
2	18.84	1.16	15.2115	$4.82x10^{-4}$	$3.91x10^{4}$	1.275	– 3.317
3	18.49	1.51	19.0473	$5.01x10^{-4}$	$3.69x10^{4}$	1.267	– 3.300
4	17.95	2.05	26.4816	$4.90x10^{-4}$	$3.66x10^{4}$	1.254	– 3.310
5	17.79	2.21	29.0887	$4.80x10^{-4}$	$3.71x10^{4}$	1.250	– 3.319

C_o (*in g/l*): **20g/*l* at 60ºC and 70% Stroke, without inhibitor**

S/N	Ce, g/*l*	C_o–Ce, g/*l*	M, g	x/m, g/g	Ce/(x/m)	Log Ce	Log(x/m)
1	18.94	1.06	14.2647	$4.70x10^{-4}$	$4.03x10^{4}$	1.277	– 3.328
2	18.80	1.20	20.2776	$3.74x10^{-4}$	$5.03x10^{4}$	1.274	– 3.427
3	18.46	1.54	25.0218	$3.89x10^{-4}$	$4.75x10^{4}$	1.266	– 3.410
4	18.11	1.89	29.4751	$4.06x10^{-4}$	$4.46x10^{4}$	1.258	– 3.391
5	17.77	2.23	37.1825	$3.79x10^{-4}$	$4.69x10^{4}$	1.250	– 3.421

B. RUBBER SEED OIL **(Sample B)**

C_o (*in g/l*): **10g/*l* at 40ºC and 50% Stroke, with inhibitor**

S/N	Ce, g/*l*	C_o–Ce, g/*l*	M, g	x/m, g/g	Ce/(x/m)	Log Ce	Log(x/m)
1	9.79	0.21	1.8024	$7.37x10^{-4}$	$1.32x10^{4}$	0.991	– 3.133
2	9.41	0.59	2.3412	$15.94x10^{-4}$	$0.59x10^{4}$	0.974	– 2.798
3	8.95	1.05	3.0681	$21.64x10^{-4}$	$0.41x10^{4}$	0.952	– 2.665
4	8.69	1.31	4.8853	$16.96x10^{-4}$	$0.51x10^{4}$	0.939	– 2.771
5	8.42	1.58	6.2418	$16.01x10^{-4}$	$0.53x10^{4}$	0.925	– 2.796

C_o (*in g/l*): **10g/*l* at 40ºC and 60% Stroke, with inhibitor**

S/N	Ce, g/*l*	C_o–Ce, g/*l*	M, g	x/m, g/g	Ce/(x/m)	Log Ce	Log(x/m)
1	9.86	0.14	2.0246	$4.37x10^{-4}$	$2.26x10^{4}$	0.994	– 3.360
2	9.57	0.43	2.8126	$6.67x10^{-4}$	$0.99x10^{4}$	0.981	– 3.015
3	9.29	0.71	4.2216	$10.64x10^{-4}$	$0.87x10^{4}$	0.968	– 2.973
4	8.94	1.06	13.6010	$4.93x10^{-4}$	$1.81x10^{4}$	0.951	– 3.307
5	8.66	1.34	14.4429	$5.81x10^{-4}$	$1.48x10^{4}$	0.938	– 3.231

C_o (*in g/l*): **10g/*l* at 40ºC and 70% Stroke, with inhibitor**

S/N	Ce, g/*l*	C_o–Ce, g/*l*	M, g	x/m, g/g	Ce/(x/m)	Log Ce	Log(x/m)
1	9.92	0.08	2.9221	$1.73x10^{-4}$	$5.73x10^{4}$	0.991	– 3.762
2	9.74	0.26	4.3012	$3.82x10^{-4}$	$2.55x10^{4}$	0.974	– 3.418
3	9.35	0.65	9.9844	$8.25x10^{-4}$	$1.13x10^{4}$	0.952	– 3.084
4	9.12	0.88	13.8692	$4.01x10^{-4}$	$2.27x10^{4}$	0.960	– 3.397
5	8.69	1.31	14.7724	$5.251x10^{-4}$	$1.66x10^{4}$	0.939	– 3.280

C_o (*in g/l*): **10g/*l* at 40ºC and 50% Stroke, without inhibitor**

S/N	Ce, g/*l*	C_o–Ce, g/*l*	M, g	x/m, g/g	Ce/(x/m)	Log Ce	Log(x/m)
1	9.83	0.17	2.8841	$3.73x10^{-4}$	$2.64x10^{4}$	0.993	– 3.428
2	9.52	0.48	3.6182	$8.39x10^{-4}$	$1.13x10^{4}$	0.979	– 3.076
3	9.12	0.88	5.0213	$11.08x10^{-4}$	$0.82x10^{4}$	0.960	– 2.995
4	8.79	1.21	5.8898	$12.99x10^{-4}$	$0.68x10^{4}$	0.943	– 2.886
5	8.44	1.56	9.2673	$10.65x10^{-4}$	$0.79x10^{4}$	0.926	– 2.973

C_o (*in g/l*): 10g/*l* at 40ºC and 60% Stroke, without inhibitor

S/N	Ce, g/*l*	C_o–Ce, g/*l*	M, g	x/m, g/g	Ce/(x/m)	Log Ce	Log(x/m)
1	9.88	0.12	3.2426	$2.34x10^{-4}$	$4.22x10^{-4}$	0.995	– 3.361
2	9.53	0.47	4.0829	$7.28x10^{-4}$	$1.31x10^{-4}$	0.979	– 3.138
3	9.21	0.79	2.2438	$22.27x10^{-4}$	$0.41x10^{-4}$	0.964	– 2.652
4	8.96	1.04	13.8591	$4.75x10^{-4}$	$1.89x10^{-4}$	0.952	– 3.323
5	8.67	1.33	16.2860	$5.16x10^{-4}$	$1.68x10^{-4}$	0.938	– 3.287

C_o (*in g/l*): 10g/*l* at 40ºC and 70% Stroke, without inhibitor

S/N	Ce, g/*l*	C_o–Ce, g/*l*	M, g	x/m, g/g	Ce/(x/m)	Log Ce	Log(x/m)
1	9.94	0.06	4.5502	$0.83x10^{-4}$	$11.98x10^{4}$	0.997	– 4.081
2	9.81	0.19	6.2133	$1.93x10^{-4}$	$5.08x10^{4}$	0.992	– 3.714
3	9.40	0.60	7.8132	$4.86x10^{-4}$	$1.93x10^{4}$	0.973	– 3.313
4	9.02	0.98	14.0234	$4.42x10^{-4}$	$2.14x10^{4}$	0.973	– 3.335
5	8.75	1.25	17.2582	$4.58x10^{-4}$	$1.91x10^{4}$	0.942	– 3.339

C_o (*in g/l*): 15g/*l* at 50ºC and 50% Stroke, with inhibitor

S/N	Ce, g/*l*	C_o–Ce, g/*l*	M, g	x/m, g/g	Ce/(x/m)	Log Ce	Log(x/m)
1	14.23	0.77	2.1031	$23.15x10^{-4}$	$0.61x10^{4}$	1.153	– 2.635
2	14.15	0.85	2.6012	$20.67x10^{-4}$	$0.68x10^{4}$	1.151	– 2.685
3	13.94	1.06	4.0133	$16.70x10^{-4}$	$0.83x10^{4}$	1.144	– 2.777
4	13.86	1.14	5.6690	$12.72x10^{-4}$	$1.09x10^{4}$	1.142	– 2.896
5	13.77	1.23	9.2419	$8.42x10^{-4}$	$1.64x10^{4}$	1.139	– 0.075

C_o (*in g/l*): 15g/*l* at 50ºC 60% Stroke, with inhibitor

S/N	Ce, g/*l*	C_o–Ce, g/*l*	M, g	x/m, g/g	Ce/(x/m)	Log Ce	Log(x/m)
1	14.30	0.70	2.1775	$20.20x10^{-4}$	$0.70x10^{4}$	1.155	– 2.692
2	14.20	0.80	3.2816	$15.39x10^{-4}$	$0.92x10^{4}$	1.152	– 2.813
3	13.97	1.03	6.3878	$10.20x10^{-4}$	$1.37x10^{4}$	1.145	– 2.991
4	13.84	1.16	14.4873	$5.06x10^{-4}$	$2.74x10^{4}$	1.141	– 3.296
5	13.80	1.20	16.3838	$4.63x10^{-4}$	$2.98x10^{4}$	1.140	– 3.334

C_o (*in g/l*): **15g/*l* at 50ºC and 70% Stroke, with inhibitor**

S/N	Ce, g/*l*	C_o–Ce, g/*l*	M, g	x/m, g/g	Ce/(x/m)	Log Ce	Log(x/m)
1	14.33	0.67	4.0000	10.59×10^{-4}	1.35×10^{4}	1.156	– 2.295
2	14.22	0.78	5.6212	8.78×10^{-4}	1.62×10^{4}	1.153	– 3.057
3	14.06	0.94	7.1121	8.36×10^{-4}	1.68×10^{4}	1.148	– 3.078
4	13.93	1.07	15.6284	4.33×10^{-4}	3.22×10^{4}	1.144	– 3.264
5	13.80	1.16	17.0026	4.31×10^{-4}	3.21×10^{4}	1.141	– 3.366

C_o (*in g/l*): **15g/*l* at 50ºC and 50% Stroke, without inhibitor**

S/N	Ce, g/*l*	C_o–Ce, g/*l*	M, g	x/m, g/g	Ce/(x/m)	Log Ce	Log(x/m)
1	14.41	0.59	4.2418	8.80×10^{-4}	1.64×10^{4}	1.159	– 3.056
2	14.12	0.88	4.9204	11.31×10^{-4}	1.25×10^{4}	1.150	– 2.947
3	13.95	1.05	5.8916	11.27×10^{-4}	1.24×10^{4}	1.145	– 2.948
4	13.66	1.34	8.2212	10.31×10^{-4}	1.32×10^{4}	1.135	– 2.987
5	13.49	1.51	11.4681	8.33×10^{-4}	1.62×10^{4}	1.130	– 2.079

C_o (*in g/l*): **15g/*l* at 50ºC and 60% Stroke, without inhibitor**

S/N	Ce, g/*l*	C_o–Ce, g/*l*	M, g	x/m, g/g	Ce/(x/m)	Log Ce	Log(x/m)
1	14.39	0.61	4.4175	8.73×10^{-4}	1.65×10^{4}	1.158	– 3.059
2	14.09	0.91	6.2444	9.22×10^{-4}	1.53×10^{4}	1.149	– 3.035
3	13.87	1.13	7.6036	9.40×10^{-4}	1.48×10^{4}	1.142	– 3.027
4	13.69	1.31	18.9128	4.38×10^{-4}	3.13×10^{4}	1.136	– 3.359
5	13.51	1.49	22.2155	4.24×10^{-4}	3.19×10^{4}	1.131	– 3.373

C_o (*in g/l*): **15g/*l* at 50ºC and 70% Stroke, without inhibitor**

S/N	Ce, g/*l*	C_o–Ce, g/*l*	M, g	x/m, g/g	Ce/(x/m)	Log Ce	Log(x/m)
1	14.33	0.67	6.3024	6.72×10^{-4}	2.13×10^{4}	1.156	– 3.173
2	14.00	1.00	6.8412	9.24×10^{-4}	1.52×10^{4}	1.146	– 3.034
3	13.77	1.23	9.2016	8.45×10^{-4}	1.63×10^{4}	1.139	– 3.073
4	13.61	1.39	19.0029	4.63×10^{-4}	2.94×10^{4}	1.134	– 3.334
5	13.44	1.56	23.5816	4.18×10^{-4}	3.22×10^{4}	1.128	– 3.378

C_o (*in g/l*): 20g/*l* at 60ºC and 50% Stroke, with inhibitor

S/N	Ce, g/*l*	C_o–Ce, g/*l*	M, g	x/m, g/g	Ce/(x/m)	Log Ce	Log(x/m)
1	18.88	1.12	5.8514	12.10×10^{-4}	1.56×10^{4}	1.275	– 2.780
2	18.43	1.57	8.4915	11.69×10^{-4}	1.58×10^{4}	1.268	– 2.731
3	17.96	2.04	11.3118	11.40×10^{-4}	1.58×10^{4}	1.257	– 2.751
4	17.71	2.29	15.7144	9.22×10^{-4}	1.92×10^{4}	1.246	– 2.830
5	17.47	1.53	22.5619	7.09×10^{-4}	2.46×10^{4}	1.240	– 2.844

C_o (*in g/l*): 20g/*l* at 60ºC and 60% Stroke, with inhibitor

S/N	Ce, g/L	C_o–Ce, g/L	M, g	x/m, g/g	Ce/(x/m)	Log Ce	Log(x/m)
1	18.94	1.06	7.4317	9.02×10^{-4}	2.10×10^{4}	1.276	– 2.871
2	18.70	1.30	10.3484	7.94×10^{-4}	2.36×10^{4}	1.272	– 2.916
3	18.22	2.78	11.8996	9.46×10^{-4}	1.93×10^{4}	1.261	– 2.955
4	17.84	2.16	18.6218	7.34×10^{-4}	2.43×10^{4}	1.250	– 3.148
5	17.52	2.46	26.1153	6.01×10^{-4}	2.92×10^{4}	1.243	– 3.185

C_o (*in g/l*): 20g/*l* at 60ºC and 70% Stroke, with inhibitor

S/N	Ce, g/*l*	C_o–Ce, g/*l*	M, g	x/m, g/g	Ce/(x/m)	Log Ce	Log(x/m)
1	18.96	1.04	9.0422	7.25×10^{-4}	2.61×10^{4}	1.277	– 3.061
2	18.73	1.27	12.1285	6.62×10^{-4}	2.58×10^{4}	1.272	– 3.040
3	18.35	1.65	16.1819	6.45×10^{-4}	2.84×10^{4}	1.263	– 3.007
4	17.91	2.09	23.4251	5.64×10^{-4}	3.18×10^{4}	1.251	– 3.142
5	17.66	2.34	29.5454	5.01×10^{-4}	3.52×10^{4}	1.245	– 3.144

C_o (*in g/l*): 20g/*l* at 60ºC and 50% Stroke, without inhibitor

S/N	Ce, g/*l*	C_o–Ce, g/*l*	M, g	x/m, g/g	Ce/(x/m)	Log Ce	Log(x/m)
1	19.08	0.98	6.2551	9.91×10^{-4}	1.93×10^{4}	1.281	– 3.004
2	18.86	1.14	6.9359	10.39×10^{-4}	1.82×10^{4}	1.276	– 2.983
3	18.39	1.61	8.2480	12.34×10^{-4}	1.49×10^{4}	1.265	– 2.909
4	17.92	2.08	12.3611	10.64×10^{-4}	1.68×10^{4}	1.253	– 2.973
5	17.85	2.15	13.4612	10.10×10^{-4}	1.77×10^{4}	1.252	– 2.996

C_o (*in g/l*): **20g/*l* at 60ºC and 60% Stroke, without inhibitor**

S/N	Ce, g/*l*	C_o–Ce, g/*l*	M, g	x/m, g/g	Ce/(x/m)	Log Ce	Log(x/m)
1	18.98	1.62	6.8827	$9.35x10^{-4}$	$1.03x10^{4}$	1.278	– 3.028
2	18.79	1.21	7.8726	$9.72x10^{-4}$	$1.93x10^{4}$	1.274	– 3.012
3	18.33	1.67	15.3102	$6.90x10^{-4}$	$2.66x10^{4}$	1.263	– 2.161
4	17.86	2.14	22.0182	$6.15x10^{-4}$	$2.90x10^{4}$	1.252	– 3.211
5	17.72	2.28	25.5783	$5.64x10^{-4}$	$3.14x10^{4}$	1.248	– 3.249

C_o (*in g/l*): **20g/*l* at 60ºC and 70% Stroke, without inhibitor**

S/N	Ce, g/*l*	C_o–Ce, g/*l*	M, g	x/m, g/g	Ce/(x/m)	Log Ce	Log(x/m)
1	18.93	1.07	8.3403	$8.11x10^{-4}$	$2.33x10^{4}$	1.277	– 3.091
2	18.74	1.26	11.6519	$6.84x10^{-4}$	$2.74x10^{4}$	1.273	– 3.165
3	18.31	1.69	16.3728	$6.53x10^{-4}$	$2.80x10^{4}$	1.263	– 3.185
4	17.87	2.13	22.7536	$6.92x10^{-4}$	$3.02x10^{4}$	1.252	– 3.228
5	17.66	2.34	26.1404	$3.24x10^{-4}$	$5.45x10^{4}$	1.247	– 3.489

C. TEMKIN AND EL-AWADY DATA FOR ECSO (**Sample A**)

C, g/*l*	r_c	r_c(at blank)	Θ	$\frac{\Theta}{(1-\Theta)}$	Log C	$\text{Log}\left[\frac{\Theta}{(1-\Theta)}\right]$	Log Θ
10.00	13.06	20.34	0.3579	0.5574	1.00	-0.2538	-0.4462
15.00	17.53	27.28	0.3578	0.5571	1.18	-0.2541	-0.4463
20.00	23.37	36.39	0.3578	0.5571	1.30	-0.2541	-0.4463

C. TEMKIN AND EL-AWADY DATA FOR ERSO (**Sample B**)

C, g/*l*	r_c	r_c(at blank)	Θ	$\frac{\Theta}{(1-\Theta)}$	Log C	$\text{Log}\left[\frac{\Theta}{(1-\Theta)}\right]$	Log Θ
10.00	11.15	20.34	0.4518	0.8242	1.00	-0.0840	-0.3450
15.00	13.04	27.28	0.5220	1.0921	1.18	0.0383	-0.2823
20.00	15.66	36.39	0.5697	1.3240	1.30	0.1219	-0.2444

APPENDIX 6- COMPOSITION OF SOME MAJOR REAGENTS USED DURING THE STUDY

REAGENT	MOLAR WEIGHT, g/mol	% PURITY	SPECIFIC GRAVITY, g/ml
n-Hexane	86.18	97.00	0.663
Ethanol	46.07	99.70	0.791
Sulphuric Acid	98.07	97.99	1.840
Chloroform	-	99.50	1.477
Petroleum Ether	-	99.08	-
Methanol	32.04	99.50	0.793
Ammonia	17.03	25.00	-
Carbon Tetrachloride	153.82	99.80	1.594
Hydrochloric Acid	36.45	35.00	1.180
Acetic Acid	50.05	99.80	1.040
Ammonium Hydroxide	17.03	33.00	0.880

APPENDIX 7- RECOMMENDED (STANDARD) FOR PHYSICOCHEMICAL CHARACTERISTICS OF MOST EDIBLE AND NON-EDIBLE OILS AS GIVEN BY FAO/WHO (1993)

PARAMETER	**FAO/WHO SPECIFICATION**	
	Edible Oils	**Non-Edible Oils**
Viscosity (*Poise*)	-	-
Refractive Index	1.466 – 1.470	1.458 – 1.466
Density *(g/ml)*	0.919 – 0.925	0.918 – 0.926
Specific Gravity	-	-
FFA Value (*mg/ml)*	≥ 0.176	≥ 0.225
Saponification Value *(mg/ml)*	189 – 195	189 – 198
Iodine value*(mg/ml)*	120 – 143	99 – 119
Peroxide Value*(mg/ml)*	<10	<10

APPENDIX 8- EPICAPAL VIEW OF THE STUDY SAMPLES

A. THE CASTOR SEED

B. THE RUBBER SEED